NAVAL POSTGRADUATE SCHOOL
Monterey, California

THESIS

TIME DOMAIN VALIDATION OF THE SIKORSKY GENERAL HELICOPTER (GENHEL) FLIGHT DYNAMICS SIMULATION MODEL FOR THE UH-60L WIDE CHORD BLADE MODIFICATION

by

Robert L. Barrie, Jr.

December 1999

Thesis Advisor: E Roberts Wood
Thesis Co-Advisor: Thomas H. Lawerence

Approved for public release; distribution is unlimited.

REPORT DOCUMENTATION PAGE

Form Approved
OMB No. 0704-0188

1. AGENCY USE ONLY ***(Leave blank)***	**2. REPORT DATE** December 1999	**3. REPORT TYPE AND DATES COVERED** Master's Thesis

4. TITLE AND SUBTITLE
Time Domain Validation of the Sikorsky General Helicopter (GenHel®) Flight Dynamics Simulation Model for the UH-60L Wide Chord Modification.

5. FUNDING NUMBERS

6. AUTHOR(S)
Captain Robert L. Barrie, Jr.

7. PERFORMING ORGANIZATION NAME(S) AND ADDRESS(ES)
Naval Postgraduate School
Monterey, CA 93943-5000

8. PERFORMING ORGANIZATION REPORT NUMBER

9. SPONSORING / MONITORING AGENCY NAME(S) AND ADDRESS(ES)
Sikorsky Aircraft Corporation
6900 Main Street P.O. Box 9729
Stratford, Connecticut 06497-9129

10. SPONSORING/MONITORING AGENCY REPORT NUMBER

11. SUPPLEMENTARY NOTES
The views expressed in this thesis are those of the author and do not reflect the official policy or position of the Department of Defense or the U.S. Government.

12a. DISTRIBUTION / AVAILABILITY STATEMENT
Approved for public release; distribution is unlimited.

12b. DISTRIBUTION CODE

13. ABSTRACT ***(Maximum 200 words)***

Helicopter design at the Sikorsky Aircraft Corporation is aided by the use of the Sikorsky General Helicopter (GenHel®) Flight Dynamics Simulation Model. Specifically, GenHel output is used by both handling qualities and maneuver loads engineers as a predictive design tool. Inherent in the use of an analytical model is the requirement for validation. This report seeks to validate the GenHel® flight dynamics simulation models used in the design of the UH-60L Wide Chord Blade (WCB) modification. Initially, comparisons are made between the current analytical models and flight test data for selected trim flight conditions and dynamic maneuvers. Based on the correlation of the data, modifications are made to the analytical model where necessary. The modified analytical model will be validated through a final comparison with test flight data. The goal of this report is to validate the use of Sikorsky's GenHel® flight simulation program as an analytic predictive tool in the design of the WCB modification and identify any areas where improvements could be applied. Validation of the WCB GenHel model serves two purposes. First it confirms the ability of GenHel to model the flight dynamic response of the UH-60L with the WCB modification. Second it confirms the predictive loads forwarded to the structural engineers during the design phase of the WCB.

14. SUBJECT TERMS Helicopter Dynamics, Mathematical Modeling	**15. NUMBER OF PAGES** 158
	16. PRICE CODE

17. SECURITY CLASSIFICATION OF REPORT Unclassified	**18. SECURITY CLASSIFICATION OF THIS PAGE** Unclassified	**19. SECURITY CLASSIFICATION OF ABSTRACT** Unclassified	**20. LIMITATION OF ABSTRACT** UL

NSN 7540-01-280-5500

Standard Form 298 (Rev. 2-89)
Prescribed by ANSI Std 239-18

TIME DOMAIN VALIDATION OF THE SIKORSKY GENERAL HELICOPTER (GENHEL) FLIGHT DYNAMICS SIMULATION MODEL FOR THE UH-60L WIDE CHORD BLADE MODIFICATION

Robert L. Barrie
Captain, United States Army
B.S., United States Military Academy, 1990

Submitted in partial fulfillment of the
requirements for the degree of

MASTER OF SCIENCE IN AERONAUTICAL ENGINEERING

from the

NAVAL POSTGRADUATE SCHOOL
December 1999

Author: ______________________________
Robert L. Barrie, Jr.

Approved by: ______________________________
E. Roberts Wood, Thesis Advisor

____
Thomas H. Lawrence, Thesis Co-Advisor

____
Gerald H. Lindsey, Chairman
Department of Aeronautics and Astronautics

ABSTRACT

Helicopter design at the Sikorsky Aircraft Corporation is aided by the use of the Sikorsky General Helicopter (GenHel®) Flight Dynamics Simulation Model. Specifically, GenHel output is used by both handling qualities and maneuver loads engineers as a predictive design tool. Inherent in the use of an analytical model is the requirement for validation. This report seeks to validate the GenHel® flight dynamics simulation models used in the design of the UH-60L Wide Chord Blade (WCB) modification. Initially, comparisons are made between the current analytical models and flight test data for selected trim flight conditions and dynamic maneuvers. Based on the correlation of the data, modifications are made to the analytical model where necessary. The modified analytical model will be validated through a final comparison with test flight data. The goal of this report is to validate the use of Sikorsky's GenHel® flight simulation program as an analytic predictive tool in the design of the WCB modification and identify any areas where improvements could be applied. Validation of the WCB GenHel model serves two purposes. First it confirms the ability of GenHel to model the flight dynamic response of the UH-60L with the WCB modification. Second it confirms the predictive loads forwarded to the structural engineers during the design phase of the WCB.

TABLE OF CONTENTS

LIST OF FIGURES

LIST OF TABLES

ACKNOWLEDGEMENT

Thanks are due to Tom Lawrence, Joe Driscoll and Aaron Tomany at Sikorsky Aircraft Corporation for their support throughout my thesis research. Their knowledge, patience and friendship made this unique learning opportunity a rewarding and enjoyable experience.

I. INTRODUCTION

Engineers at Sikorsky Aircraft use General Helicopter (GenHel®) Flight Dynamics Software as a design tool for predicting handling qualities and structural loading characteristics. Inherent in the use of an analytical model is the requirement for validation. All mathematical models are guilty until proven innocent [Ref. 1]. Sikorsky has a validated GenHel® model of the UH-60 BLACK HAWK helicopter. The model was originally developed under contract from NASA in 1980 and has been refined throughout the development cycle of the aircraft. The analytical model was recently modified to reflect the latest BLACK HAWK design evolution, the Wide Chord Blade (WCB).

Customer demands for increases to the mission gross weight and performance requirements of the UH-60 BLACK HAWK helicopter resulted in a requirement for increased rotor solidity. Sikorsky's solution to the problem is an all-composite blade referred to as the Wide Chord Blade. The WCB is equal in length to the current UH-60 blade and maintains the same nominal non-linear twist distribution which provides an effective linearized value of –18 degrees. Improvements were attained through the incorporation of enhanced SC1095 airfoils, a 16% increase in chord length, and the addition of 20° anhedral swept tips. The 16% increase in chord length increases blade chord from 20.88 inches to 24.25 inches. The 20° anhedral swept tip is initiated at blade radius (r/R) value of 96 percent. A detailed description of the WCB is provided in Chapter II.

WCB performance characteristics used to modify the GenHel® models were determined through a combination of wind tunnel testing and theoretical analysis. Lift and drag maps for the new blades were empirically derived and dynamic stall characteristics were approximated using theory.

The new WCB GenHel® mathematical models were used to predict structural and handling qualities design parameters. The majority of the GenHel® predictive analysis was focused on quantifying the increase in performance derived from the improved

blades. Specifically, determining if the increased aerodynamic performance of the WCB would expand the aerodynamic envelope of the BLACK HAWK beyond the current structural envelope. Flight testing of the new blade's performance on the UH-60 commenced in March of 1999.

The WCB flight test data used in this analysis was collected during 95 flight hours from 18 Mar 99 through 23 Jul 99 at Sikorsky's West Palm Beach Flight Test Center. This report seeks to validate the predictive use of GenHel® derived design parameters through correlation with measured flight test data recorded during the UH-60L Wide Chord Blade test program and identify any areas where improvements could be applied. Validation of the WCB GenHel® models serves two purposes. First, it confirms the ability of GenHel® to model the flight dynamic response of the UH-60L with the WCB modification. Second, it confirms the predictive loads forwarded to the structural engineers during the design phase of the WCB.

The report begins with a background discussion of the WCB, an overview of GenHel®, and a description of the correlation techniques, procedures and parameters. Chapter III defines the two GenHel® models currently used at Sikorsky to model the WCB. Chapter IV contains the trim flight correlation of these two models and Chapter V contains dynamic maneuver correlations. After thorough correlation of the two current models, the models were modified in an effort to gain a better understanding of the downwash and interference effects of the new rotor system. Chapter VI first describes the modifications, and then correlates the modified model with both trim and dynamic test flight data. Finally, conclusions are drawn and recommendations for future correlation efforts are made.

II. BACKGROUND

A. DESCRIPTION OF THE WIDE CHORD BLADE MODIFICATION

The Wide Chord Blade modification was born out of a desire to meet customer demands for improved performance and increased component life in a cost-efficient manner. Figure 1 presents a schematic of the WCB. The WCB incorporates a

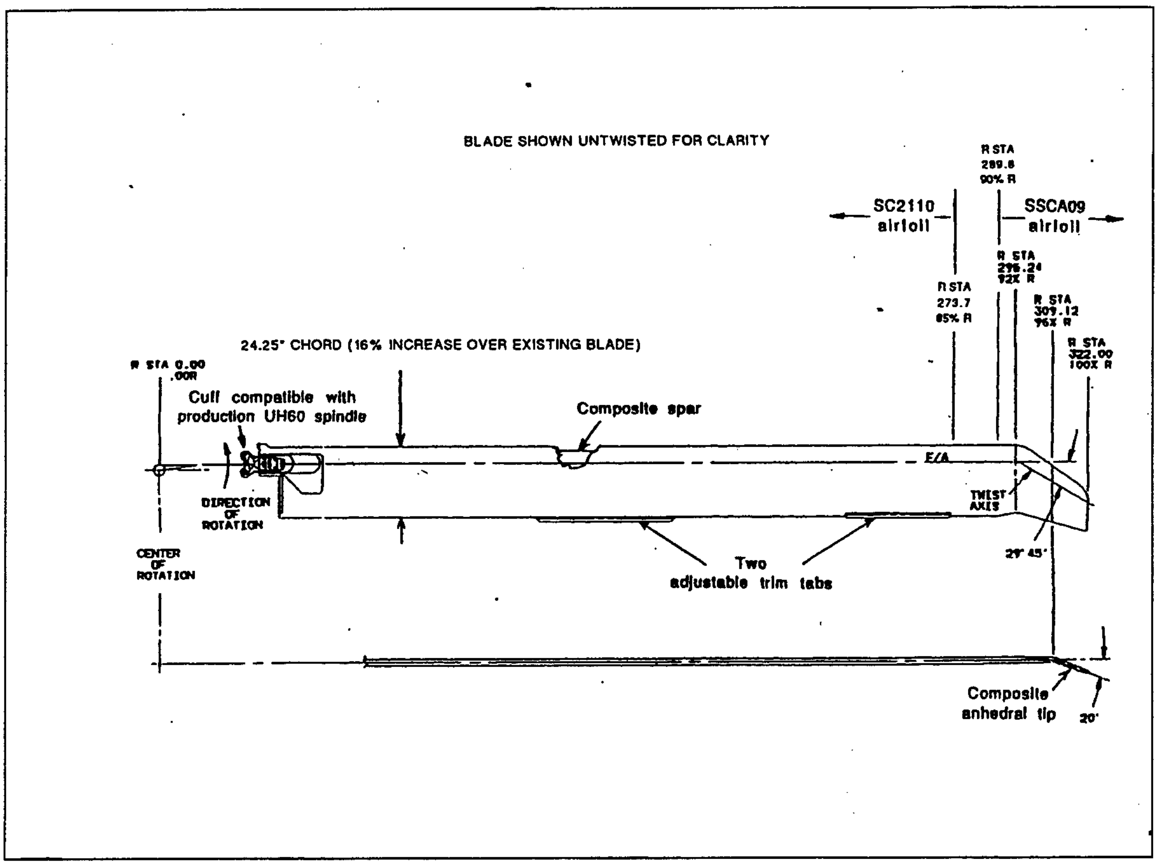

Figure 1 Wide Chord Blade Schematic [From Ref. 2]

wider chord blade, advanced airfoil, and anhedral tip. Advantages of the composite WCB include increased service life, improved damage tolerance, improved crack propagation properties, elimination of BIM requirements, reduced tip corrosion, and

reduced production costs for material and labor [Ref. 2]. An aerodynamic comparison between the standard UH-60 rotor blade and the WCB is presented below in Table 1.

Table 1 Aerodynamic Comparison of Rotor Blades [From Ref. 2]

	Standard H-60 Blade	Wide Chord Blade
Blade		
Chord (16% increase)	20.88 in.	24.25 in.
Solidity(10% increase)	0.0826	0.0909
Twist	-18° equivalent	-18° equivalent
Tip		
Anhedral	0°	20° outer 4% radius
Sweep @ .25 chord	20° outer 7% radius	29.75° outer 8% radius
Taper	none	1:0.6 outer 8% radius
Airfoil Section	SC1095	SSC-A09

B. OVERVIEW OF GENHEL®

The GenHel® mathematical model is a total force, non-linear, large angle representation with six rigid-body degrees of freedom. The main rotor model is based on a blade element analysis which develops total rotor forces and moments from a combination of aerodynamic, mass, and inertial loads acting on the simulated blade. The model allows for rotor system modeling of rigid blades with flap, lag and rotor speed degrees of freedom. For analysis purposes, the rotor system is divided into equal annular areas. By doing so, computational effort is weighted towards areas of higher dynamic pressures and computation time is minimized. [Ref. 3]

The program is composed of modules that can be modified to create an aircraft specific model. Figure 2 illustrates the modular architecture of GenHel®.

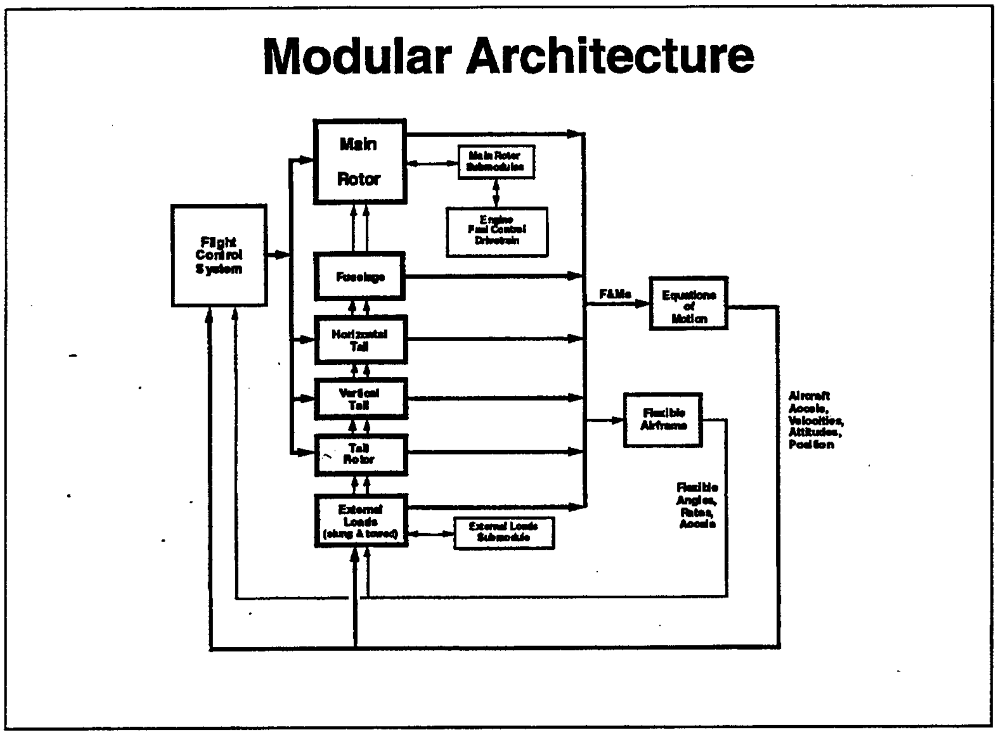

Figure 2 Illustration of GenHel® Modular Architecture [From Ref. 4]

Modules are modified by changing their geometric, mass and aerodynamic properties to reflect those of the desired aircraft. The program is capable of modeling a vast array of helicopter dynamics and complex interactions. Downwash, sidewash and interference effects are derived at each module via theoretical and empirical methods. In addition to the downwash values calculated at each panel, fuselage downwash correction terms are added as a side force, rolling moment and pitching moment (Y,L, and M). Their values are empirically derived from BLACK HAWK and Seahawk flight test data and are applied at the center of gravity (CG) as functions of sideslip (β). The wide-ranging capabilities of GenHel® are evidenced in Figure 3.

GenHel® works by calculating and summing the forces and moments of each module at each time step and passing these values to the equations of motion module. The equations of motion module calculates accelerations by dividing the applied forces and moments by the airframe weights and inertias.

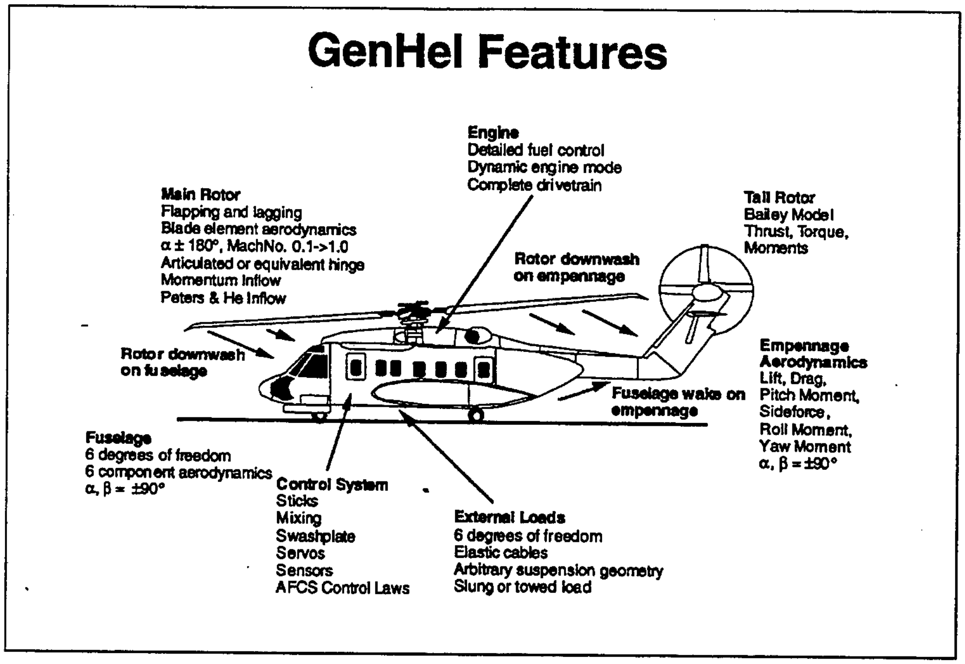

Figure 3 GenHel® Capabilities [From Ref. 4]

Accelerations are then integrated to obtain the velocities, angular rates, positions and attitudes. Earth axis reference values are obtained using Euler transformations.

Maneuvers are simulated with GenHel® in two steps. The first step is to establish trim flight conditions at the desired initial conditions. Adjustable trimmers allow the user to specify the desired method to drive the aircraft's linear and angular accelerations to zero. Once trim flight is established, control inputs are introduced which produce the desired maneuver. Both trim and dynamic output data is recorded in the computer for follow-on analysis.

C. CORRELATION DESCRIPTION

This section describes the aircraft configurations used, the GenHel® models used, the test flight data acquisition procedures, the parameters used, and the correlation procedure used in this report.

1. Aircraft Configurations

Limited flight test data restricted the correlation to the two aircraft configurations described in Table 2.

Table 2 Aircraft Configurations

Configuration One	Gross Weight (GW) Center of Gravity (FSCG) Density Altitude	16825 pounds 364 inches 3000 feet
Configuration Two	Gross Weight (GW) Center of Gravity (FSCG) Density Altitude	22000 pounds 360 inches 3000 feet

These two configurations are the aft center of gravity limits for the non-ESSS aircraft at their respective weights [Ref. 5]. At each flight condition, level trim, trim turns, and dynamic maneuvers are examined.

2. GenHel® Models

The three analytical models examined in this report are the Handling Qualities model (HQ model), the Maneuver Loads model (ML model) and the Modified Maneuver Loads model (Mod ML model). Chapter III describes the HQ and ML models. In Chapter IV, the HQ and ML models are correlated to trim test flight data. In Chapter V, the HQ and ML models are correlated to dynamic test flight data. After thorough correlation of the HQ and ML models, the ML model was modified in an effort to gain a better understanding of the downwash and interference effects of the new rotor system. Chapter VI first describes the modifications, and then correlates the Mod ML model with both trim and dynamic test flight data.

3. Test Flight Data Acquisition

Flight tests were conducted in UH-60L Serial Number 84-23953 with a clean aircraft. Flights 744, 747, 793, and 795 of the H-60 Growth Rotor Test Plan were used for correlation. Flights 744 and 747 were conducted at GW 16825 , FSCG 364 , and 3000 ft DA, and flights 793 and 795 were conducted at GW 22000, FSCG 360, 3000 ft DA. Table 3 summarizes the use of test flight data. All data was recorded as a raw data

file on the computer system in West Palm Beach. Data was manipulated for analysis using ADAPS2 computer software.

Table 3 Summary of Test Flight Data Usage

	Configuration One GW 16825, FSCG 364, 3000 ft DA	Configuration Two GW 22000, FSCG 360, 3000 ft DA
Trim, Level	Flight 744 Runs 24-30	Flight 793 Runs 32-37
Trim, Fixed Coll Turn	Flight 747 Runs 33-35, 36-39	No Test Data Available
Dynamic Maneuvers	Flight 747 Runs 43 ,51 ,55, 58, 61, 64, 67	Flight 795 Runs 42, 48, 49, 83, 86, 89, 92

a. Configuration One: GW 16825, FSCG 364, 3000 ft DA.

Trim, level flight, test data was obtained from flight 744, run numbers 24-30. Trim, fixed collective, turning flight, test data was obtained from flight 747 run numbers 33-35 and 36-39. Dynamic maneuver test data was obtained from flight 747, runs 43, 51, 55, 58, 61, 64 and 67.

b. GW 22000, FSCG 360, 3000 ft DA.

Trim, level flight, test data was obtained from flight 793 run numbers 32-37. Dynamic maneuver test data was obtained from flight 795 run numbers 42, 48, 49, 83, 86, 89, and 92.

4. Correlation Parameters

The following parameters are correlated for trim flight: stick positions, aircraft attitudes, stabilator bending, main rotor shaft bending, and main rotor torque. For dynamic maneuvers, the correlation parameters are: stick positions, SAS output positions, aircraft attitude, aircraft rates, and aircraft accelerations. Table 4 shows all of

the correlation parameters, their units, and their corresponding GenHel® and ADAPS2 mneumonics. For consistency, all stick positions are depicted in percentage (%), all angles are in degrees (deg) and all hub moments are in foot-pound (ft-lb) and all stabilator bending moments are in inch-pounds (in-lb).

Table 4 Correlation Parameters

Parameter	GenHel			ADAPS2		
	Mnemonic	Units	Notes	Mnemonic	Units	Notes
Input Parameters						
RUN NUMBER				RUNNO:D:RUN		
GROSS WEIGHT	WEIGHT	lbs		W:D:1X	lb	
LONGITUDINAL CENTER OF GRAVITY	FSCG	in		CG:D:1X	in	
PRESSURE ALTITUDE	HTRIM	ft		H:D:1X	feet	
DENSITY ALTITUDE	-	-		HD:D:1X	feet	
TRUE AIRSPEED	V	knots		VT:D:1X	knots	
OUTSIDE AIR TEMPERATURE	OAT	deg F		ITATBOOM:D:1X	deg C	convert to deg F
Control Inputs						
LONGITUDINAL CYCLIC DISPLACEMENT	XBPC	%	Full forward = 0	LGSTKP:D:1X	%	10 inches total
LATERAL CYCLIC DISPLACEMENT	XAPC	%	Full left = 0	LATSTKP:D:1X	%	10 inches total
COLLECTIVE DISPLACEMENT	XCPC	%	Full down = 0	COLLSTKP:D:1X	%	10 inches total
PEDAL DISPLACEMENT	XPPC	%	Full left = 0	PEDP:D:1X	%	5.38 inches total
STABILATOR INCIDENCE ANGLE	IP1,IP2	deg	Panel 1=Panel 2	STABLAIC:D:1X	deg	
LONGITUDINAL SAS ACTUATOR OUTPUT POS	XBILS	in	5%-a+ 5%-d = 1in total	LGSASOP:D:1X	%	convert to inches
LATERAL SAS ACTUATOR OUTPUT POSITION	XAILS	in	5%-a+ 5%-d = 1in total	LATSASOP:D:1X	%	convert to inches
YAW SAS ACTUATOR OUTPUT POSITION	XPILS	in	5%-a+ 5%-d = .538 in total	YAWSASOP:D:1X	%	convert to inches
States						
ROLL ATTTIUDE	PHIB	deg		ROLLATT:D:1X	deg	
PITCH ATTITUDE	THETAB	deg		PITCHATT:D:1X	deg	
YAW ATTITUDE	PSIB	deg		HEADING:D:1X	deg	
ROLL RATE	PDEG	deg/s		ROLLRAT:D:1X	deg/s	
PITCH RATE	QDEG	deg/s		PITCHRAT:D:1X	deg/s	
YAW RATE	RDEG	deg/s		YAWRAT:D:1X	deg/s	
ROLL ACCELERATION	PDOT	rad/s2	convert to deg/s2	ROLLACC:D:1X	deg/s2	
PITCH ACCELERATION	QDOT	rad/s2	convert to deg/s2	PITCHACC:D:1X	deg/s2	
YAW ACCELERATION	RDOT	rad/s2	convert to deg/s2	YAWACC:D:1X	deg/s2	
AIRCRAFT SIDESLIP	BETFRE	deg		SIDESLIP:D:1X	deg	
AIRCRAFT ANGLE OF ATTACK	ALFREE	deg		ATTACK	deg	
Loads						
MR SHAFT SPEED	OMGMR	rad/s		NRRPM	RPM	convert to rad/s
MR SHP	HPMR	hp		HPMR:D:1X	hp	
MR SHAFT TORQUE	QHBMR	ft-lb	Filtered,ref to shaft axis	MRSEQ1:D:1X	ft-lb	
MR MAST LAT BENDING	LHBMR	ft-lb	Filtered,ref to shaft axis	MRSEBL1:A:1U	in-lb	First Harmonic In-Plane Bending
MR MAST LONG BENDING	MHBMR	ft-lb	Filtered,ref to shaft axis			
MR THRUST	THBMR	lb		MRSAXLD:D:1X	lb	
RIGHT HORIZONTAL STAB LIFT	ZP1	lb	Link to bending moment	-	-	
RIGHT HORIZONTAL STAB FLAT BEND	-	-		STBNBM1R:S:1M	in-lb	
LEFT HORIZONTAL STAB LIFT	ZP2	lb	Link to bending moment	-	-	
LEFT HORIZONTAL STAB FLAT BEND				STBNBM1L:S:1M	in-lb	

Manipulation of the data was required in two instances where GenHel® output and test flight data were not in direct correlation. The first case was the main rotor shaft bending moment and the second case was the stabilator bending moment.

a. Main Rotor Shaft Bending

In-plane main rotor shaft bending (MRSEBL1) is measured during flight test by a bending bridge on the main rotor shaft extension in the shaft axis system.

Harmonic analysis reveals the amplitude of the first harmonic bending moment (MRSEBL1:A:1U) which is used for correlation. GenHel® outputs main rotor force and moments at the center of rotation. Figure 4 illustrates the shaft axis system and the location of the hub forces and moments.

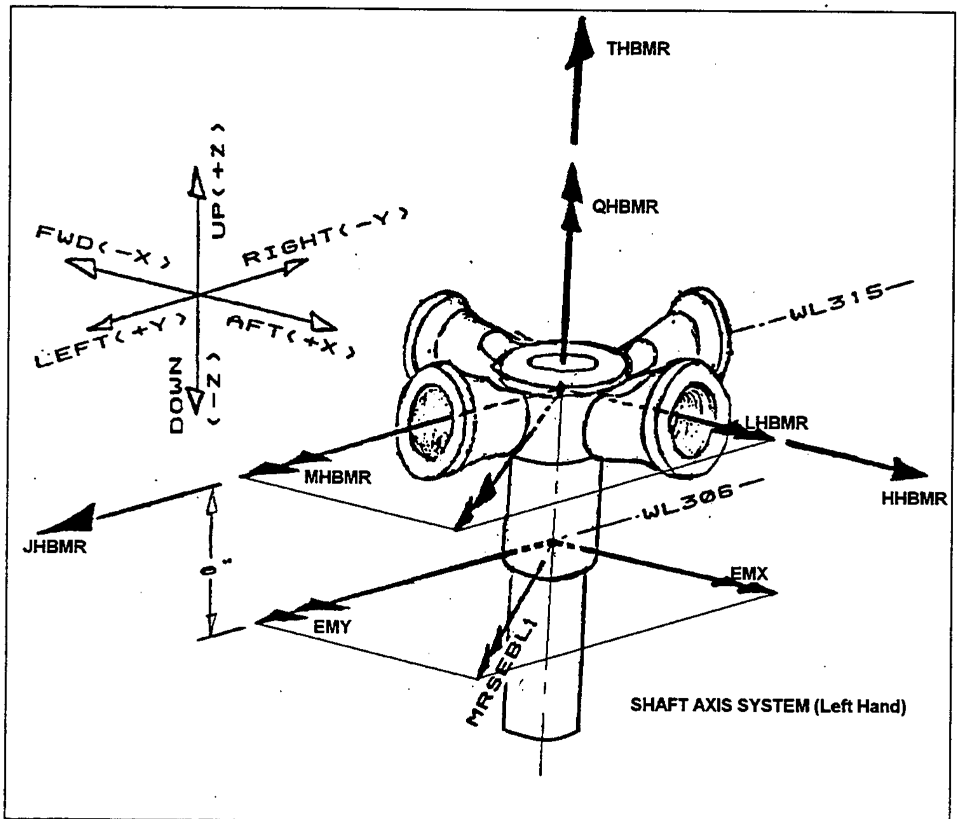

Figure 4 Shaft Axis System and Hub Moment Definition

The filtered in-plane forces and moments computed by GenHel® at the center of rotation (HHBMR, JHBMR, LHBMR, MHBMR) are replaced by equivalent bending moments at the shaft extender (EMY, EMX).

$$EMX = LHBMR - JHBMR(e) \qquad \text{Eqn. (1)}$$

$$EMY = MHBMR + HHBMR(e) \qquad \text{Eqn. (2)}$$

$$\text{In-Plane Bending} = (EMX^2 + EMY^2)^{.5} \qquad \text{Eqn. (3)}$$

Equation 3 is used to determine the GenHel® in-plane bending value for correlation.

b. *Stabilator Flatwise Bending*

Similar to the main rotor shaft bending moment, the bending moment on the stabilator is not directly output by GenHel®. GenHel® calculates point loads for the left and right stabilator panels in body axis coordinates. Stabilator bending is measured during flight test with bending bridges (STBNBM1R and STBNBM1L) located 18.1 inches from the aircraft centerline on both the left and right stabilator wings (stabilator local axes). Bending up is positive.

For correlation, the point loads calculated by GenHel® are transferred to the stabilator local axis (see Figure 5) and are used to derive an equivalent bending moment at the location of the bending bridge (local axes).

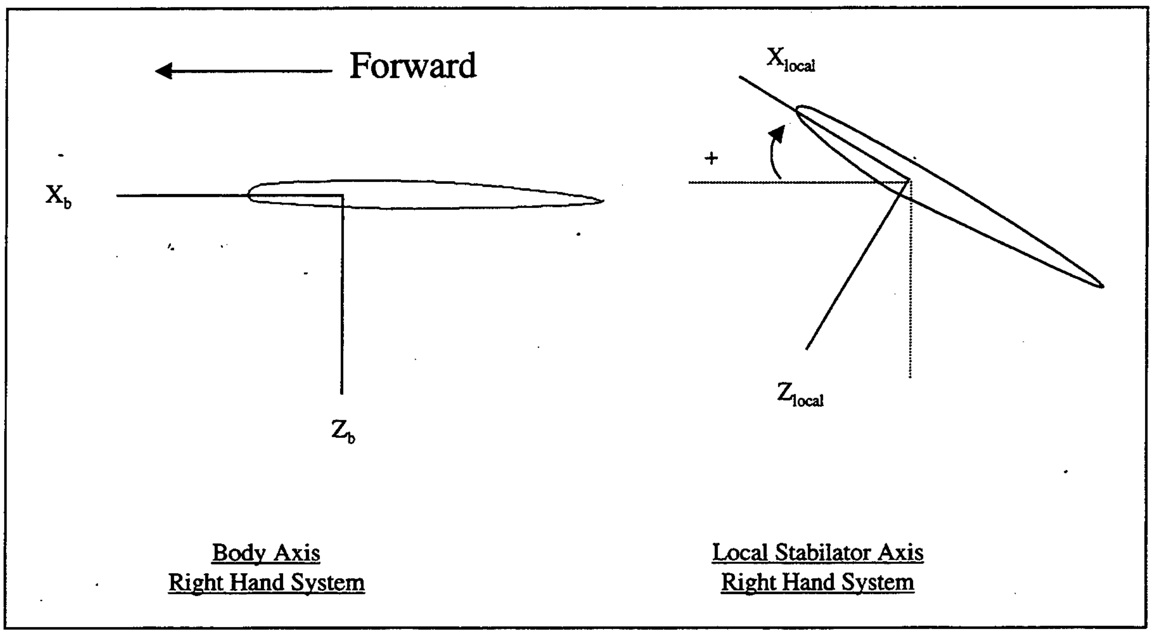

Figure 5 Local Stabilator Axis

The key to deriving the bending moment on the stabilator is an accurate estimation of the spanwise pressure distribution. Accurately predicting this distribution in the turbulent airflow over the stabilator is a difficult task at best. Suprisingly, during the loads survey/envelope expansion program of the SH-60B, it was determined that a uniform distribution provides a good estimate of the spanwise lift for steady, level flight [Ref. 6]. For the purposes of this report their assumption is carried forward. Figure 6

illustrates the procedure employed in order to derive the equivalent bending moment from the GenHel® point load. The point load from GenHel® is translated to the stabilator local axis, distributed evenly across the span, and integrated to determine the shear load distribution. Integration of the shear load distribution provides the bending moment distribution. This simplified method for determining the analytical bending moment does not give due credit to the complexity of the problem, yet it will provide a consistent baseline from which to judge the models' responses.

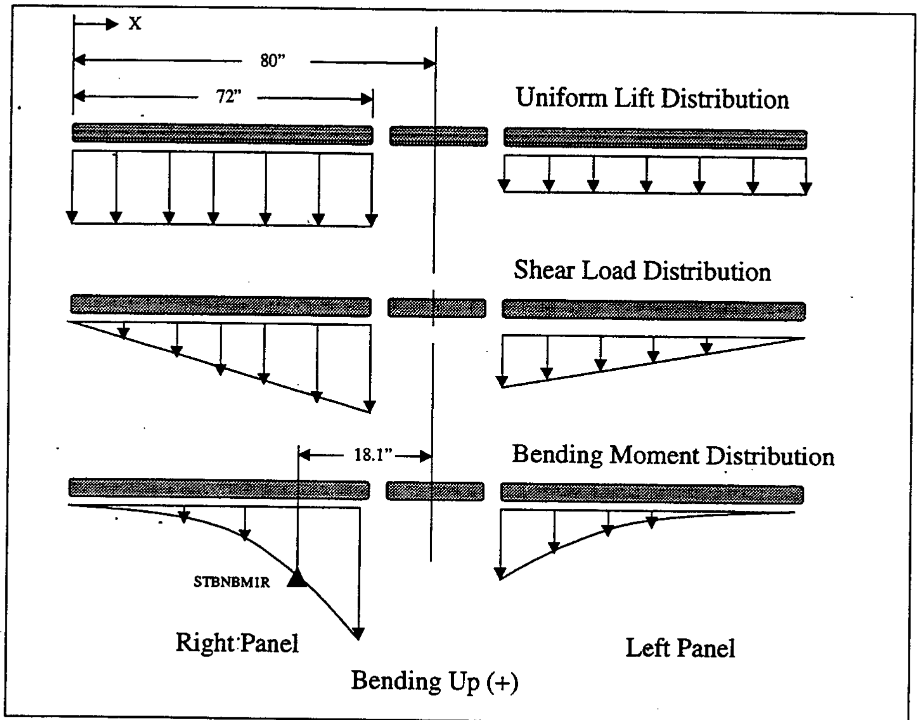

Figure 6 Stabilator Loads Estimation

5. Correlation Procedure

a. Trim Runs

Trim test flight run data was obtained from the Test Flight Center using a data tabulation program in ADAPS2. GenHel® data was obtained for correlation from trim print-outs commanded after the model was established in the desired trim conditions (level flight or collective fixed turn). For level flight, GenHel® was trimmed using pitch

attitude to trim longitudinal acceleration, roll attitude to trim lateral acceleration(>60 knots), collective to trim vertical acceleration, and cyclic and pedals to trim the angular accelerations. Runs were conducted from 40-150 knots in 10 knot increments, 155 knots, and 160 knots. For the collective fixed turns, the yaw rate required to match the flight test angle of bank was determined by Equation 4. Velocity and rate of descent were commanded to match flight test. Runs were conducted in left and right 30°, 45°, and 60° roll angles .

$$\dot{\psi} = \frac{g(\tan\phi)}{V} \qquad \text{Eqn. (4)}$$

The test and analytical data was then transferred to a spreadsheet for further manipulation and graphing. Appendix A contains sample GenHel® command files used to establish trim conditions in the models. Appendix B contains the processed trim flight data for these flights.

b. Dynamic Runs

Dynamic test flight run data was obtained from the Test Flight Center in raw form via the CTDIF function in ADAPS2. All dynamic test flight data was acquired at V_h. For correlation of dynamic maneuvers, the GenHel® model was first established in trim, level flight at the conditions defined in the run log. The maneuver was then commanded in the model by the actual test flight stick inputs using Input B. Inputs were not commanded for the off-axis cylic input. For example, to simulate a longitudinal stick pulse, the lateral cyclic was held constant at trim value, while the test pilot's inputs were commanded in the model for the longitudinal cyclic, collective, and pedal deflections. This precluded the introduction of any off-axis bias due to modeling inaccuracies of the pitch-to-roll or roll-to-pitch coupling. Input A was used concurrently to remove any trim bias which may have existed from trim flight stick positions. The GenHel® output data was then saved in SAVRUN format for further manipulation and graphing in MATLAB®. Appendix A contains sample GenHel® command files used to run dynamic maneuvers.

THIS PAGE INTENTIONALLY LEFT BLANK

III. GENHEL® UH-60L WIDE CHORD BLADE MODEL DESCRIPTIONS

A. HANDLING QUALITIES MODEL

The WCB Handling Qualities (HQ) Model was developed by modifying the standard UH-60L model to reflect the geometric, inertial, and aerodynamic properties of the WCB. The baseline HQ model used in this report has the filename "UH60LWCB". In order to ensure accurate correlation, the model was further modified to reflect the current main and tail rotor rigging of the test aircraft (84-23953). Table 5 presents the main and tail rotor rigging values used in this report. The primary change from the

Table 5 Main and Tail Rotor Rigging Values

Main Rotor Engineering Rig Check – Aircraft 84-23953
Date: 2/25/99
Blade: Black
Engineer: Anne West

Coll Position	Long Position	Lateral Position	Pedal Position	0 Degrees (Tail)	90 Degrees	180 Degrees (Nose)	270 Degrees	Long Control	Lat Control	Coll Control
Pinned	Aft	Pinned	Pinned	11.4	19.2	5.5	-2.7	-11.0	-3.0	8.4
Pinned	Block	Pinned	Pinned	11.2	11.4	5.4	5.2	-3.1	-2.9	8.3
High	Block	Pinned	Pinned	20.1	16.8	12.0	15.2	-0.8	-4.1	16.0
Low	Block	Pinned	Pinned	2.7	6.7	-0.8	-5.2	-6.0	-1.8	0.9
High	Aft	Pinned	Pinned	19.8	26.1	12.2	5.8	-10.2	-3.8	16.0
Low	Forward	Left	Pinned	8.4	-12.7	-7.1	13.7	13.2	-7.8	0.6
Pinned	Block	Pinned	Right	11.4	7.4	5.5	10.0	1.3	-3.0	8.6
Pinned	Block	Pinned	Left	11.3	16.1	5.2	0.0	-8.1	-3.1	8.2
Pinned	Forward	Pinned	Right	10.6	-10.5	5.7	26.9	18.7	-2.5	8.2
Pinned	Aft	Left	Left	16.1	18.8	0.3	-3.1	-11.0	-7.9	8.0
Pinned	Forward	Right	Left	2.0	-5.5	13.8	21.7	13.6	5.9	8.0
High	Aft	Pinned	Left	19.7	26.0	11.7	5.6	-10.2	-4.0	15.8
High	Forward	Pinned	Right	18.1	-1.9	12.6	33.2	17.6	-2.8	15.5
High	Forward	Right	Left	9.3	-1.7	20.9	32.5	17.1	5.8	15.3
High	Aft	Left	Right	23.9	22.1	8.8	10.3	-5.9	-7.6	16.3
Low	Aft	Right	Right	-5.8	9.6	8.6	-7.6	-8.6	7.2	1.2
Low	Aft	Left	Left	8.1	8.8	-7.0	-8.1	-8.5	-7.6	0.5

Tail Rotor Engineering Rig Check – Aircraft 84-23953
Date: 3/9/99
Blade: Blue
Engineer: Anne West

Coll Position	Pedal Position	Blade Angle @ Cuff
Pinned	Left	19.6
Pinned	Right	-11.8
Pinned	Pinned	3.1
Low	Pinned	-3.6
High	Pinned	12.0
High	Left	19.8
High	Right	-2.4
Low	Right	-11.9
Low	Left	11.9

baseline HQ model was the inclusion of 3° of tail rotor bias present on the test aircraft. Appendix A contains sample GenHel® command files used to modify and establish trim conditions with the HQ Model.

B. MANEUVER LOADS MODEL

The HQ model described above is primarily used as a handling qualities tool. The WCB Maneuver Loads (ML) model was created from the HQ model in order to make GenHel® output compatible with software used for structural analysis. To use GenHel® as a tool for predictive analysis of aircraft structural loads, several modifications to the HQ model are required.

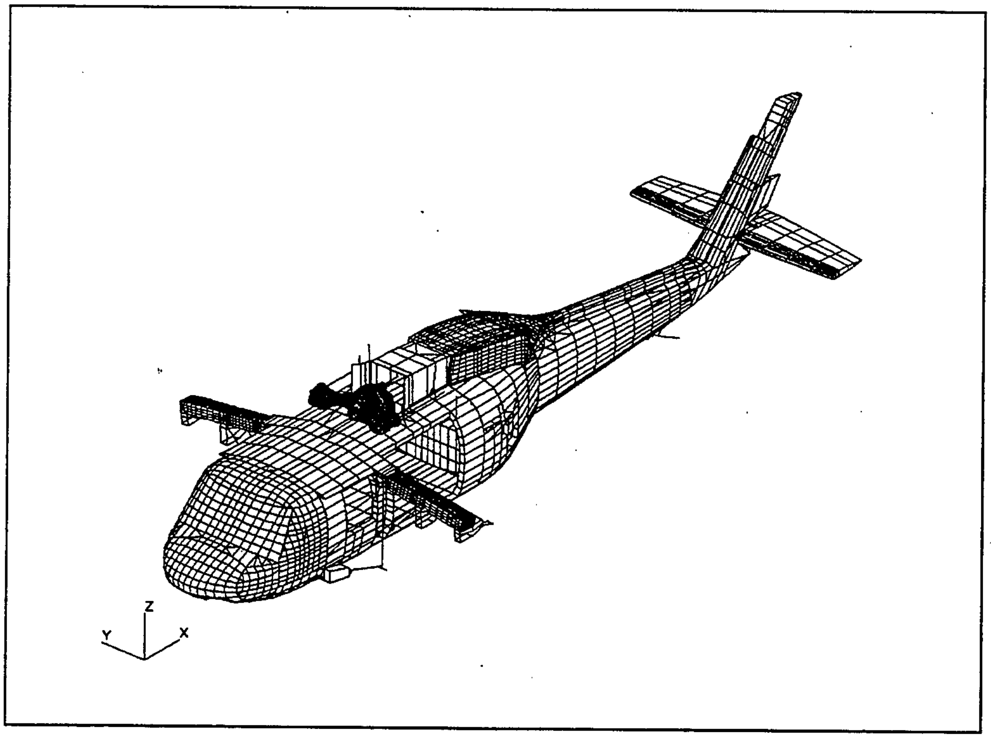

Figure 7 Sikorsky H-60 NASTRAN® Model

The first modification involves the downwash correction terms used in the HQ model. The downwash correction terms derived from BLACK HAWK and Seahawk flight test data (described in Chapter II) were added to the HQ model at the CG. Their

presence at the CG results in an imbalance of forces if applied directly as boundary conditions for NASTRAN® analysis . To remedy this problem, the downwash correction forces and moments (Y, L, and M) are instead added at the fuselage waterline and buttline in the ML model.

Also added to the fuselage waterline and buttline in the ML model are changes in forces in moments (Z,Y,L, and N). These changes account for the differences which exist between unpowered wind tunnel tests (where fuselage aerodynamic data is derived) and powered flight. The changes are based on S-92 powered wind tunnel tests.

Changes were also made to the stabilator and tail rotor modules. The stabilator modules in the HQ model have equal main rotor downwash values on the left and right stabilator panels. In reality, the right stabilator panel would see larger downwash magnitudes than the left panel. The ML model was modified to reflect a more accurate picture of the downwash seen by the stabilator by changing the main rotor interference maps to reflect a greater downwash distribution on the right side of the stabilator. Additionally, tail rotor flapping moments derived from test data are applied at the tail rotor center of rotation and included in the total tail rotor bending moment.

The ML model used in this report has the filename "H60WCBML". Rigging and mass data were confirmed prior to correlation. Appendix A contains sample GenHel® command files used to run dynamic maneuvers with the ML model.

THIS PAGE INTENTIONALLY LEFT BLANK

IV. HQ AND ML MODELS TRIM FLIGHT CORRELATION

A. DISCUSSION

1. Level Flight (Figures 8-17)

For both configurations, all stick positions trend well with no deviations greater than 14%. Longitudinal cyclic is consistently 2% aft of test data and lateral cyclic is consistently 6-7% right of test data. Collective correlates well from 40-100 knots then under predicts (max –14%) from 100-160 knots. Pedal position correlates well from 40-100 knots then diverges to a maximum of 8-9% right of test. The collective and pedal divergence is linked to an under estimation of torque in the same speed regime. Less torque requires less collective which requires less left pedal.

Pitch attitude trends very well and is consistently 2 degrees lower than test data. The yaw and roll attitude are difficult to correlate because of the transition of the trim variables. At airspeeds greater than 120 knots, yaw is within 1 degree of test data.

Stabilator bending is under predicted by both models on the right panel and is under predicted by the ML model on the left panel. The HQ model correlates very well with the left panel bending moment.

Main rotor shaft bending is more accurately predicted by the HQ model. In both configurations, and for both models, the 40-60 knot range is modeled poorly.

2. Turns (Figures 18-22)

Longitudinal cyclic correlates very well in both left and right turns. Both models under predict the amount of left cyclic required to hold left turns and both models over predict the amount of right cyclic to hold right turns. For the pedals, likewise, both models under predict the left pedal required in a left turn and over predict the amount of right pedal to hold a right turn.

Pitch attitude is slightly under predicted in turns as was the case in level flight.

Stabilator bending trends well, however the values are suspect due to our assumption of uniform lift distribution's requirement for level flight. The HQ model correlates well with main rotor shaft bending. The ML model trends well but under predicts bending in both left and right turns.

B. CORRELATION PLOTS

1. Level Flight Trim Plots GW 16825 lb, FSCG 364, 3000 ft DA

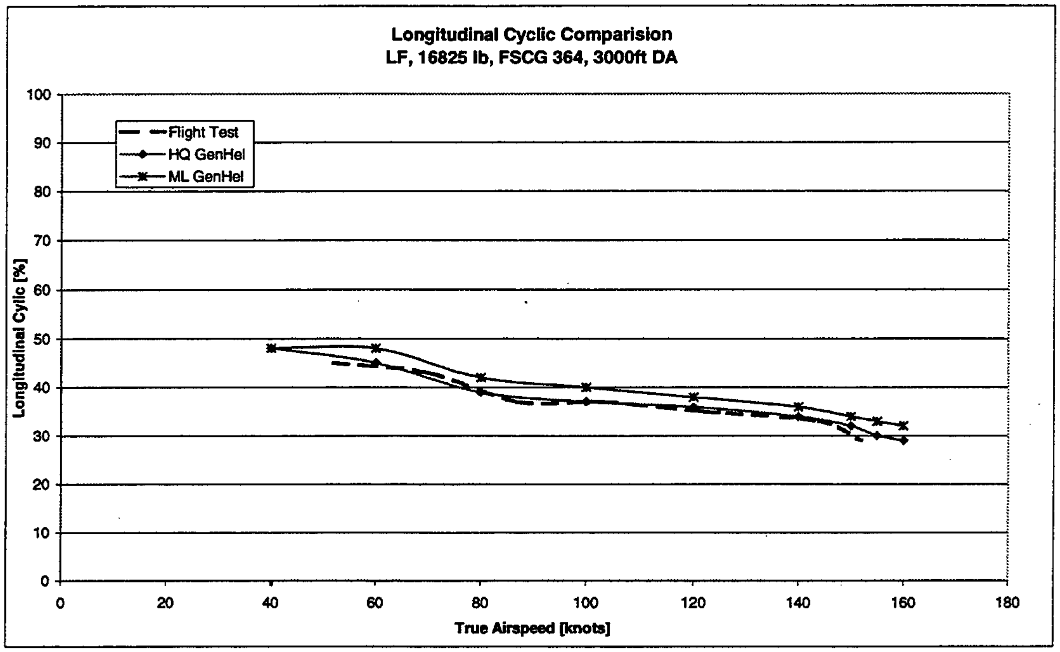

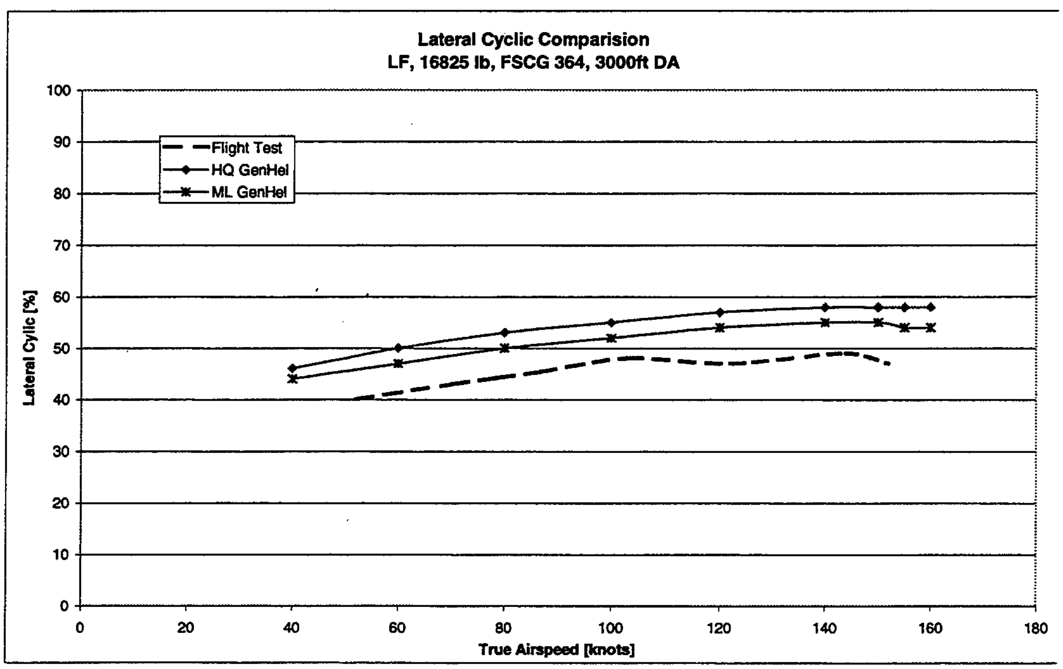

Figure 8 Trim LF Cyclic Comparison 16825 lb, FSCG 364 in, 3000 ft DA

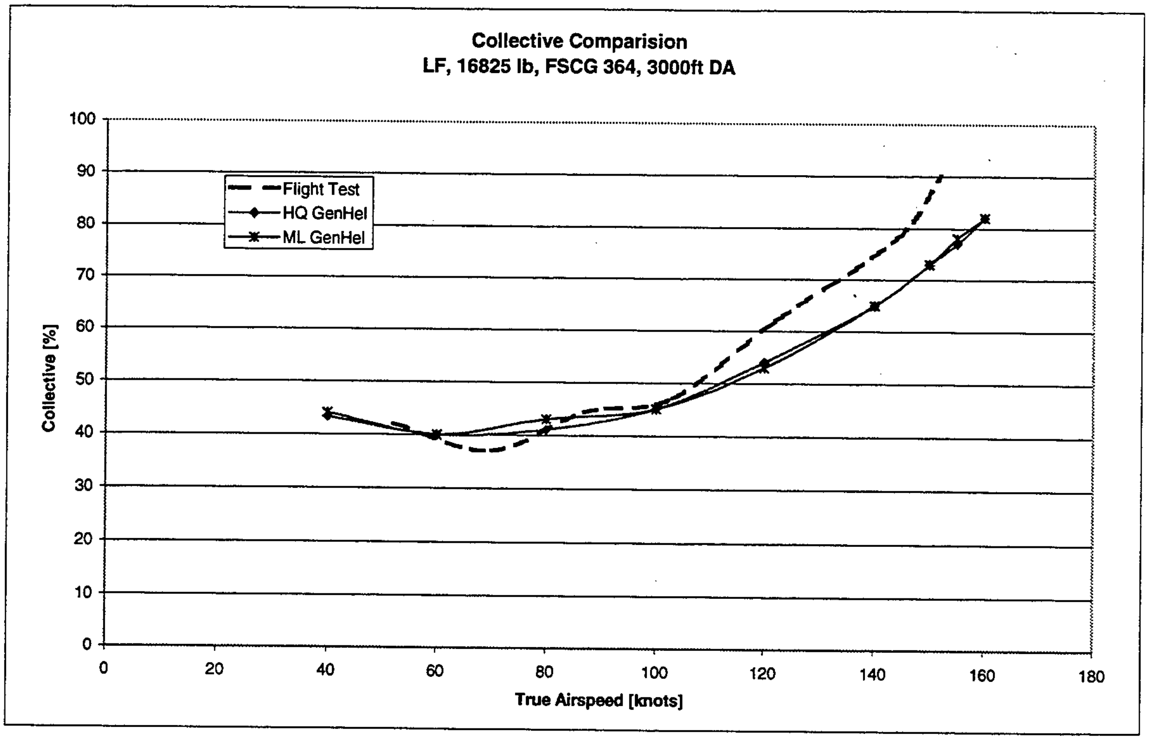

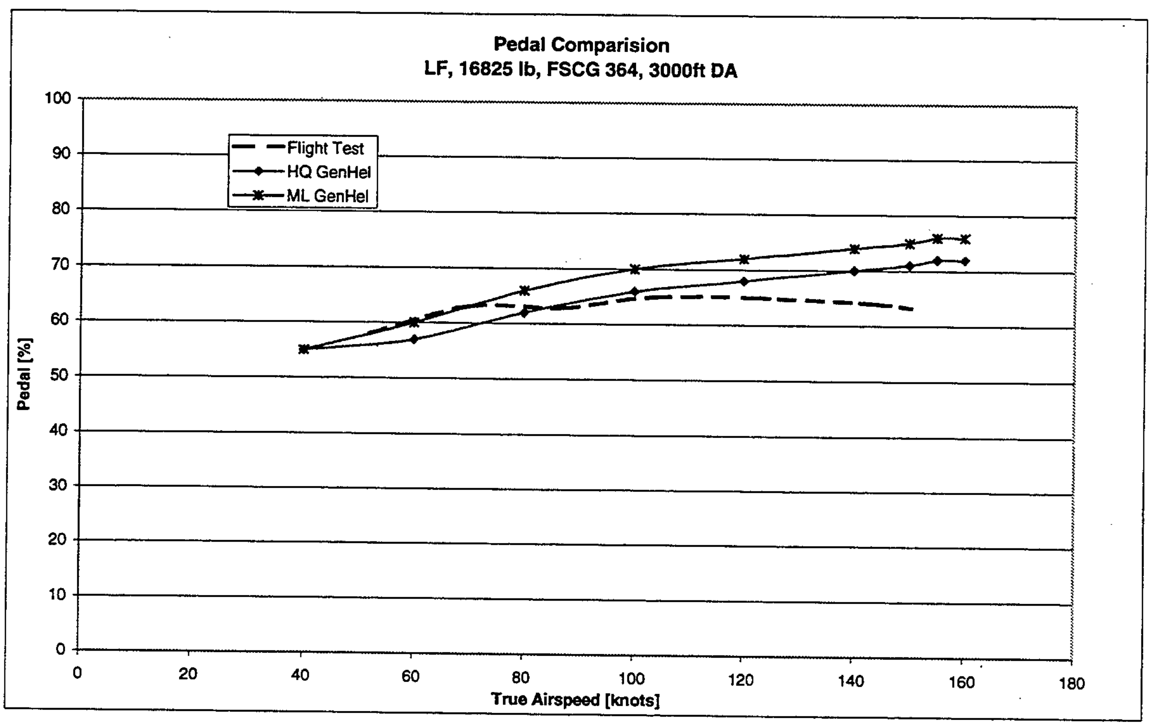

Figure 9 Trim LF Collective and Pedal Comparison 16825 lb, FSCG 364 in, 3000 ft DA

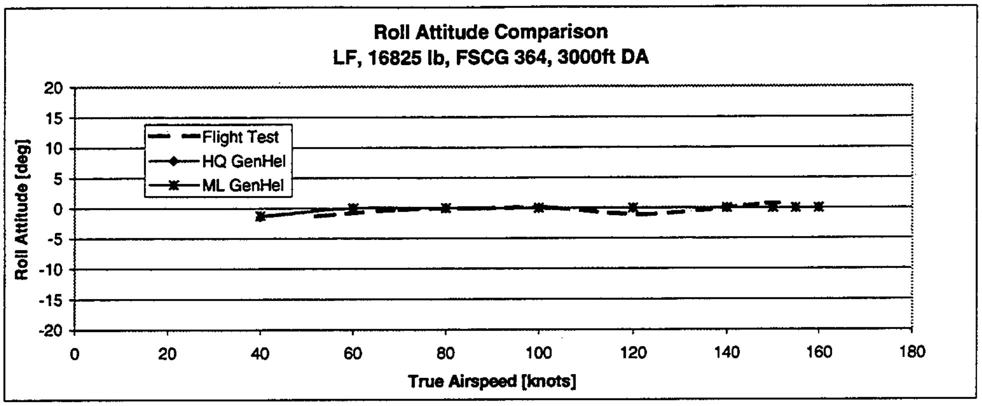

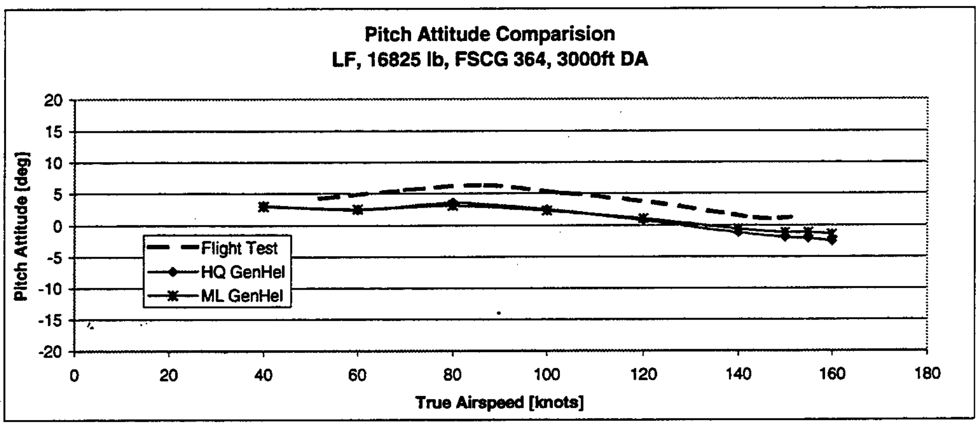

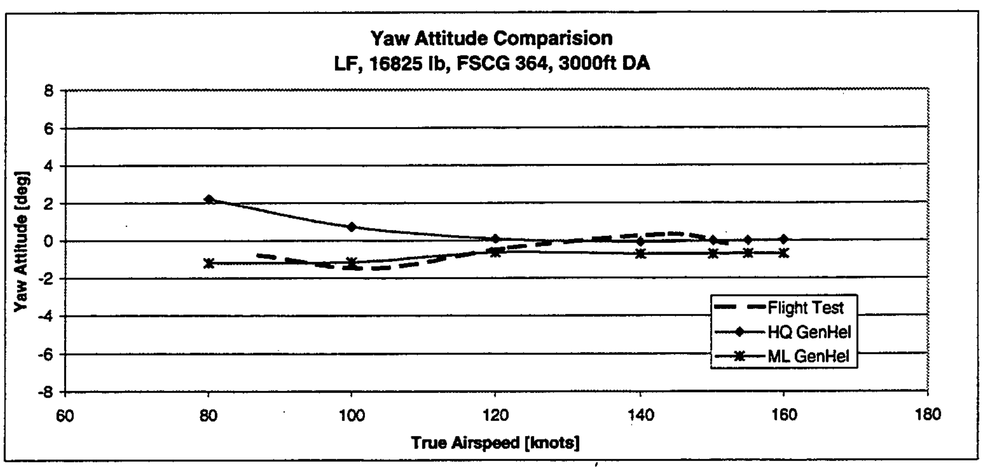

Figure 10 Trim LF Attitude Comparison 16825 lb, FSCG 364 in, 3000 ft DA

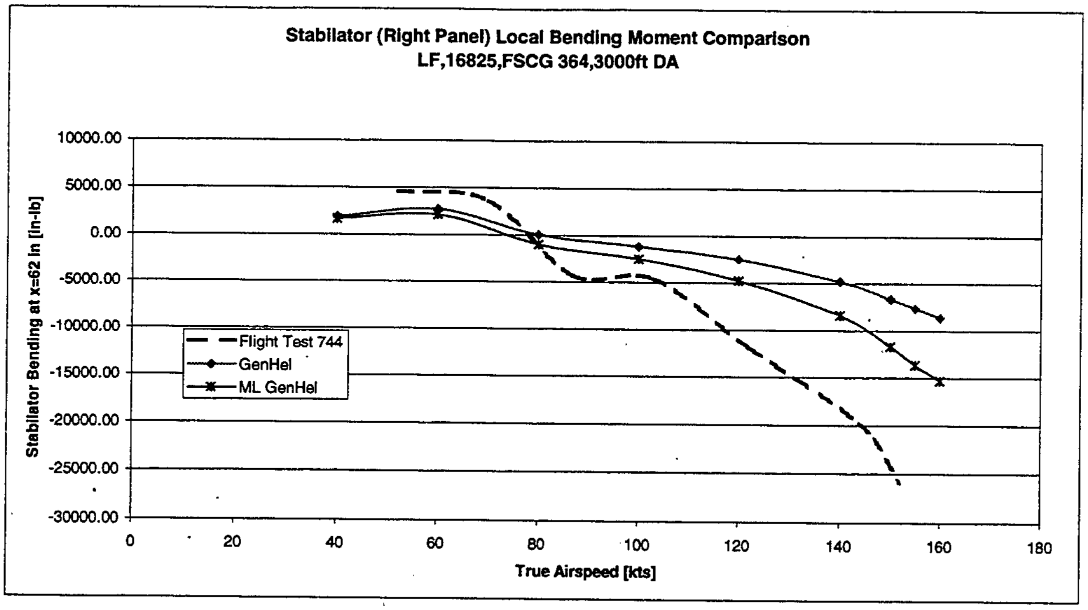

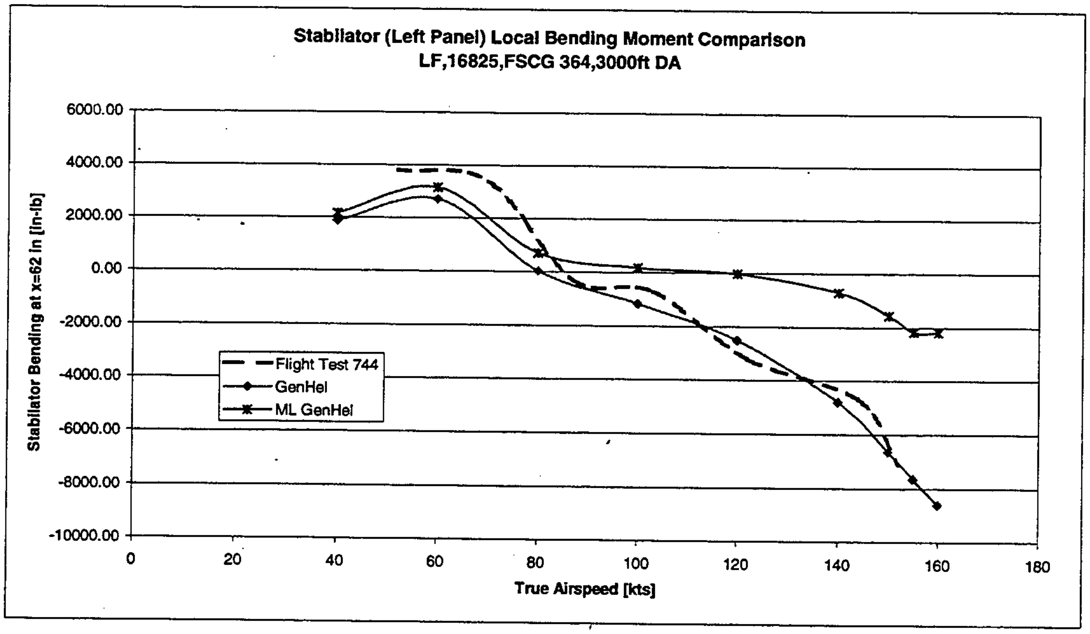

Figure 11 Trim LF Stabilator Bending Comparison 16825 lb, FSCG 364 in, 3000 ft DA

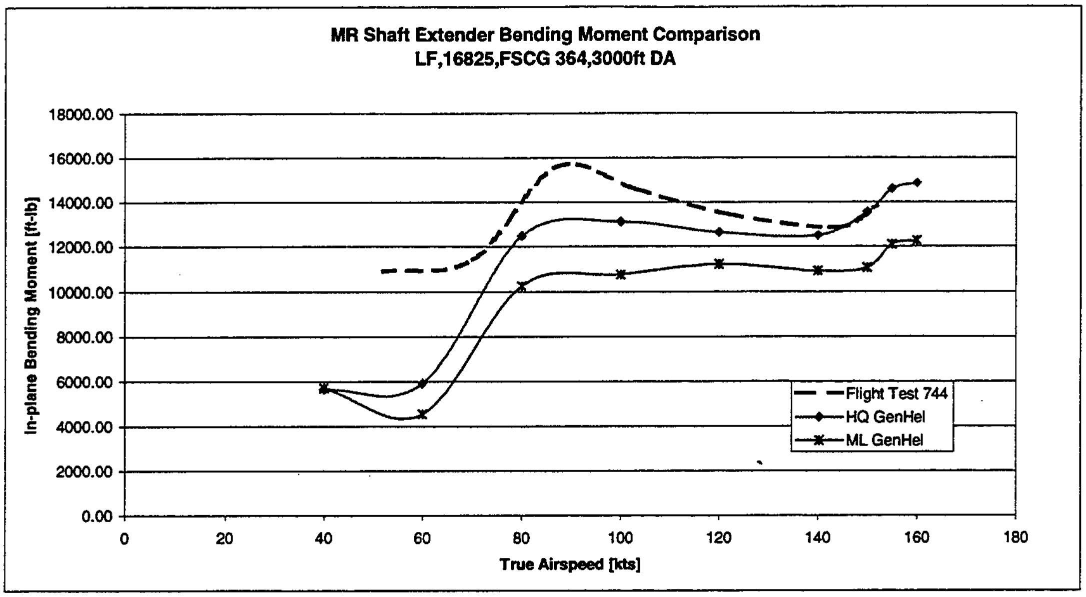

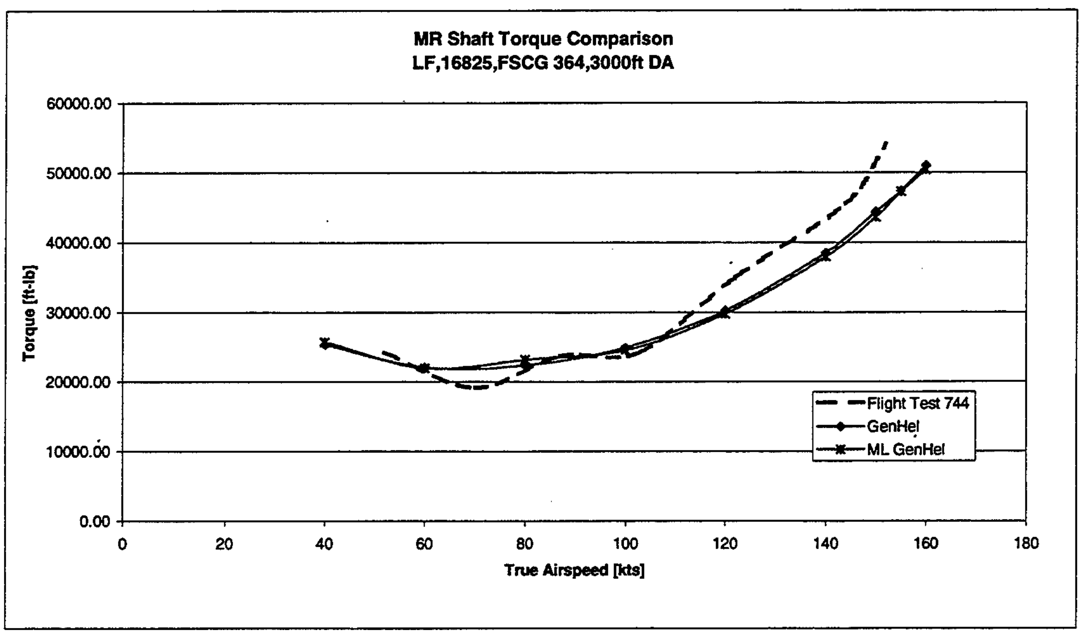

Figure 12 Trim LF MR Shaft Moment Comparison 16825 lb, FSCG 364 in, 3000 ft DA

2. Level Flight Trim Data 22000 lb, FSCG 360, 3000 ft DA

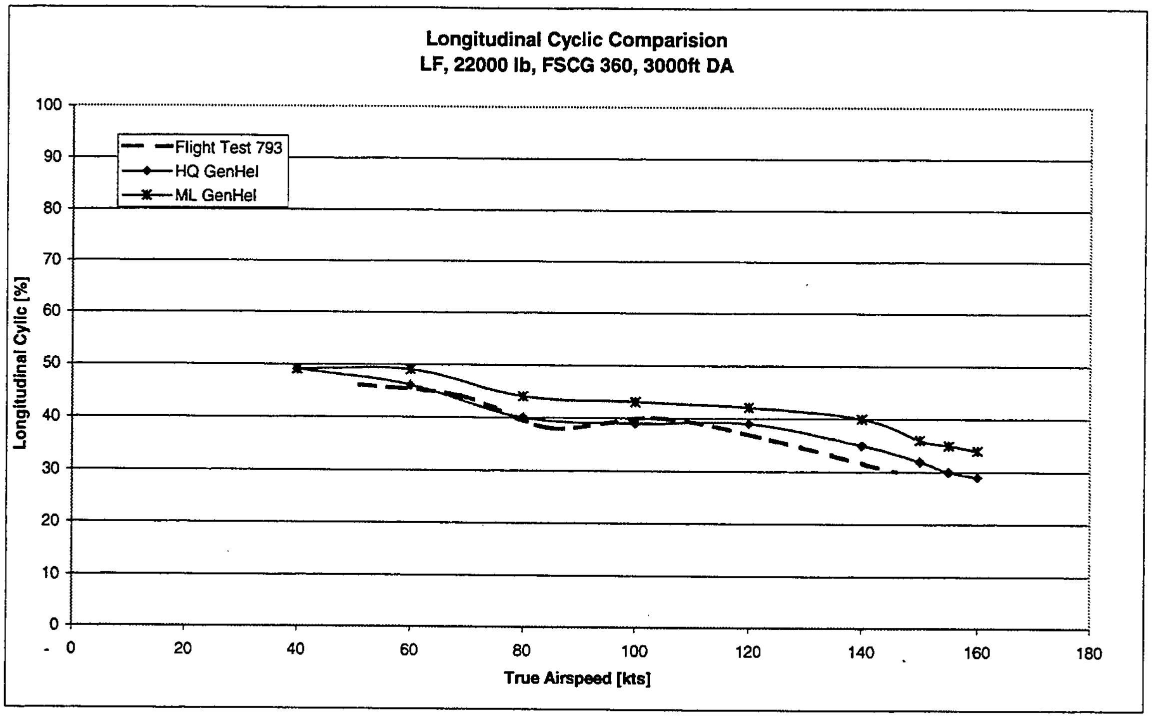

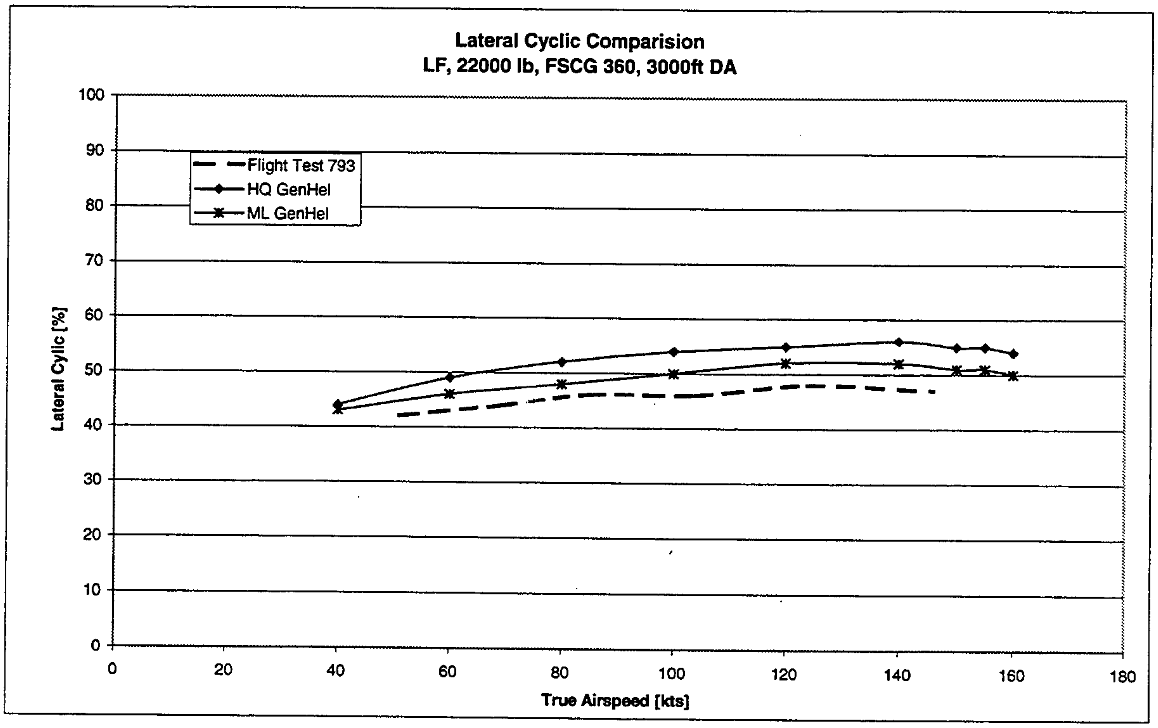

Figure 13 Trim LF Cyclic Comparison 22000 lb, FSCG 360 in, 3000 ft DA

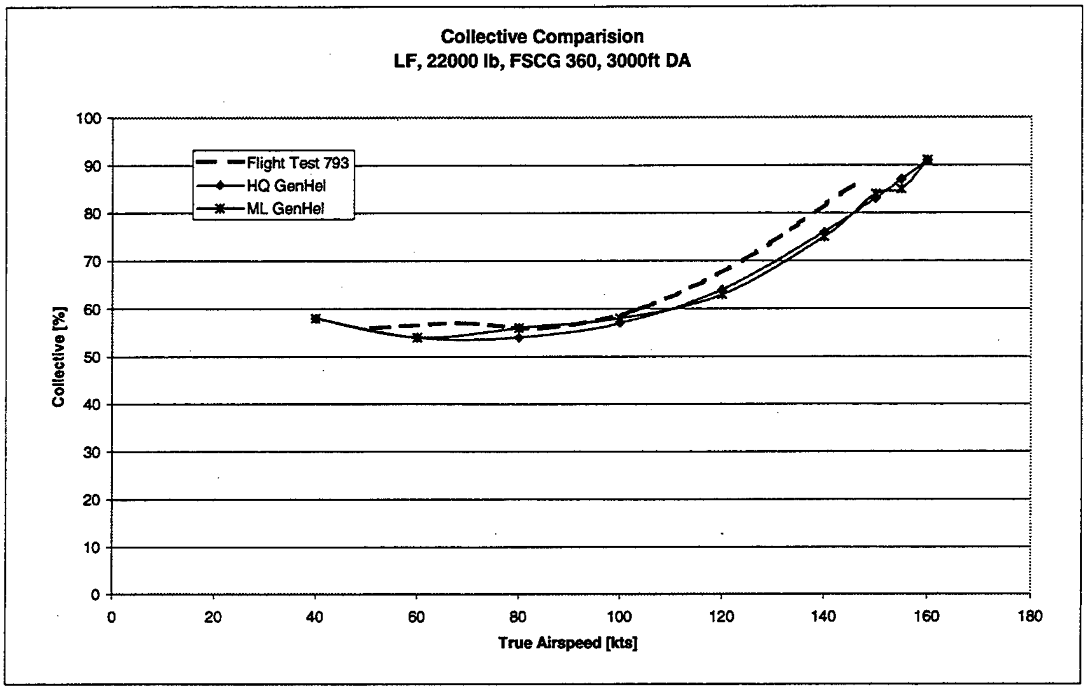

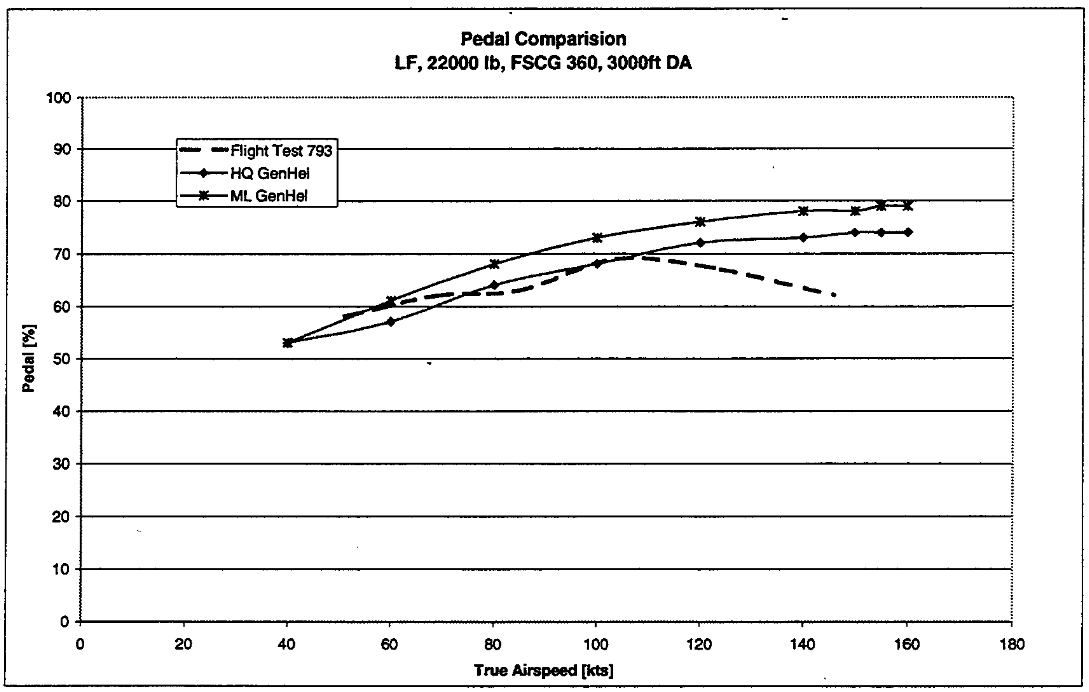

Figure 14 Trim LF Collective and Pedal Comparison 22000 lb, FSCG 360 in, 3000 ft DA

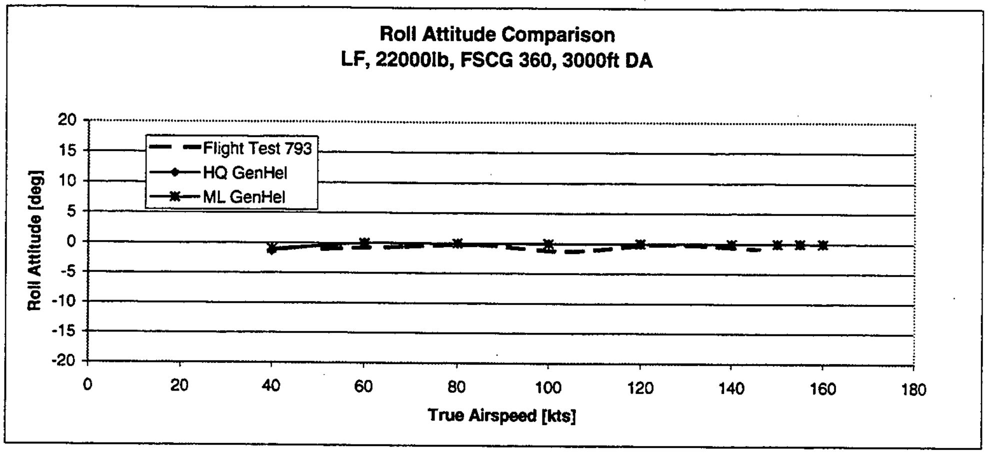

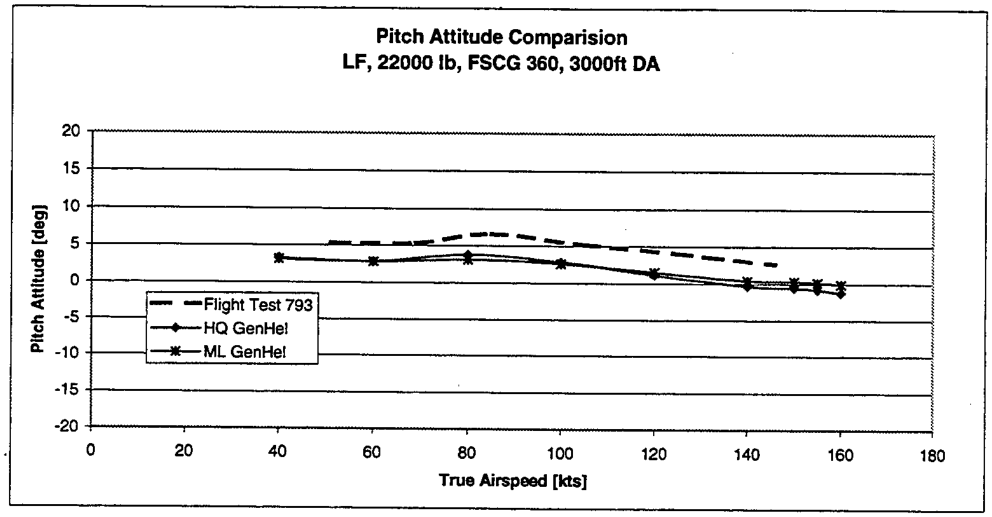

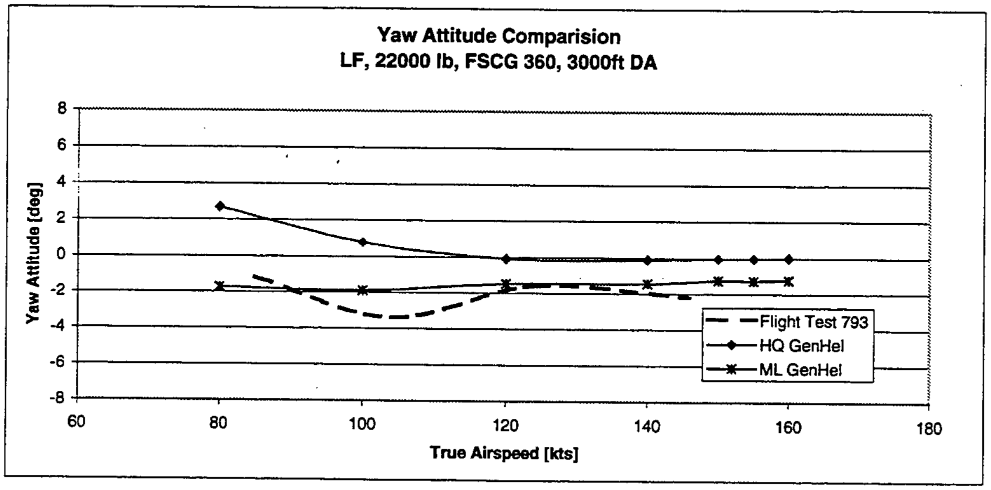

Figure 15 Trim LF Attitude Comparison 22000 lb, FSCG 360 in, 3000 ft DA

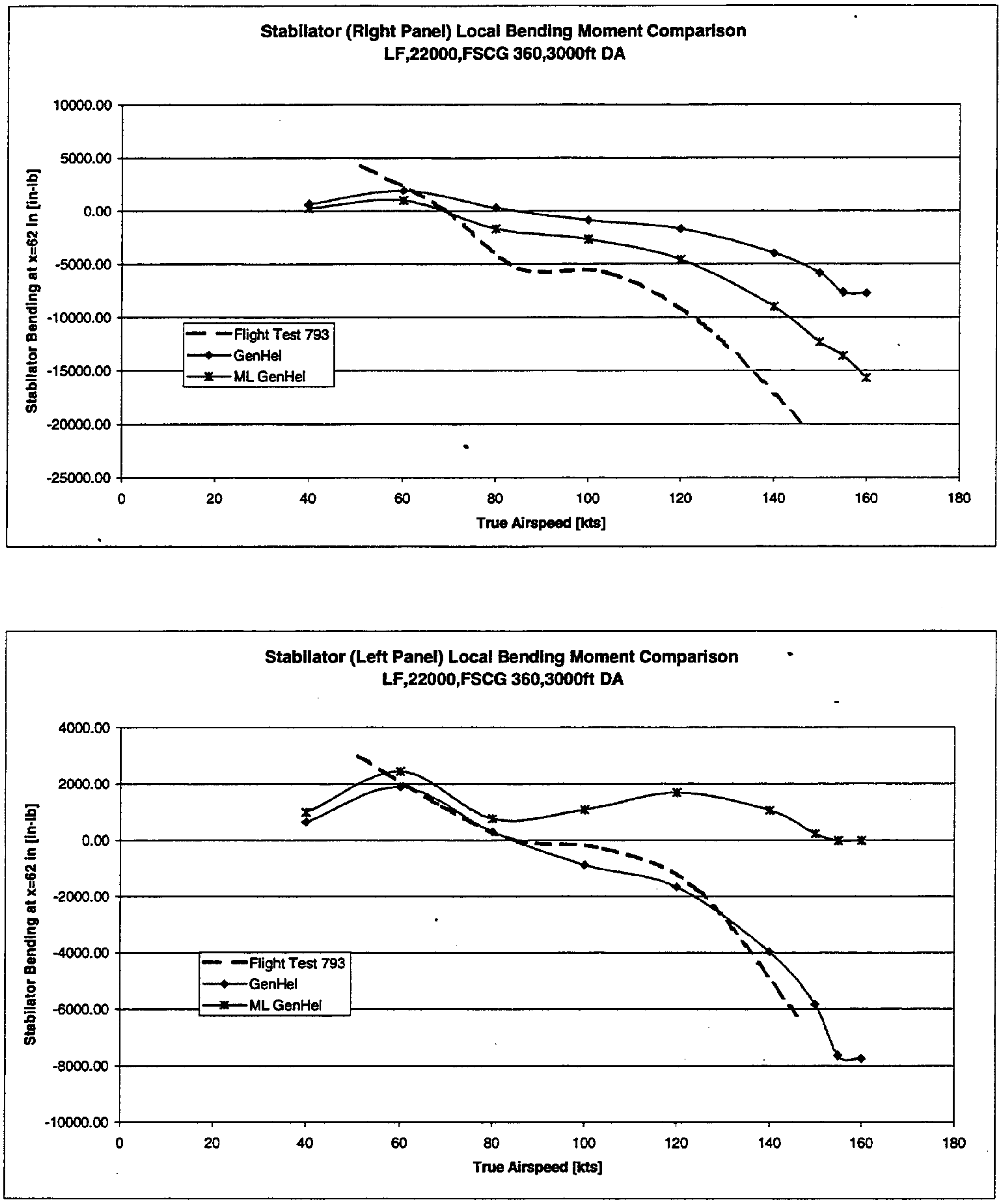

Figure 16 Trim LF Stabilator Bending Comparison 22000 lb, FSCG 360 in, 3000 ft DA

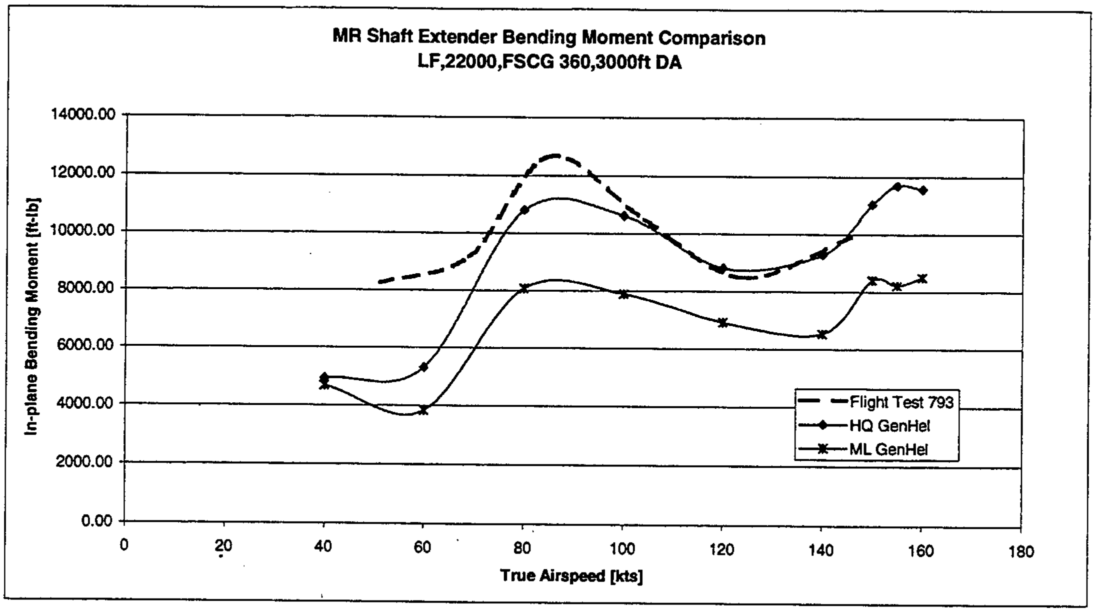

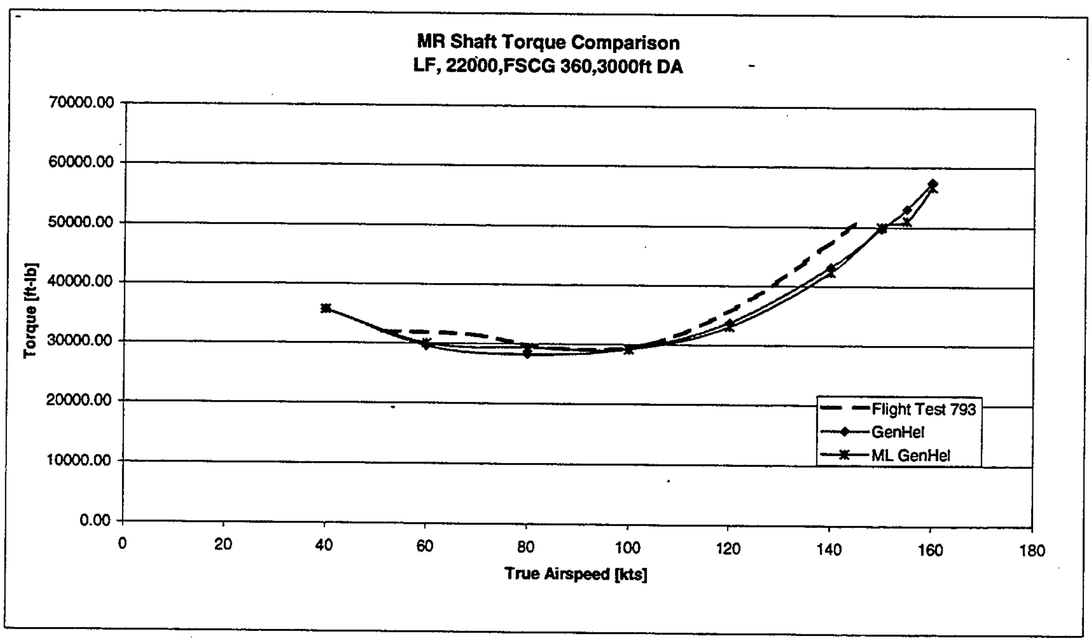

Figure 17 Trim LF MR Shaft Moment Comparison 22000 lb, FSCG 360 in, 3000 ft DA

3. Turning Flight Trim Plots 16825 lb, FSCG 364, 3000 ft DA

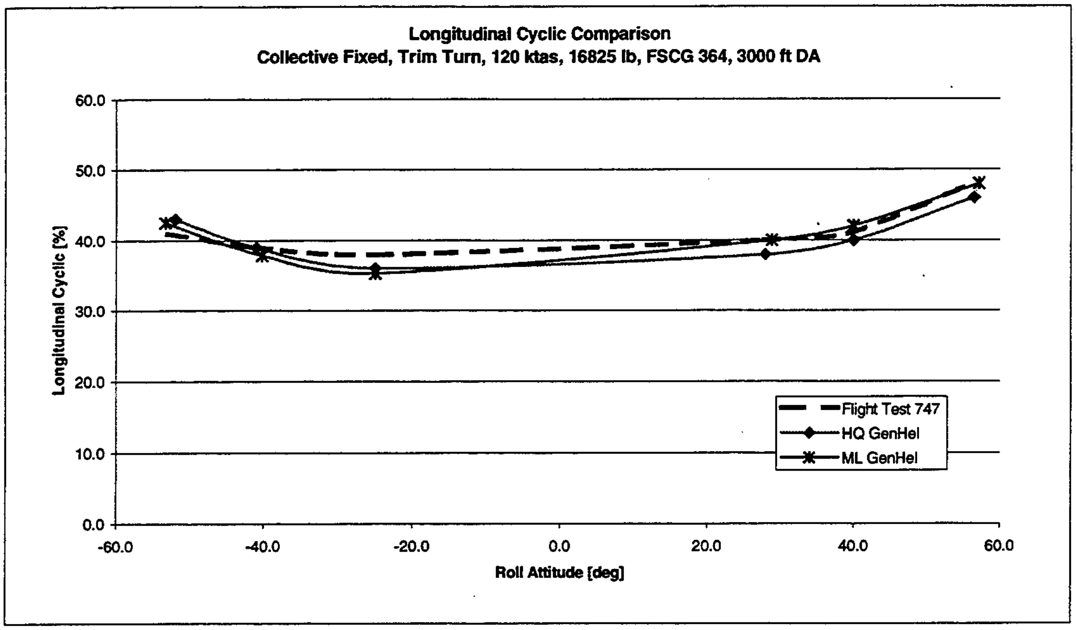

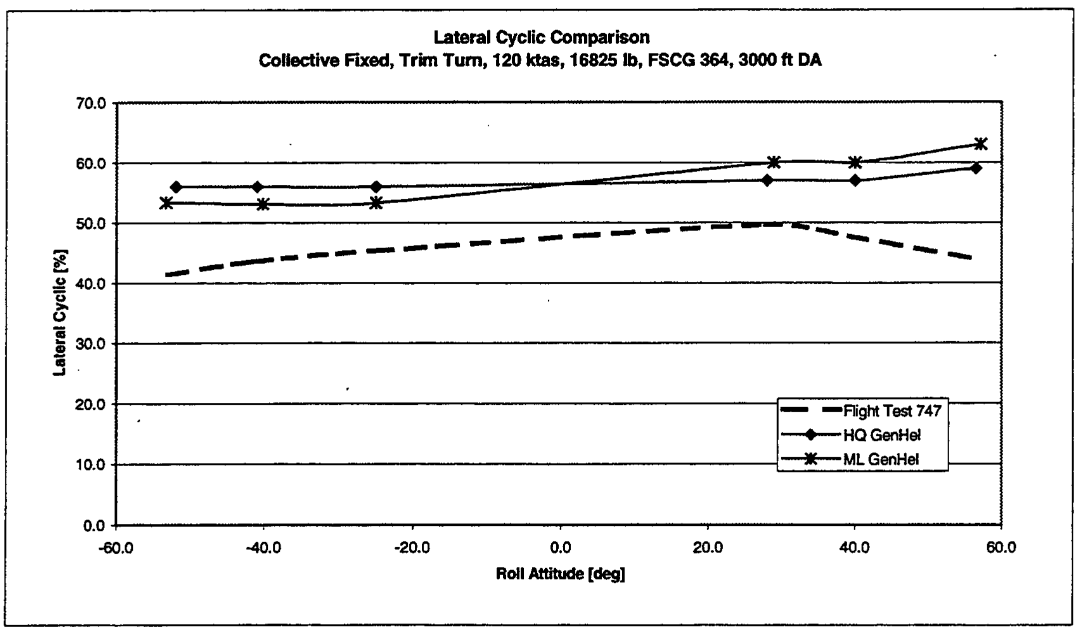

Figure 18 Trim Turn Cyclic Comparison 16825 lb, FSCG 364 in, 3000 ft DA

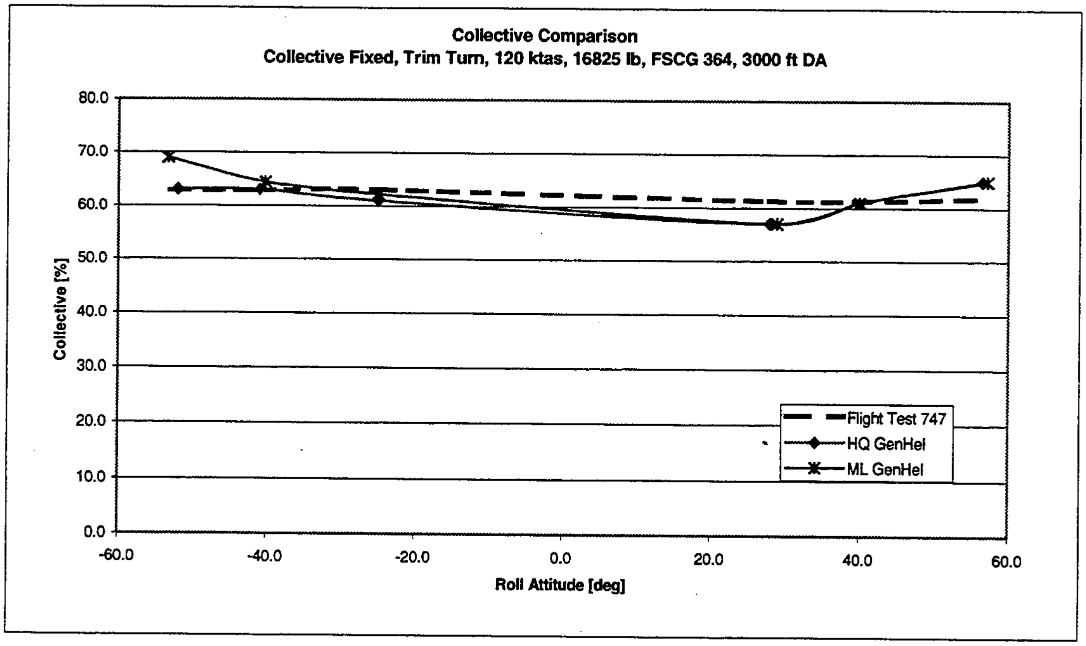

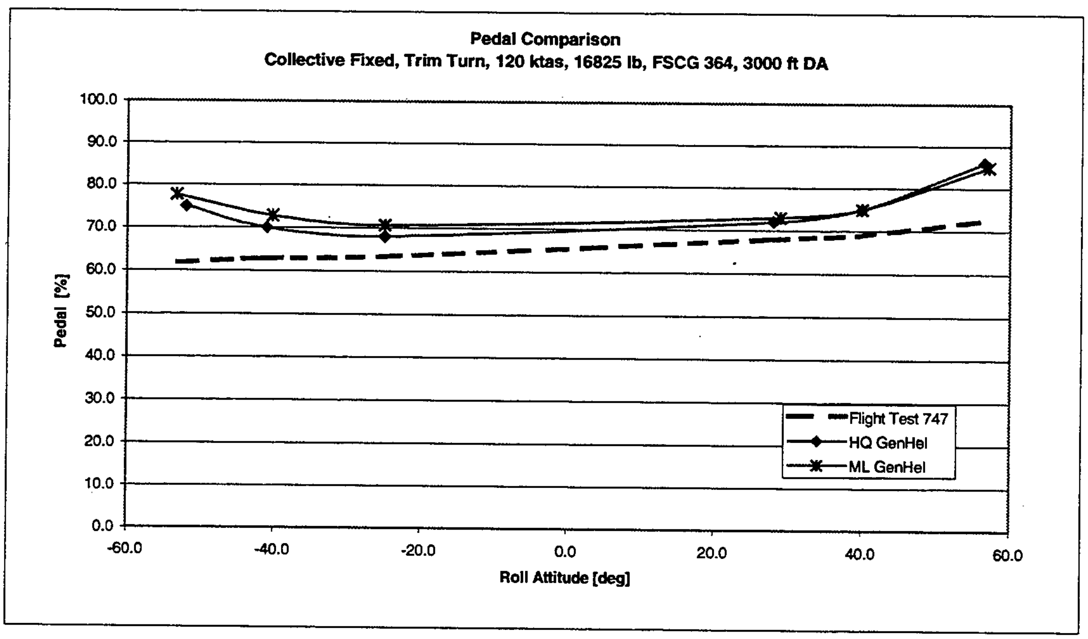

Figure 19 Trim Turn Collective and Pedal Comparison 16825 lb, FSCG 364 in, 3000 ft DA

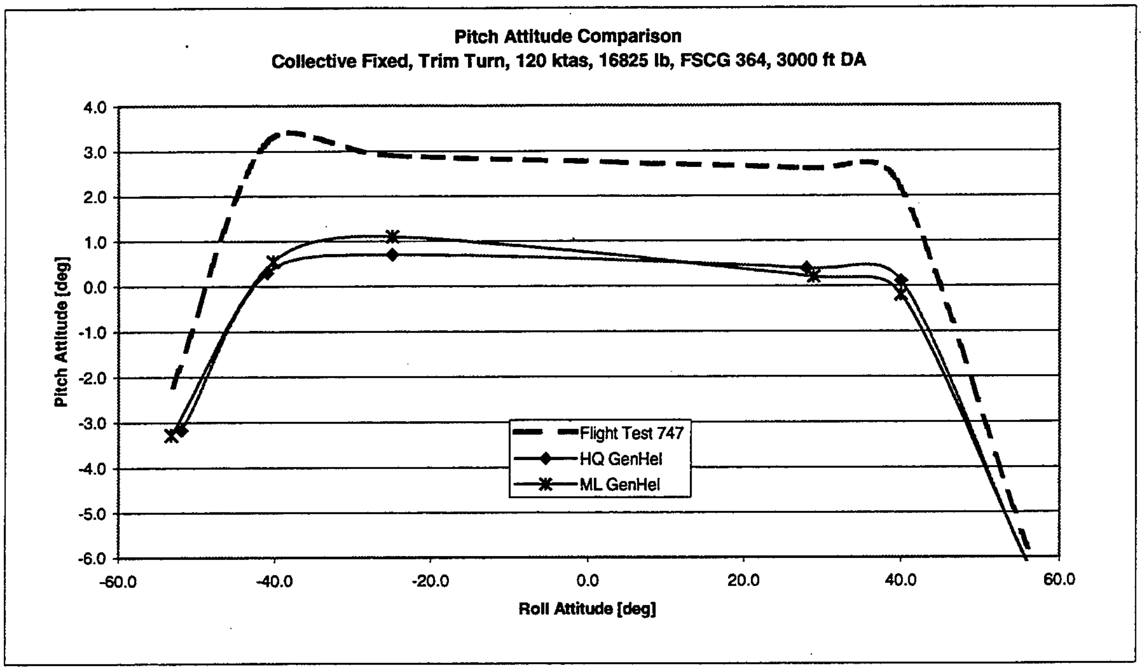

Figure 20 Trim Turn Pitch Attitude Comparison 16825 lb, FSCG 364 in, 3000 ft DA

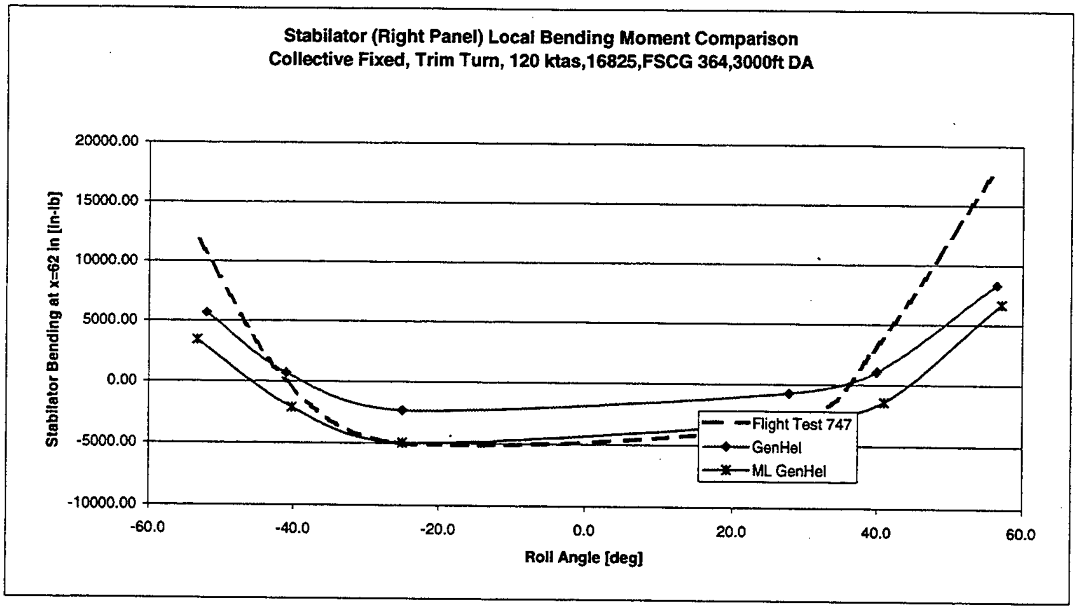

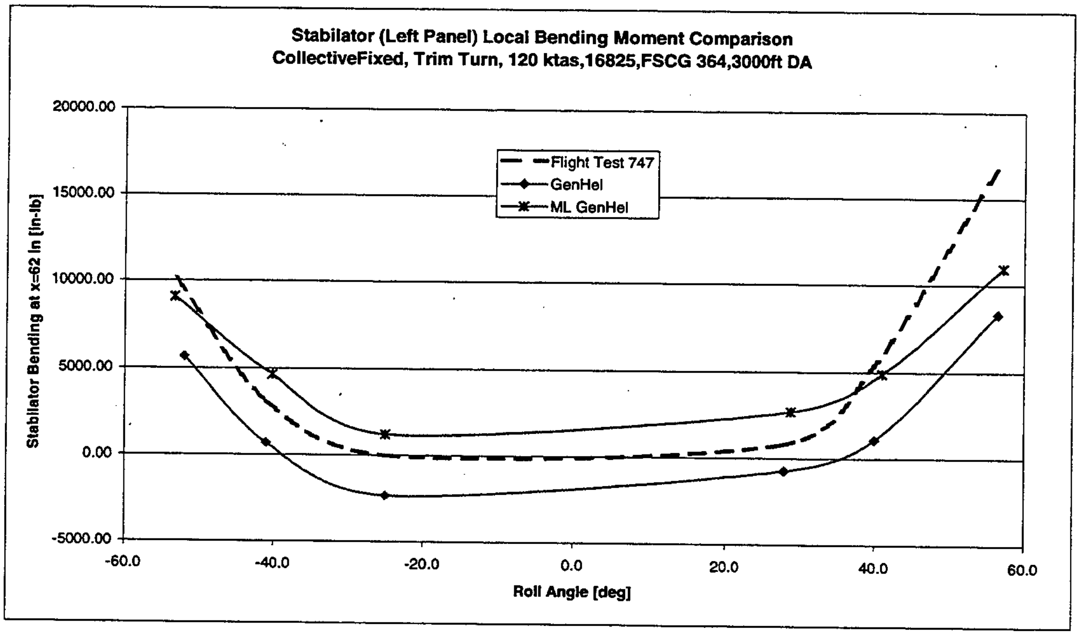

Figure 21 Trim Turn Stabilator Bending Comparison 16825 lb, FSCG 364 in, 3000 ft DA

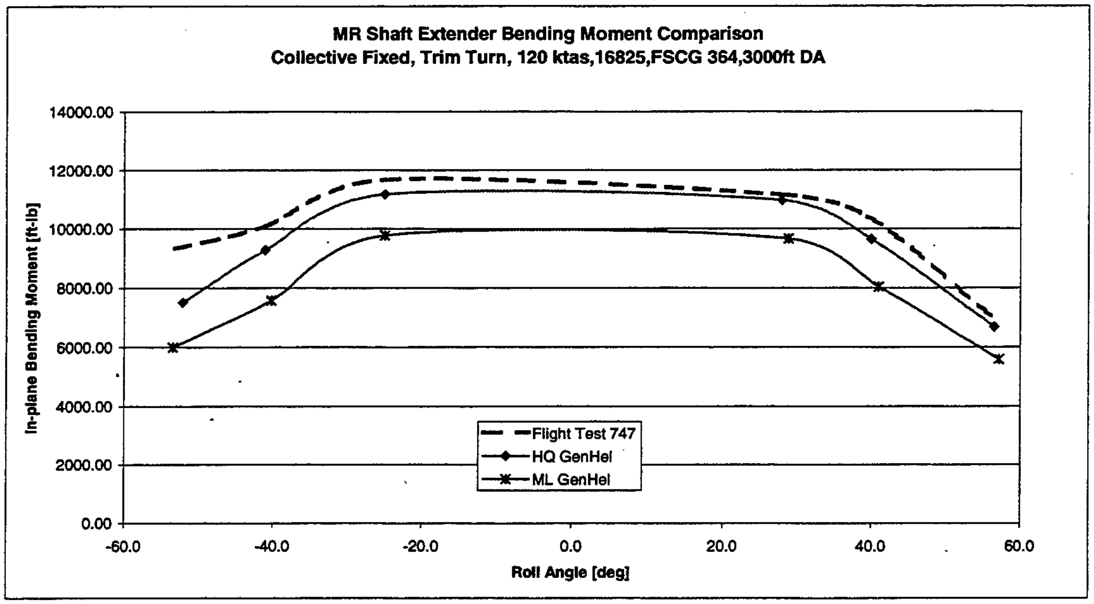

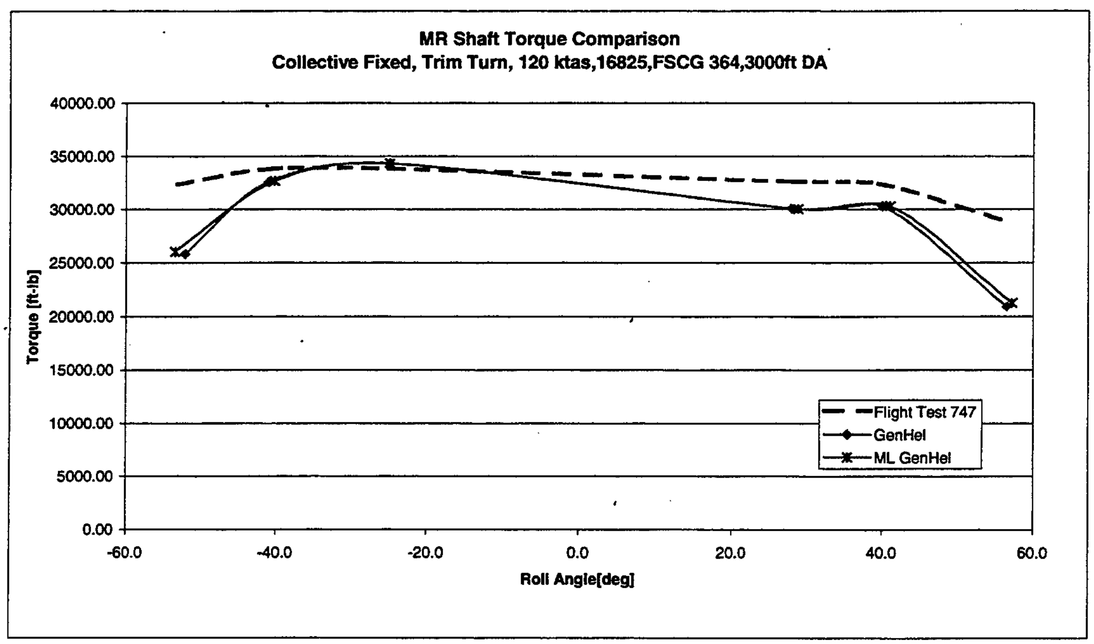

Figure 22 Trim Turn MR Shaft Moment Comparison 16825 lb, FSCG 364 in, 3000 ft DA

THIS PAGE INTENTIONALLY LEFT BLANK

V. HQ AND ML DYNAMIC MANEUVER CORRELATION

A. DISCUSSION

The time domain analysis of the HQ and ML models yielded very good results. Longitudinal and lateral step and pulse inputs were evaluated for both configurations. Both models had excellent correlation of the on-axis response to pulse inputs.

In both configurations, both models under predicted the attitude response to forward and right step inputs and over predicted the attitude response to left lateral steps. The attitude responses in question may have been skewed by the authors lack of experience in controlling the off-axis response. This is evidenced by the nearly flawless results obtained during the relatively quick pulse inputs compared to the less remarkable results obtained during the slower developing step inputs. More careful management of the off-axis controls is required for step input analysis.

B. CORRELATION PLOTS

1. Dynamic Correlation Plots, 16825 lb, FSCG 364, 3000 ft DA

a. Forward Longitudinal Step Flight 953-747 Run 043

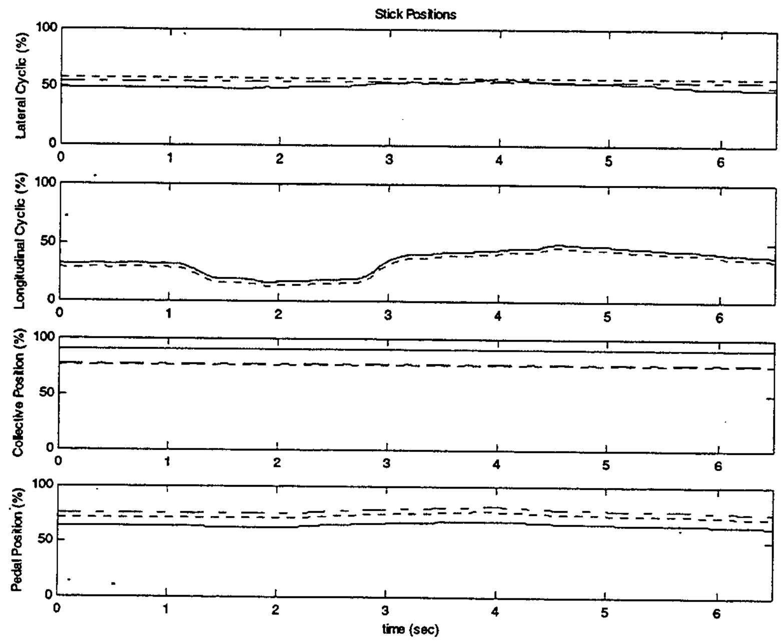

Figure 23 Flight 953-747 Run 043 Stick Positions 16825, FSCG 364, 3000 ft DA

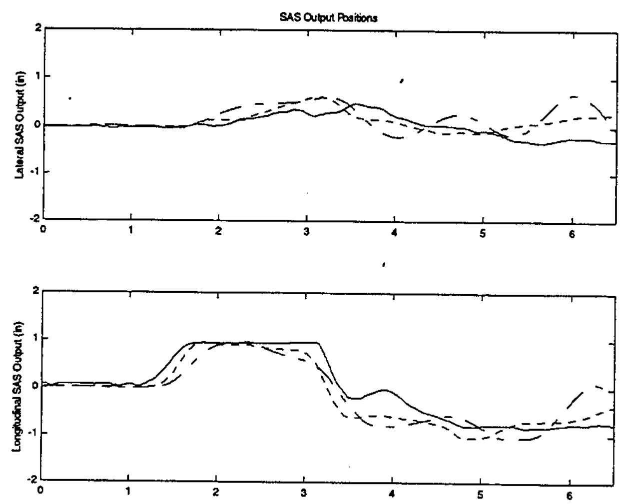

Figure 24 Flight 953-747 Run 043 SAS Positions 16825, FSCG 364, 3000 ft DA

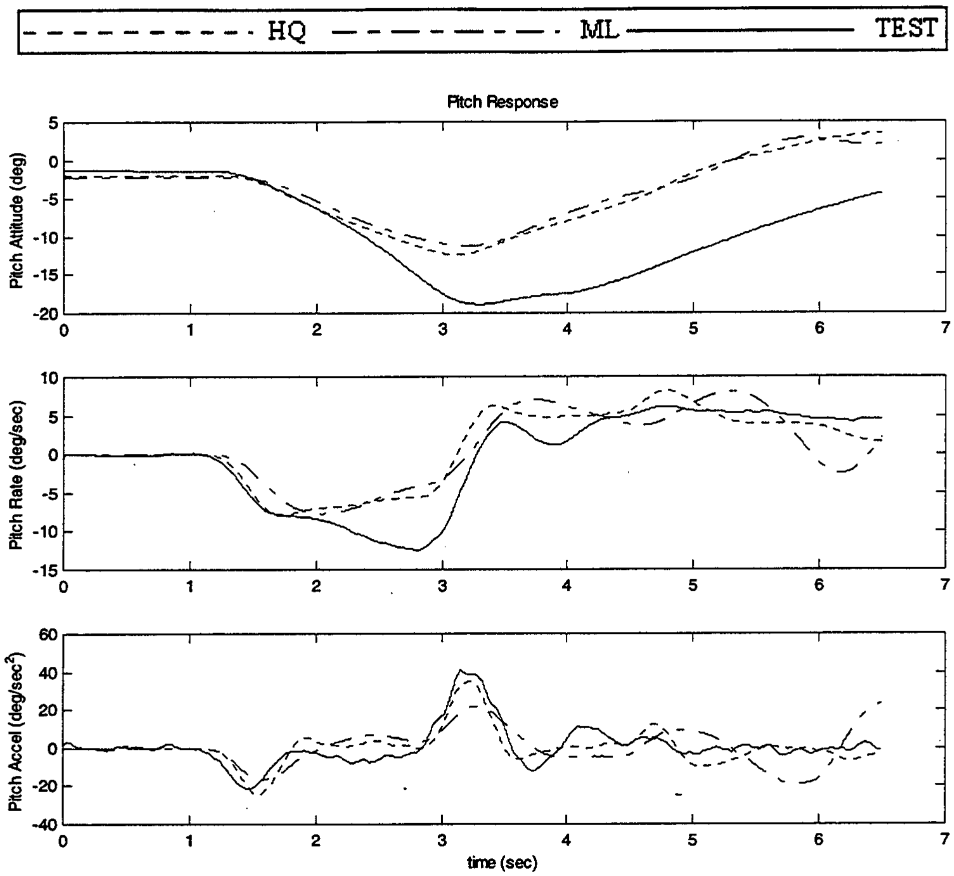

Figure 25 Flight 953-747 Run 043 On-Axis Response 16825, FSCG 364, 3000 ft DA

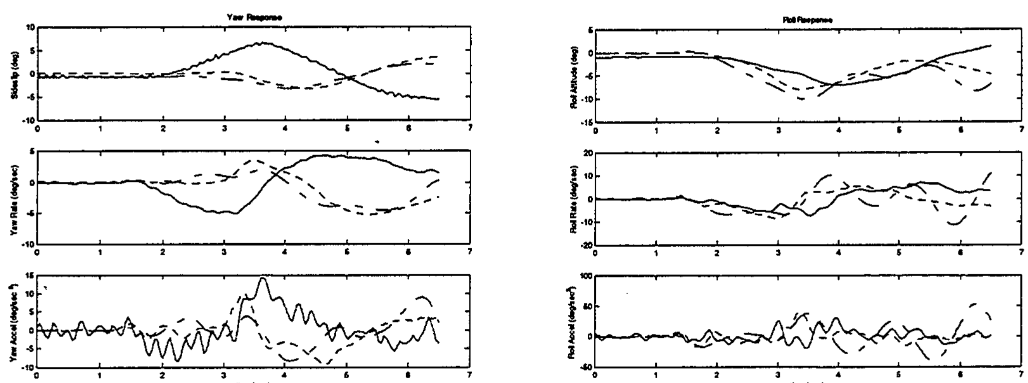

Figure 26 Flight 953-747 Run 043 Off-Axis Response 16825, FSCG 364, 3000 ft DA

b. Left Lateral Step, Flight 953-747 Run 051

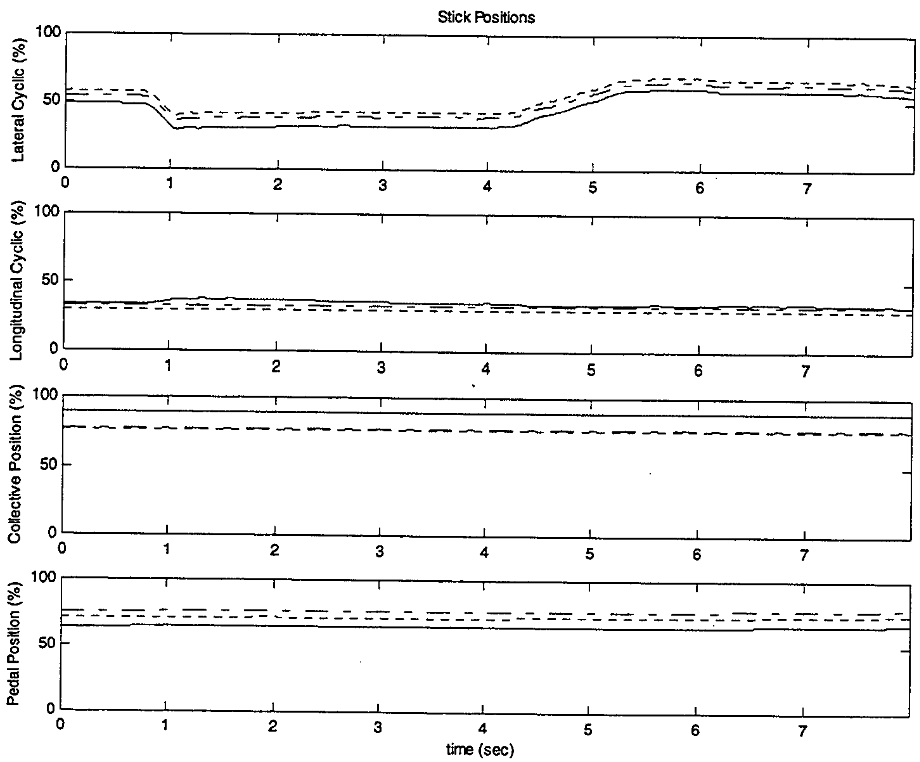

Figure 27 Flight 953-747 Run 051 Stick Positions 16825, FSCG 364, 3000 ft DA

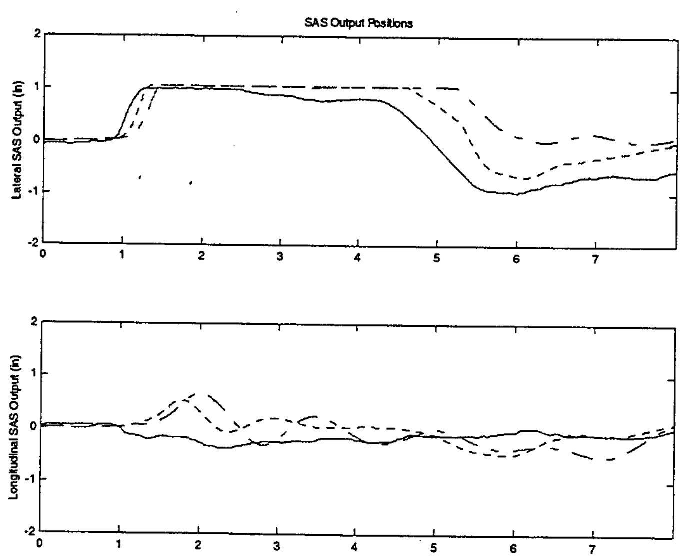

Figure 28 Flight 953-747 Run 051 SAS Positions 16825, FSCG 364, 3000 ft DA

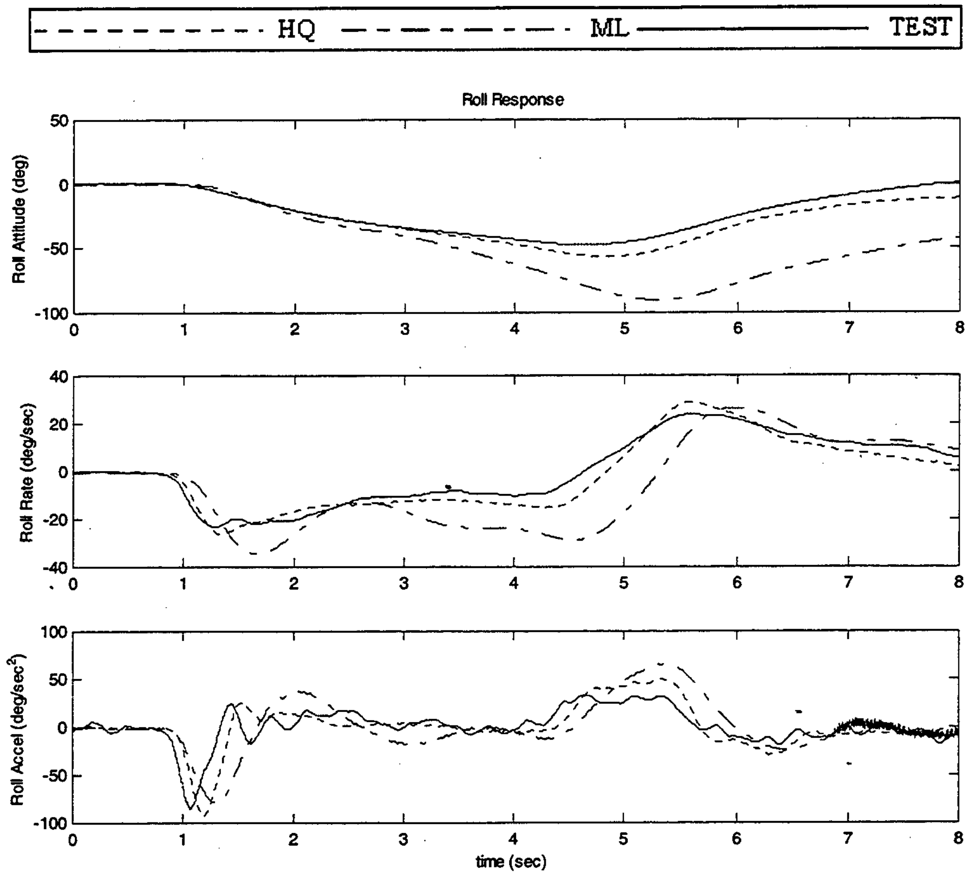

Figure 29 Flight 953-747 Run 051 On-Axis Response 16825, FSCG 364, 3000 ft DA

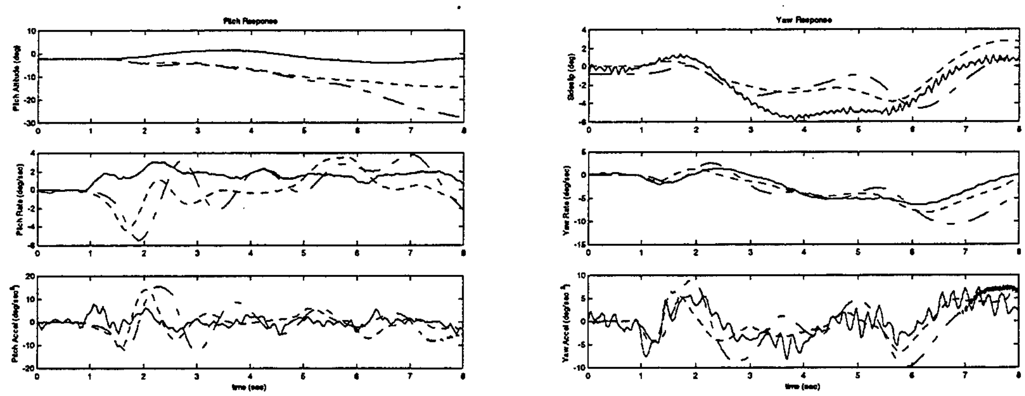

Figure 30 Flight 953-747 Run 051 Off-Axis Response 16825, FSCG 364, 3000 ft DA

c. *Right Lateral Step, Flight 953-747 Run 055*

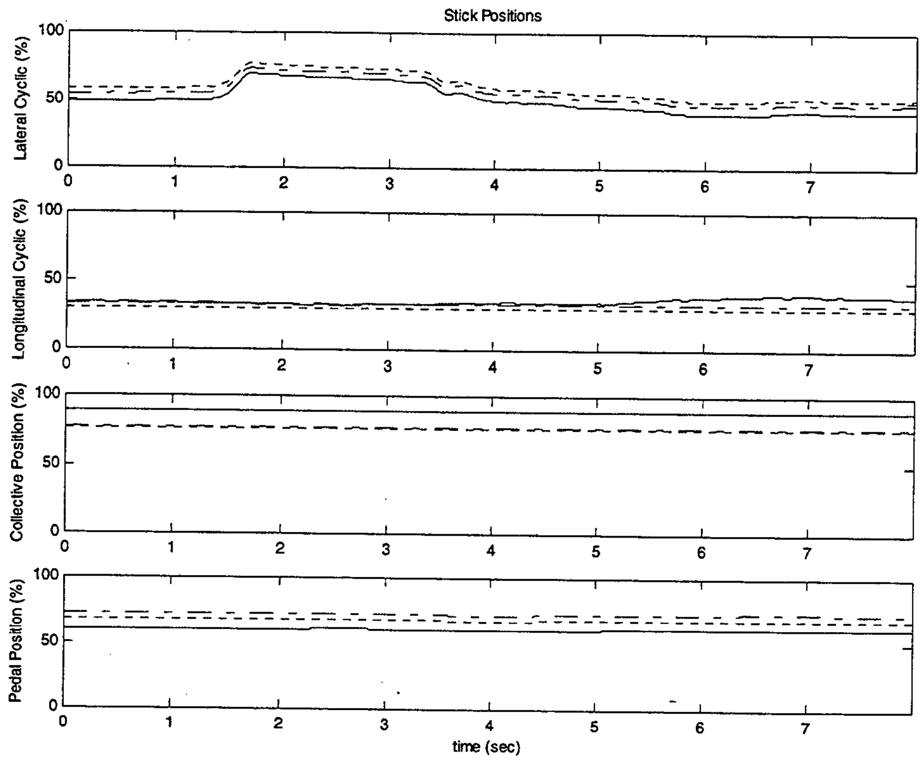

Figure 31 Flight 953-747 Run 055 Stick Positions 16825, FSCG 364, 3000 ft DA

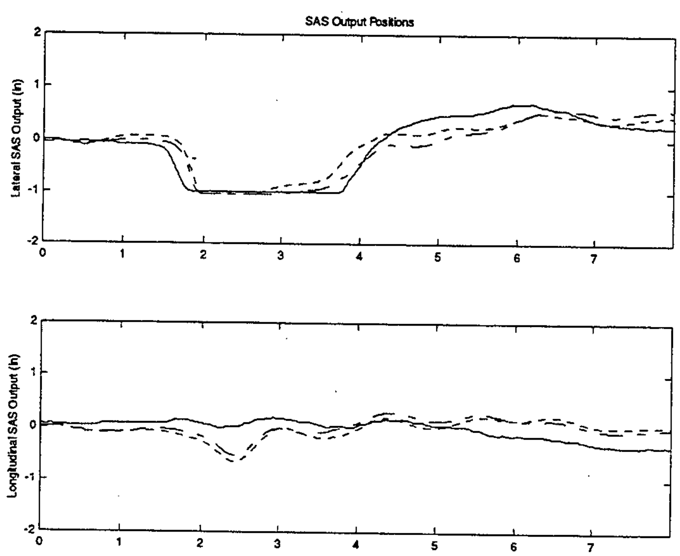

Figure 32 Flight 953-747 Run 055 SAS Positions 16825, FSCG 364, 3000 ft DA

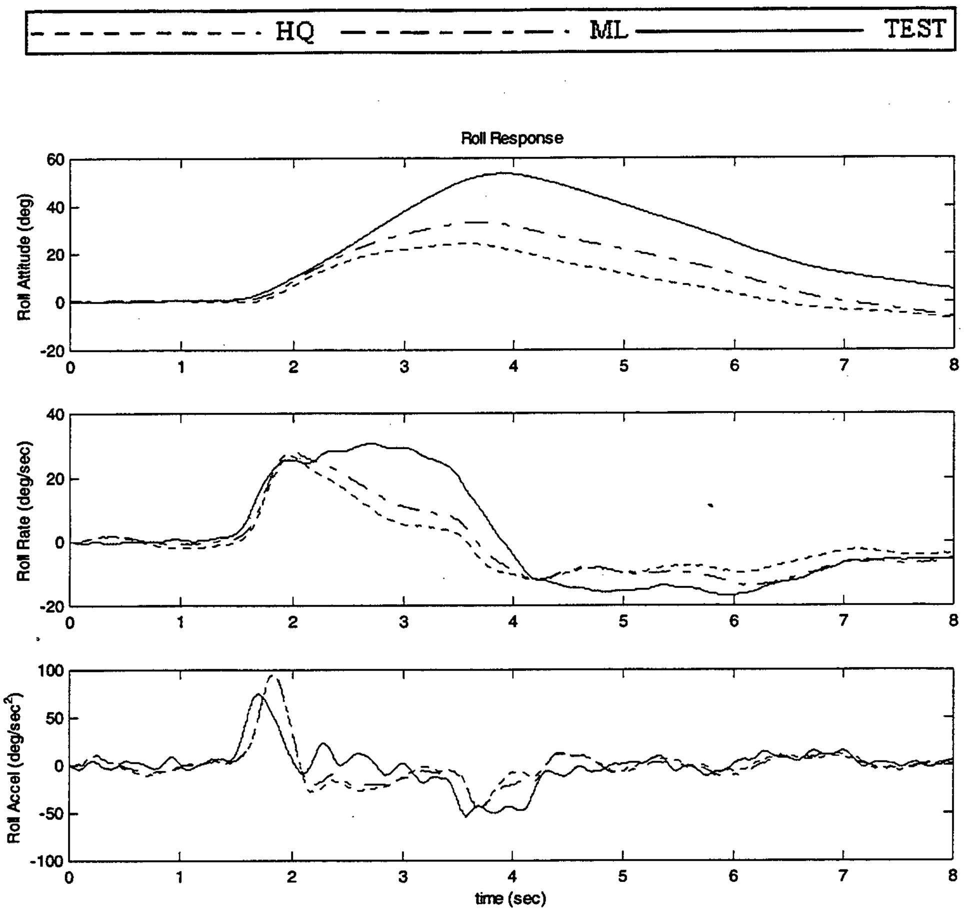

Figure 33 Flight 953-747 Run 055 On-Axis Response 16825, FSCG 364, 3000 ft DA

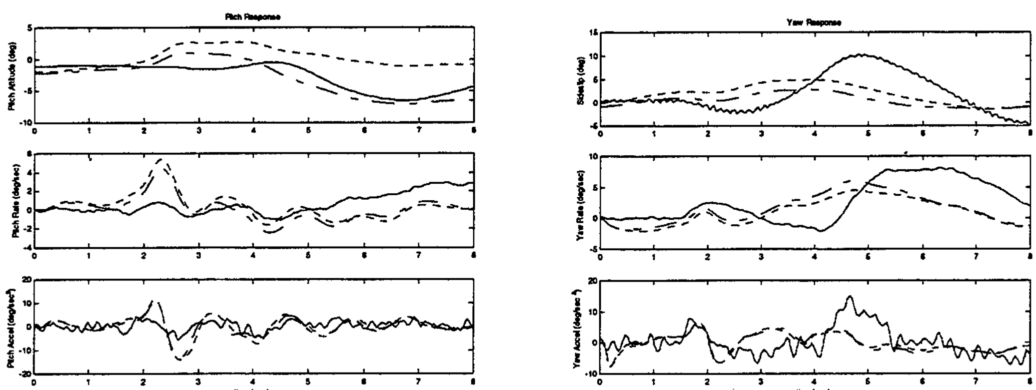

Figure 34 Flight 953-747 Run 055 Off Axis Response 16825, FSCG 364, 3000 ft DA

d. *Forward Longitudinal Pulse, Flight 953-747 Run 058*

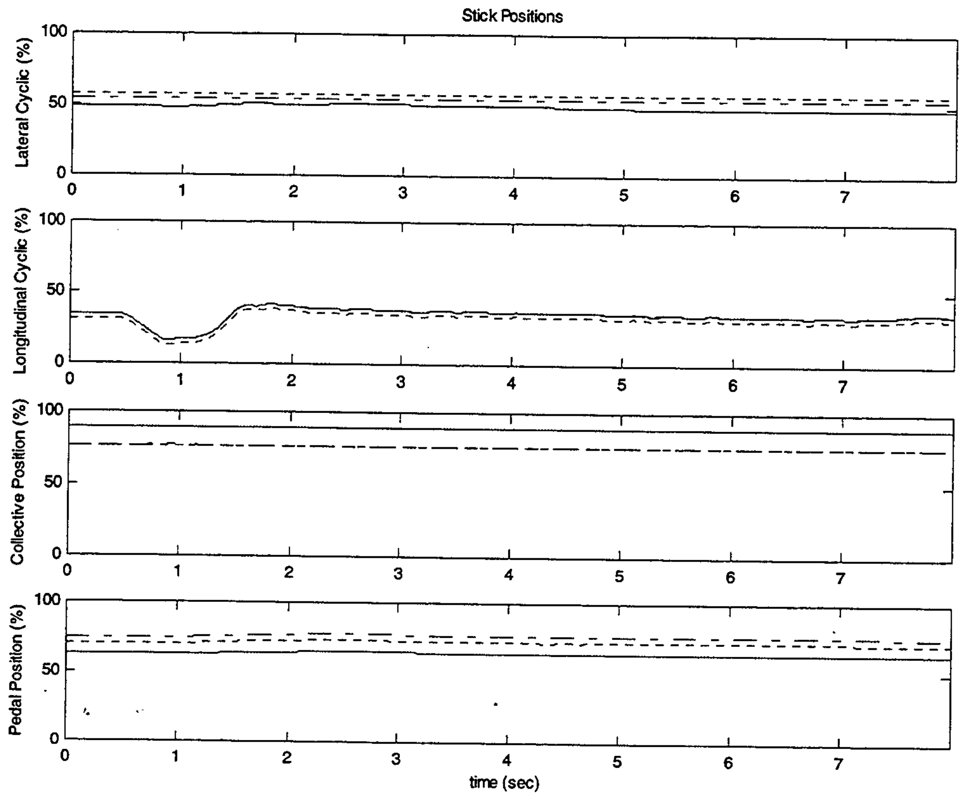

Figure 35 Flight 953-747 Run 058 Stick Positions 16825, FSCG 364, 3000 ft DA

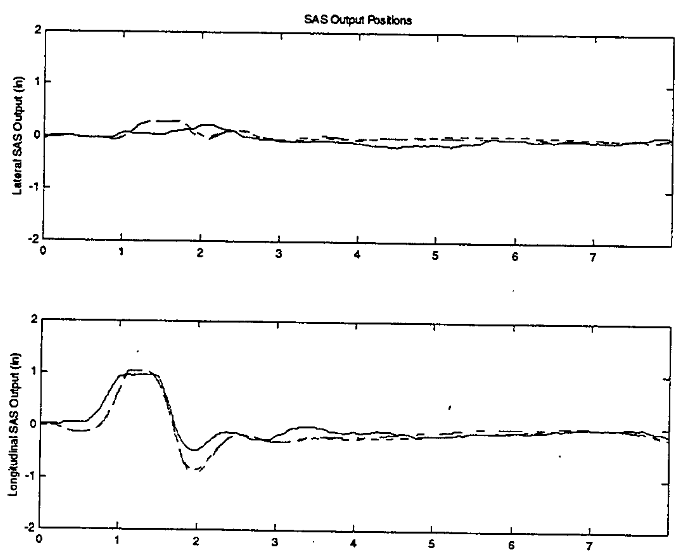

Figure 36 Flight 953-747 Run 058 SAS Positions 16825, FSCG 364, 3000 ft DA

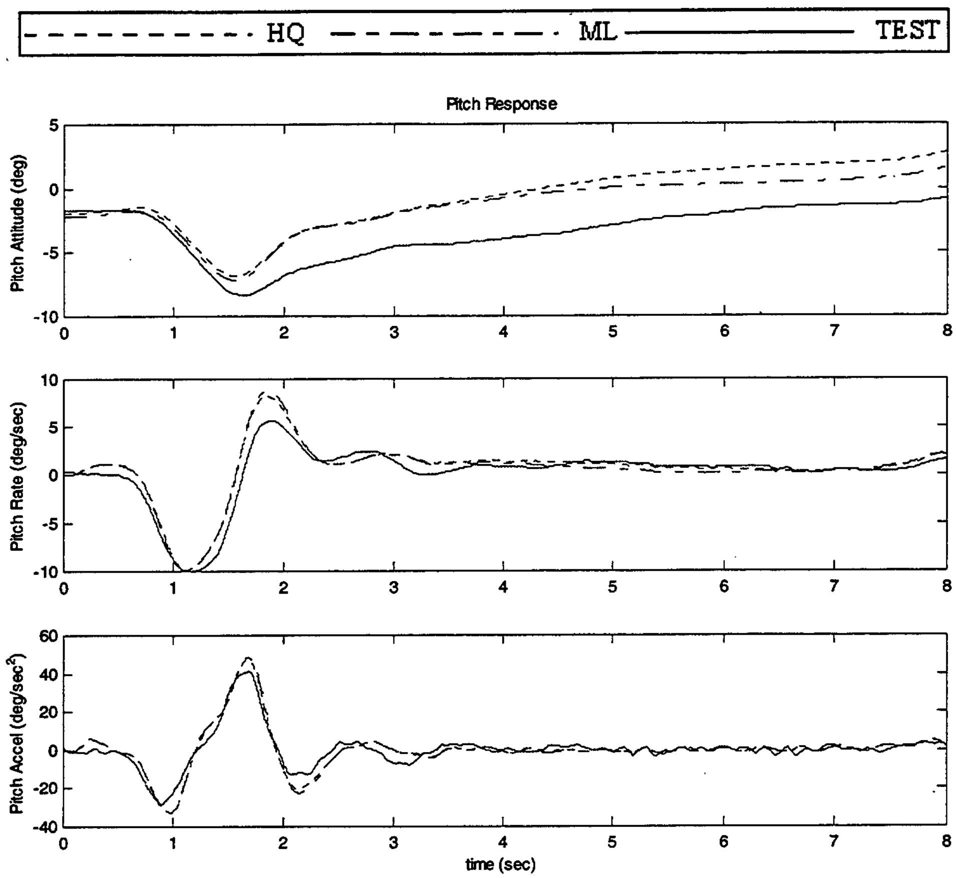

Figure 37 Flight 953-747 Run 058 On-Axis Response 16825, FSCG 364, 3000 ft DA

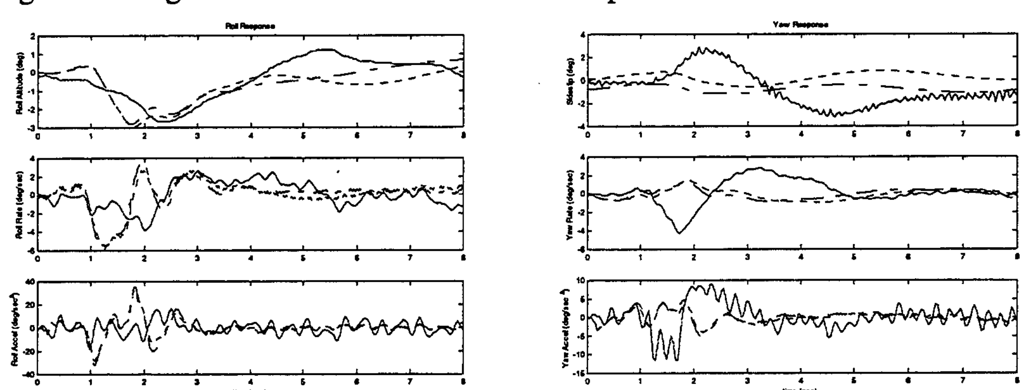

Figure 38 Flight 953-747 Run 058 Off-Axis Response 16825, FSCG 364, 3000 ft DA

e. Aft Longitudinal Pulse, Flight 953-747 Run 061

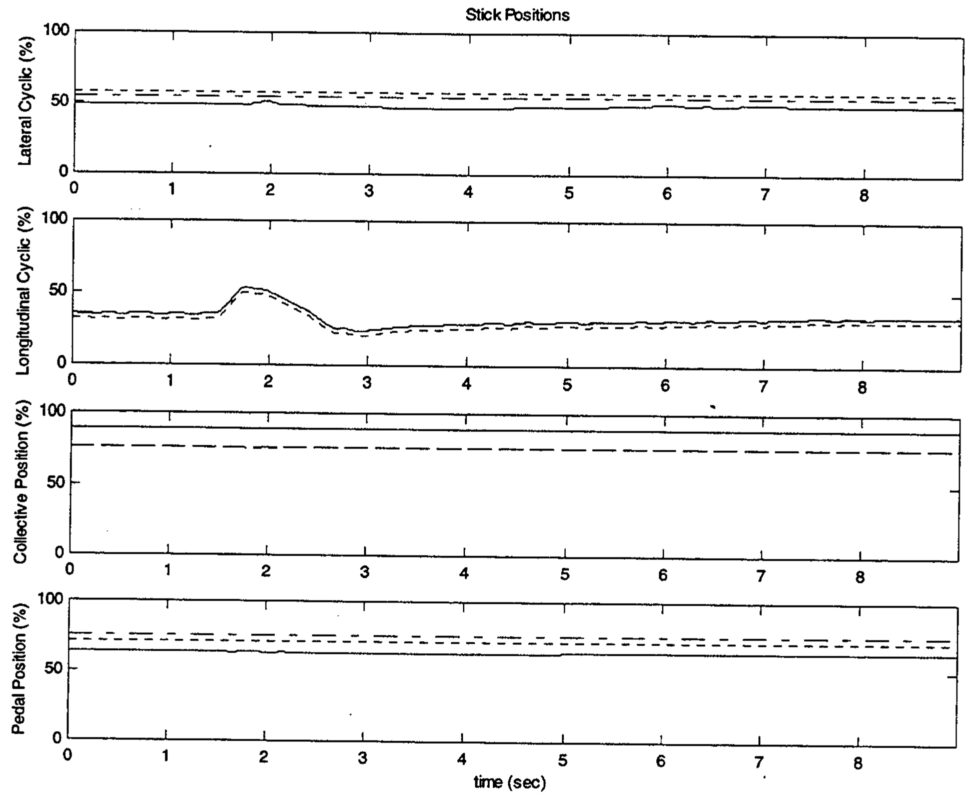

Figure 39 Flight 953-747 Run 061 Stick Positions 16825, FSCG 364, 3000 ft DA

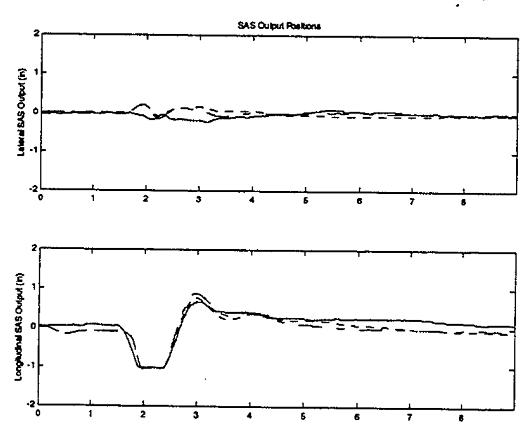

Figure 40 Flight 953-747 Run 061 SAS Positions 16825, FSCG 364, 3000 ft DA

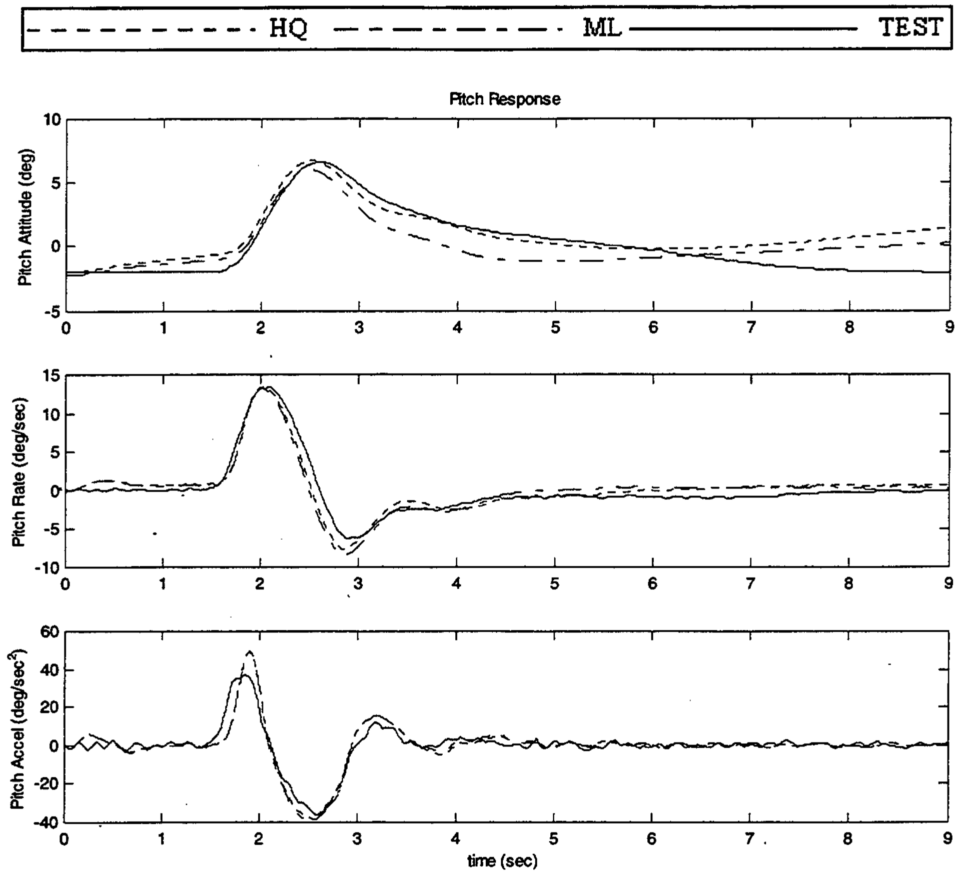

Figure 41 Flight 953-747 Run 061 On-Axis Response 16825, FSCG 364, 3000 ft DA

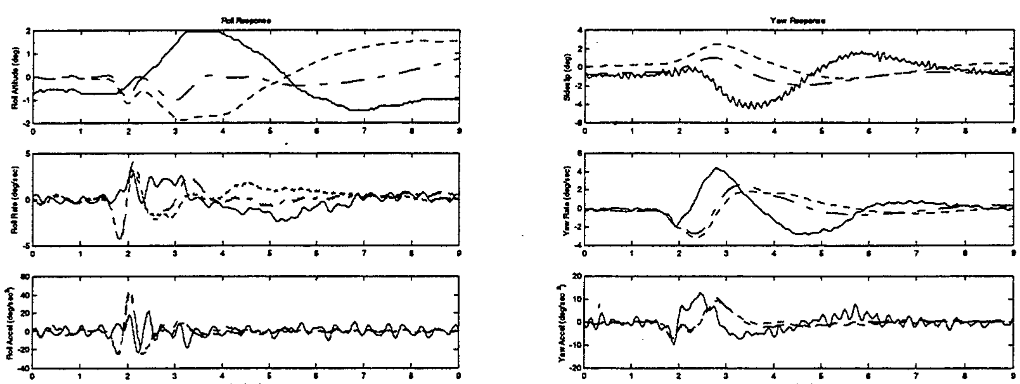

Figure 42 Flight 953-747 Run 061 Off-Axis Response 16825, FSCG 364, 3000 ft DA

f. Left Lateral Pulse, Flight 953-747 Run 064

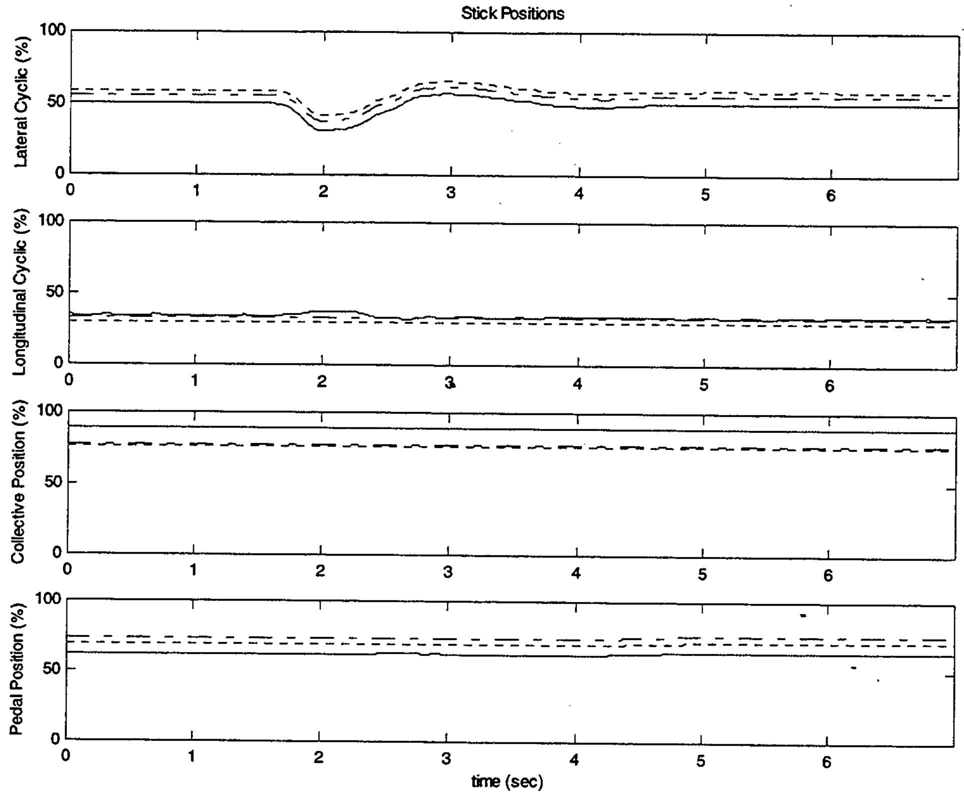

Figure 43 Flight 953-747 Run 064 Stick Positions 16825, FSCG 364, 3000 ft DA

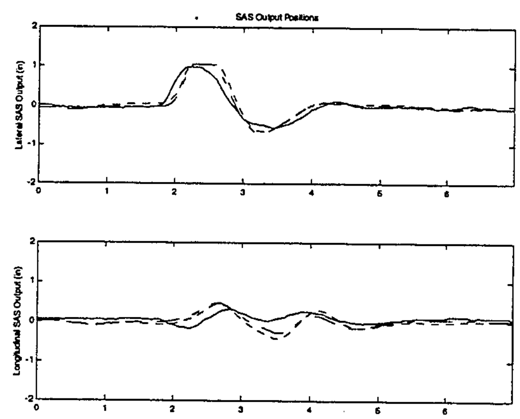

Figure 44 Flight 953-747 Run 064 SAS Positions 16825, FSCG 364, 3000 ft DA

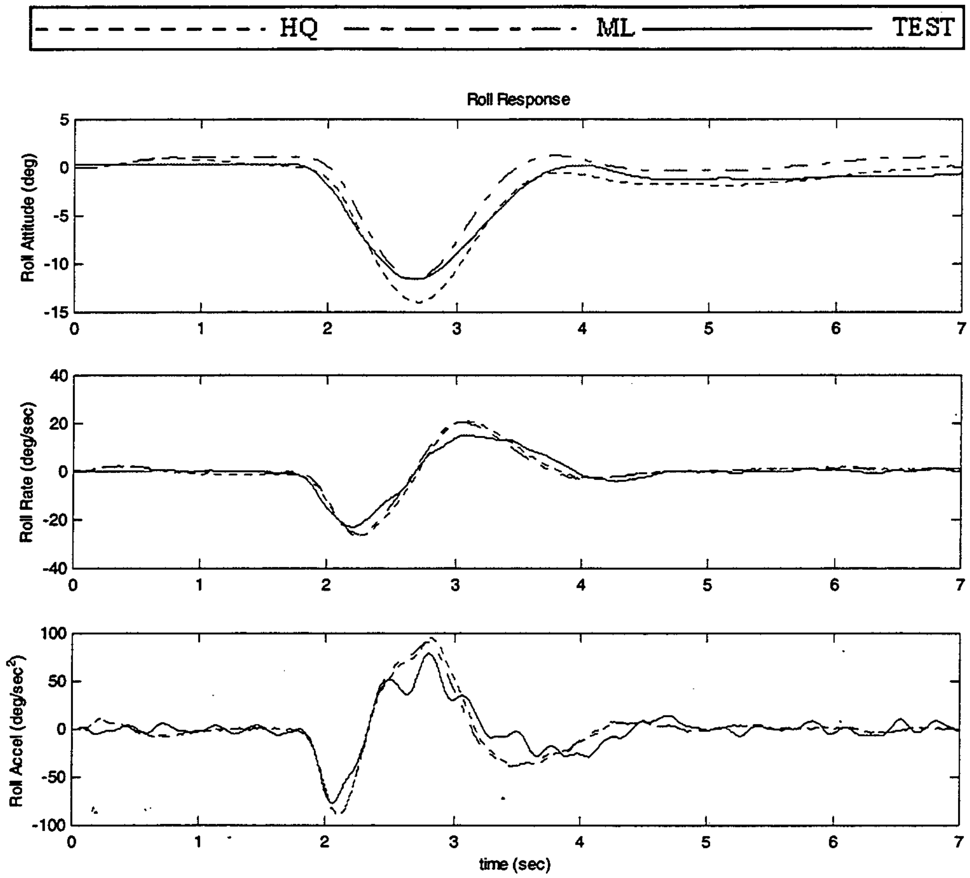

Figure 45 Flight 953-747 Run 064 On-Axis Response 16825, FSCG 364, 3000 ft DA

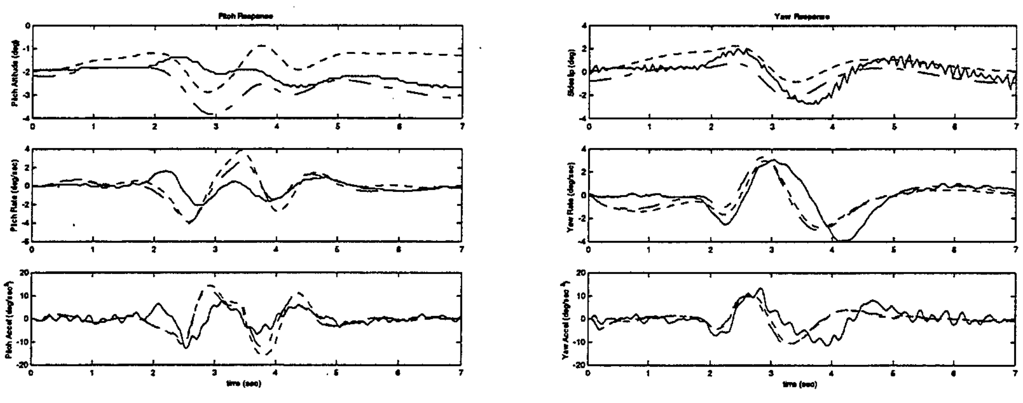

Figure 46 Flight 953-747 Run 064 Off-Axis Response 16825, FSCG 364, 3000 ft DA

g. *Right Lateral Pulse, Flight 953-747 Run 067*

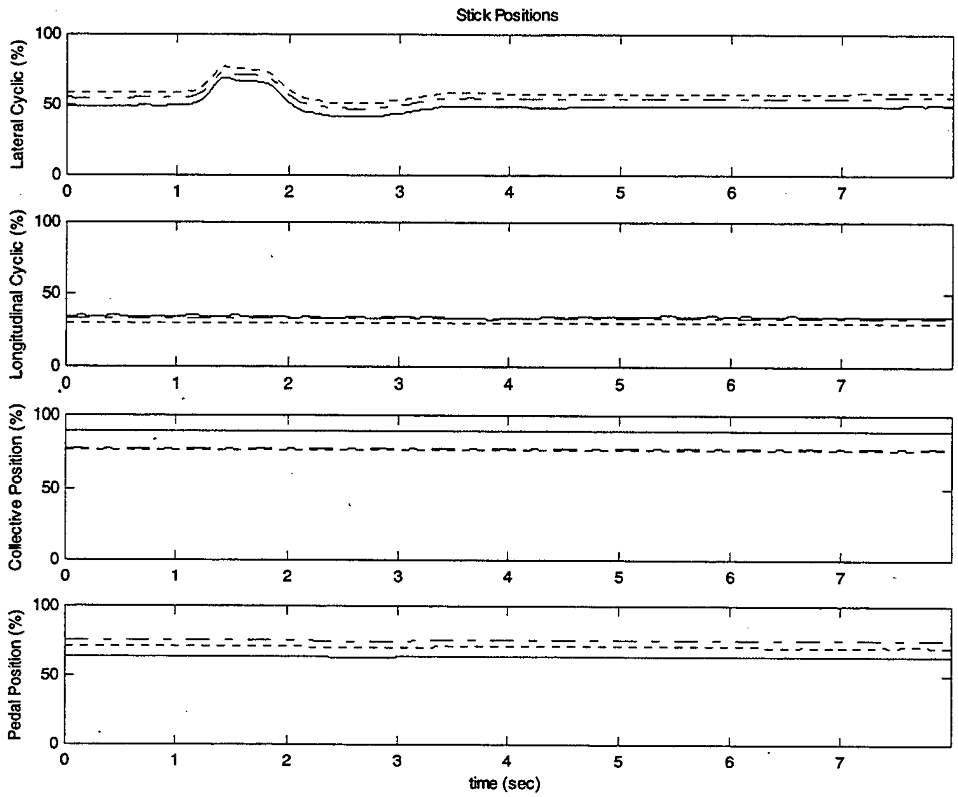

Figure 47 Flight 953-747 Run 067 Stick Positions 16825, FSCG 364, 3000 ft DA

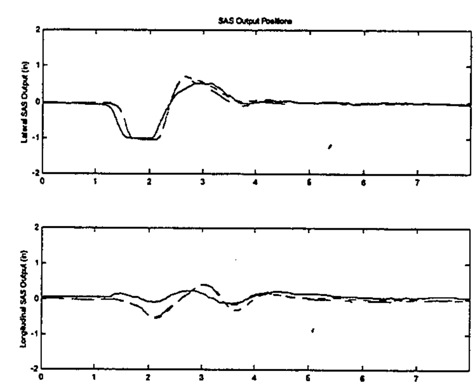

Figure 48 Flight 953-747 Run 067 SAS Positions 16825, FSCG 364, 3000 ft DA

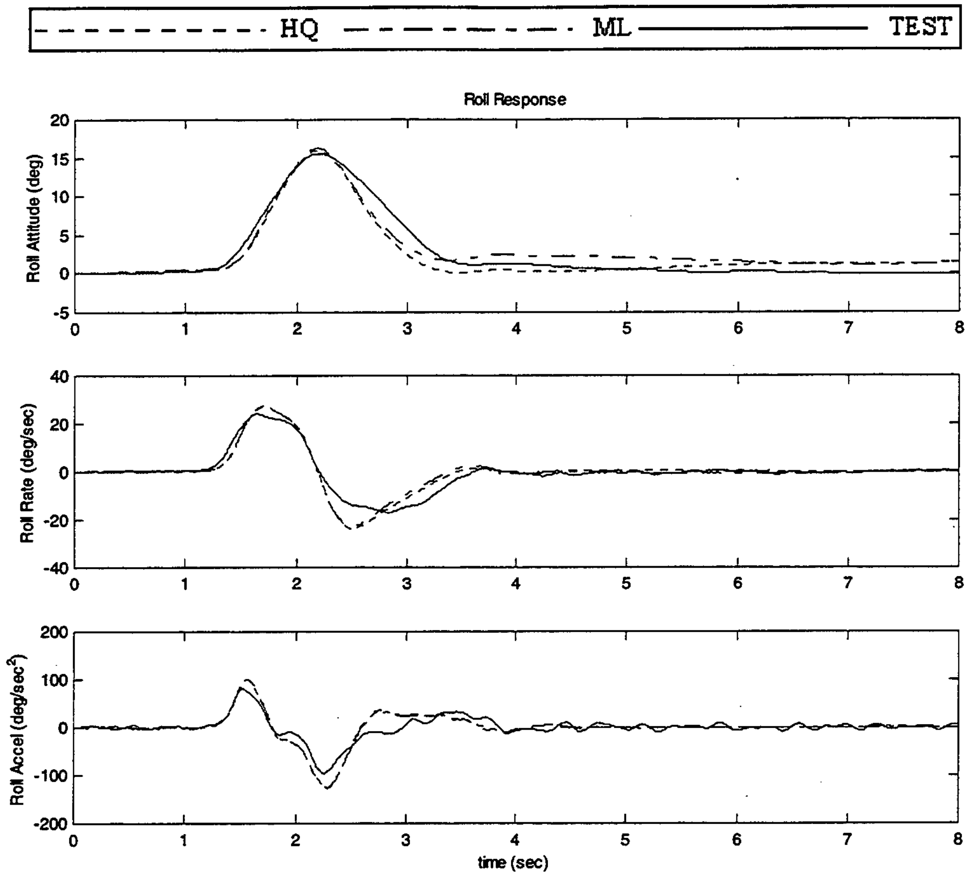

Figure 49 Flight 953-747 Run 067 On-Axis Response 16825, FSCG 364, 3000 ft DA

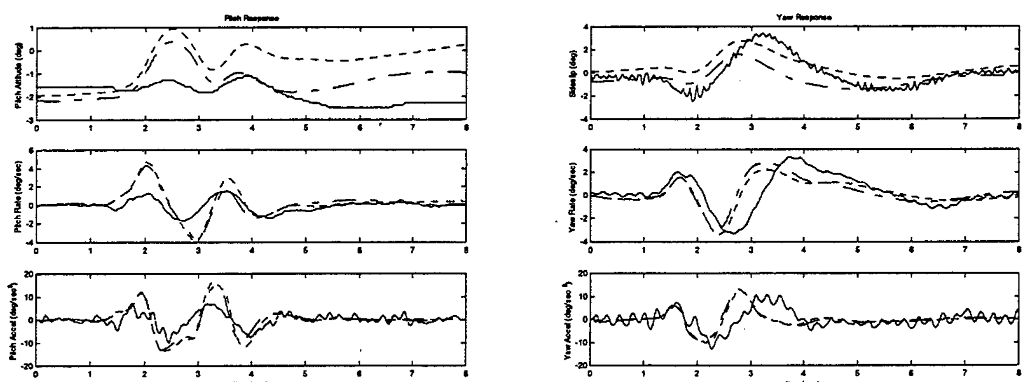

Figure 50 Flight 953-747 Run 067 Off-Axis Response 16825, FSCG 364, 3000 ft DA

2. Dynamic Correlation Plots 22000 lb, FSCG 360, 3000 ft DA

a. Aft Longitudinal Step, Flight 953-795 Run 042

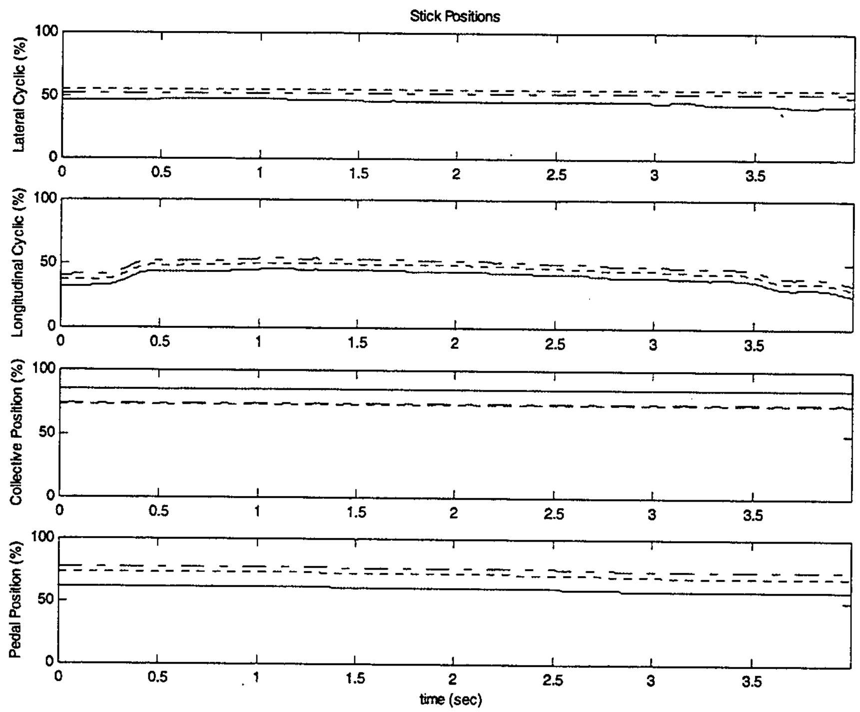

Figure 51 Flight 953-795 Run 042 Stick Positions 22000, FSCG 360, 3000 ft DA

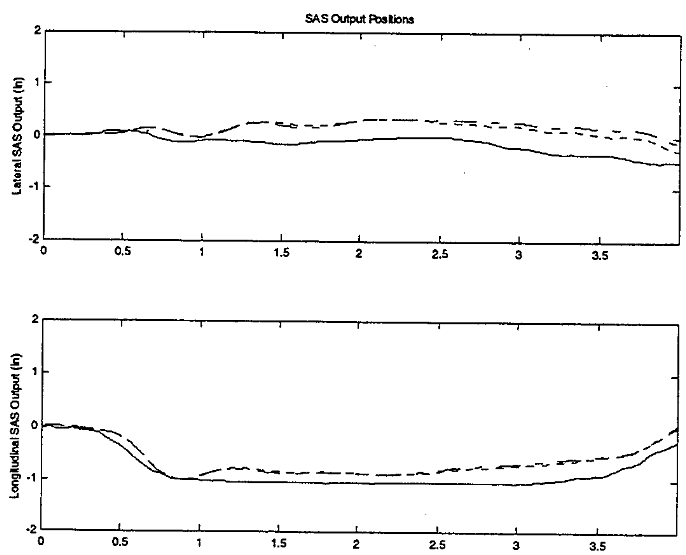

Figure 52 Flight 953-795 Run 042 SAS Positions 22000, FSCG 360, 3000 ft DA

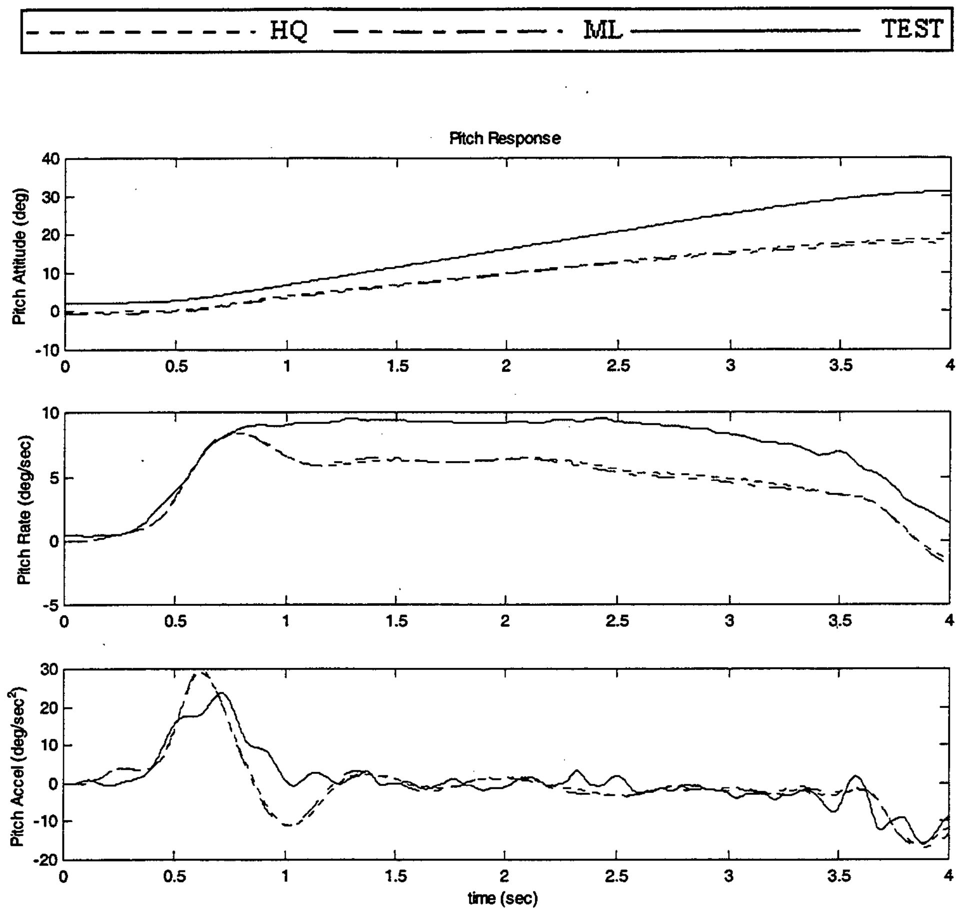

Figure 53 Flight 953-795 Run 042 On-Axis Response 22000, FSCG 360, 3000 ft DA

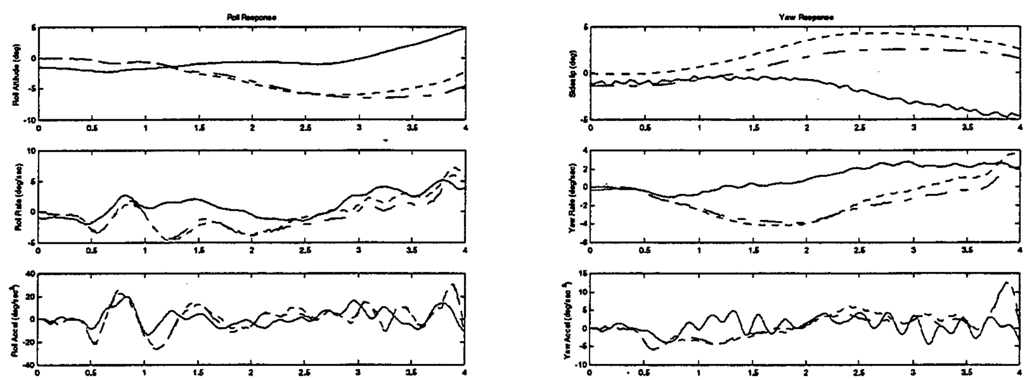

Figure 54 Flight 953-795 Run 042 Off-Axis Response 22000, FSCG 360, 3000 ft DA

b. ***Left Lateral Step, Flight 953-795 Run 048***

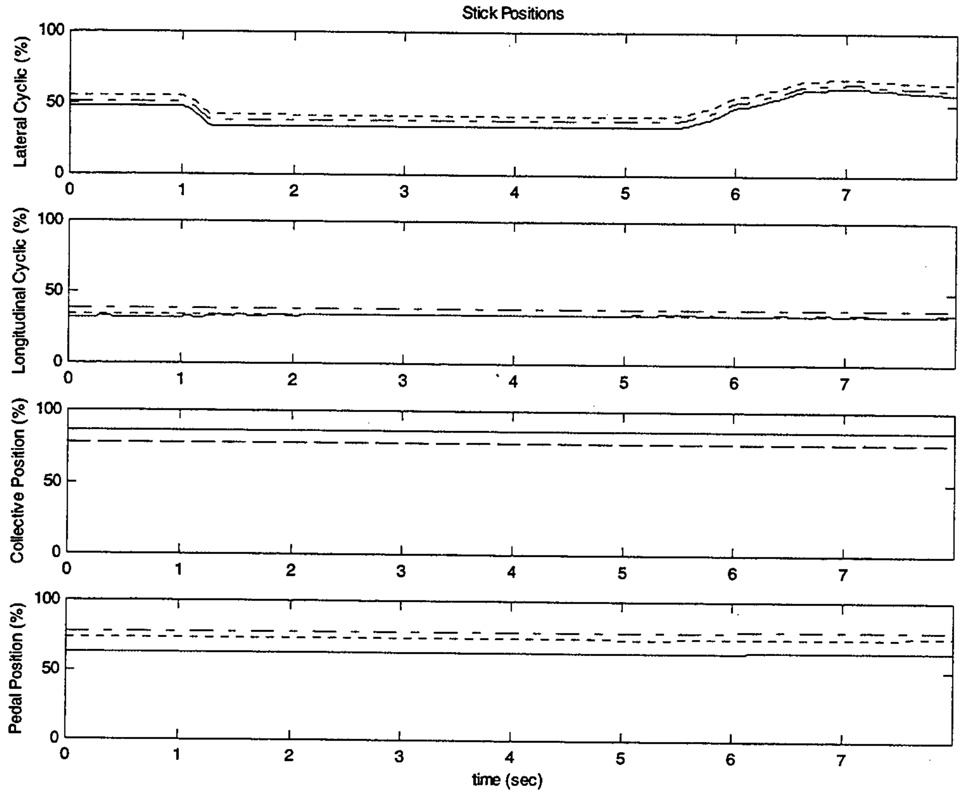

Figure 55 Flight 953-795 Run 048 Stick Positions 22000, FSCG 360, 3000 ft DA

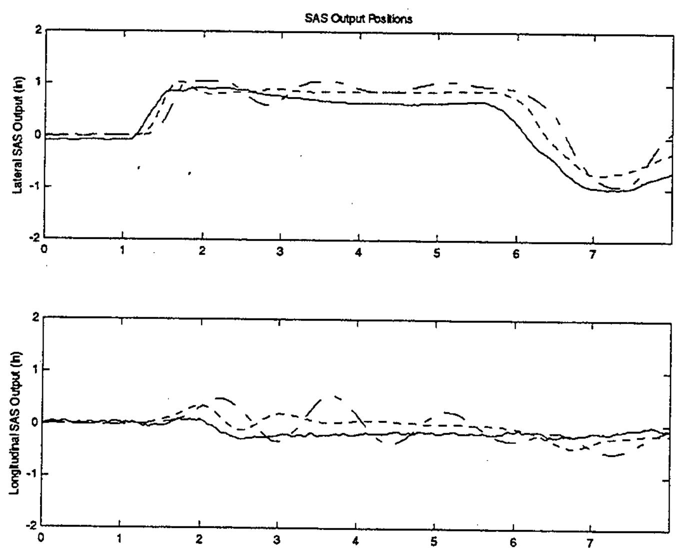

Figure 56 Flight 953-795 Run 048 SAS Positions 22000, FSCG 360, 3000 ft DA

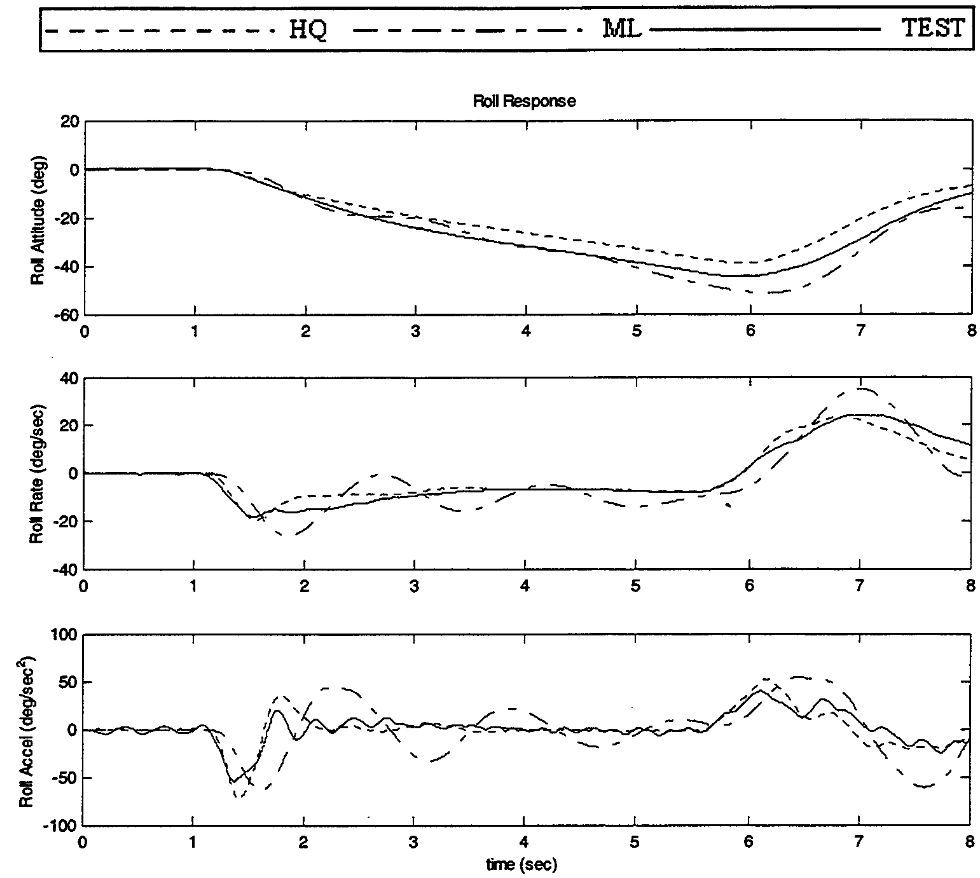

Figure 57 Flight 953-795 Run 048 On-Axis Response 22000, FSCG 360, 3000 ft DA

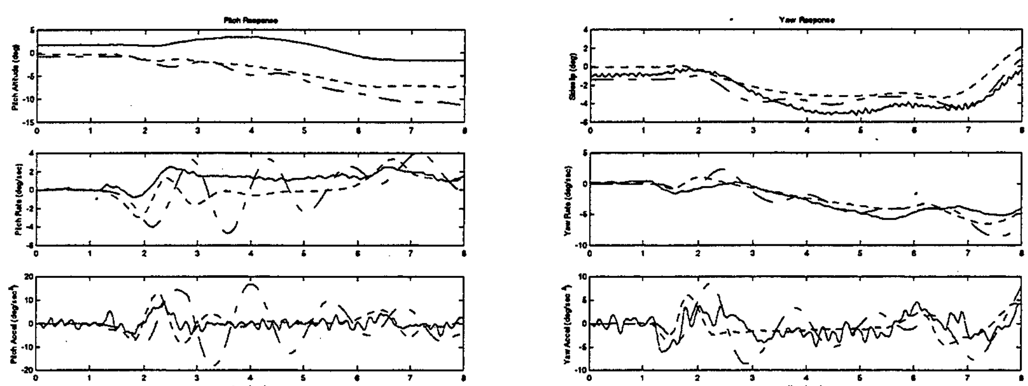

Figure 58 Flight 953-795 Run 048 Off-Axis Response 22000, FSCG 360, 3000 ft DA

c. *Right Lateral Step, Flight 953-795 Run 049*

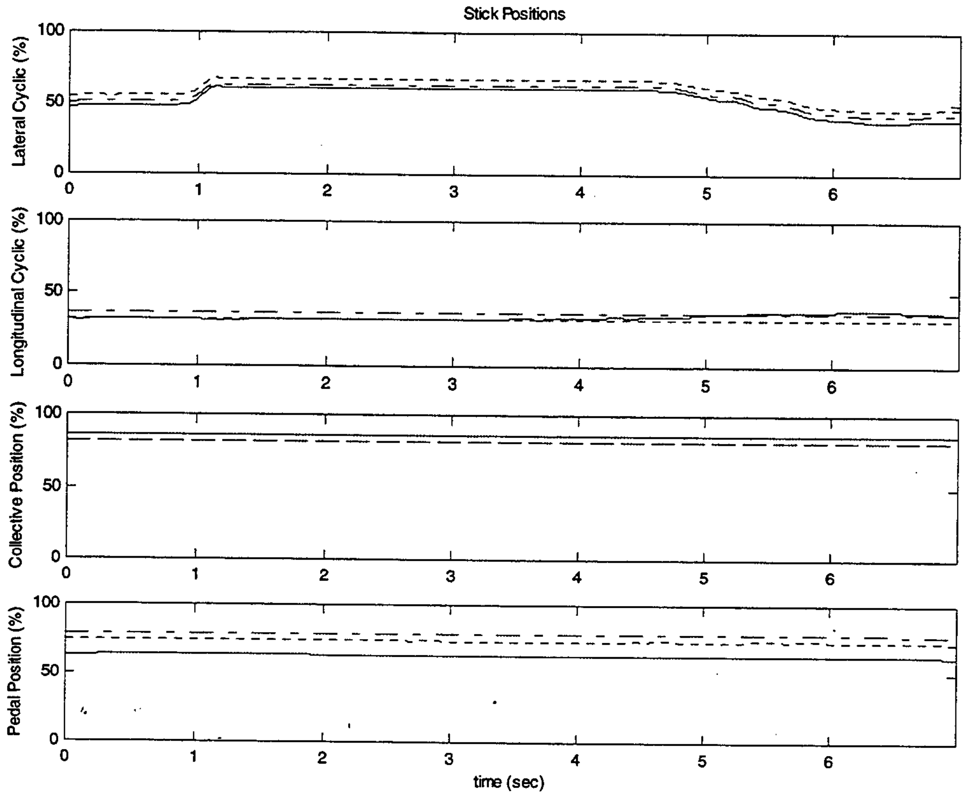

Figure 59 Flight 953-795 Run 049 Stick Positions 22000, FSCG 360, 3000 ft DA

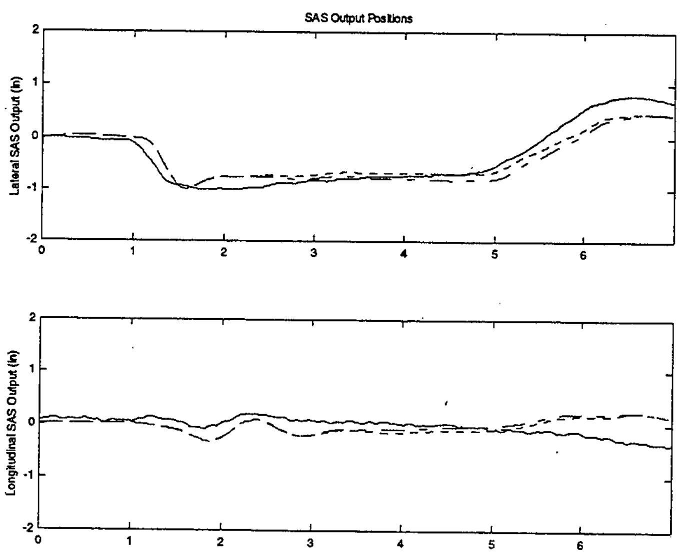

Figure 60 Flight 953-795 Run 049 SAS Positions 22000, FSCG 360, 3000 ft DA

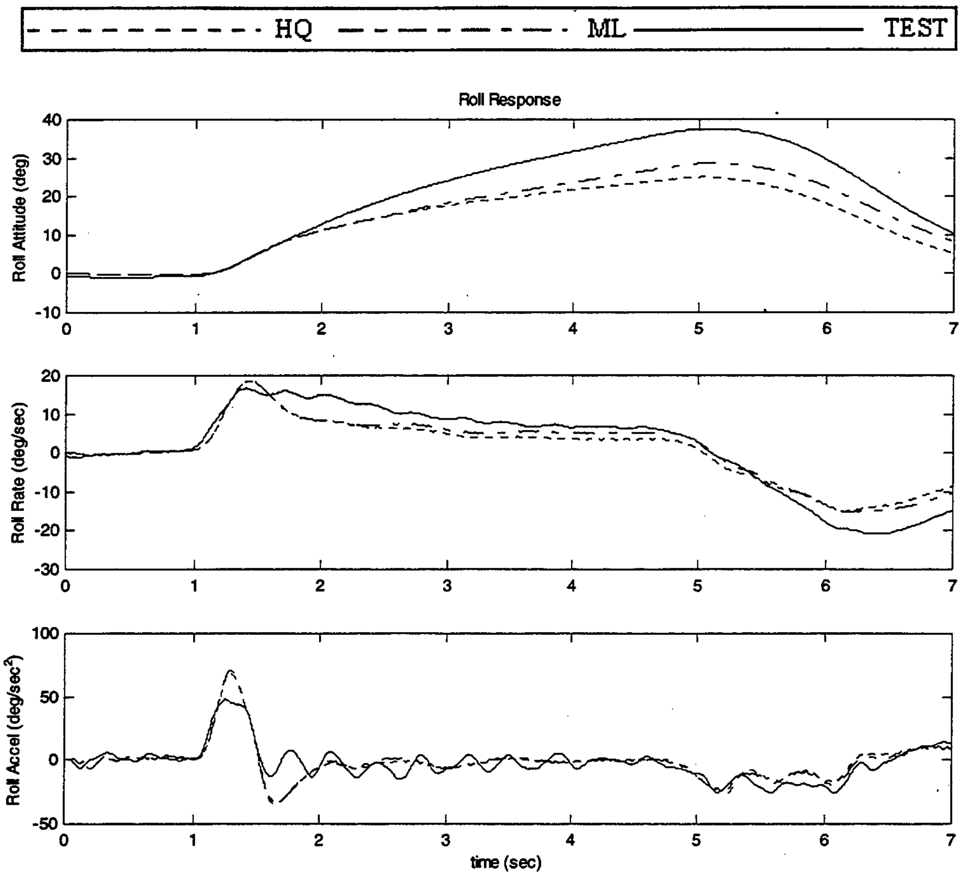

Figure 61 Flight 953-795 Run 049 On-Axis Response 22000, FSCG 360, 3000 ft DA

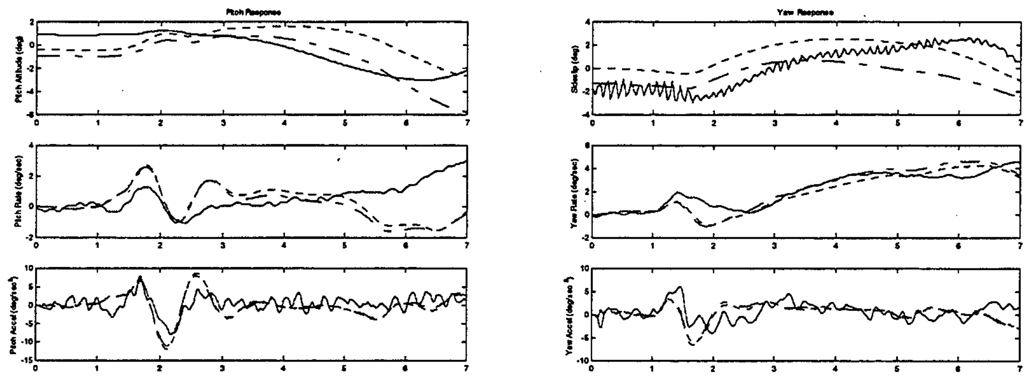

Figure 62 Flight 953-795 Run 049 Off-Axis Response 22000, FSCG 360, 3000 ft DA

d. *Forward Longitudinal Pulse, Flight 953-795 Run 083*

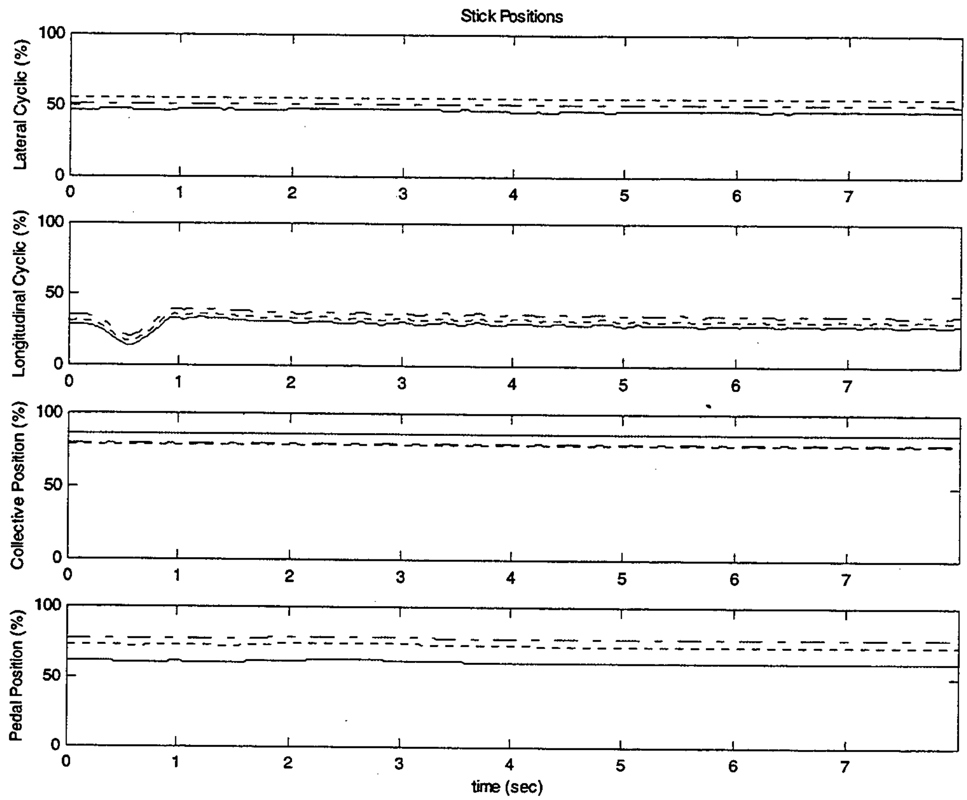

Figure 63 Flight 953-795 Run 083 Stick Positions 22000, FSCG 360, 3000 ft DA

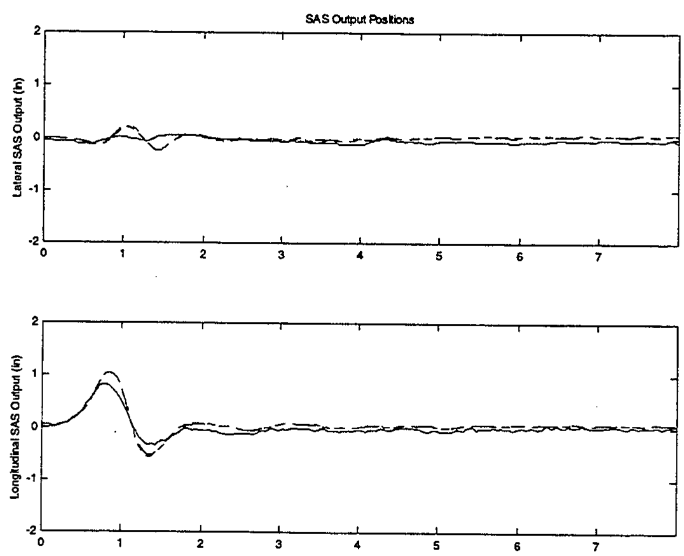

Figure 64 Flight 953-795 Run 083 SAS Positions 22000, FSCG 360, 3000 ft DA

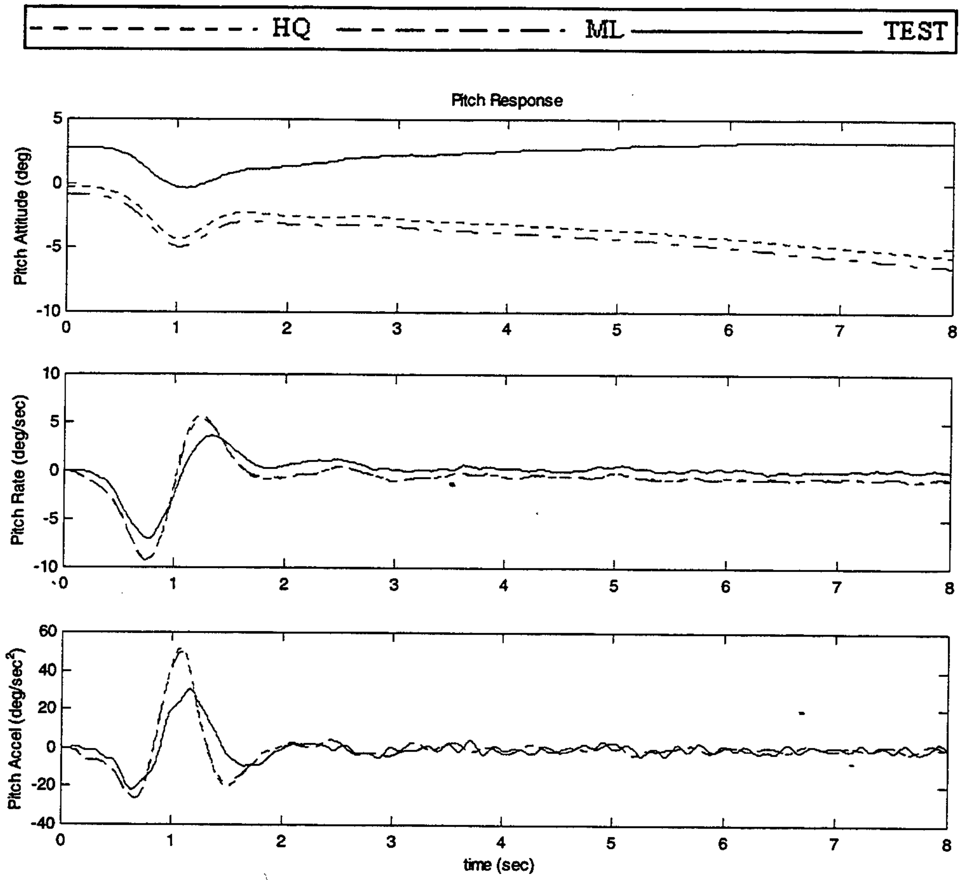

Figure 65 Flight 953-795 Run 083 On-Axis Response 22000, FSCG 360, 3000 ft DA

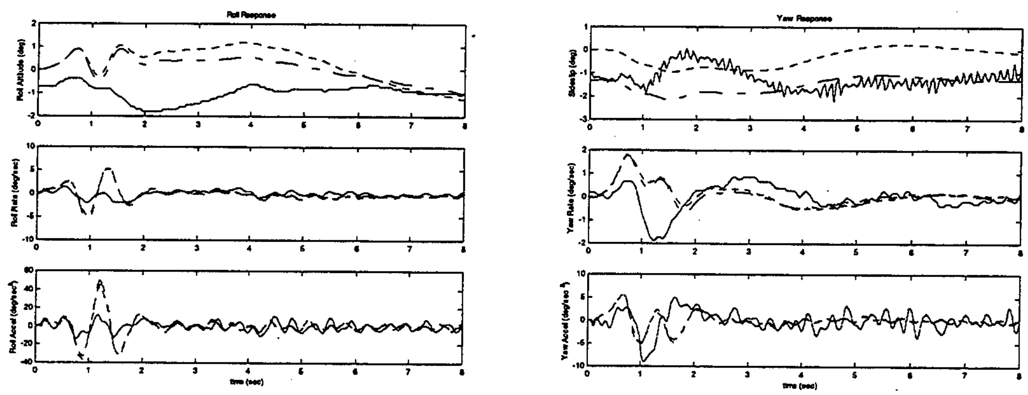

Figure 66 Flight 953-795 Run 083 Off-Axis Response 22000, FSCG 360, 3000 ft DA

e. *Aft Longitudinal Pulse, Flight 953-795 Run 086*

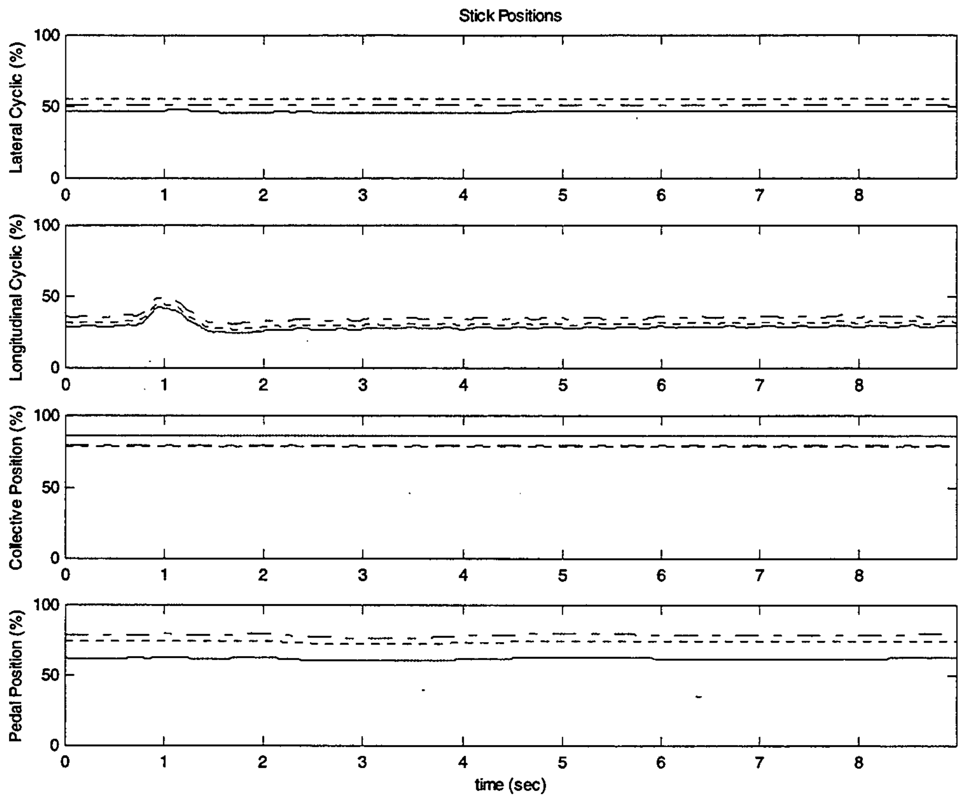

Figure 67 Flight 953-795 Run 086 Stick Positions 22000, FSCG 360, 3000 ft DA

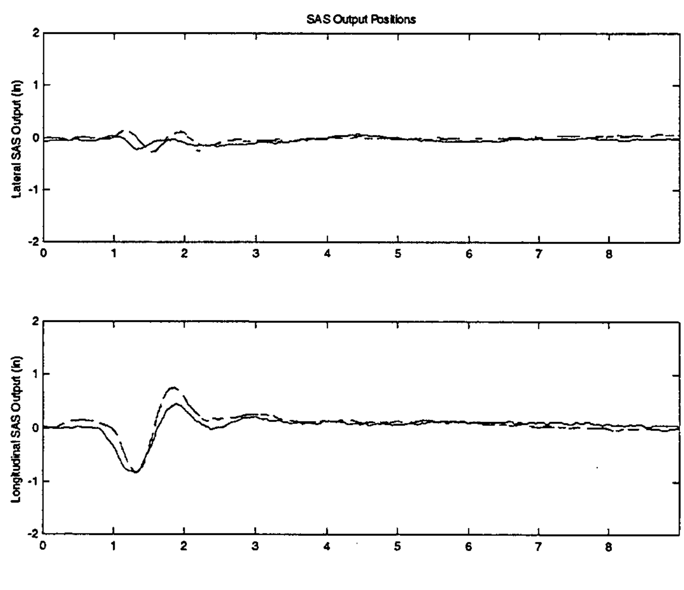

Figure 68 Flight 953-795 Run 086 SAS Positions 22000, FSCG 360, 3000 ft DA

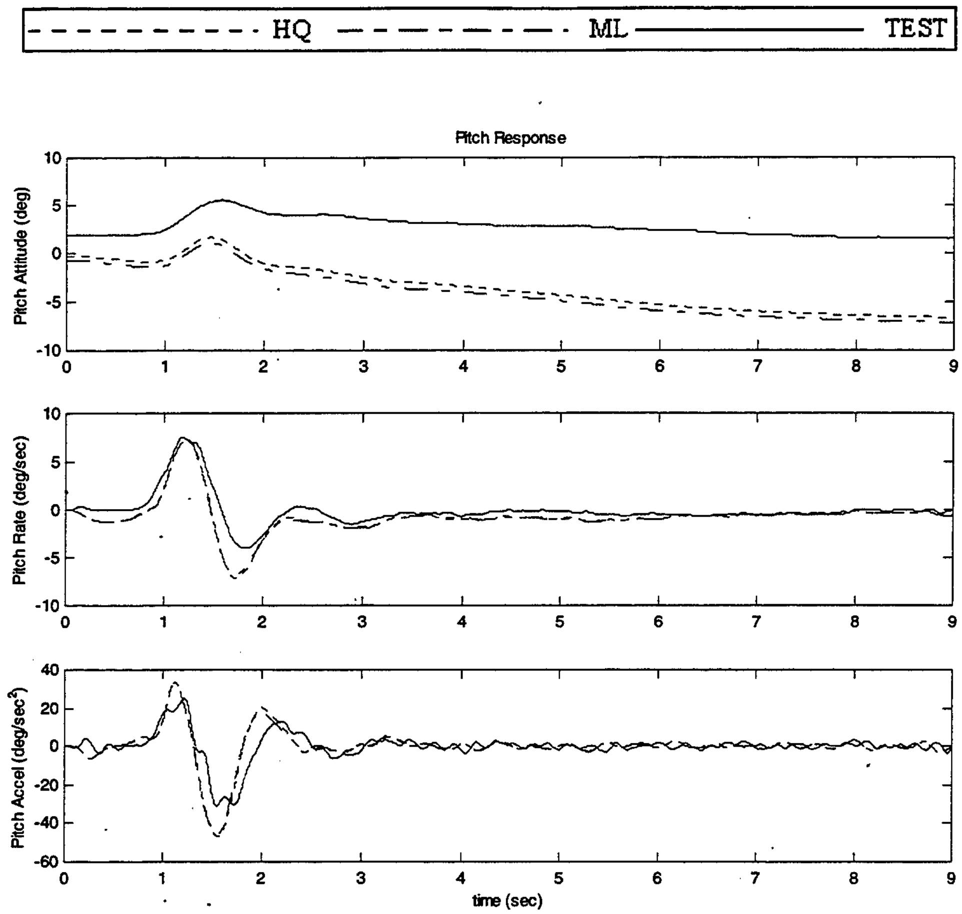

Figure 69 Flight 953-795 Run 086 On-Axis Response 22000, FSCG 360, 3000 ft DA

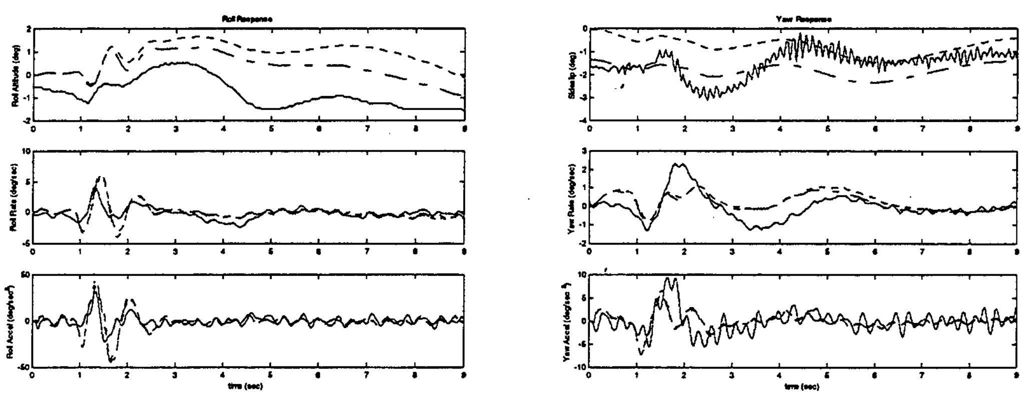

Figure 70 Flight 953-795 Run 086 Off-Axis Response 22000, FSCG 360, 3000 ft DA

f. *Left Lateral Pulse, Flight 953-795 Run 089*

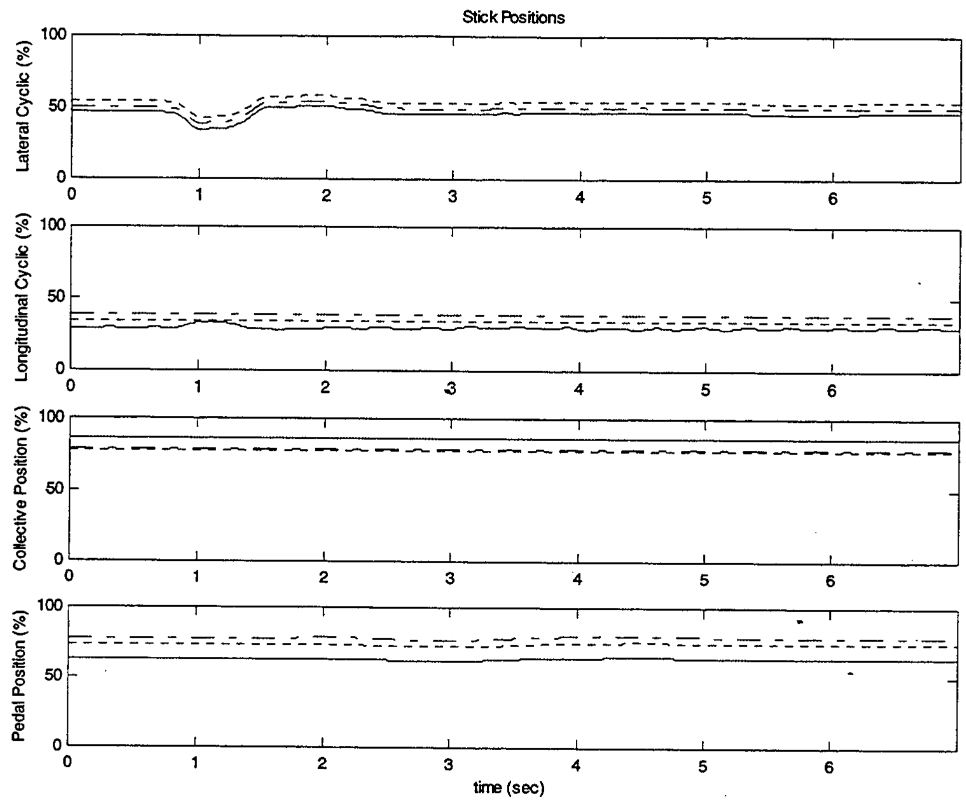

Figure 71 Flight 953-795 Run 089 Stick Positions 22000, FSCG 360, 3000 ft DA

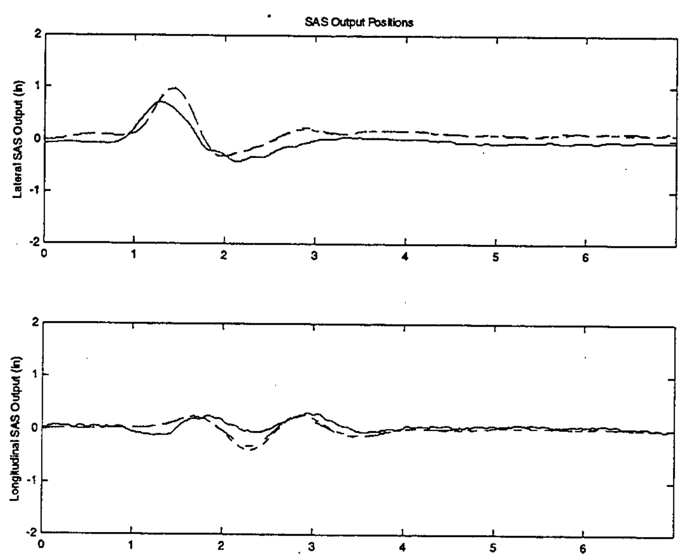

Figure 72 Flight 953-795 Run 089 SAS Positions 22000, FSCG 360, 3000 ft DA

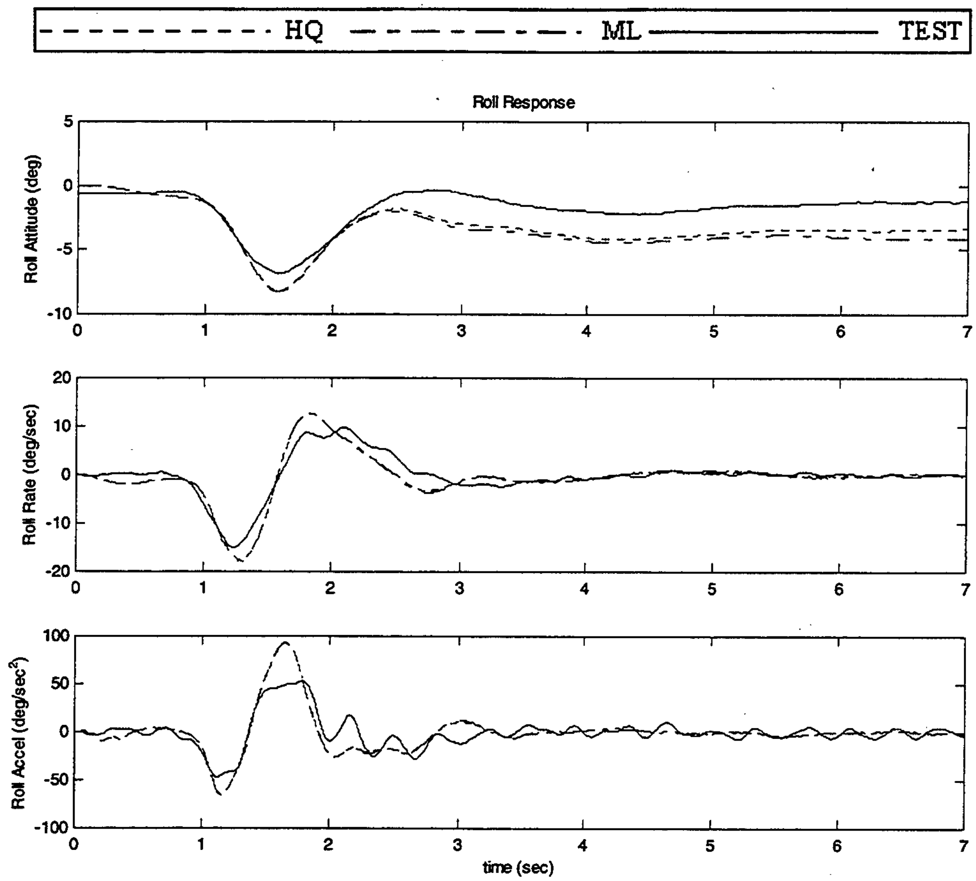

Figure 73 Flight 953-795 Run 089 On-Axis Response22000, FSCG 360, 3000 ft DA

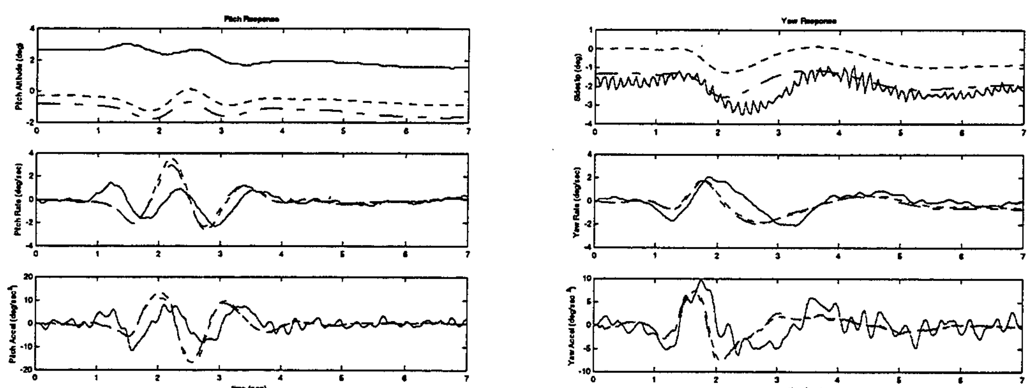

Figure 74 Flight 953-795 Run 089 Off-Axis Response 22000, FSCG 360, 3000 ft DA

g. *Right Lateral Pulse, Flight 953-795 Run 092*

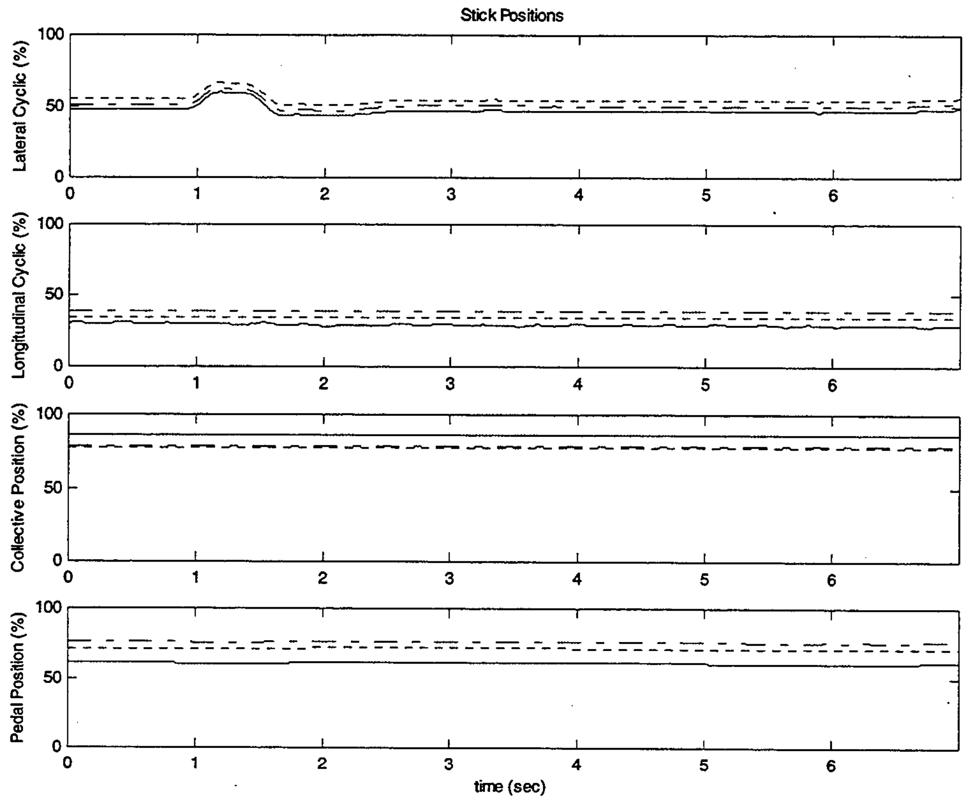

Figure 75 Flight 953-795 Run 092 Stick Positions 22000, FSCG 360, 3000 ft DA

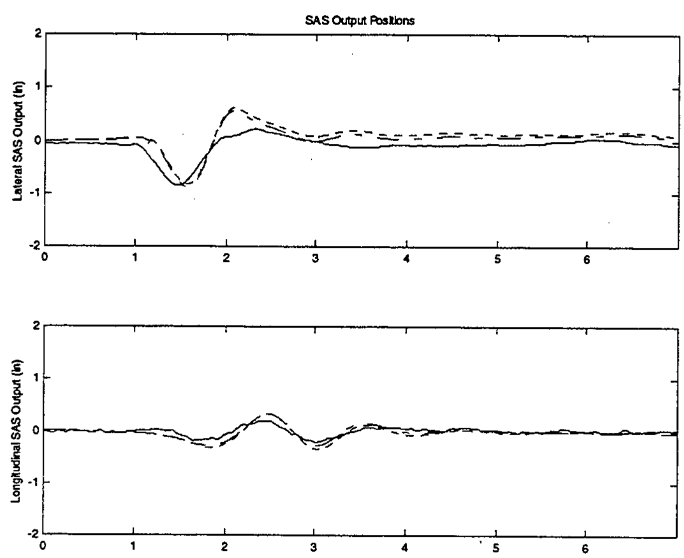

Figure 76 Flight 953-795 Run 092 SAS Positions 22000, FSCG 360, 3000 ft DA

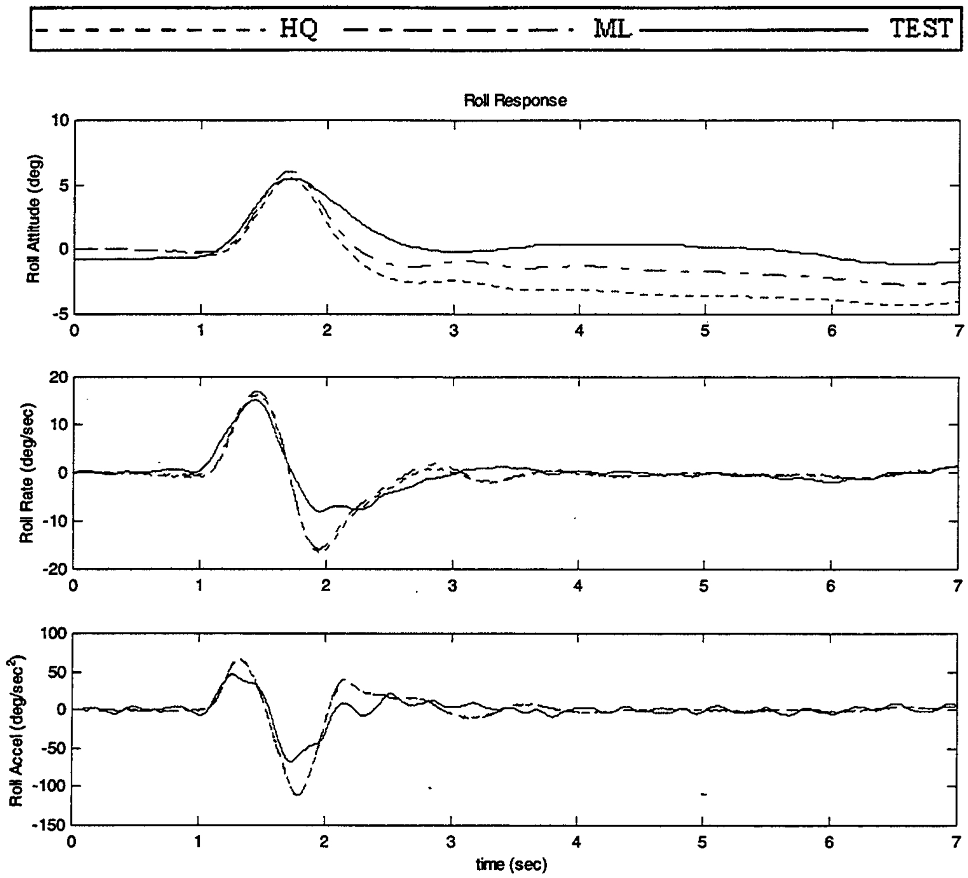

Figure 77 Flight 953-795 Run 092 On-Axis Response 22000, FSCG 360, 3000 ft DA

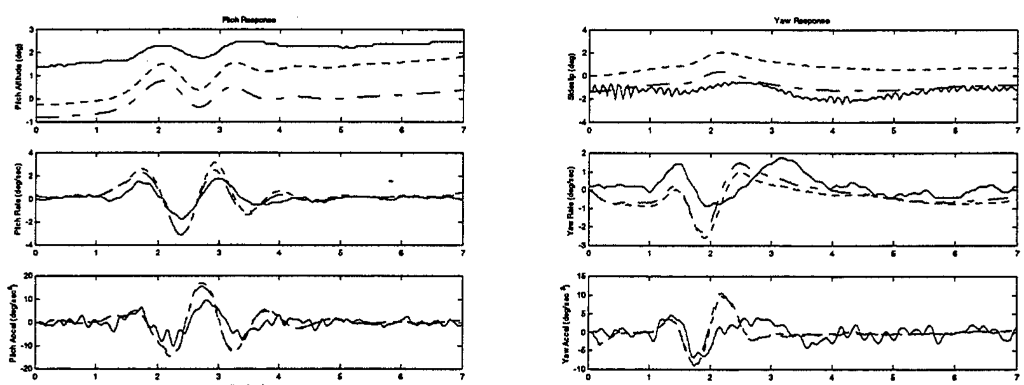

Figure 78 Flight 953-795 Run 092 Off-Axis Response 22000, FSCG 360, 3000 ft DA

THIS PAGE INTENTIONALLY LEFT BLANK

VI. MODIFIED ML MODEL CORRELATION

A. EXPLANATION OF THE MODIFICATIONS

This chapter catalogs the modifications which were made to the ML model in an effort to document the effects on stabilator and main rotor shaft bending moments due to:

1. Downwash correction terms.
2. Forces and moments added as a result of powered wind tunnel tests.
3. Interference on the horizontal tail.

This effort was precipitated by the apparent under prediction of the stabilator bending values by both the HQ and the ML models in trim flight. This entire analysis is hostage to our assumption of uniform lift distribution on the stabilator. Table 6 depicts the terms in question and their GenHel® variable names. All plots examined in this section include the baseline HQ and ML models for reference and comparison.

Table 6 Modification Parameters

Term	Source	Action	GenHel® Variable Name
Downwash Correction Terms on Fuselage	UH-60 / SH-60 Test Data	Side Force	Lodata\YDWCMP
		Rolling Moment	Lodata\LDWCMP
		Pitching Moment	Lodata\MDWCMP
Δ Forces on Fuselage	S-92 Powered Wind Tunnel Tests	Lift Force	Lodata\FL1MAP Lodata\FL2MAP
		Side Force	Lodata\FY1MAP Lodata\FY2MAP
		Rolling Moment	Lodata\FR1MAP Lodata\FR2MAP
		Yawing Moment	Lodata\MRDNQFMP
Horizontal Tail Interference	Test And Theory	Right Panel Velocity	Lodata\DAEPP1MP Lodata\DBEPP1MP
		Left Panel Velocity	Lodata\DAEPP2MP Lodata\DBEPP2MP

The effects of the forces added from S-92 powered wind tunnel test were negligible and thus attention was focused on the downwash correction terms and the horizontal tail interference. Figure 79 depicts the effects of separately removing the downwash correction terms and the stabilator interference terms on the main rotor shaft

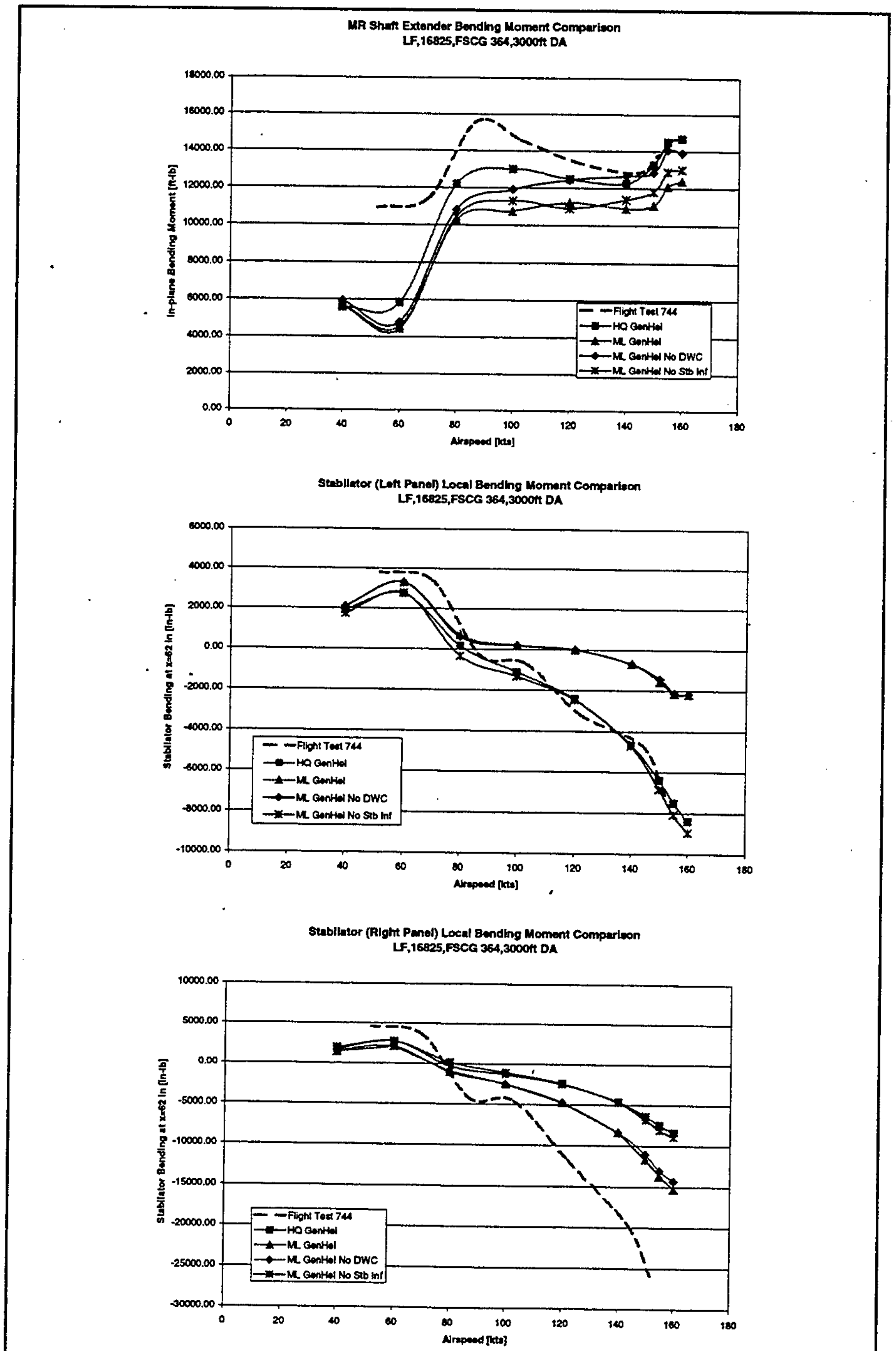

Figure 79 Baseline Removal of Downwash Correction Terms and Stabilator Interference

bending and the stabilator bending to establish a baseline for further analysis.

Figure 79 shows that the baseline ML model (with downwash correction terms) has the same stabilator bending values as the ML model with the downwash correction terms removed. There is, however, a difference in the main rotor shaft bending. The impact of the downwash correction terms is witnessed at the main rotor shaft, where the bending values for the model without the downwash correction terms are higher than that of the baseline ML model at high speed. The downwash correction terms essentially lower main rotor shaft bending values without effecting stabilator bending.

The left panel stabilator values correlate well with the stabilator interference velocities removed. If our assumption of uniform lift distribution was correct, then GenHel® still under-predicts the download seen on the right panel.

The second round of investigations involved removing the stabilator interference velocities from the left panel and observing increasing values of right panel stabilator interference. Figure 80 shows the results of this analysis. As expected, as the interference velocities are increased over the right panel, the stabilator bending values increase, inducing an increase in the main rotor shaft bending moment. Increasing the stabilator interference velocity by a factor of two brought the right stabilator panel bending moment to a close correlation with the test data. In doing so, however, the main rotor shaft bending values increased beyond an acceptable limit.

The next investigation examines the effects of changing the magnitudes of the downwash correction terms on the main rotor shaft bending moment. Figure 81 depicts the results. Increasing the pitching moment downwash term (MDWCMP) decreases the bending at the main rotor shaft without changing the loads seen by the stabilator. However, no physics-based justification for this change can be provided. For the purposes of this report, the values depicted graphically as 1.5 x MDWCMP (-75 ft^3 from baseline) are used for MDWCMP in order to achieve a better correlation.

The last modification was an increase in 2 square feet of fuselage drag to account for test equipment external to the aircraft. In summary, the final Modified ML Model used no left stabilator interference, twice the baseline value of right stabilator

interference, -75 ft^3 MDWCMP, and increased the fuselage flat plate area by 2 square feet. The GenHel® command file used to trim the Mod ML model is located in Appendix A.

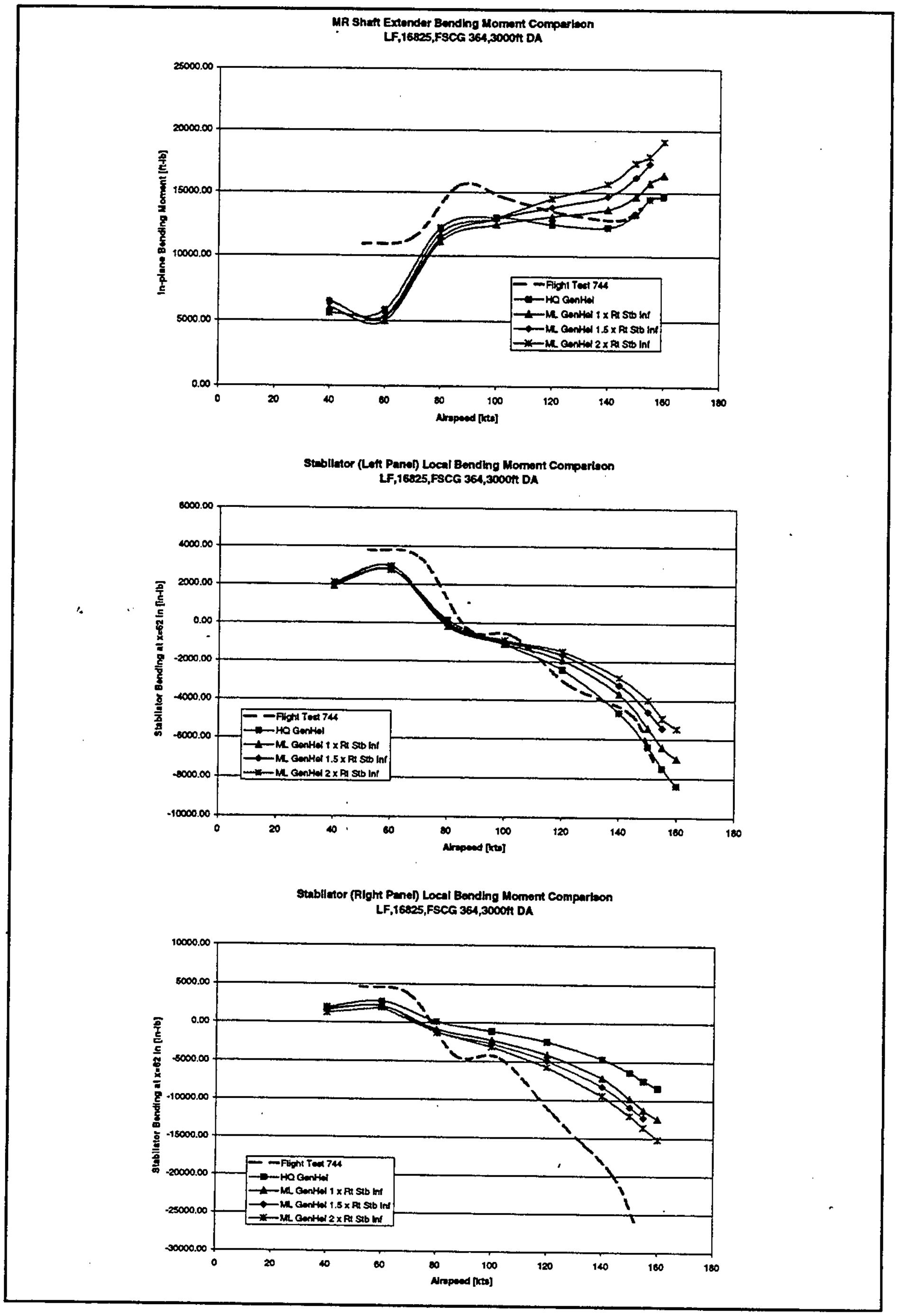

Figure 80 Increasing Right Panel Interference, Left Panel Interference Removed

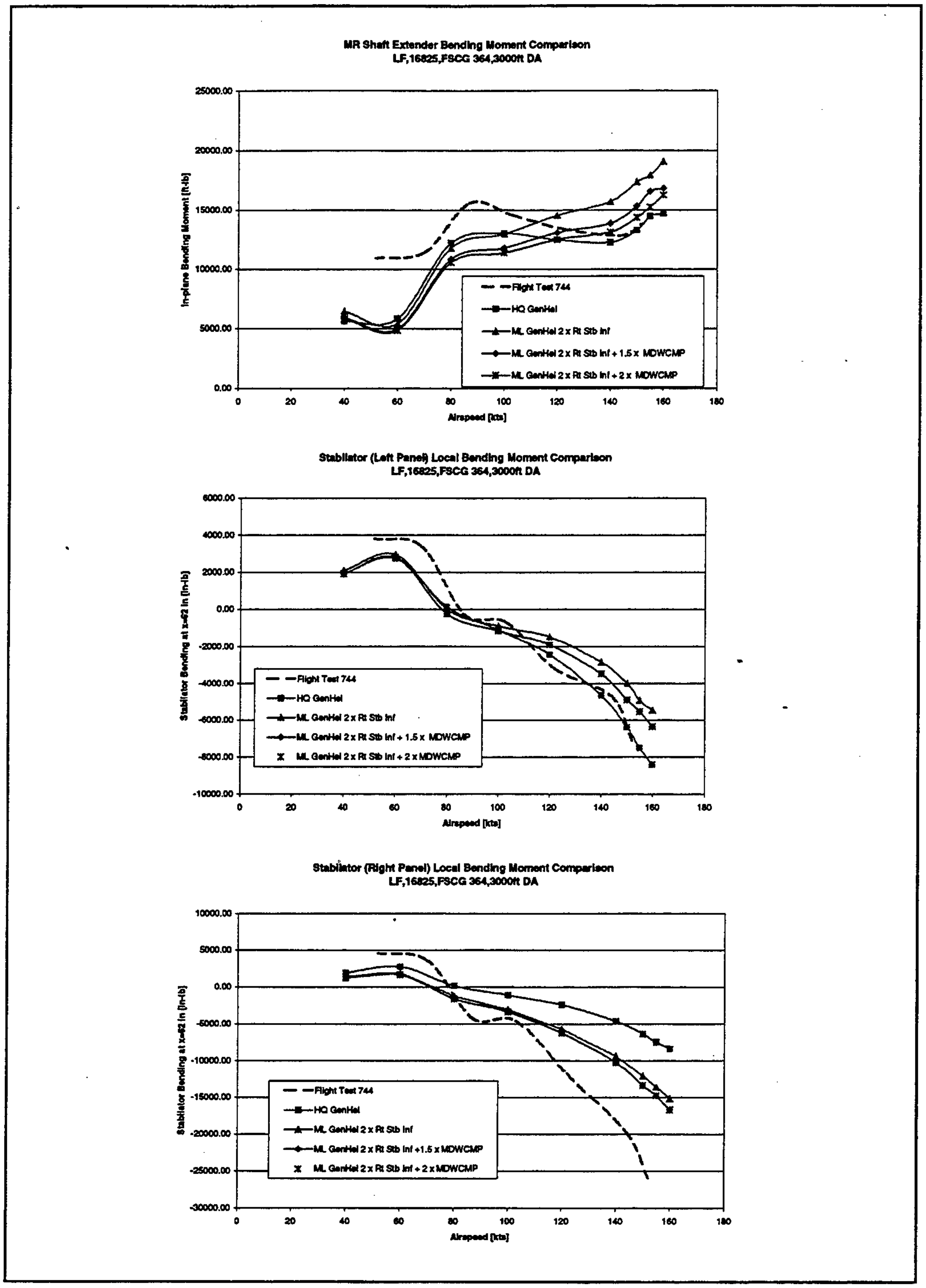

Figure 81 Modified Down Wash Correction Terms

The following sections correlate the Mod ML model in a manner similar to the HQ and ML models.

B. TRIM CORRELATION

In all areas but main rotor shaft bending and stabilator bending the Mod ML model values closely mirror those of the HQ and ML models. As described in the previous section, the modifications created the desired increase in the stabilator bending moment. The resultant increase in main rotor shaft bending was partially offset by the modification to the pitching moment portion of the downwash correction. Clearly a better picture of the flow over the stabilator and in the rotor wake is required to justify these changes.

1. Modified Level Flight Trim Plots GW 16825 lb, FSCG 364, 3000 ft DA

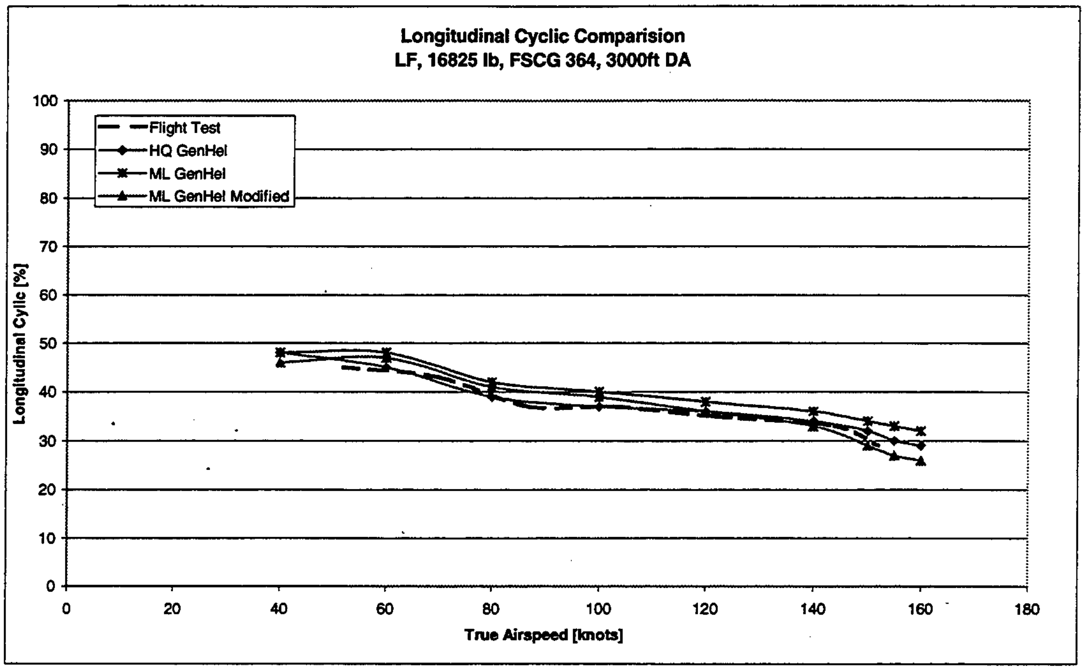

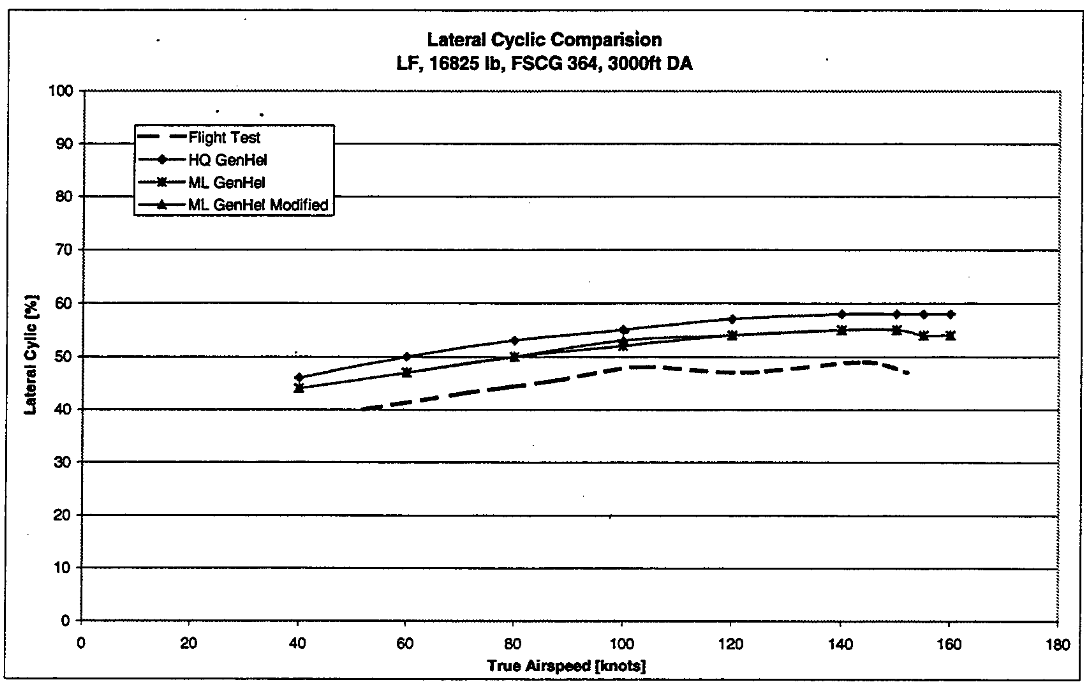

Figure 82 Modified Trim LF Cyclic Comparison 16825 lb, FSCG 364 in, 3000 ft DA

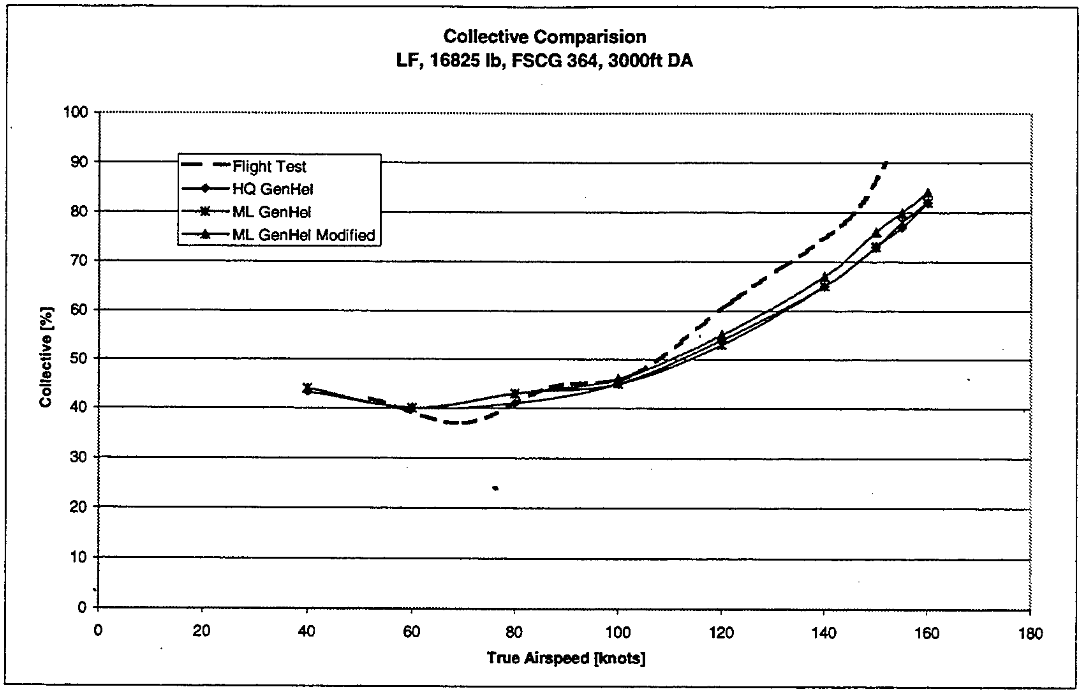

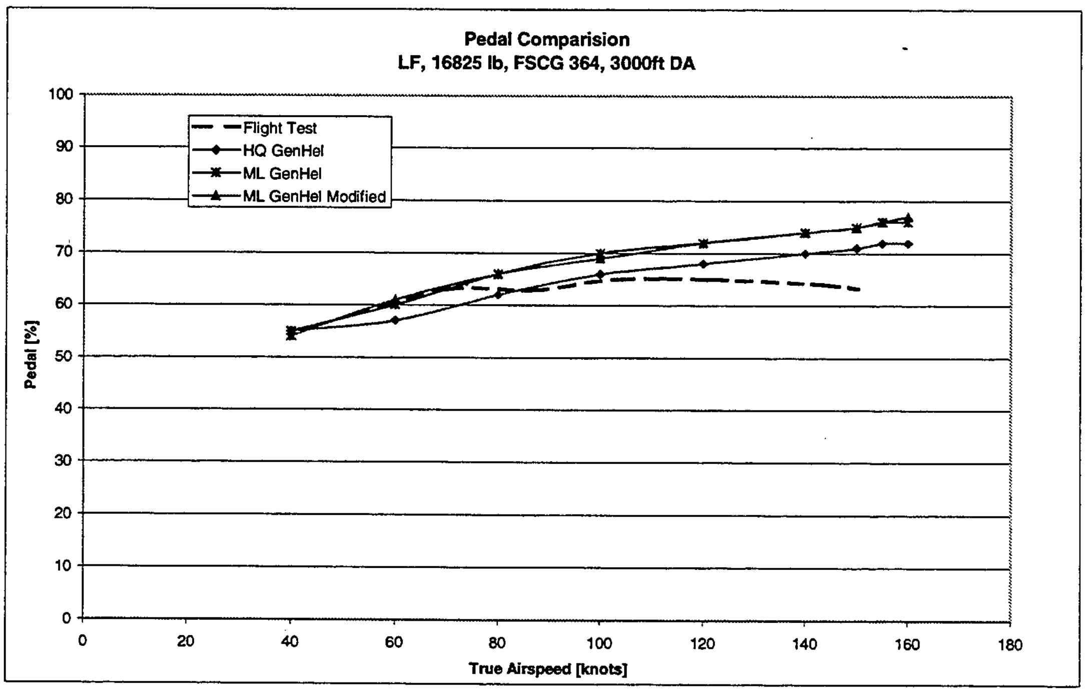

Figure 83 Modified Trim LF Collective and Pedal Comparison 16825 lb, FSCG 364 in, 3000 ft DA

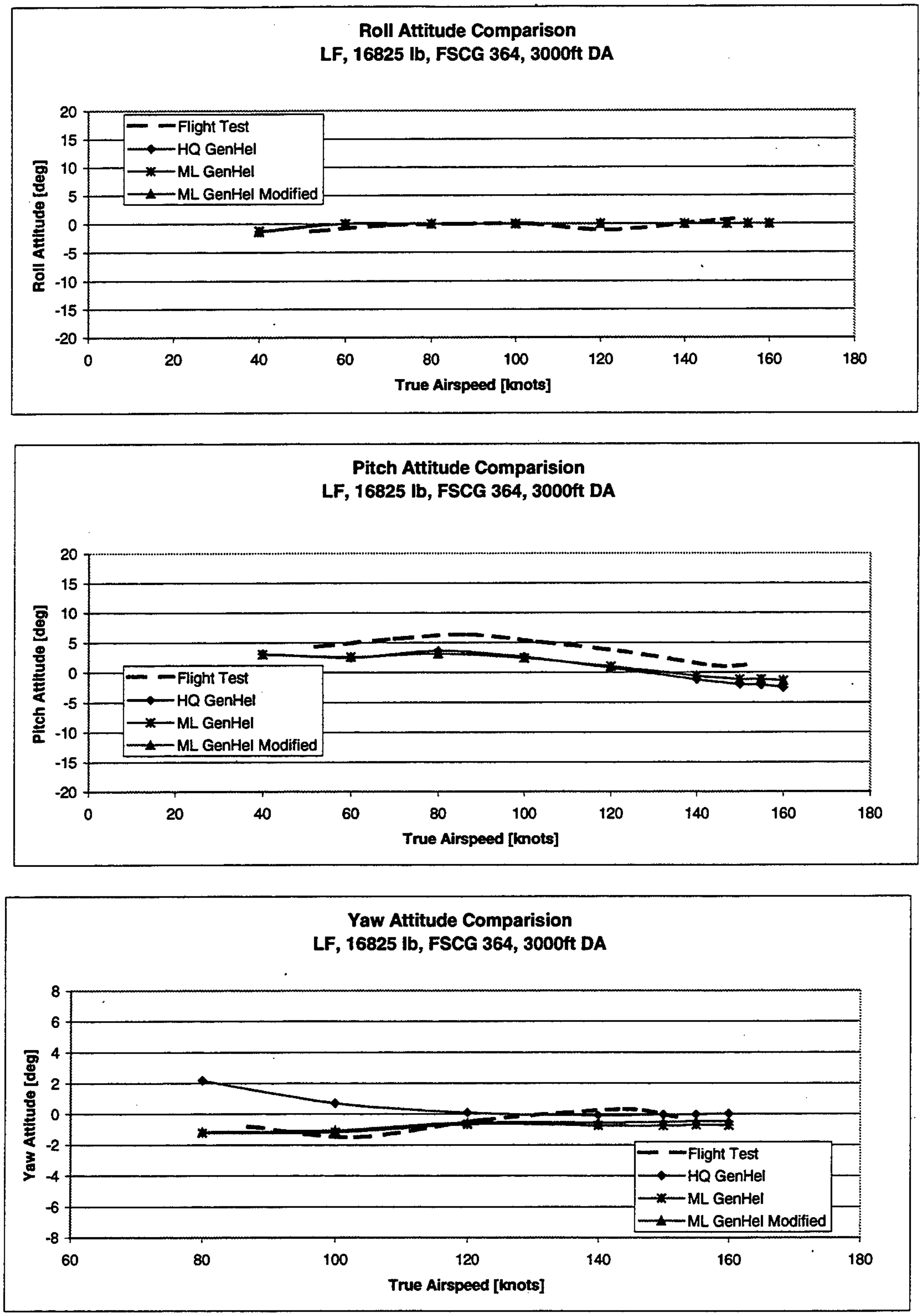

Figure 84 Modified Trim LF Attitude Comparison 16825 lb, FSCG 364 in, 3000 ft DA

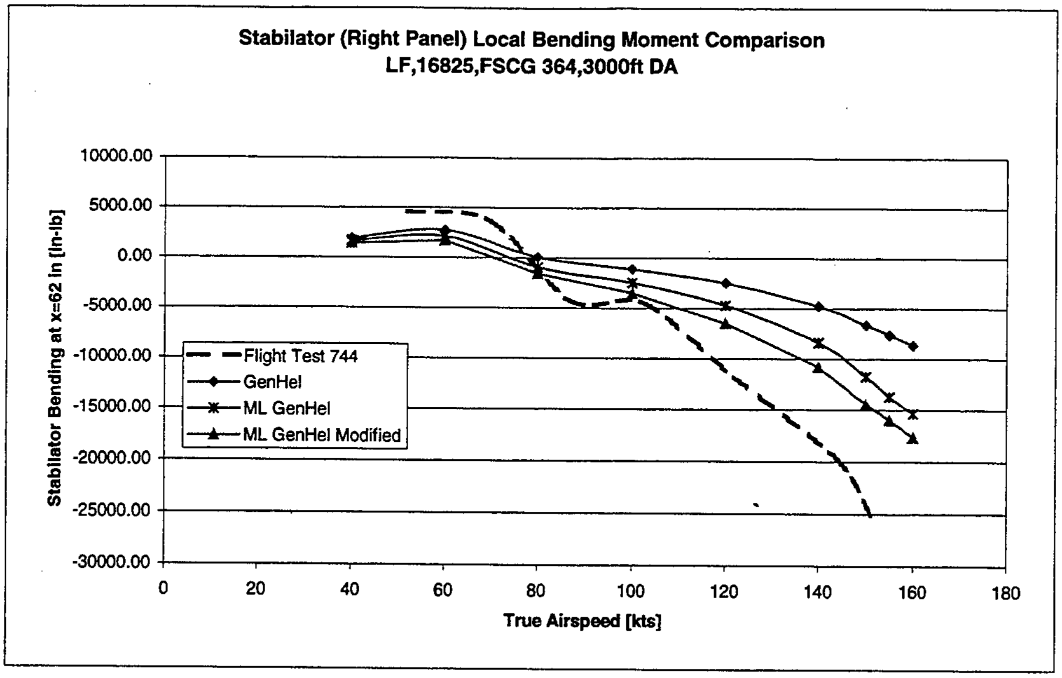

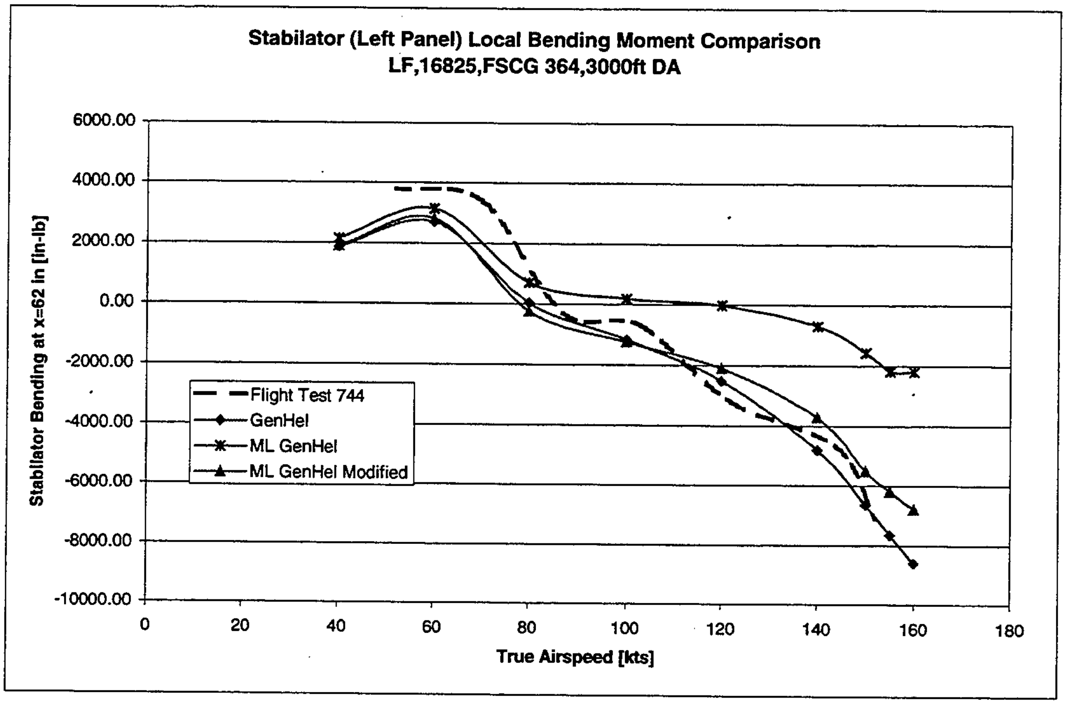

Figure 85 Modified Trim LF Stabilator Bending Comparison 16825 lb, FSCG 364 in, 3000 ft DA

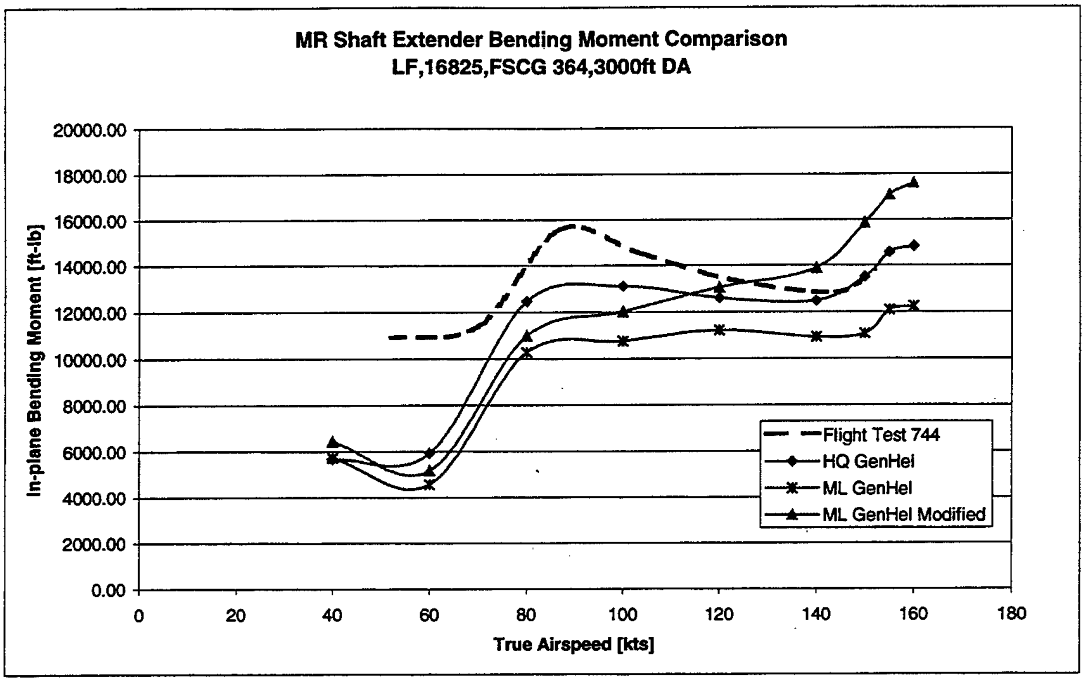

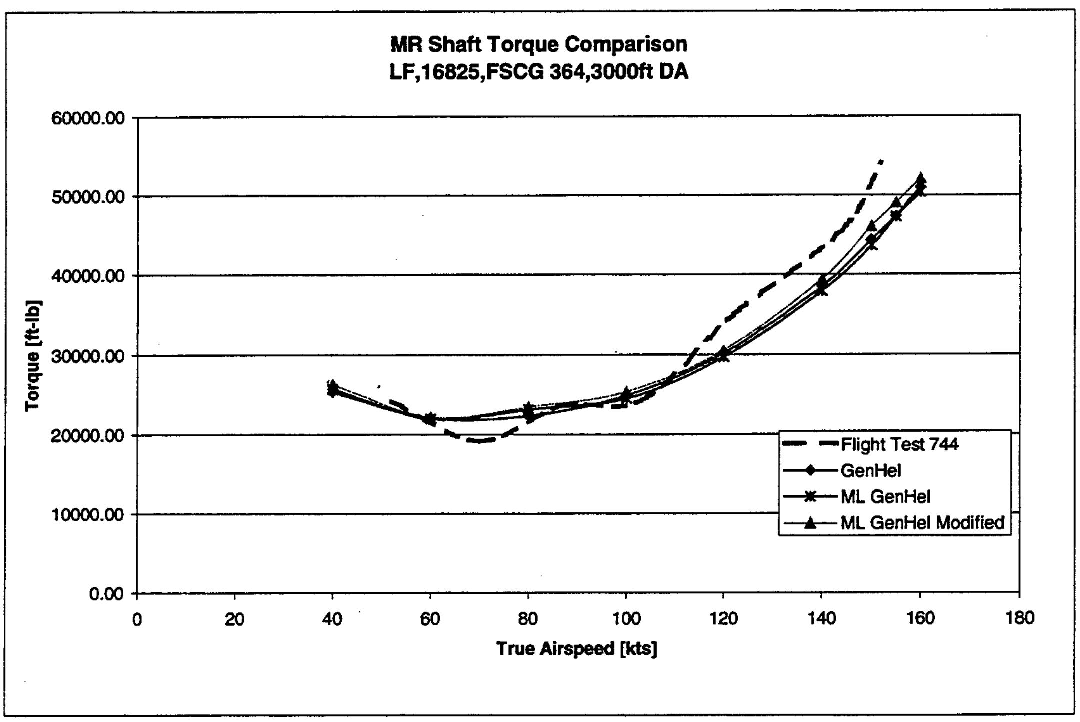

Figure 86 Modified Trim LF MR Shaft Moment Comparison 16825 lb, FSCG 364 in, 3000 ft DA

2. Modified Level Flight Trim Plots GW 22000 lb, FSCG 360, 3000 ft DA

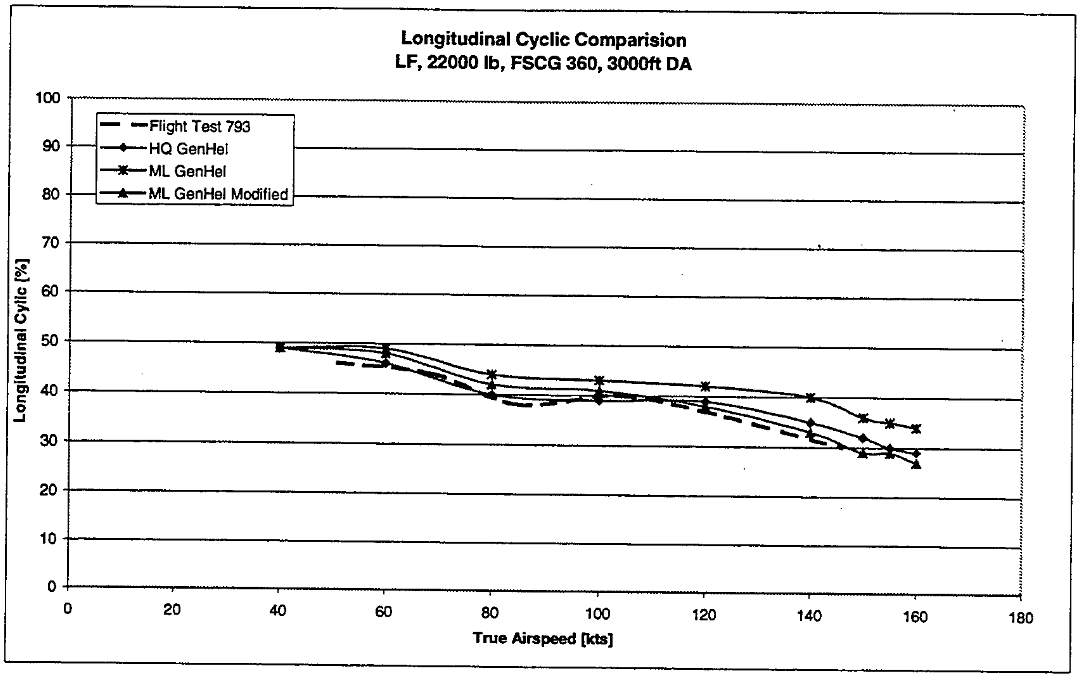

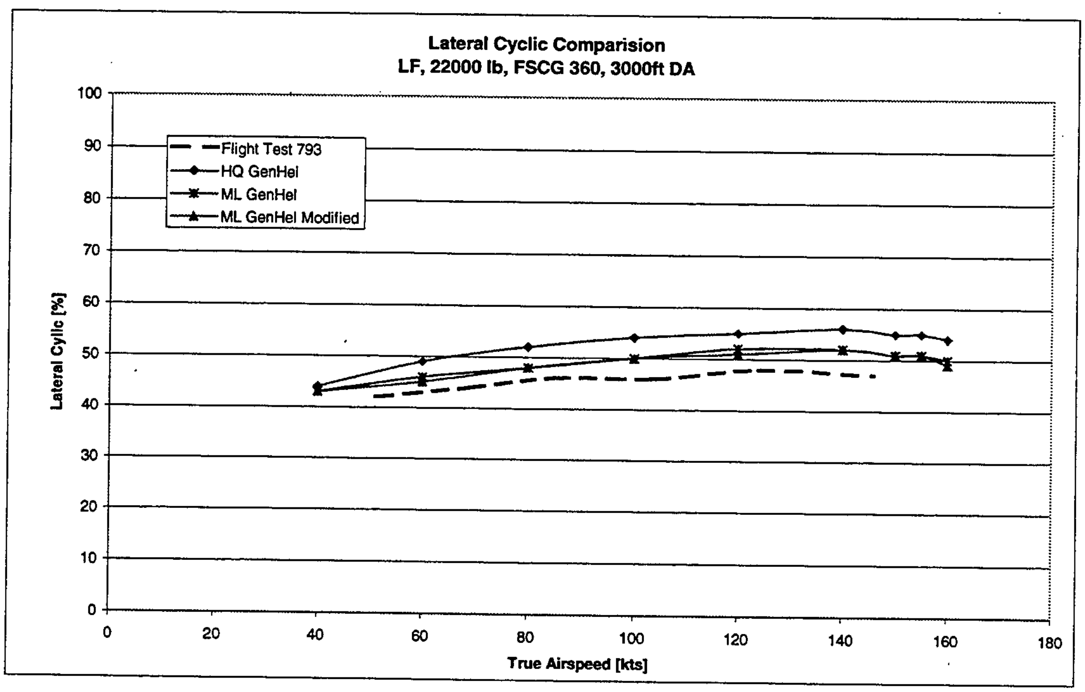

Figure 87 Modified Trim LF Cyclic Comparison 22000 lb, FSCG 360 in, 3000 ft DA

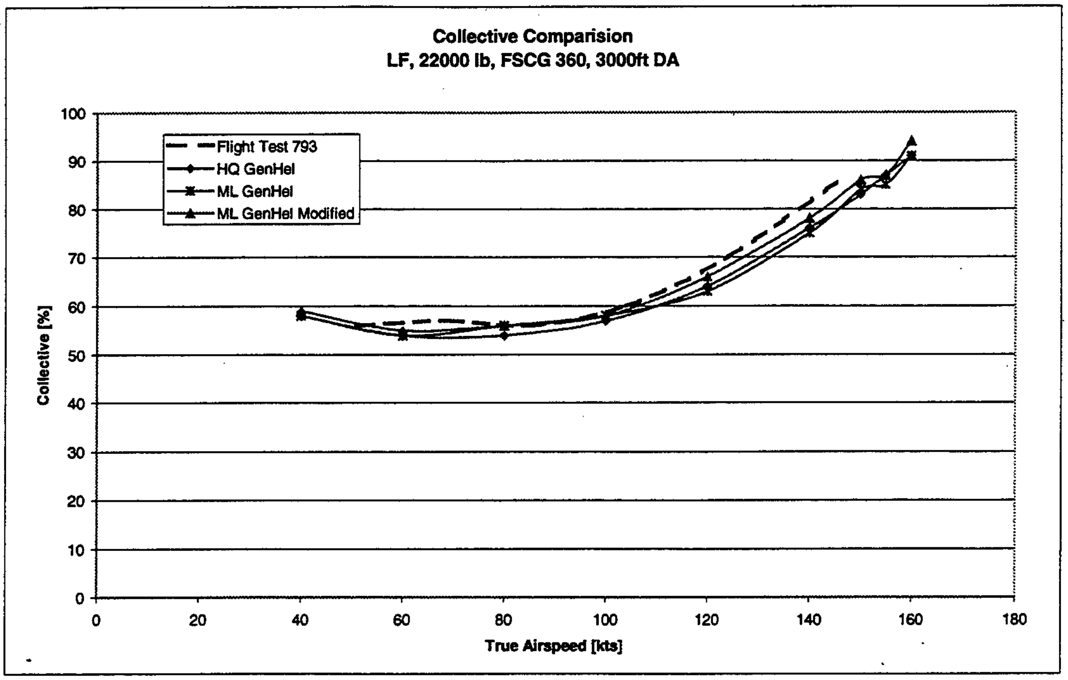

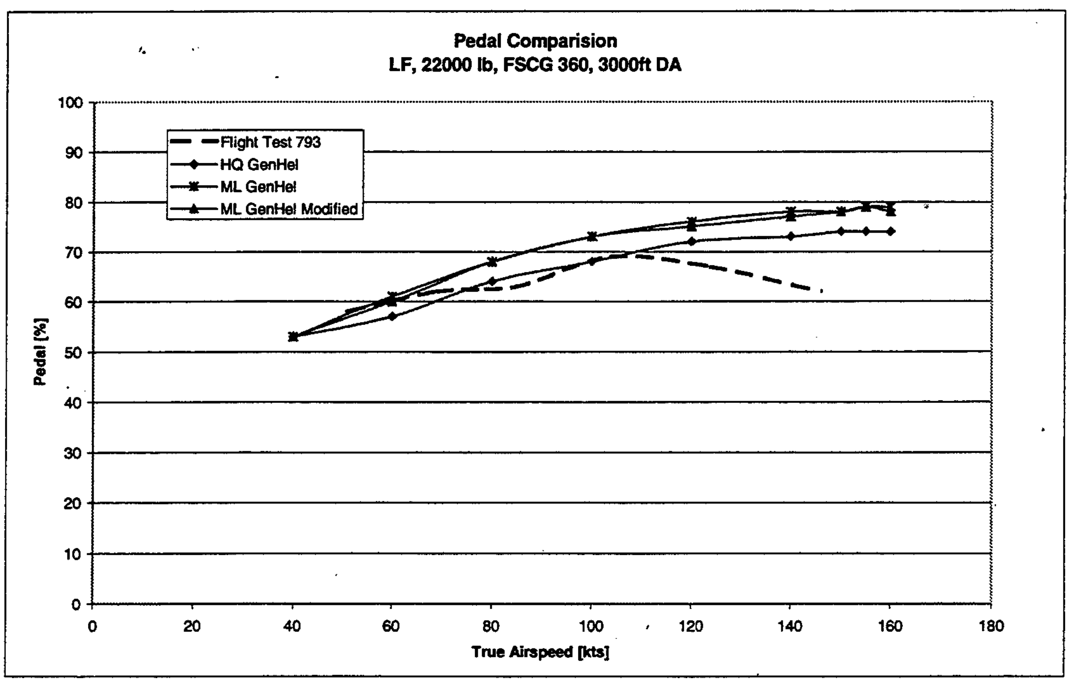

Figure 88 Modified Trim LF Collective and Pedal Comparison 22000 lb, FSCG 360 in, 3000 ft DA

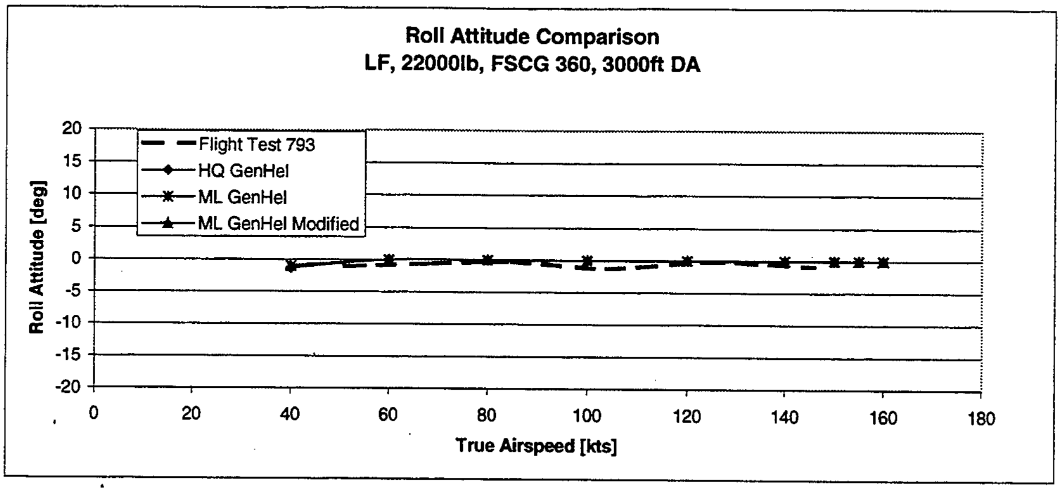

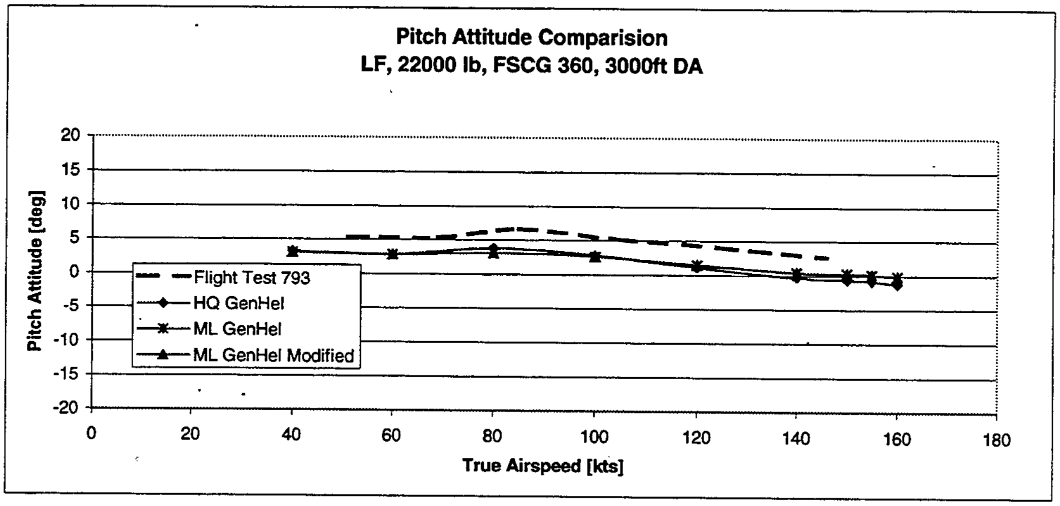

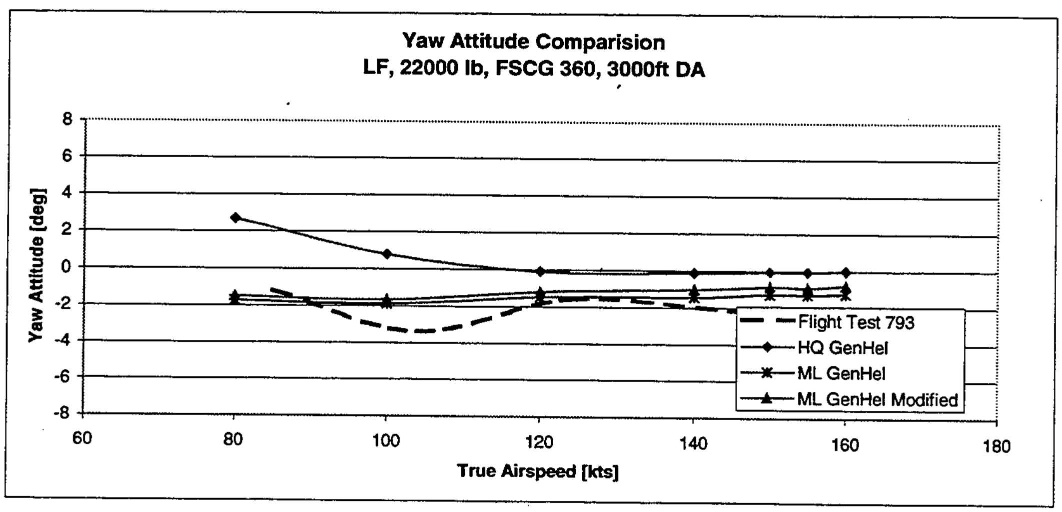

Figure 89 Modified Trim LF Attitude Comparison 22000 lb, FSCG 360 in, 3000 ft DA

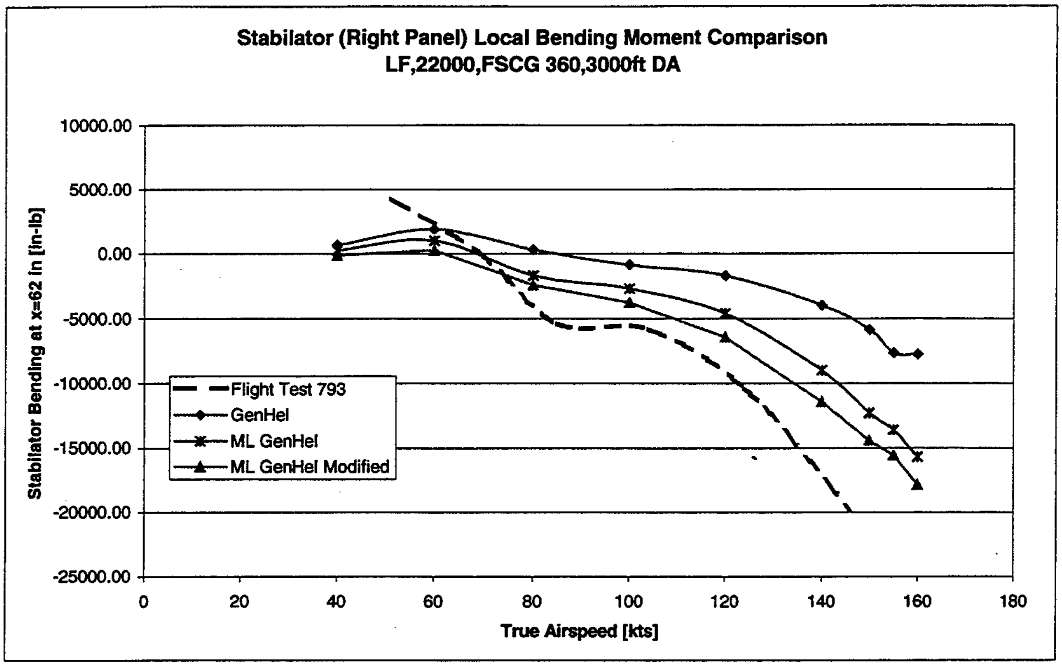

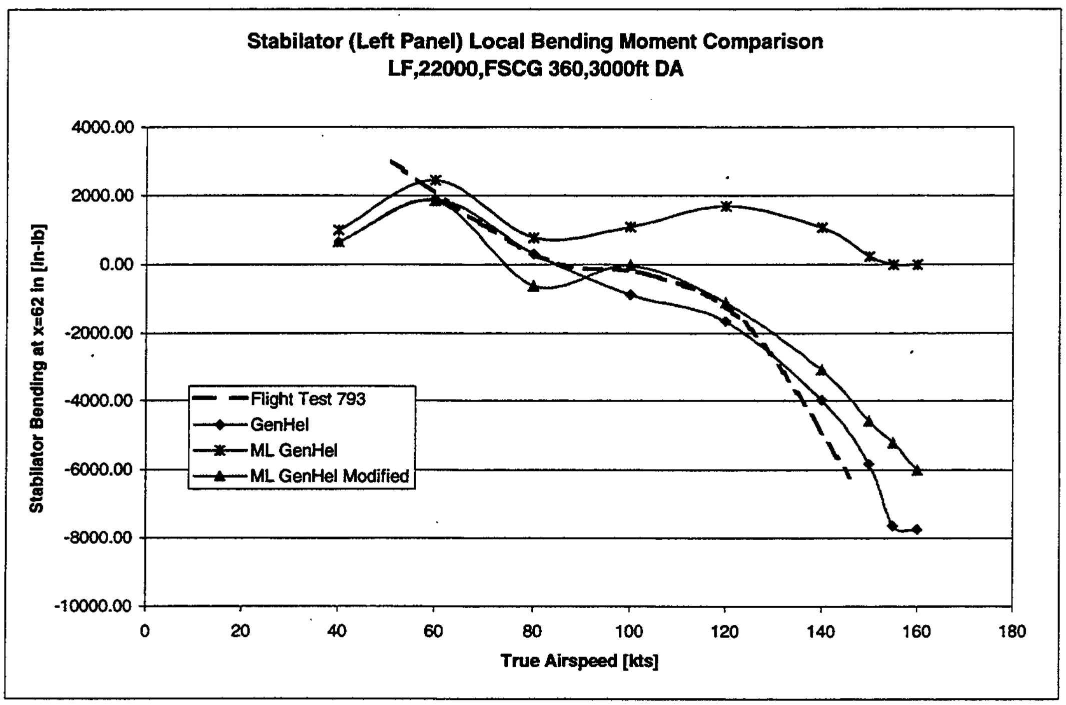

Figure 90 Modified Trim LF Stabilator Bending Comparison 22000 lb, FSCG 360 in, 3000 ft DA

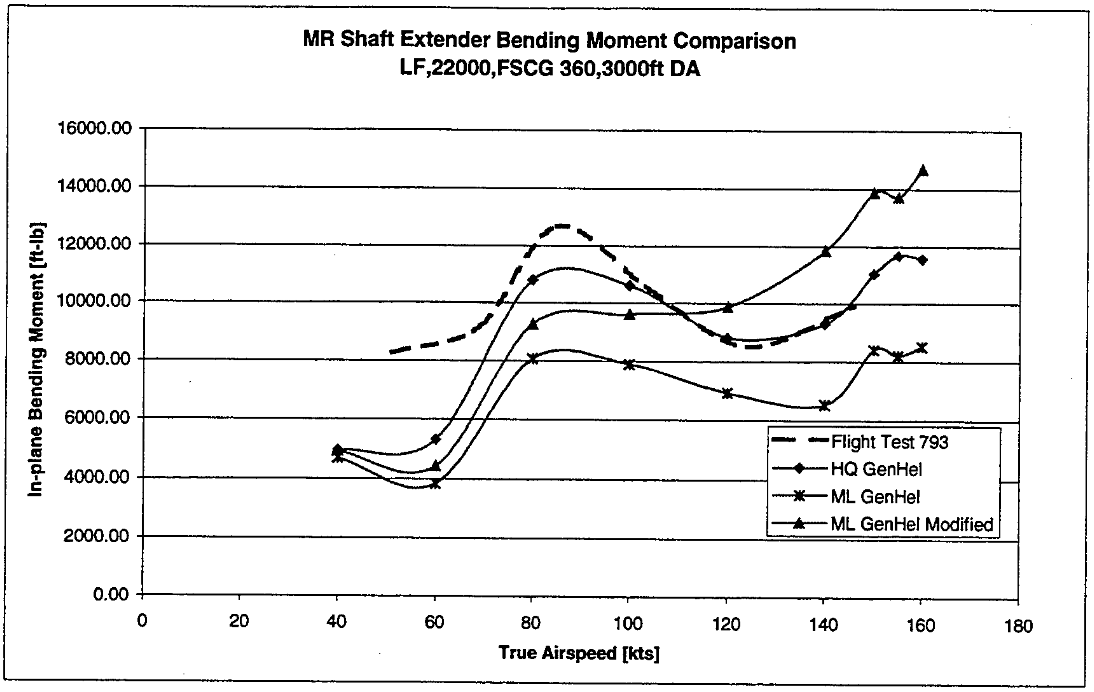

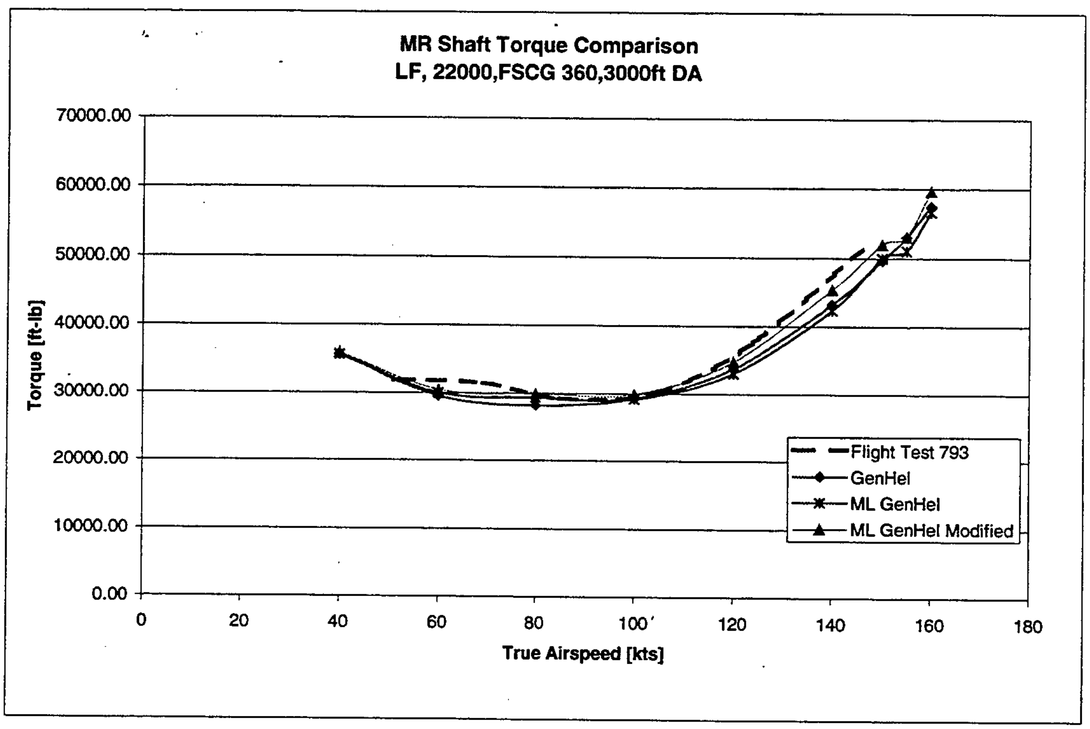

Figure 91 Modified Trim LF MR Shaft Moment Comparison 22000 lb, FSCG 360 in, 3000 ft DA

3. Modified Turning Flight Trim Plots 16825 lb, FSCG 364, 3000 ft DA

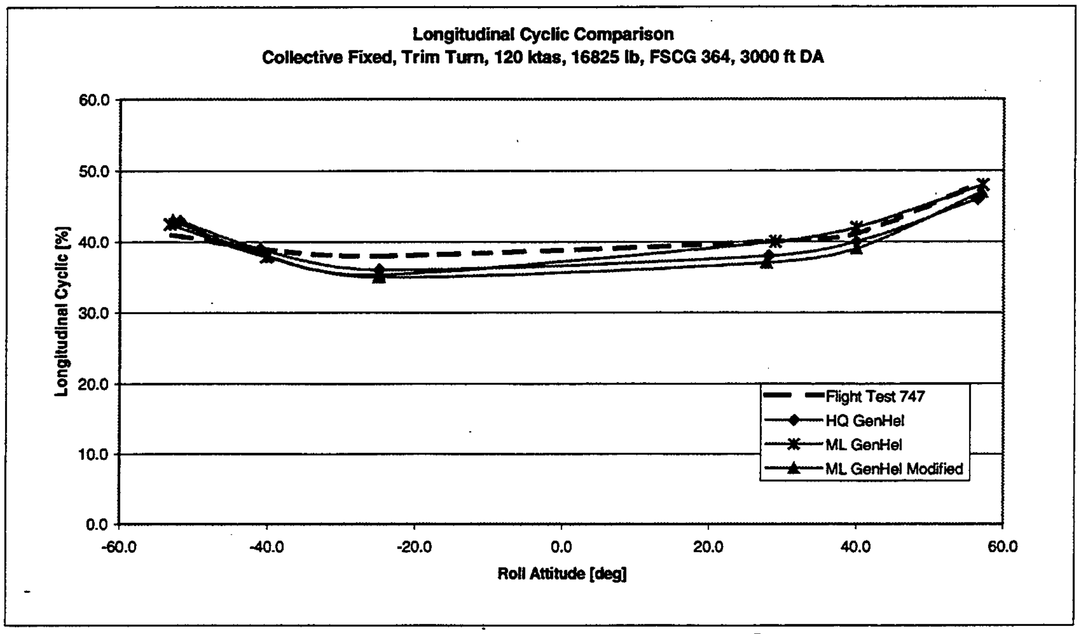

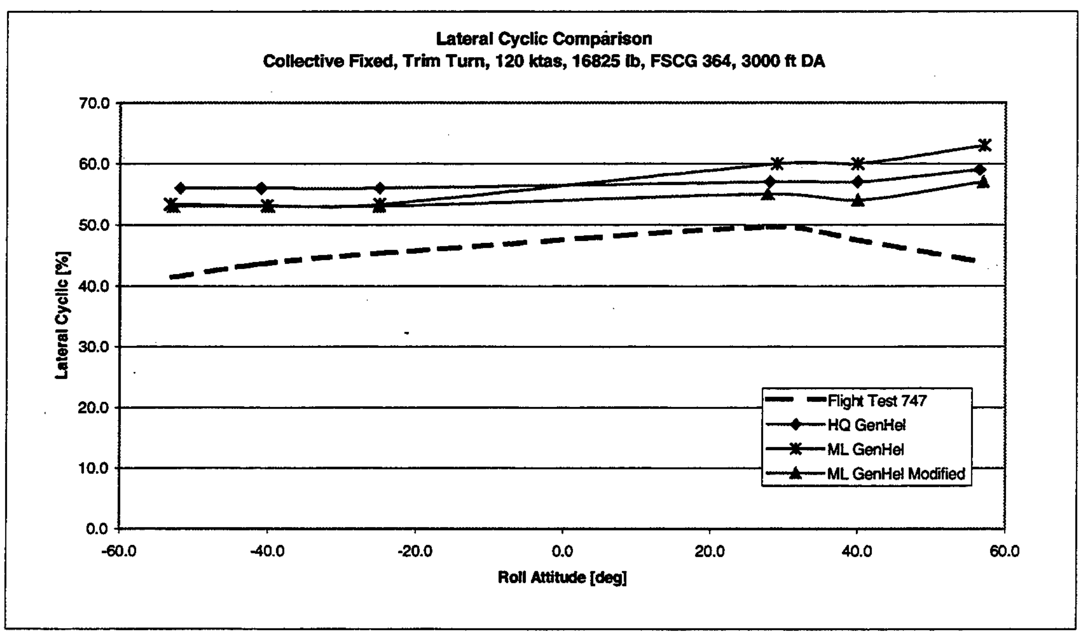

Figure 92 Modified Trim Turn Cyclic Comparison 16825 lb, FSCG 364 in, 3000 ft DA

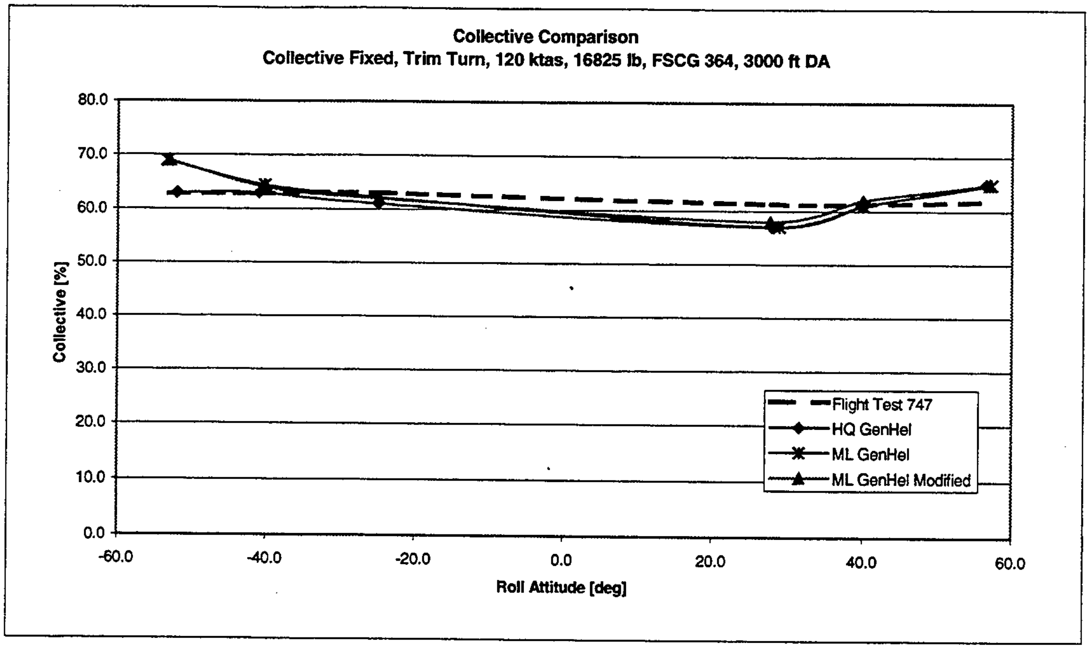

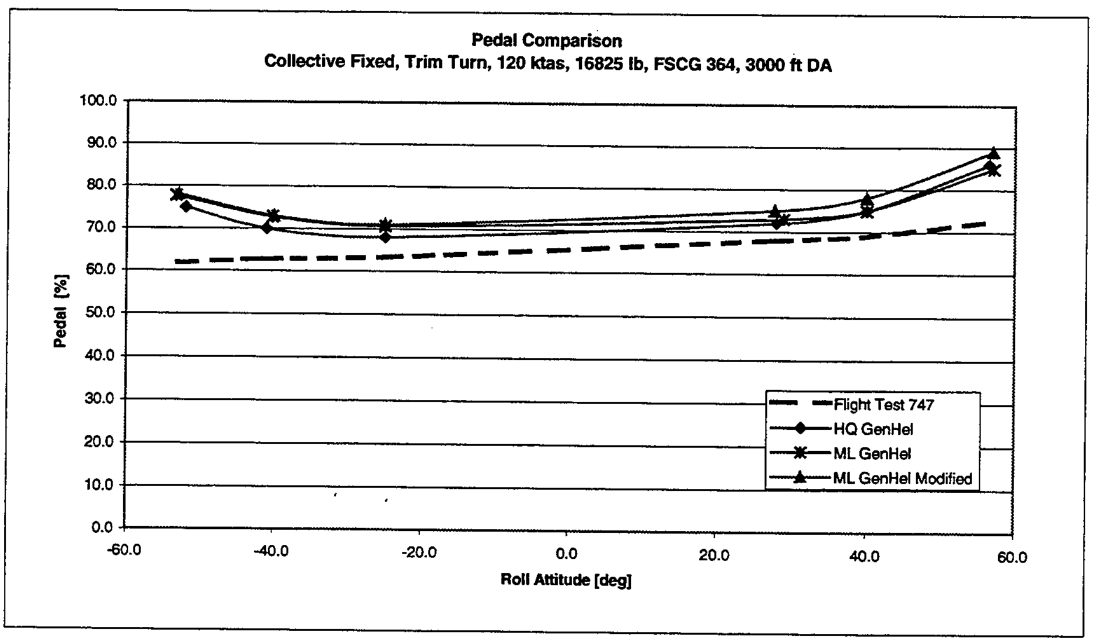

Figure 93 Modified Trim Turn Collective and Pedal Comparison 16825 lb, FSCG 364 in, 3000 ft DA

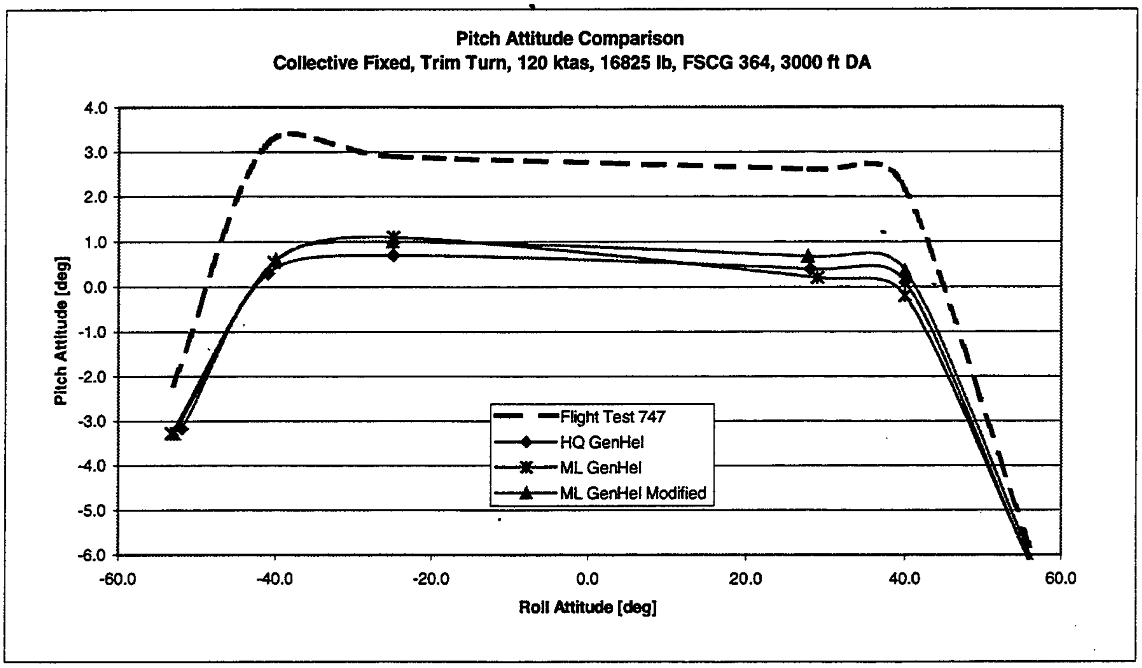

Figure 94 Modified Trim Turn Pitch Attitude Comparison 16825 lb, FSCG 364 in, 3000 ft DA

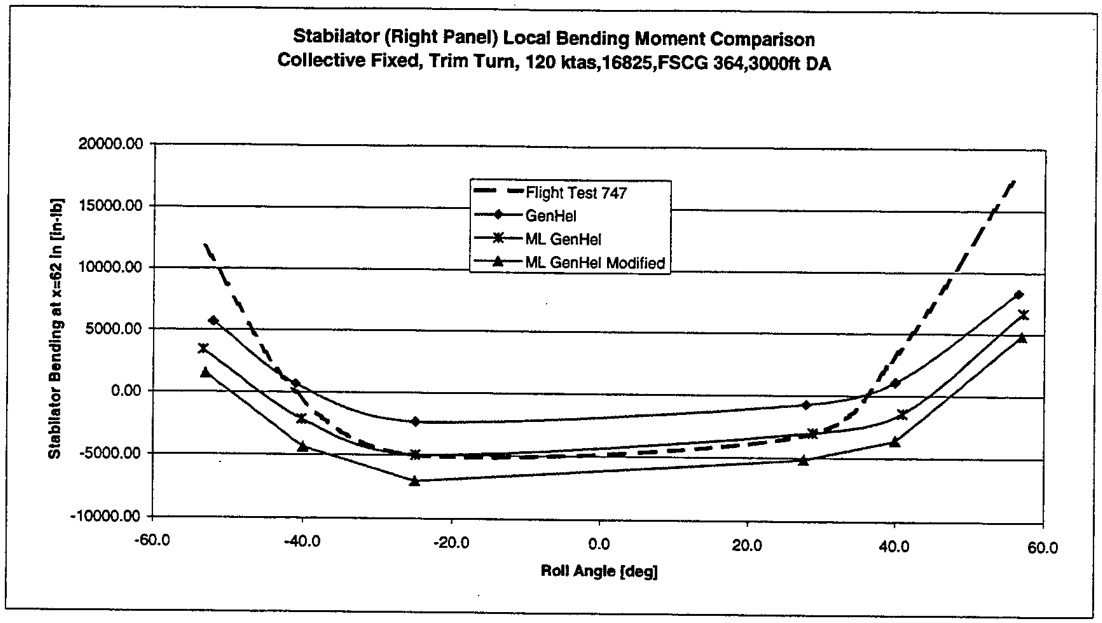

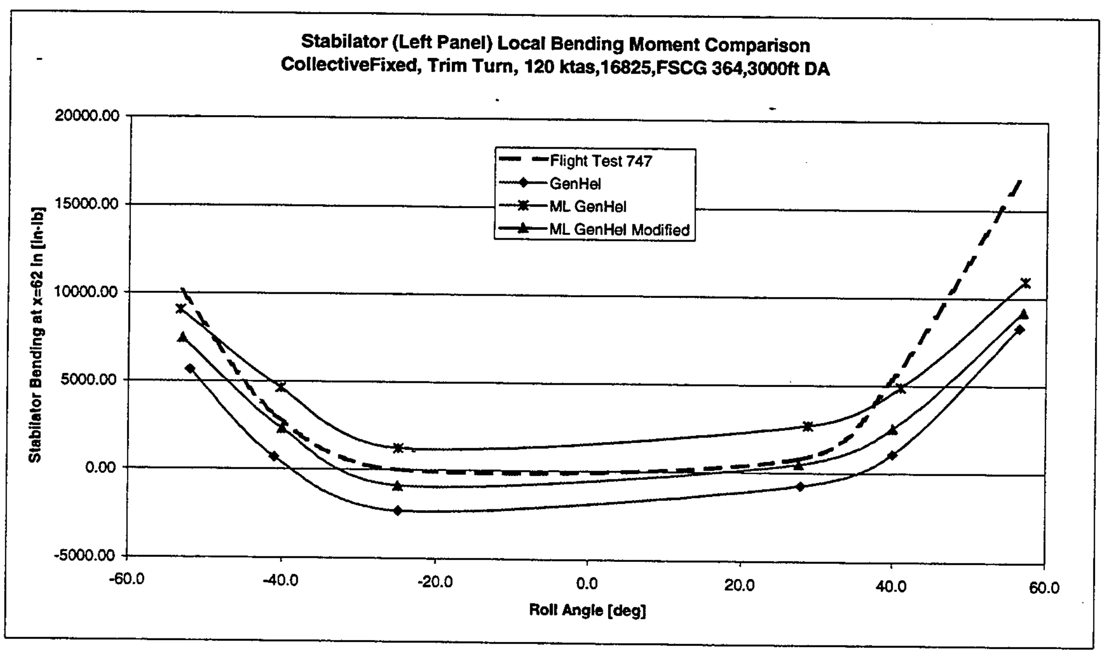

Figure 95 Modified Trim Turn Stabilator Bending Comparison 16825 lb, FSCG 364 in, 3000 ft DA

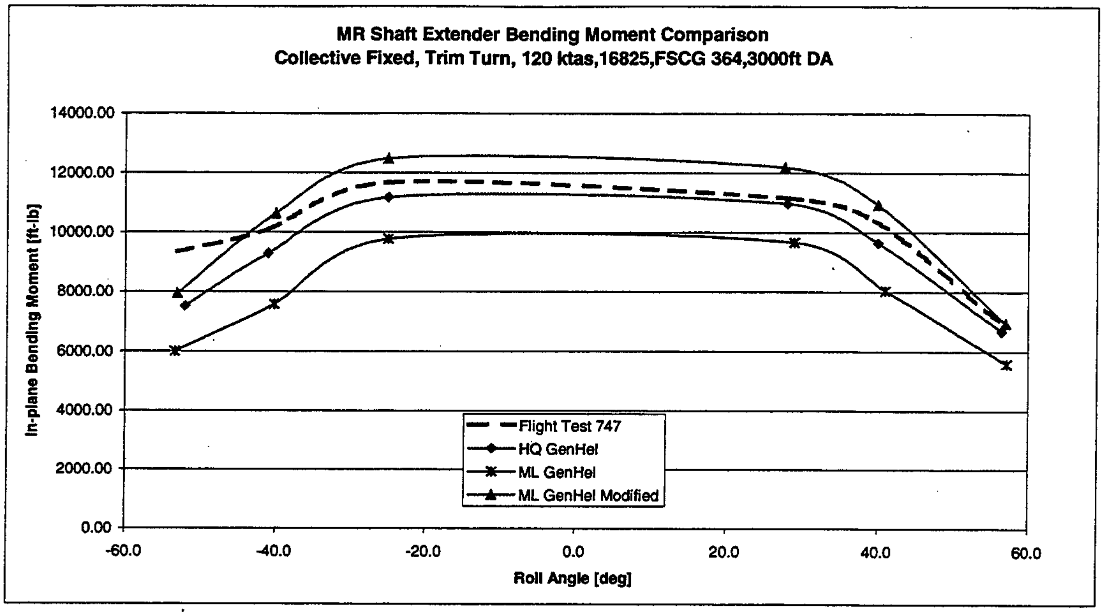

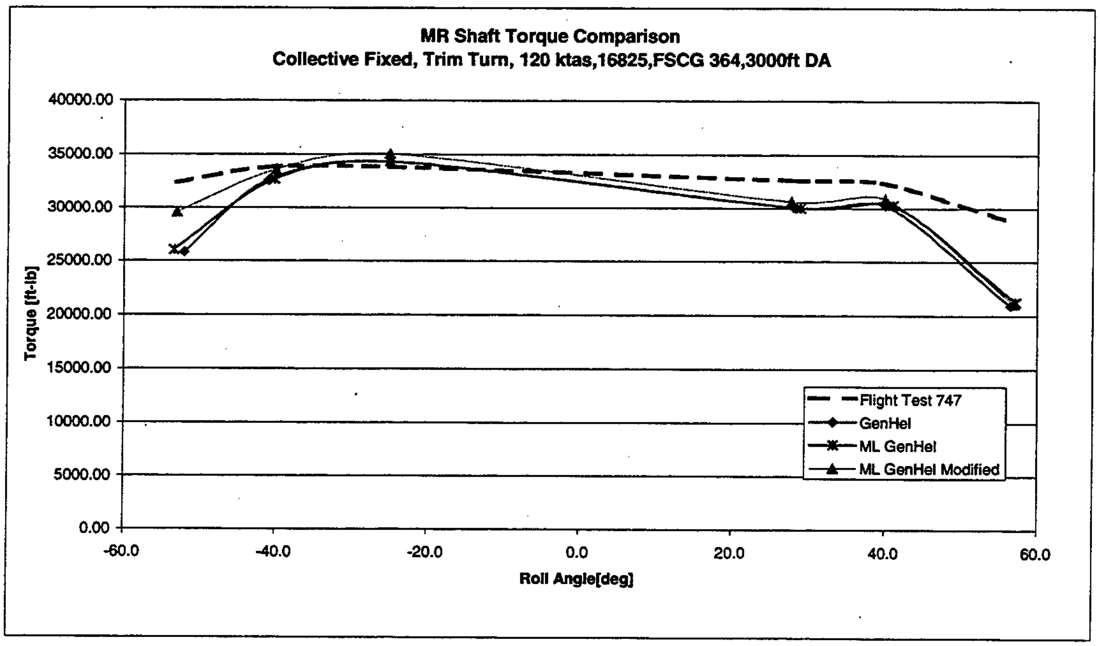

Figure 96 Modified Trim Turn MR Shaft Moment Comparison 16825 lb, FSCG 364 in, 3000 ft DA

C. DYNAMIC CORRELATION

Similar to the HQ and ML time domain response, the Mod ML model correlated well with test data in response to pulse inputs. Step response likewise exhibited similar characteristics to that of the HQ and ML models. The model under predicted the attitude response to the forward and right step and over predicted the roll attitude response to the left lateral step function.

THIS PAGE INTENTIONALLY LEFT BLANK

Dynamic Correlation, 16825, FSCG 364, 3000 ft DA

a. Forward Longitudinal Step, Modified 953-747 Run 043

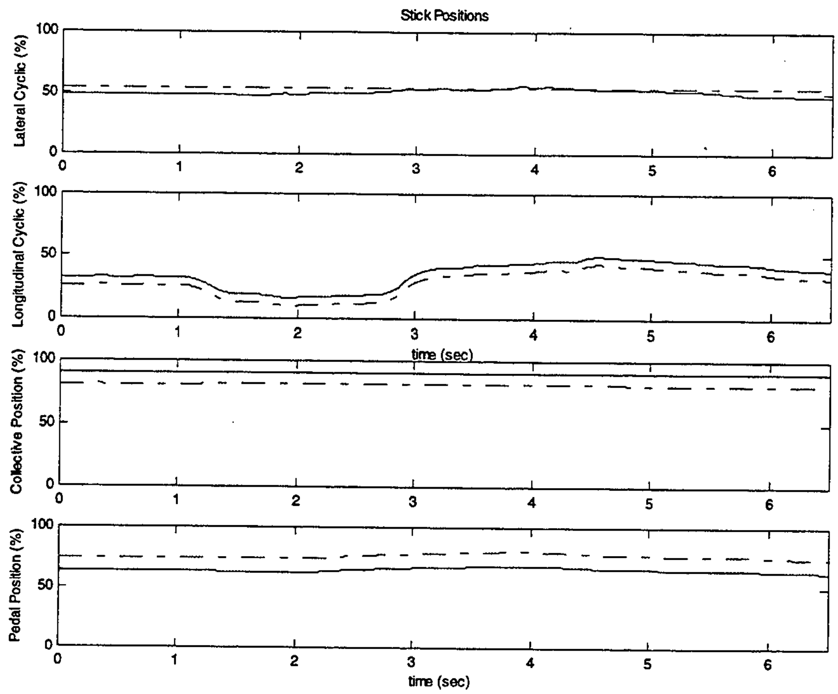

Figure 97 Modified 953-747 Run 043 Stick Positions 16825,FSCG 364, 3000 ft DA

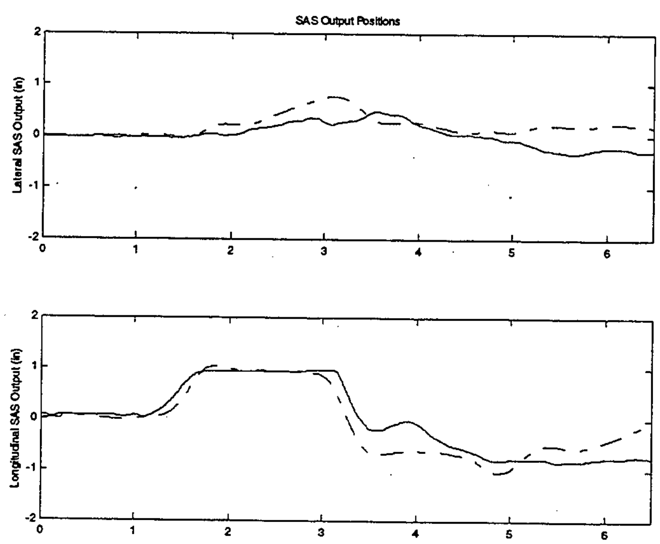

Figure 98 Modified 953-747 Run 043 SAS Positions 16825,FSCG 364, 3000 ft DA

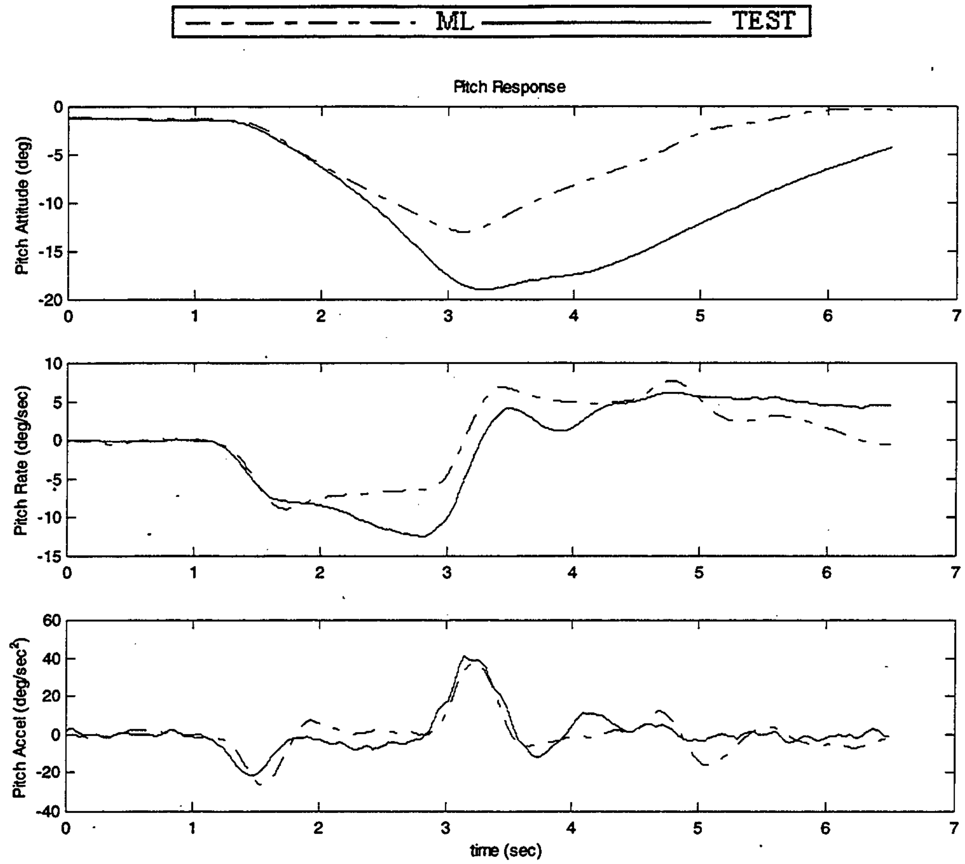

Figure 99 Modified 953-747 Run 043 On-Axis Response 16825,FSCG 364, 3000 ft DA

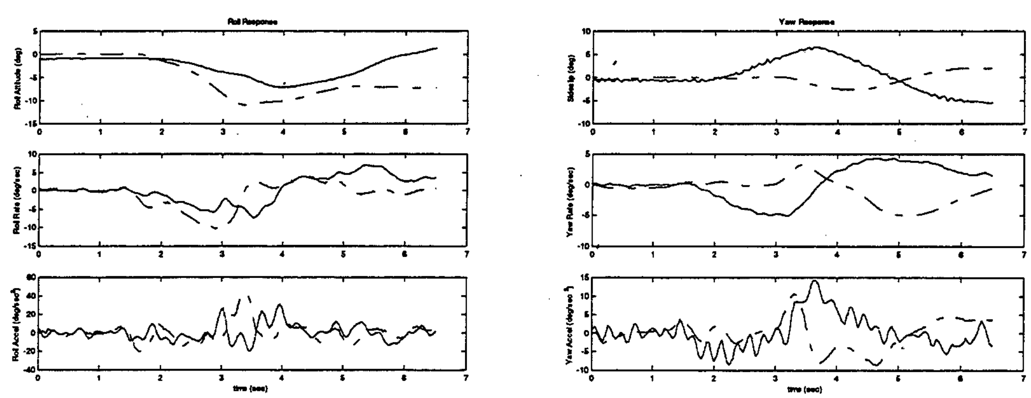

Figure 100 Modified 953-747 Run 043 Off-Axis Response 16825,FSCG 364, 3000 ft DA

b. *Left Lateral Step, Modified 953-747 Run 051*

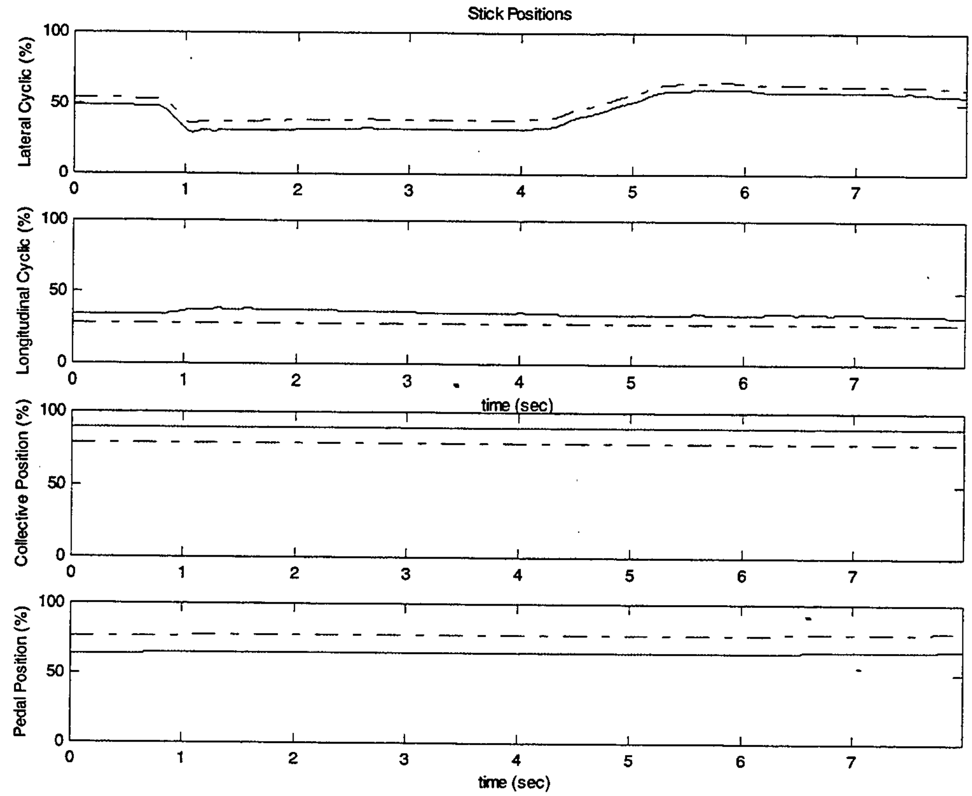

Figure 101 Modified 953-747 Run 051 Stick Positions 16825,FSCG 364, 3000 ft DA

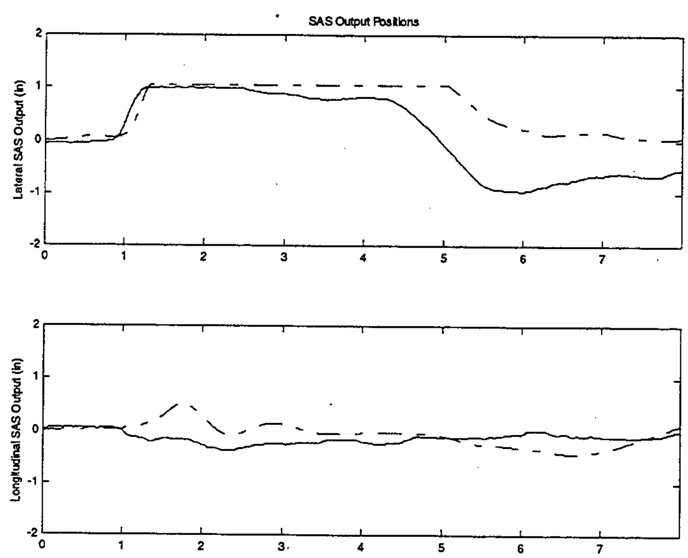

Figure 102 Modified 953-747 Run 051 SAS Positions 16825,FSCG 364, 3000 ft DA

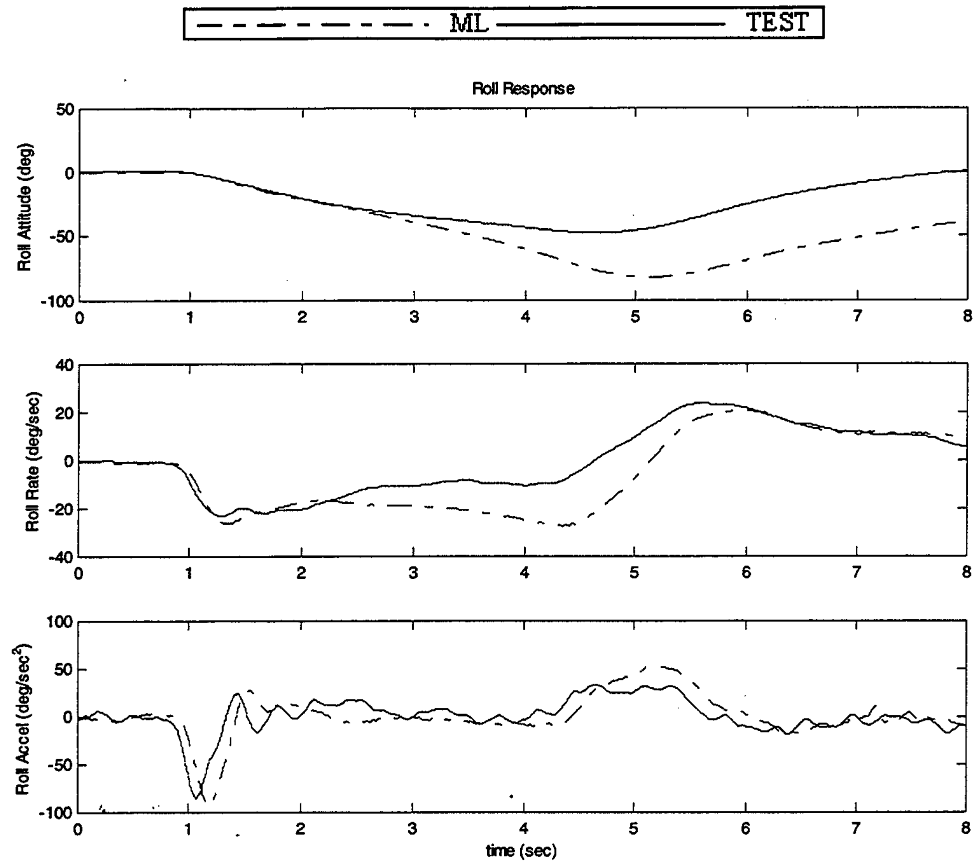

Figure 103 Modified 953-747 Run 051 On-Axis Response 16825,FSCG 364, 3000 ft DA

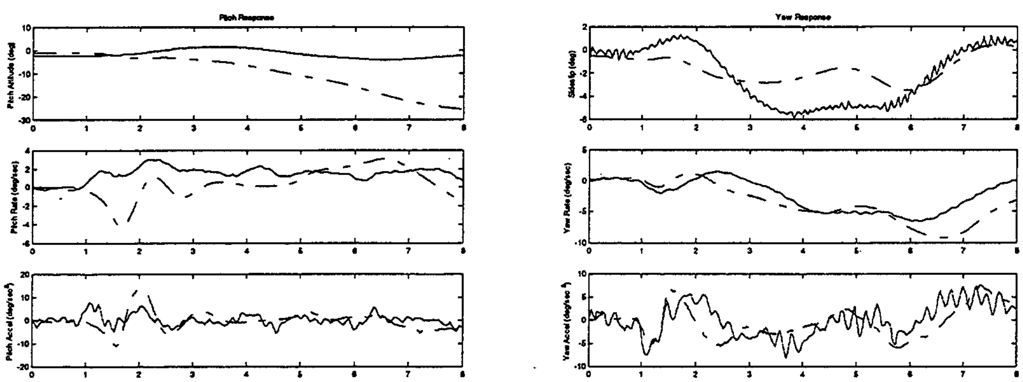

Figure 104 Modified 953-747 Run 051 Off-Axis Response 16825,FSCG 364, 3000 ft DA

c. Right Lateral Step, Modified 953-747 Run 055

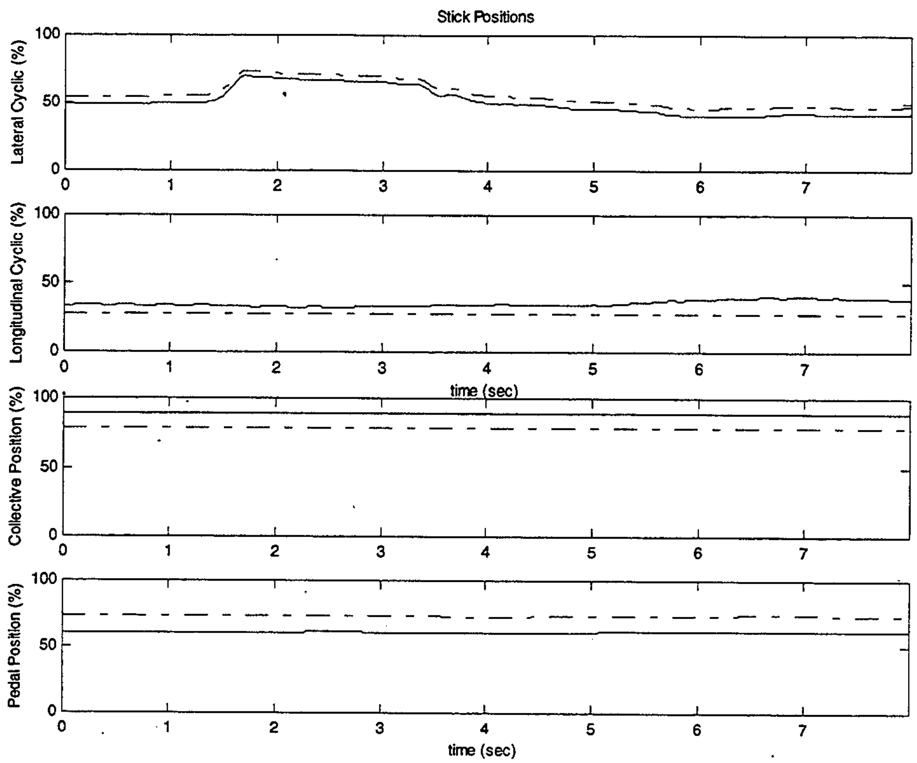

Figure 105 Modified 953-747 Run 055 Stick Positions 16825,FSCG 364, 3000 ft DA

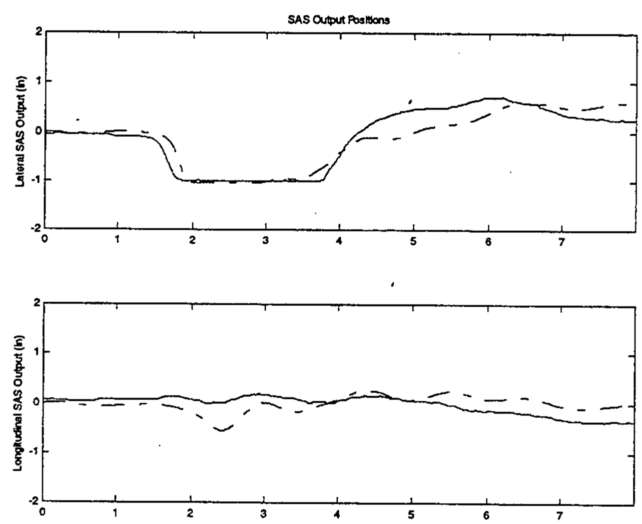

Figure 106 Modified 953-747 Run 055 SAS Positions 16825,FSCG 364, 3000 ft DA

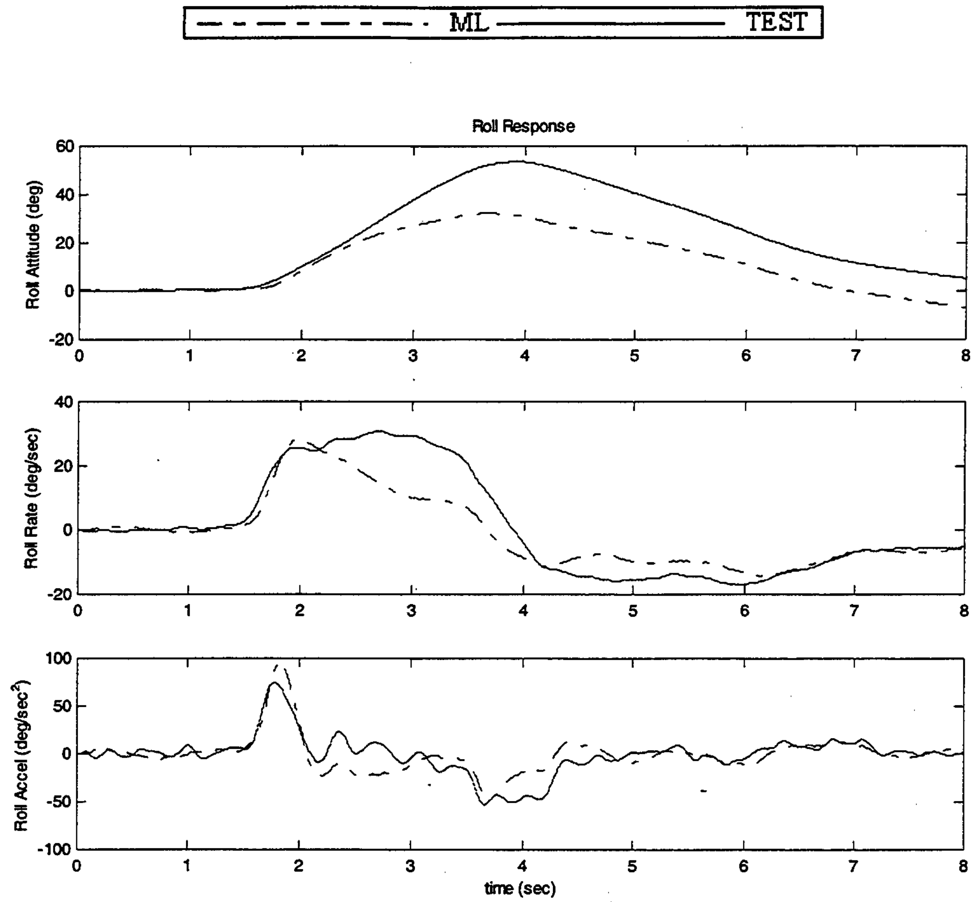

Figure 107 Modified 953-747 Run 055 On-Axis Response 16825,FSCG 364, 3000 ft DA

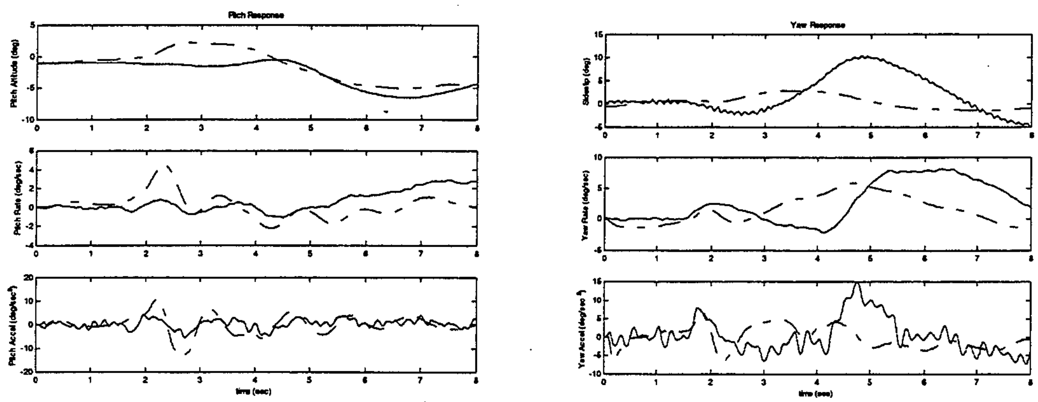

Figure 108 Modified 953-747 Run 055 Off-Axis Response 16825,FSCG 364, 3000 ft DA

d. *Forward Longitudinal Pulse, Modified 953-747 Run 058*

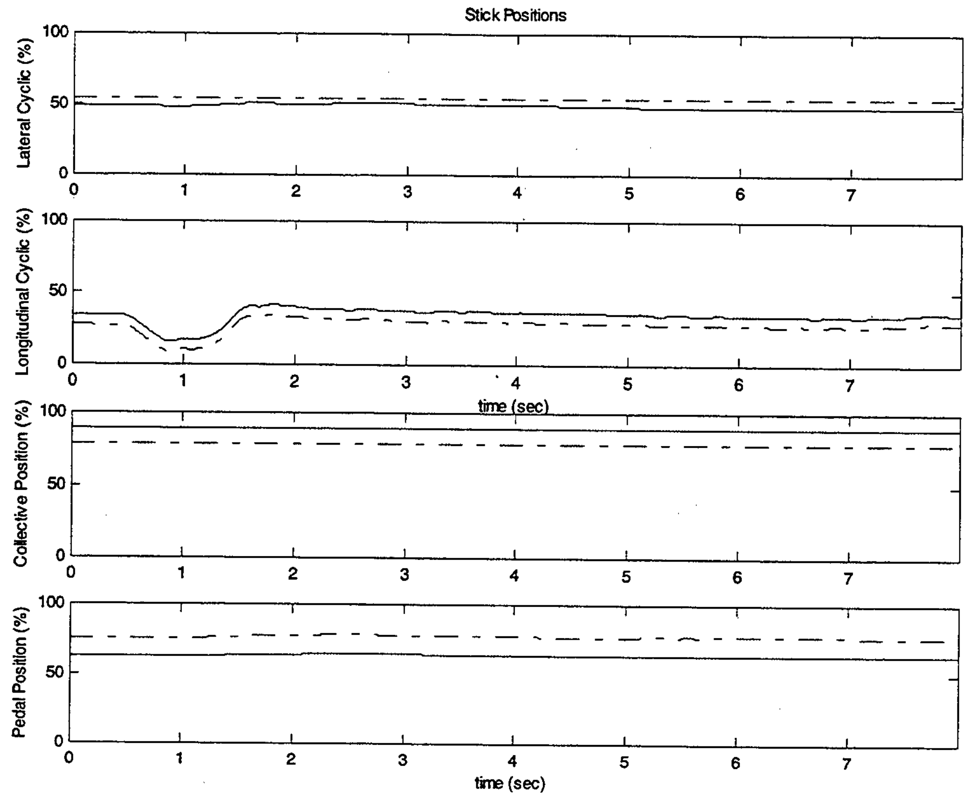

Figure 109 Modified 953-747 Run 058 Stick Positions 16825,FSCG 364, 3000 ft DA

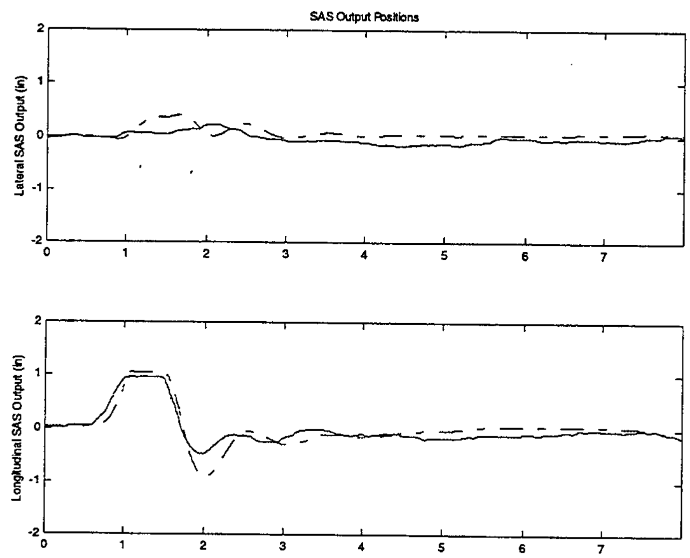

Figure 110 Modified 953-747 Run 058 SAS Positions 16825,FSCG 364, 3000 ft DA

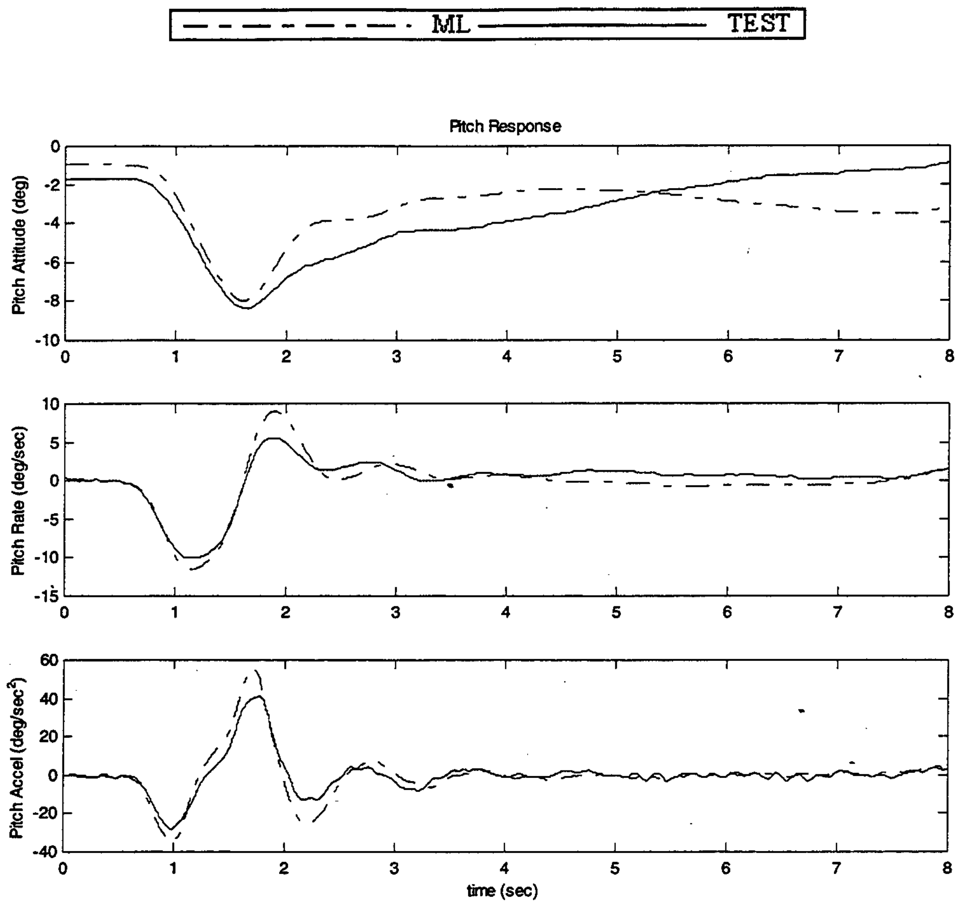

Figure 111 Modified 953-747 Run 058 On-Axis Response 16825,FSCG 364, 3000 ft DA

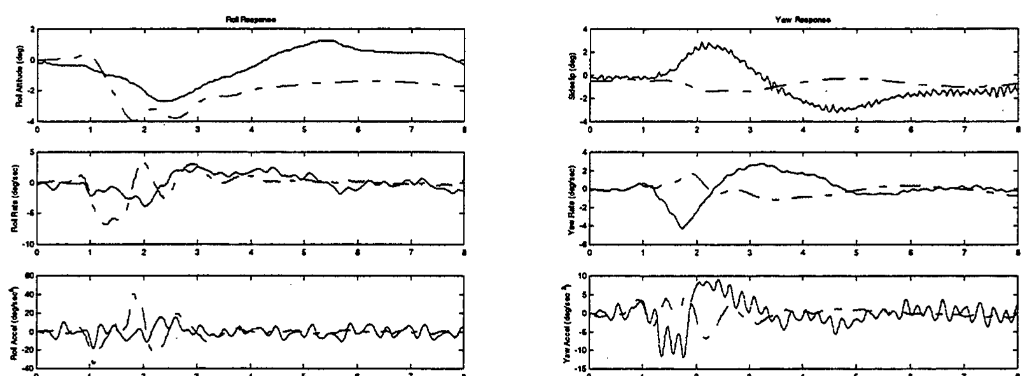

Figure 112 Modified 953-747 Run 058 Off-Axis Response 16825,FSCG 364, 3000 ft DA

e. Aft Longitudinal Pulse, Modified 953-747 Run 061

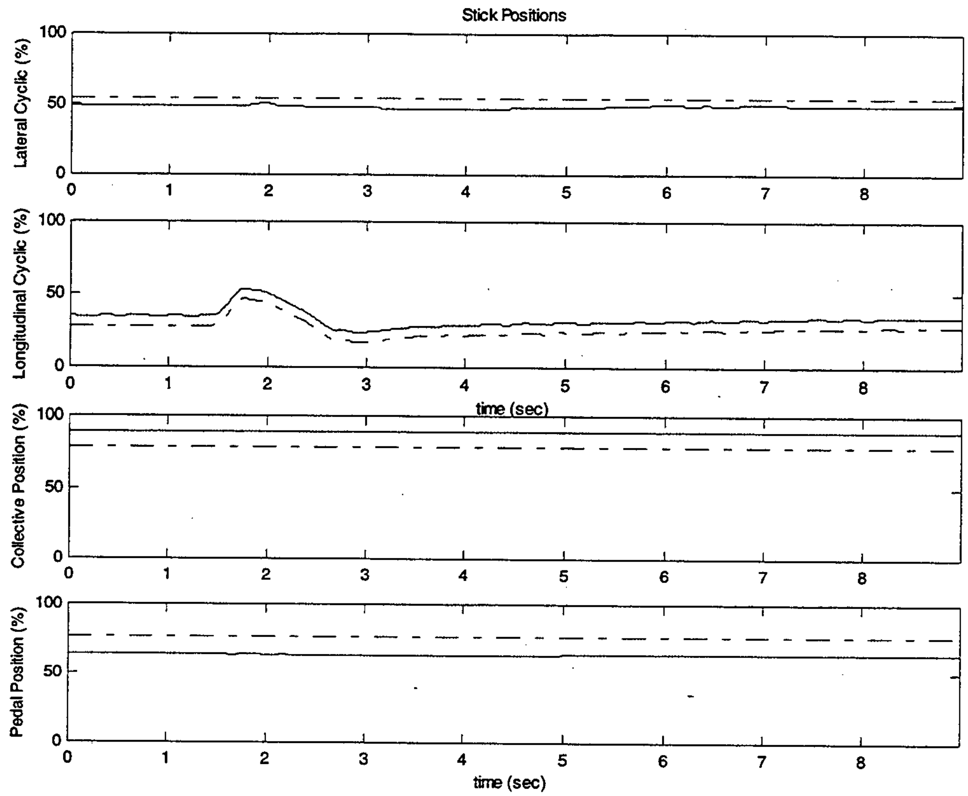

Figure 113 Modified 953-747 Run 061 Stick Positions 16825,FSCG 364, 3000 ft DA

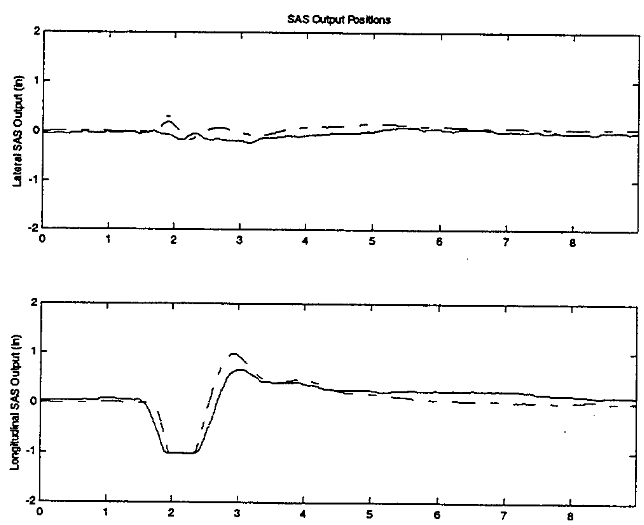

Figure 114 Modified 953-747 Run 061 SAS Positions 16825,FSCG 364, 3000 ft DA

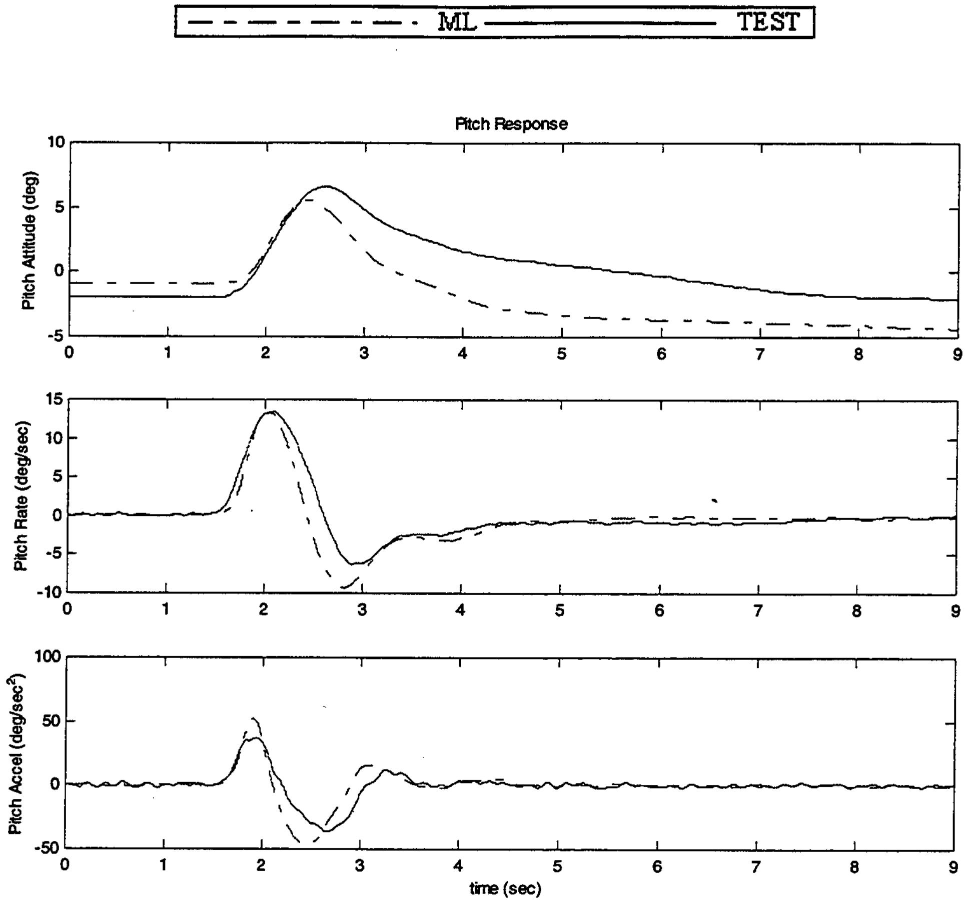

Figure 115 Modified 953-747 Run 061 On-Axis Response 16825,FSCG 364, 3000 ft DA

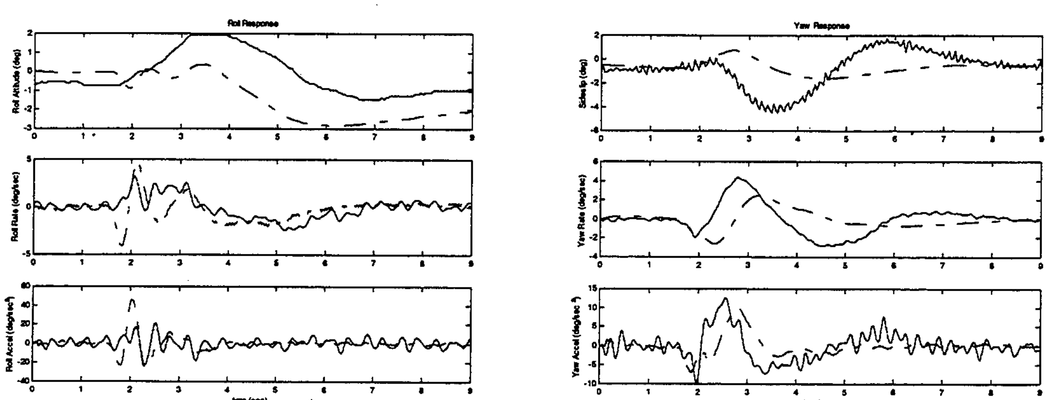

Figure 116 Modified 953-747 Run 061 Off-Axis Response 16825,FSCG 364, 3000 ft DA

f. Left Lateral Pulse, Modified 953-747 Run 064

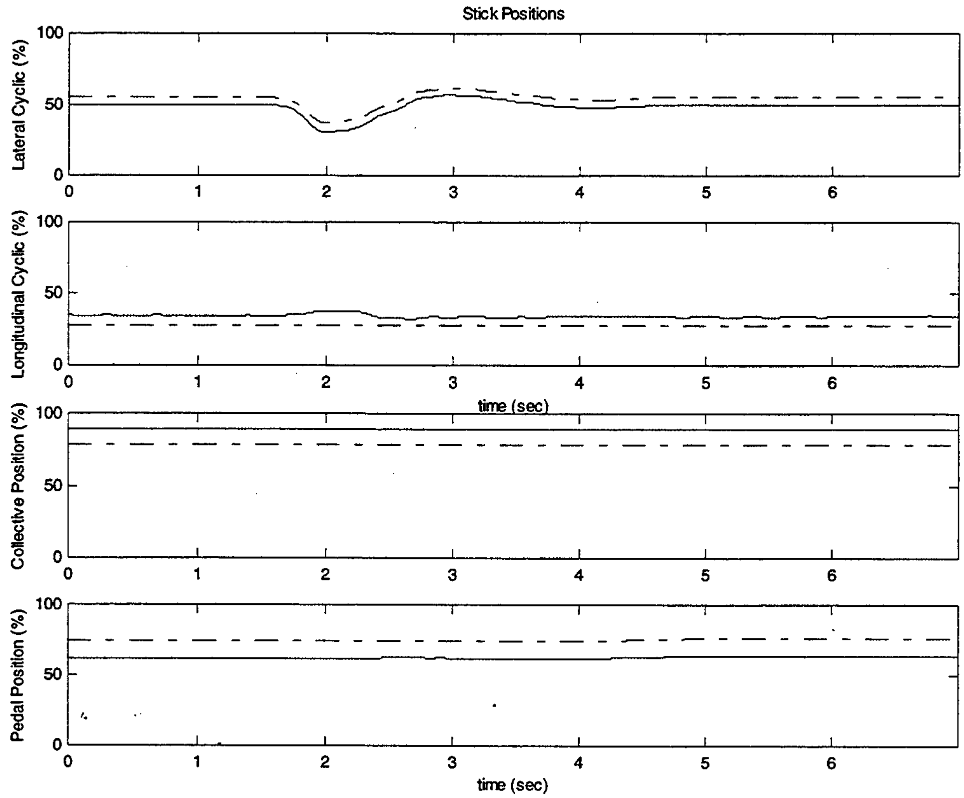

Figure 117 Modified 953-747 Run 064 Stick Positions 16825,FSCG 364, 3000 ft DA

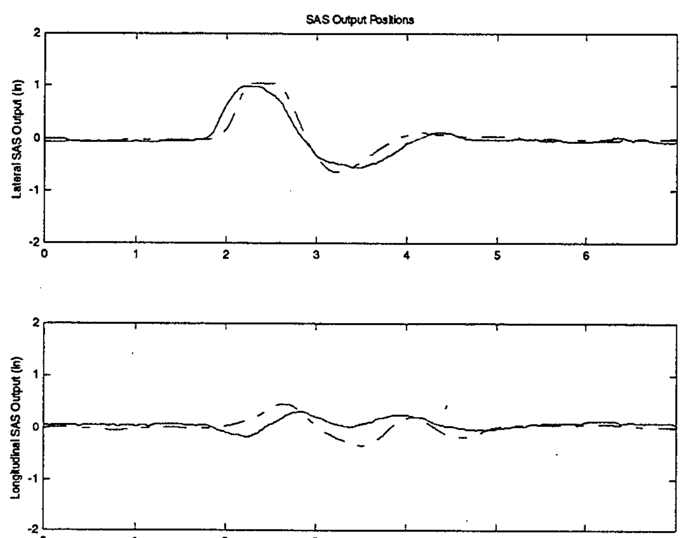

Figure 118 Modified 953-747 Run 064 SAS Positions 16825,FSCG 364, 3000 ft DA

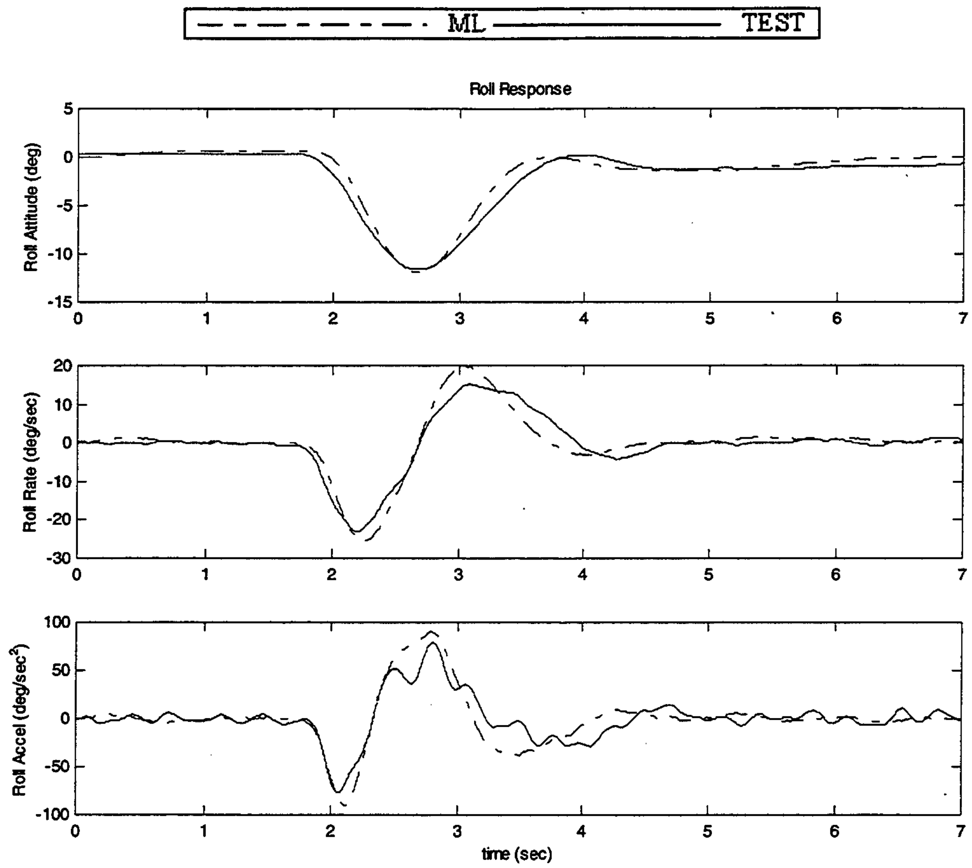

Figure 119 Modified 953-747 Run 064 On-Axis Response 16825,FSCG 364, 3000 ft DA

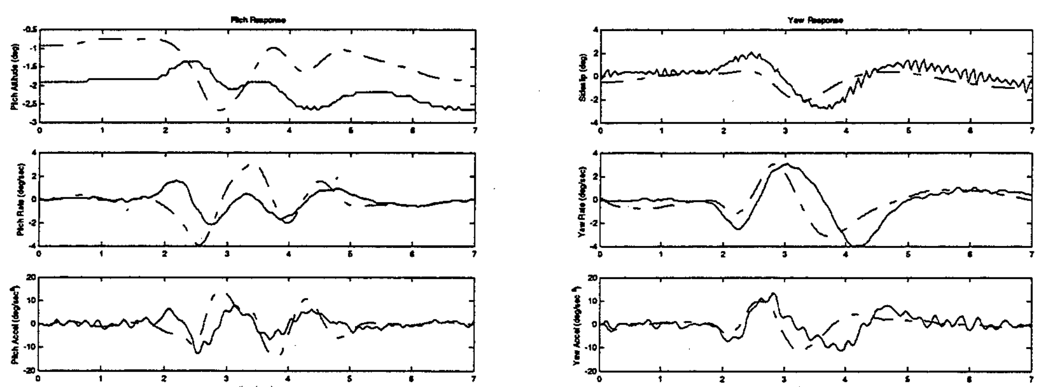

Figure 120 Modified 953-747 Run 064 Off-Axis Response 16825,FSCG 364, 3000ft DA

g. *Right Lateral Pulse, Modified 953-747 Run 067*

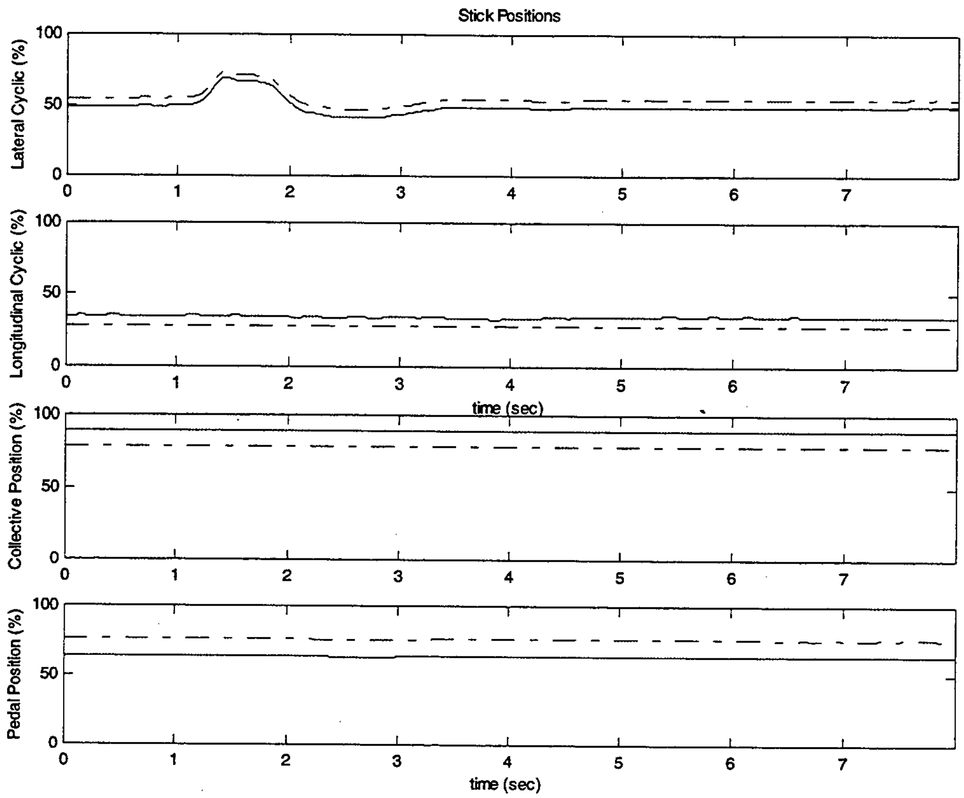

Figure 121 Modified 953-747 Run 067 Stick Positions 16825,FSCG 364, 3000 ft DA

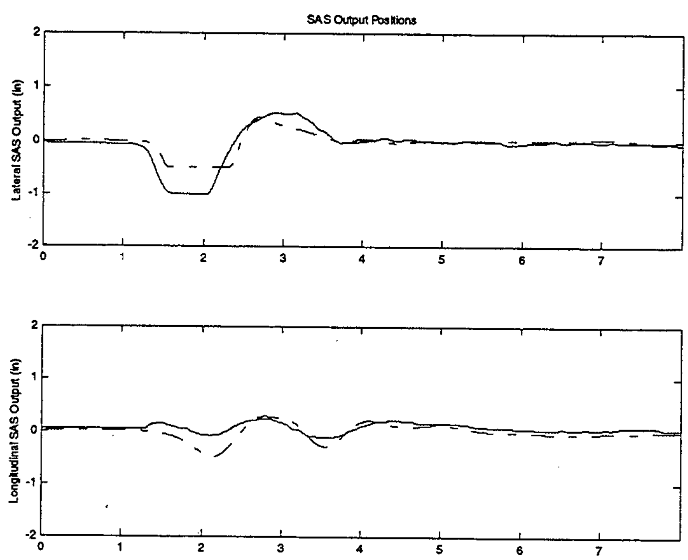

Figure 122 Modified 953-747 Run 067 SAS Positions 16825,FSCG 364, 3000 ft DA

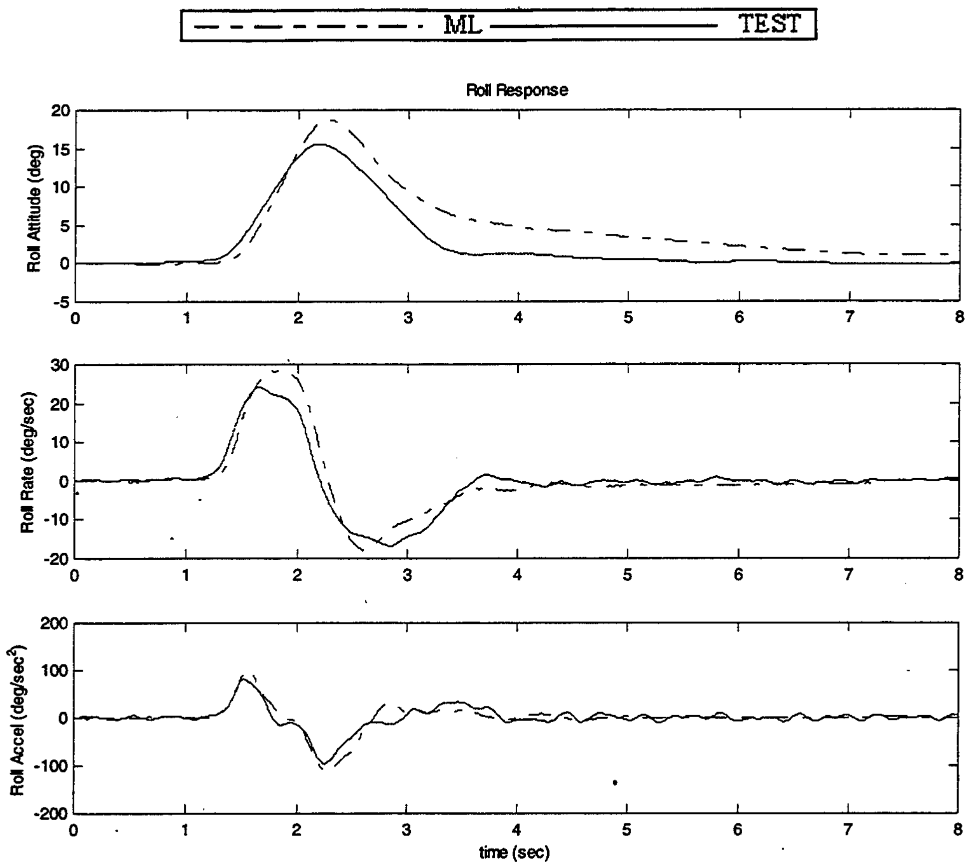

Figure 123 Modified 953-747 Run 067 On-Axis Response 16825,FSCG 364, 3000 ft DA

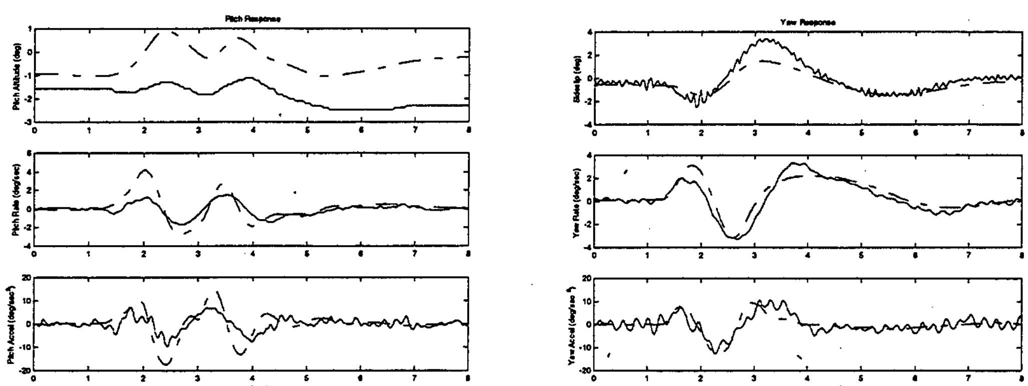

Figure 124 Modified 953-747 Run 067 Off-Axis Response 16825,FSCG 364, 3000ft DA

2. Dynamic Correlation, 22000, FSCG 360, 3000 ft DA

a. Aft Longitudinal Step, Modified 953-795 Run 042

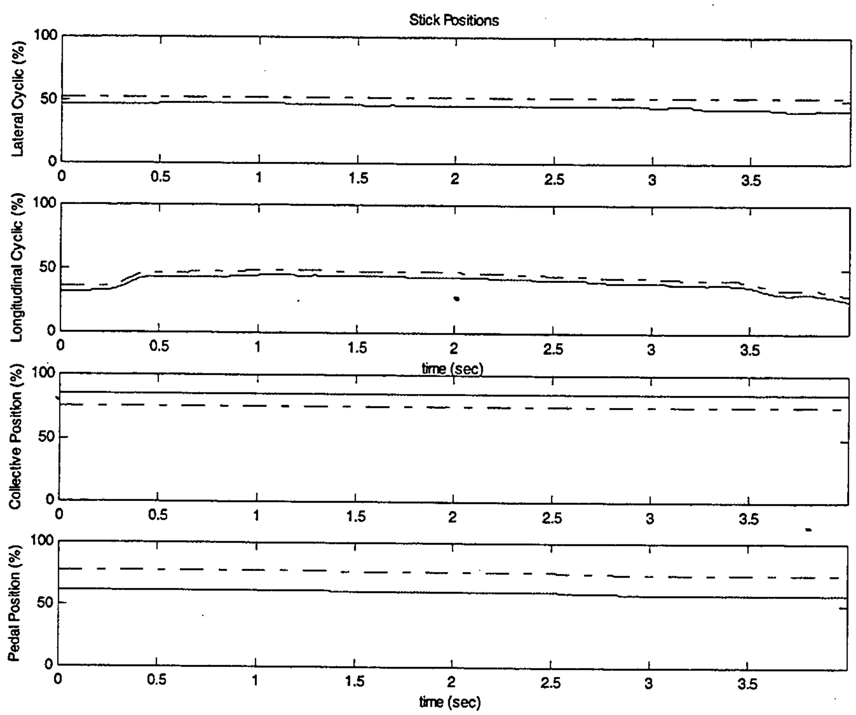

Figure 125 Modified 953-795 Run 042 Stick Positions 22000,FSCG 360, 3000ft DA

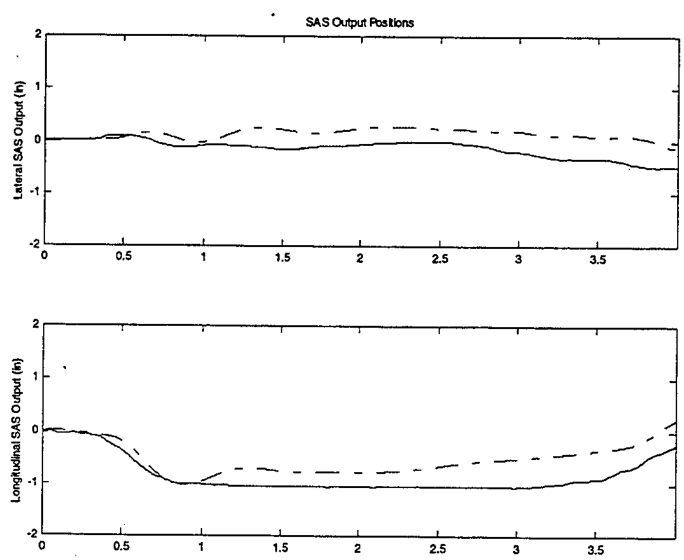

Figure 126 Modified 953-795 Run 042 SAS Positions 22000,FSCG 360, 3000ft DA

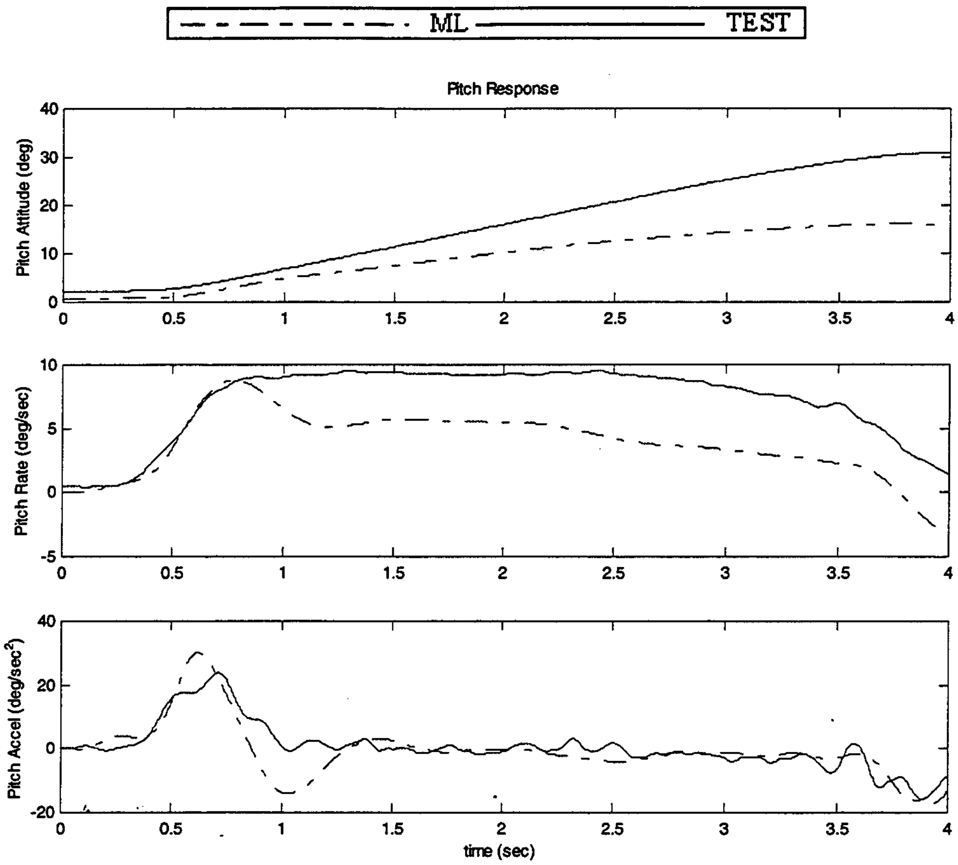

Figure 127 Modified 953-795 Run 042 On-Axis Response 22000,FSCG 360, 3000ft DA

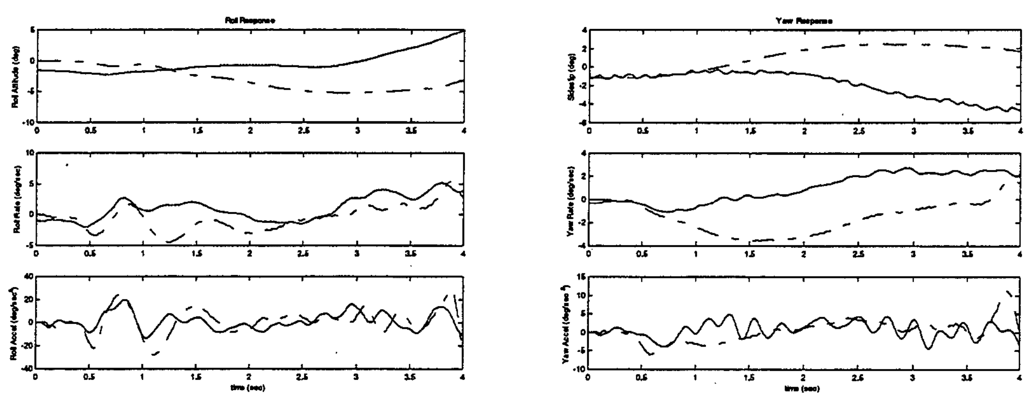

Figure 128 Modified 953-795 Run 042 Off-Axis Response 22000,FSCG 360, 3000ft DA

b. Left Lateral Cyclic, Modified 953-795 Run 048

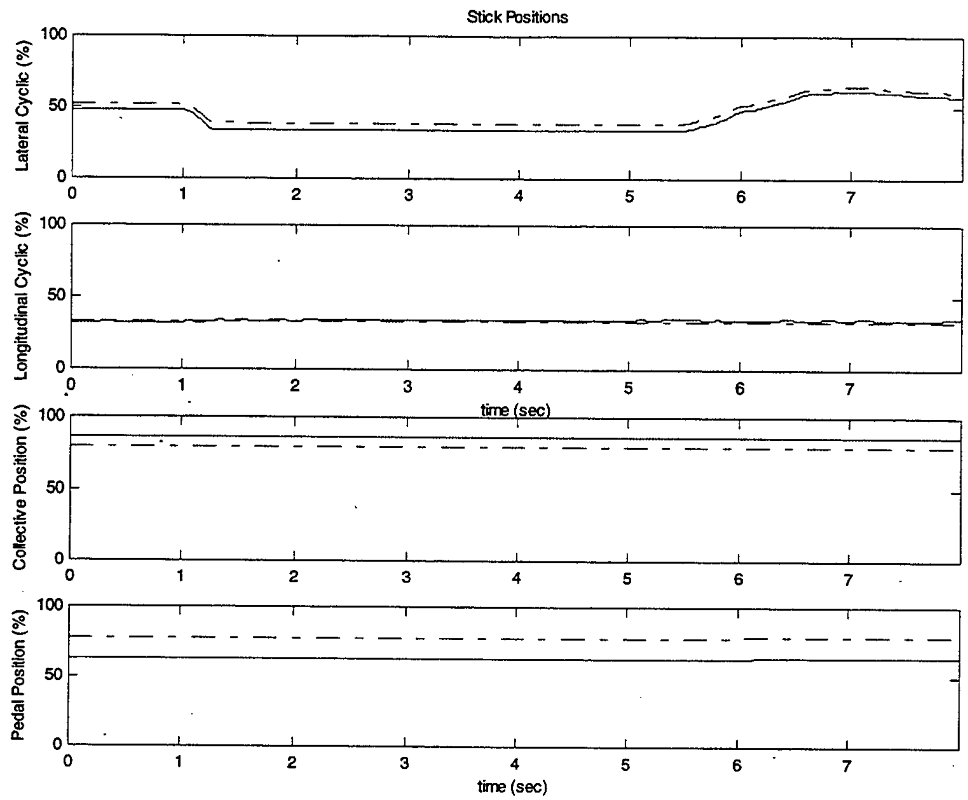

Figure 129 Modified 953-795 Run 048 Stick Positions 22000,FSCG 360, 3000ft DA

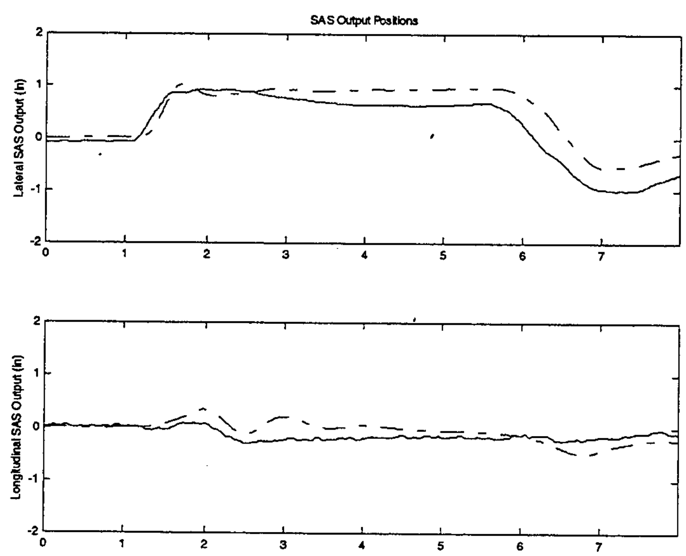

Figure 130 Modified 953-795 Run 048 SAS Positions 22000,FSCG 360, 3000ft DA

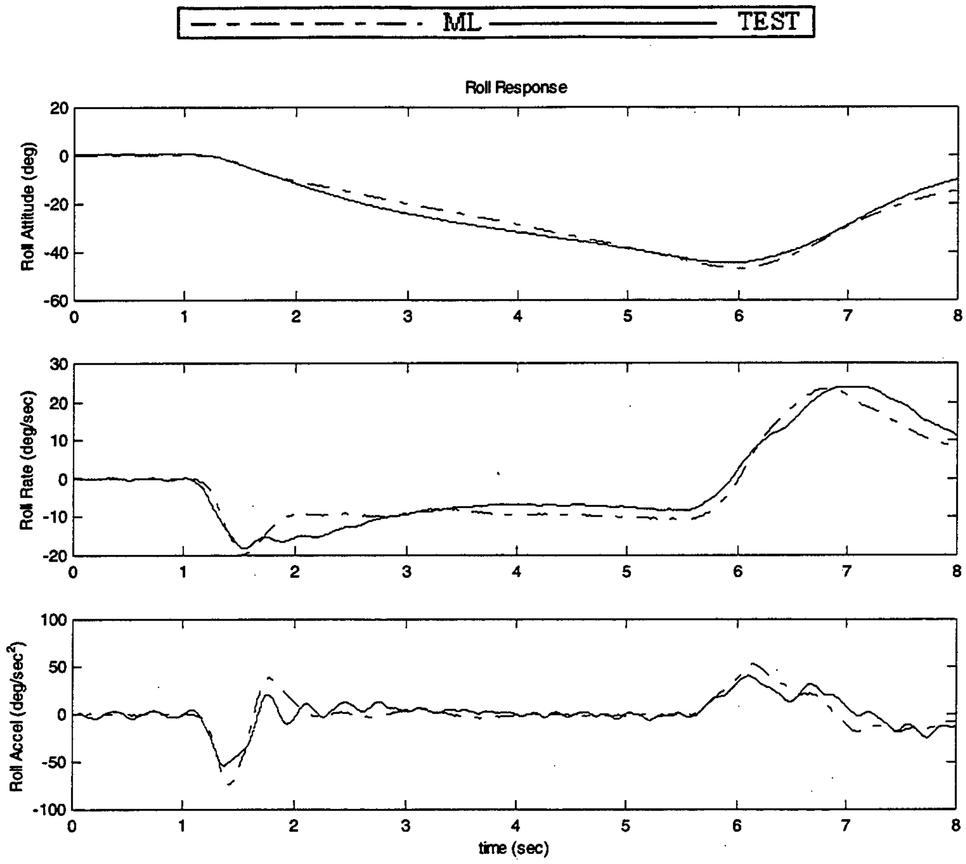

Figure 131 Modified 953-795 Run 048 On-Axis Response 22000,FSCG 360, 3000ft DA

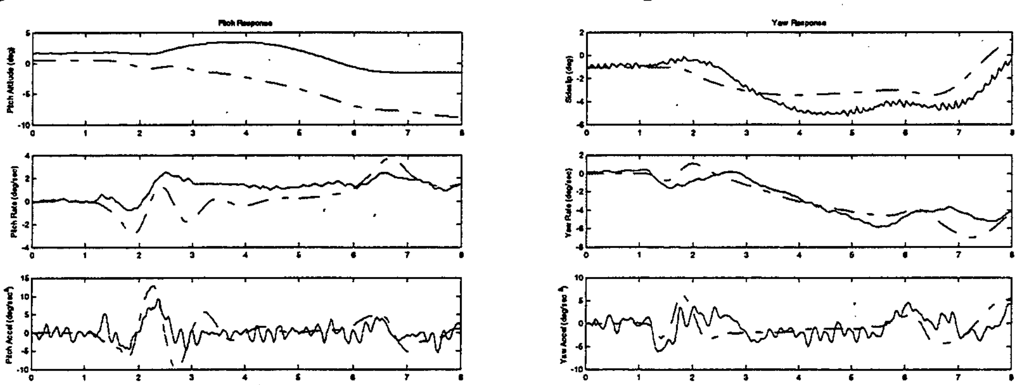

Figure 132 Modified 953-795 Run 048 Off-Axis Response 22000,FSCG 360, 3000ft DA

c. *Right Lateral Step, Modified 953-795 Run 049*

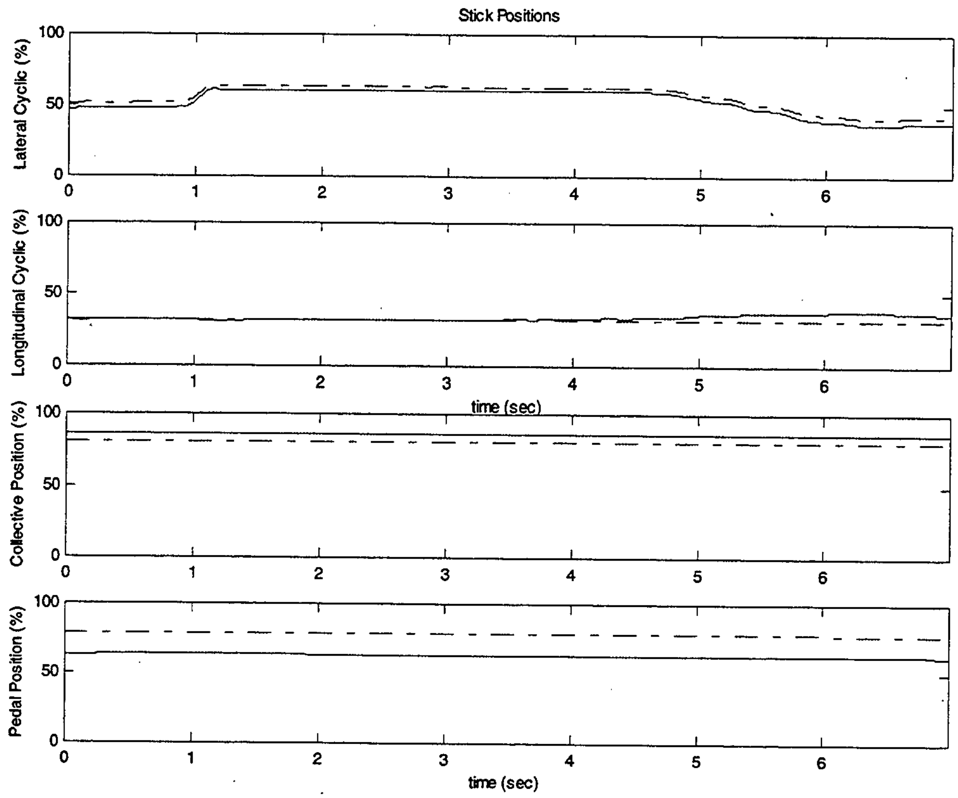

Figure 133 Modified 953-795 Run 049 Stick Positions 22000,FSCG 360, 3000ft DA

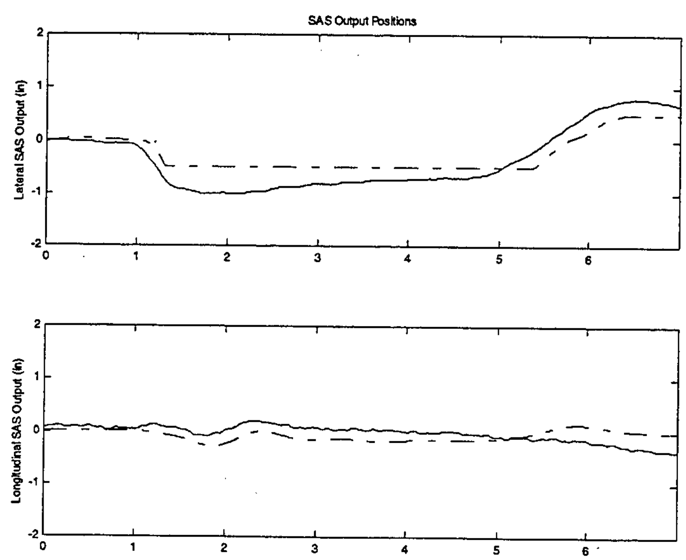

Figure 134 Modified 953-795 Run 049 SAS Positions 22000,FSCG 360, 3000ft DA

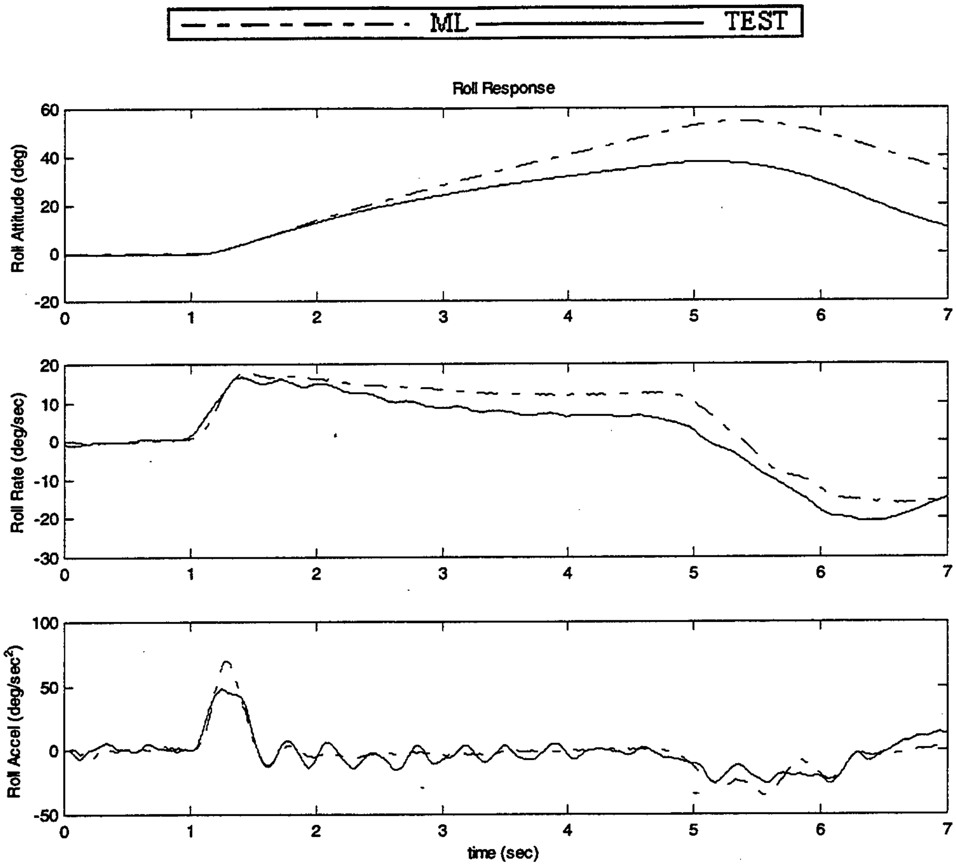

Figure 135 Modified 953-795 Run 049 On-Axis Response 22000,FSCG 360, 3000ft DA

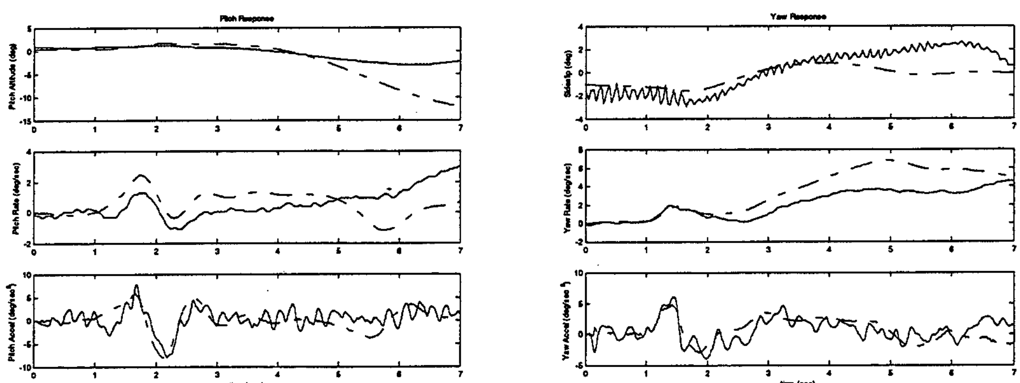

Figure 136 Modified 953-795 Run 049 Off-Axis Response 22000,FSCG 360, 3000ft DA

d. *Forward Longitudinal Pulse, Modified 953-795 Run 083*

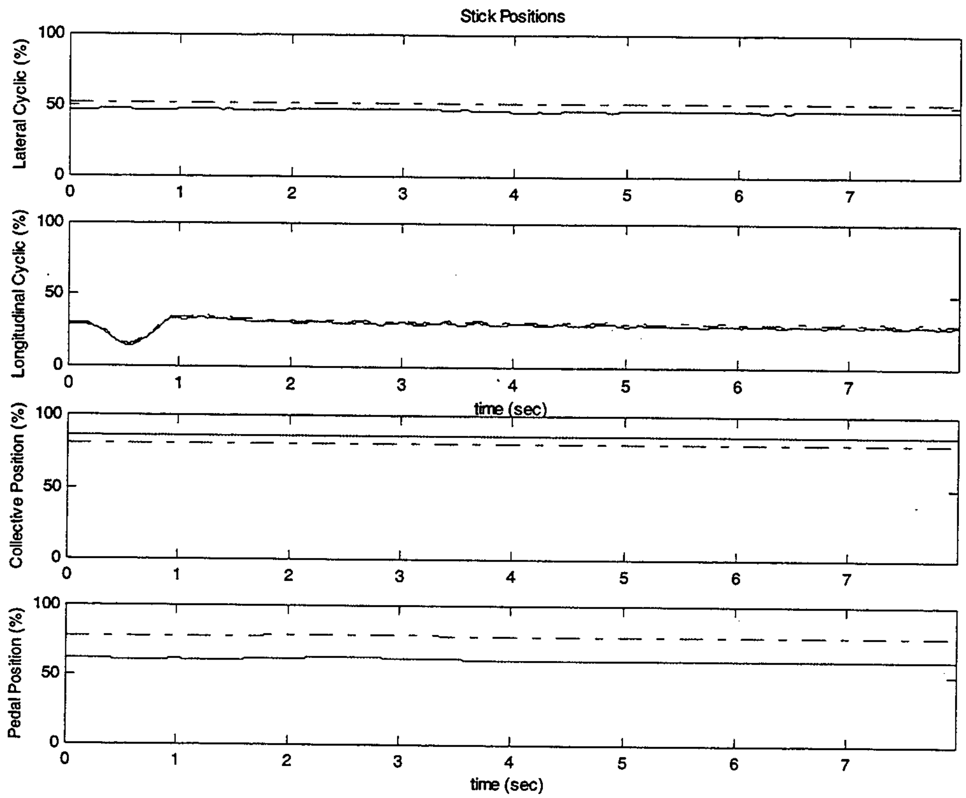

Figure 137 Modified 953-795 Run 083 Stick Positions 22000,FSCG 360, 3000ft DA

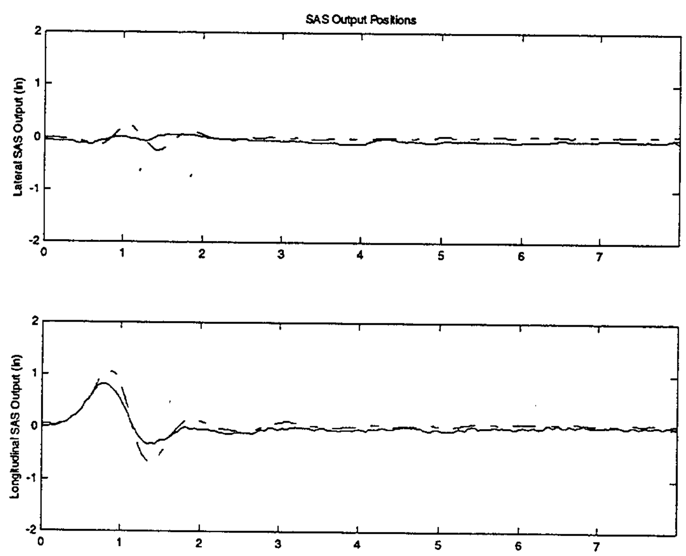

Figure 138 Modified 953-795 Run 083 SAS Positions 22000,FSCG 360, 3000ft DA

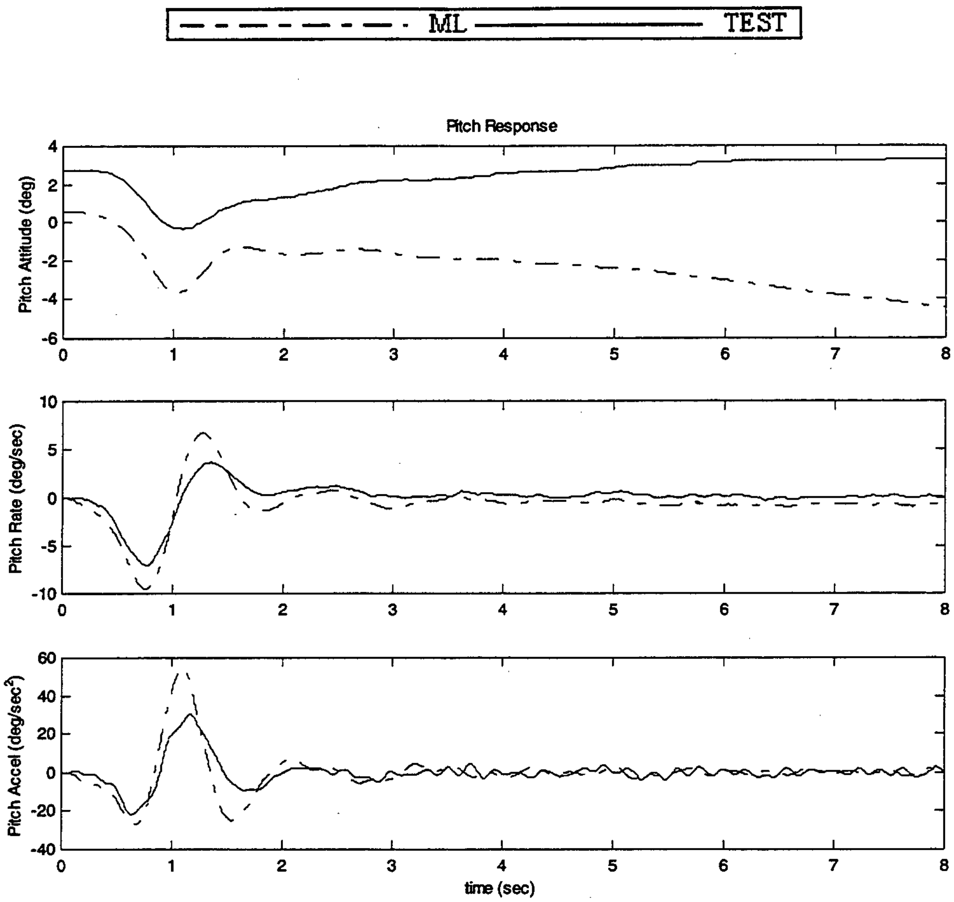

Figure 139 Modified 953-795 Run 083 On-Axis Response. 22000,FSCG 360, 3000ft DA

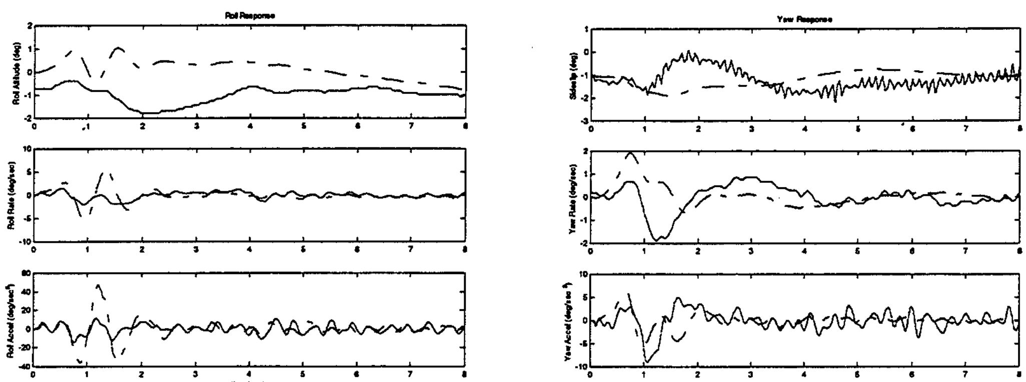

Figure 140 Modified 953-795 Run 083 Off-Axis Response 22000,FSCG 360, 3000ft DA

e. *Aft Longitudinal Pulse, Modified 953-795 Run 086*

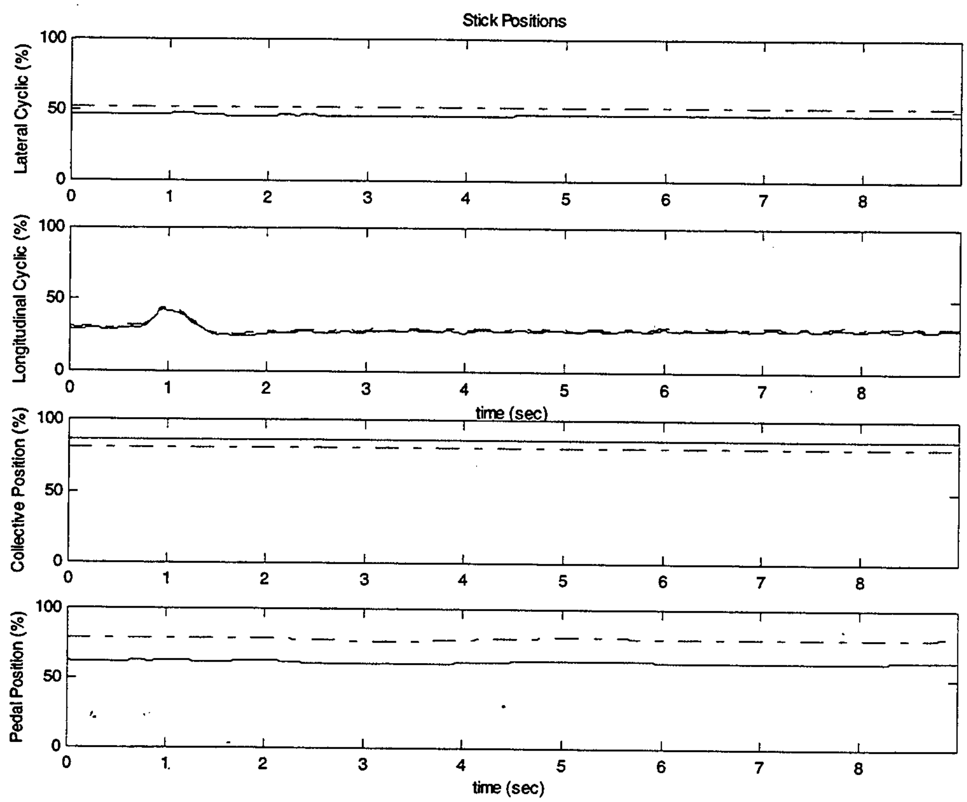

Figure 141 Modified 953-795 Run 086 Stick Positions 22000,FSCG 360, 3000ft DA

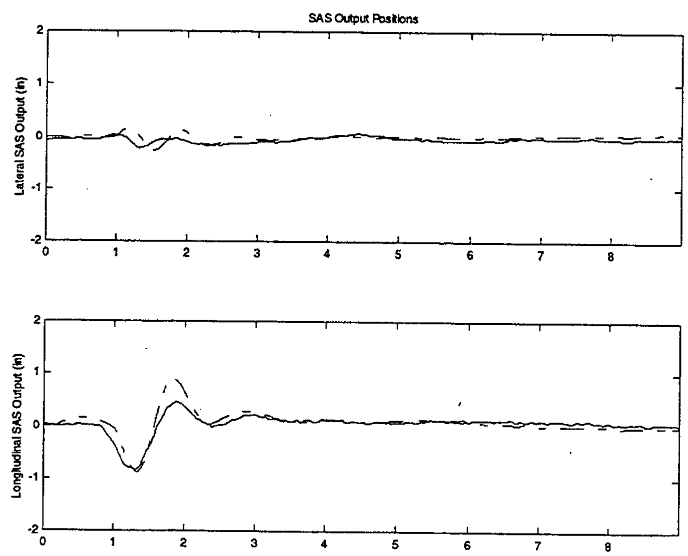

Figure 142 Modified 953-795 Run 086 SAS Positions 22000,FSCG 360, 3000ft DA

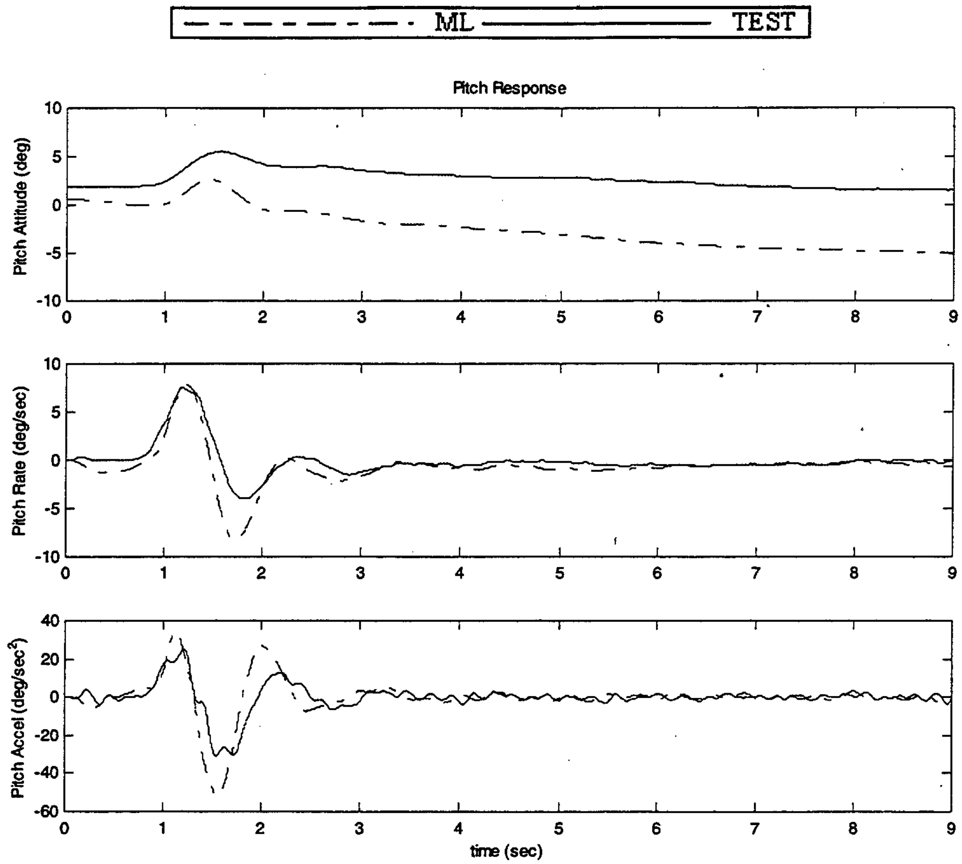

Figure 143 Modified 953-795 Run 086 On-Axis Response 22000,FSCG 360, 3000ft DA

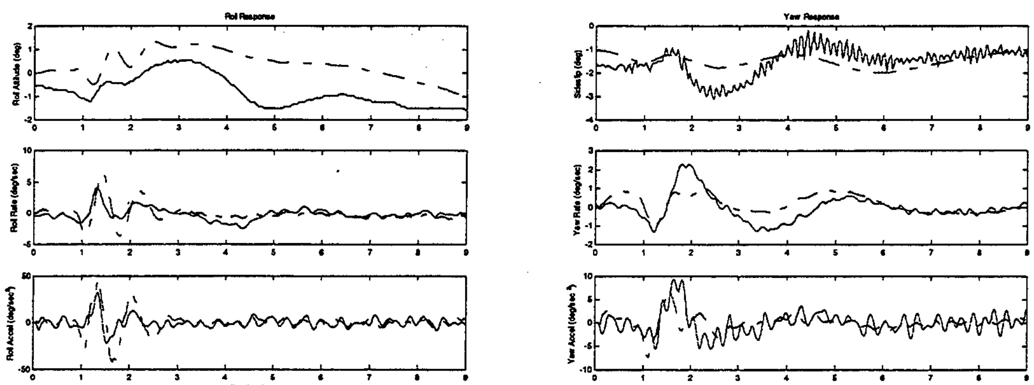

Figure 144 Modified 953-795 Run 086 Off-Axis Response 22000,FSCG 360, 3000ft DA

f. Left Lateral Pulse, Modified 953-795 Run 089

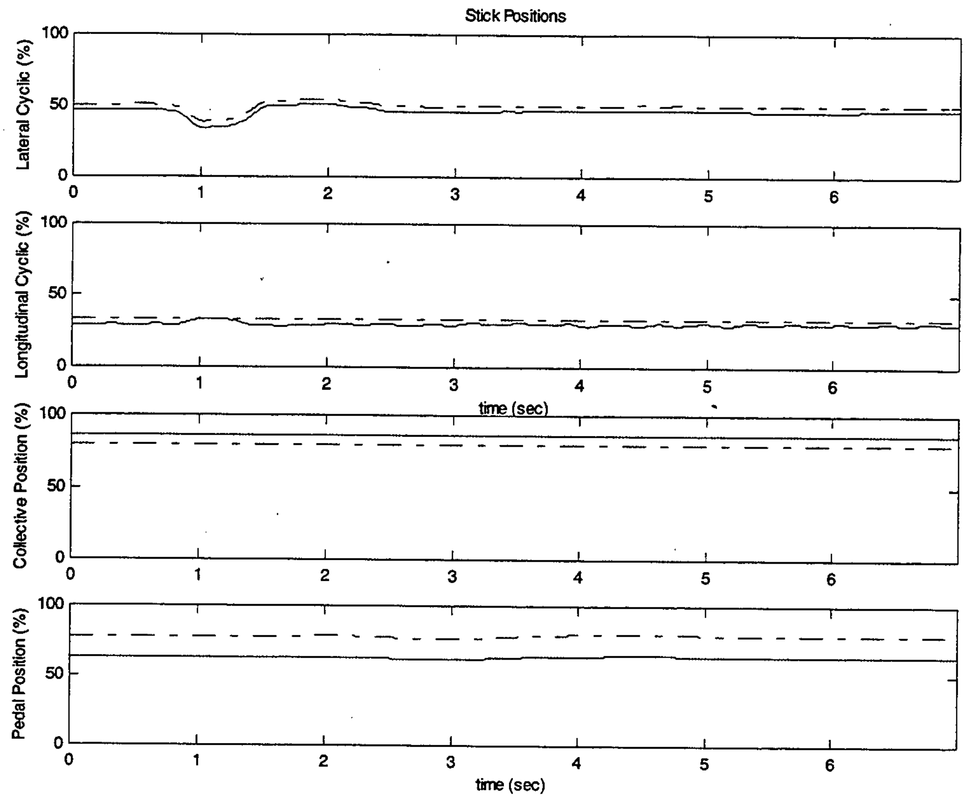

Figure 145 Modified 953-795 Run 089 Stick Positions 22000,FSCG 360, 3000ft DA

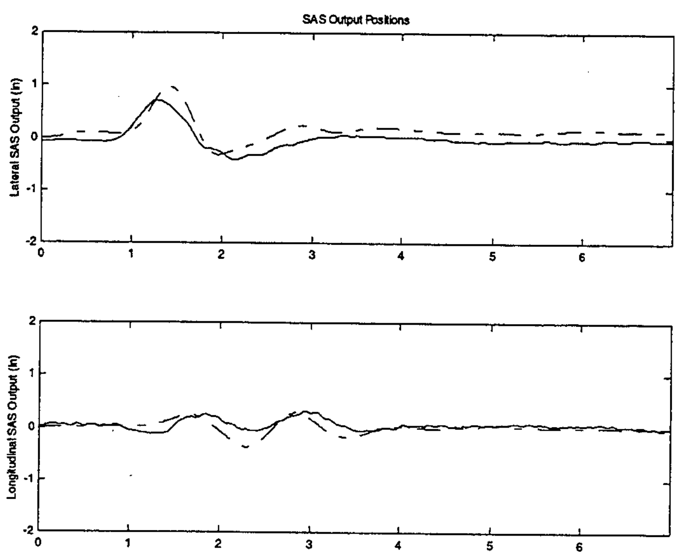

Figure 146 Modified 953-795 Run 089 SAS Positions 22000,FSCG 360, 3000ft DA

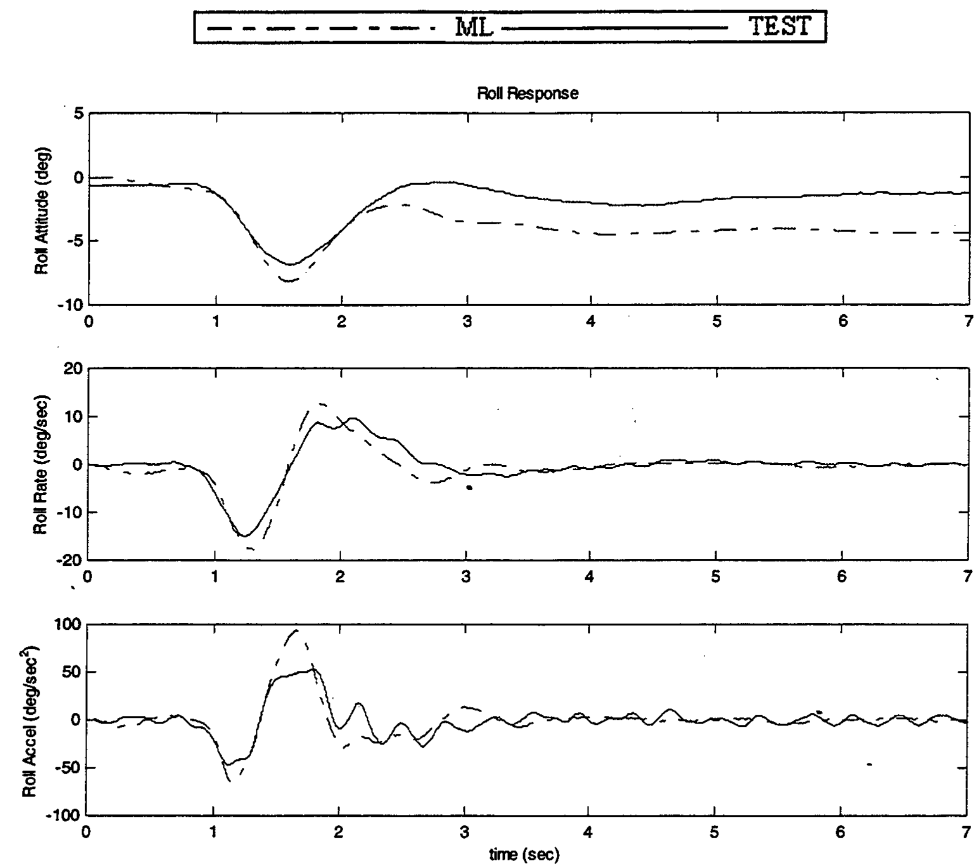

Figure 147 Modified 953-795 Run 089 On-Axis Response 22000,FSCG 360, 3000ft DA

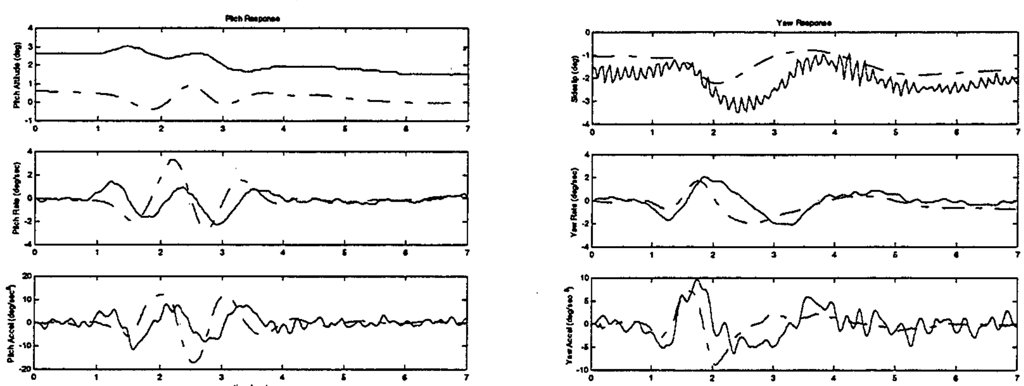

Figure 148 Modified 953-795 Run 089 Off-Axis Response 22000,FSCG 360, 3000ft DA

g. *Right Lateral Pulse, Modified 953-795 Run 092*

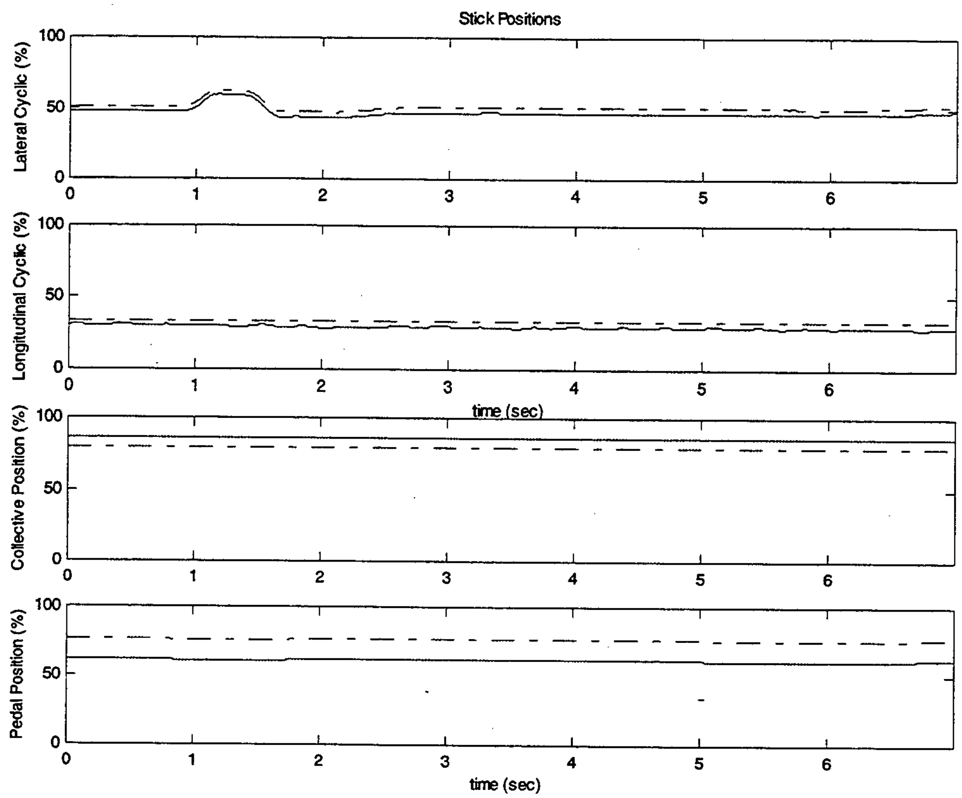

Figure 149 Modified 953-795 Run 092 Stick Positions 22000,FSCG 360, 3000ft DA

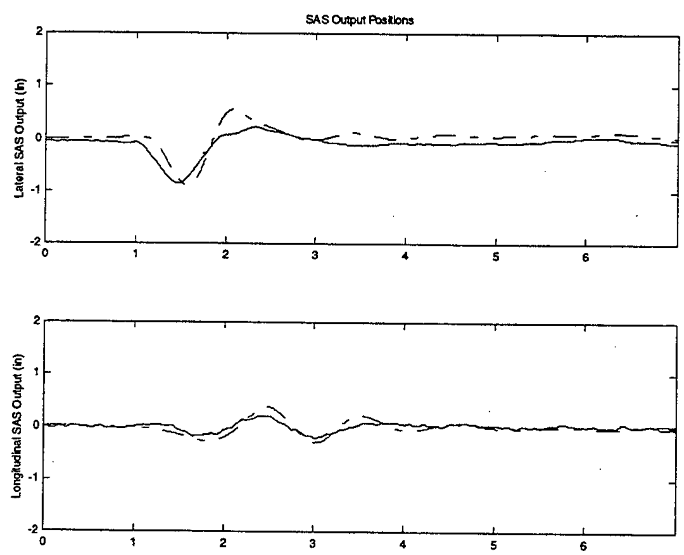

Figure 150 Modified 953-795 Run 092 SAS Positions 22000,FSCG 360, 3000ft DA

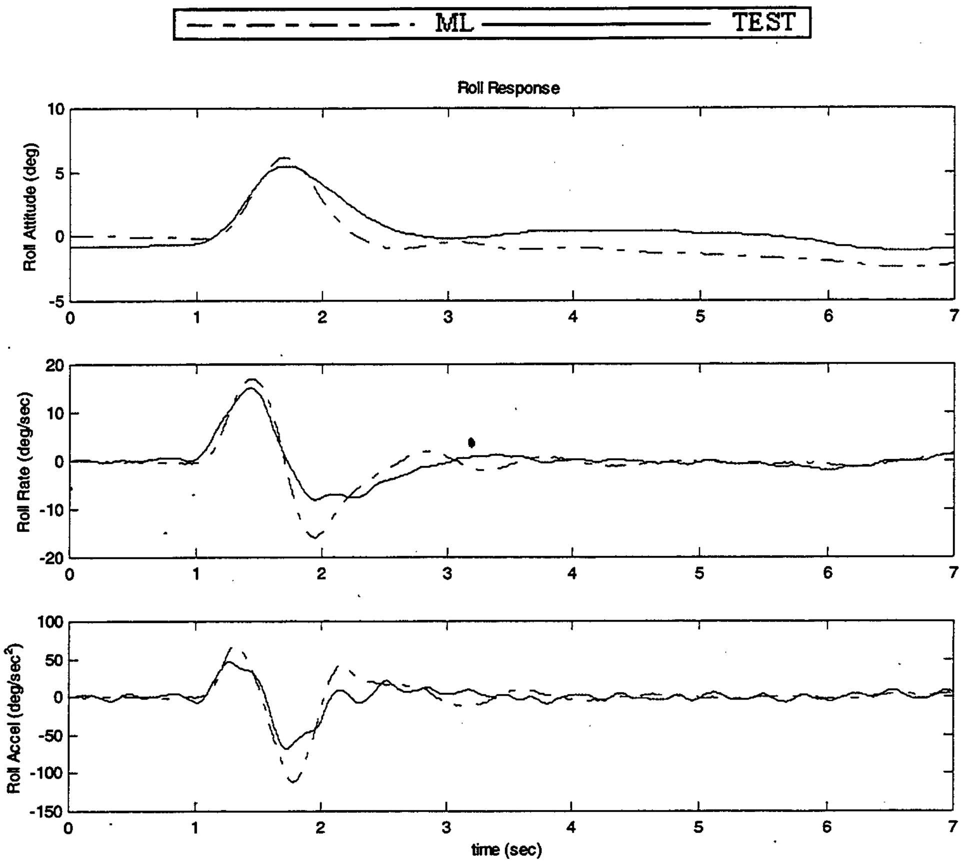

Figure 151 Modified 953-795 Run 092 On-Axis Response 22000,FSCG 360, 3000ft DA

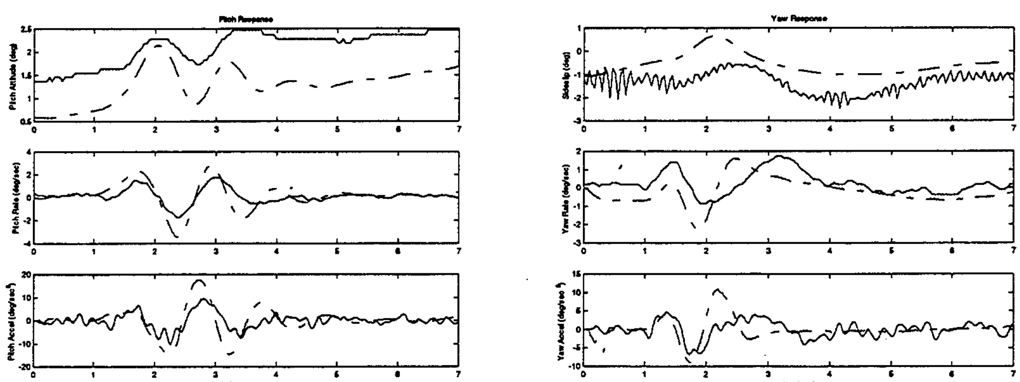

Figure 152 Modified 953-795 Run 092 Off-Axis Response 22000,FSCG 360, 3000ft DA

THIS PAGE INTENTIONALLY LEFT BLANK

VII. CONCLUSIONS AND RECOMMENDATIONS

A. CONCLUSIONS

This report examined two aircraft configurations in trim and dynamic flight maneuvers with three mathematical models. Several conclusions can be drawn from the results.

Trim analysis revealed very good correlation of the models in all regions with some degradation in the high-speed regimes. Unfortunately, this area (V_h) was where all of the available test flight data for analysis of handling qualities performance was recorded. Considering that all dynamic maneuvers covered in this report were conducted at V_h and at the aircraft's aft center of gravity limits, the on-axis response correlated very well. The lack of correlation in the off-axis response is more attributable to the author's lack of modeling experience than to a problem with the models.

The fact that the handling qualities model most accurately modeled the main rotor shaft bending while having the least accurate prediction of stabilator bending casts doubt on the assumption of uniform lift distribution across the stabilator. In other words, the point loads generated by GenHel® on the stabilator most likely generate a larger bending moment than was assumed in this report.

B. RECOMMENDATIONS

Recommendations for future correlation work include:

1. During time-domain analysis, attempt to more closely monitor the off-axis response.
2. Request handling quality test runs at lower airspeeds.
3. Further study is required regarding the relationship between the shaft bending values and the stabilator bending. Clearly a more accurate picture of the flow across the stabilator would allow for more accurate modeling. Another option is to increase the number of bending bridges on the stabilator so as to remove the requirement for a distribution assumption.

THIS PAGE INTENTIONALLY LEFT BLANK

APPENDIX A. SAMPLE GENHEL® COMMAND FILES

Sample Command File for HQ Model Trim Run

```
S
HTRIM=3000
OAT=48.32
WEIGHT=16825
FSCG=364
TRMPRT=1
MXTHR(1)=24.9
ENGIN=.F
&RETURN &
ED
MS
S
A
V
40
60
80
100
120
140
150
155
160
&RETURN &
E
E
```

Sample Command File for HQ Model Dynamic Run (Lateral Input)

```
ED
ML
I
INPUTB
16
&RETURN &
E
C
I
1
ST
XA(2)
N
-4.46447
&RETURN &
```

```
I
2
ST
XC(2)
N
-7.87920
&RETURN &
I
3
ST
XP(2)
N
-3.76958
&RETURN &
E
E
S
WEIGHT=22000
FSCG=360
HTRIM=3000
V=40
OAT=48.32
TIMLIM=10
DSASSW=.T.
ASASSW=.T.
MXTHR(1)=24.9
ENGIN=.F.
TRMPRT=.F.
TFILMR=0.29
TFILTM=0.0
VARPB(1)=A'XA(3)
VARPB(2)=A'XC(3)
VARPB(3)=A'XP(3)
FILENMPB='795_048.CTDIF
SLOADPB=.T.
RMBIASPB=.T.
ADAPS=.T.
VNAMEWPB(1)='LATSTKI
VNAMEWPB(2)='COLLSTKI
VNAMEWPB(3)='PEDI
TMVRSR(1)=A'WEIGHT
TMVRSR(2)=A'FSCG
TMVRSR(3)=A'HTRIM
TMVRSR(4)=A'V
TMVRSR(5)=A'OAT
TMVRSR(6)=A'TIMLIM
VARSR(1)=A'XAPC
VARSR(2)=A'XBPC
VARSR(3)=A'XCPC
VARSR(4)=A'XPPC
VARSR(5)=A'XAILS
VARSR(6)=A'XBILS
VARSR(7)=A'PHIB
```

```
VARSR(8)=A'THETAB
VARSR(9)=A'BETFRE
VARSR(10)=A'PDEG
VARSR(11)=A'QDEG
VARSR(12)=A'RDEG
VARSR(13)=A'PDOT
VARSR(14)=A'QDOT
VARSR(15)=A'RDOT
VARSR(16)=A'QHBMR
VARSR(17)=A'LHBMR
VARSR(18)=A'MHBMR
VARSR(19)=A'ZP1
VARSR(20)=A'ZP2
&RETURN &
```

Sample Command File for HQ Model Dynamic Run (Longitudinal Input)

```
ED
ML
I
INPUTB
16
&RETURN &
E
C
I
1
ST
XB(2)
N
3.11422
&RETURN &
I
2
ST
XC(2)
N
-7.80865
&RETURN &
I
3
ST
XP(2)
N
-3.67734
&RETURN &
E
E
S
```

```
WEIGHT=22000
FSCG=360
HTRIM=3000
V=40
OAT=48.32
TIMLIM=10
DSASSW=.T.
ASASSW=.T.
MXTHR(1)=24.9
ENGIN=.F.
TRMPRT=.F.
TFILMR=0.29
TFILTM=0.0
VARPB(1)=A'XB(3)
VARPB(2)=A'XC(3)
VARPB(3)=A'XP(3)
FILENMPB='795_041.CTDIF
SLOADPB=.T.
RMBIASPB=.T.
ADAPS=.T.
VNAMEWPB(1)='LGSTKI
VNAMEWPB(2)='COLLSTKI
VNAMEWPB(3)='PEDI
TMVRSR(1)=A'WEIGHT
TMVRSR(2)=A'FSCG
TMVRSR(3)=A'HTRIM
TMVRSR(4)=A'V
TMVRSR(5)=A'OAT
TMVRSR(6)=A'TIMLIM
VARSR(1)=A'XAPC
VARSR(2)=A'XBPC
VARSR(3)=A'XCPC
VARSR(4)=A'XPPC
VARSR(5)=A'XAILS
VARSR(6)=A'XBILS
VARSR(7)=A'PHIB
VARSR(8)=A'THETAB
VARSR(9)=A'BETFRE
VARSR(10)=A'PDEG
VARSR(11)=A'QDEG
VARSR(12)=A'RDEG
VARSR(13)=A'PDOT
VARSR(14)=A'QDOT
VARSR(15)=A'RDOT
VARSR(16)=A'QHBMR
VARSR(17)=A'LHBMR
VARSR(18)=A'MHBMR
VARSR(19)=A'ZP1
VARSR(20)=A'ZP2
&RETURN &
```

Sample Command File for ML Model Trim Run

```
ED
ML
D
6
D
6
D
6
D
6
E
MS
S
A
V
40
60
80
100
120
140
150
155
160
&RETURN &
E
E
S
HTRIM=3000
OAT=48.32
WEIGHT=16825
FSCG=364
TRMPRT=1
MXTHR(1)=24.9
ENGIN=.F
&RETURN &
```

Sample Command File for ML Model Dynamic Run (Lateral input)

```
ED
ML
D
6
D
6
D
6
D
6
```

```
D
15
I
INPUTB
15
&RETURN &
I
INPUTA
16
&RETURN &
E
C
I
1
ST
XA(2)
N
-4.46447
&RETURN &
I
2
ST
XC(2)
N
-7.87920
&RETURN &
I
3
ST
XP(2)
N
-3.76958
&RETURN &
E
E
S
WEIGHT=22000
FSCG=360
HTRIM=3000
V=40
OAT=48.32
TIMLIM=10
DSASSW=.T.
ASASSW=.T.
MXTHR(1)=24.9
ENGIN=.F.
TRMPRT=.F.
TFILMR=0.29
TFILTM=0.0
VARPB(1)=A'XA(3)
VARPB(2)=A'XC(3)
VARPB(3)=A'XP(3)
FILENMPB='795_048.CTDIF
```

```
SLOADPB=.T.
RMBIASPB=.T.
ADAPS=.T.
VNAMEWPB(1)='LATSTKI
VNAMEWPB(2)='COLLSTKI
VNAMEWPB(3)='PEDI
TMVRSR(1)=A'WEIGHT
TMVRSR(2)=A'FSCG
TMVRSR(3)=A'HTRIM
TMVRSR(4)=A'V
TMVRSR(5)=A'OAT
TMVRSR(6)=A'TIMLIM
VARSR(1)=A'XAPC
VARSR(2)=A'XBPC
VARSR(3)=A'XCPC
VARSR(4)=A'XPPC
VARSR(5)=A'XAILS
VARSR(6)=A'XBILS
VARSR(7)=A'PHIB
VARSR(8)=A'THETAB
VARSR(9)=A'BETFRE
VARSR(10)=A'PDEG
VARSR(11)=A'QDEG
VARSR(12)=A'RDEG
VARSR(13)=A'PDOT
VARSR(14)=A'QDOT
VARSR(15)=A'RDOT
VARSR(16)=A'QHBMR
VARSR(17)=A'LHBMR
VARSR(18)=A'MHBMR
VARSR(19)=A'ZP1
VARSR(20)=A'ZP2
&RETURN &
```

Sample Command File for ML Model Dynamic Run (Longitudinal Input)

```
ED
ML
D
6
D
6
D
6
D
6
D
15
I
INPUTB
15
&RETURN &
```

```
I
INPUTA
16
&RETURN &
E
C
I
1
ST
XB(2)
N
3.11422
&RETURN &
I
2
ST
XC(2)
N
-7.80865
&RETURN &
I
3
ST
XP(2)
N
-3.67734
&RETURN &
E
E
S
WEIGHT=22000
FSCG=360
HTRIM=3000
V=40
OAT=48.32
TIMLIM=10
DSASSW=.T.
ASASSW=.T.
MXTHR(1)=24.9
ENGIN=.F.
TRMPRT=.F.
TFILMR=0.29
TFILTM=0.0
VARPB(1)=A'XB(3)
VARPB(2)=A'XC(3)
VARPB(3)=A'XP(3)
FILENMPB='795_041.CTDIF
SLOADPB=.T.
RMBIASPB=.T.
ADAPS=.T.
VNAMEWPB(1)='LGSTKI
VNAMEWPB(2)='COLLSTKI
VNAMEWPB(3)='PEDI
```

```
TMVRSR(1)=A'WEIGHT
TMVRSR(2)=A'FSCG
TMVRSR(3)=A'HTRIM
TMVRSR(4)=A'V
TMVRSR(5)=A'OAT
TMVRSR(6)=A'TIMLIM
VARSR(1)=A'XAPC
VARSR(2)=A'XBPC
VARSR(3)=A'XCPC
VARSR(4)=A'XPPC
VARSR(5)=A'XAILS
VARSR(6)=A'XBILS
VARSR(7)=A'PHIB
VARSR(8)=A'THETAB
VARSR(9)=A'BETFRE
VARSR(10)=A'PDEG
VARSR(11)=A'QDEG
VARSR(12)=A'RDEG
VARSR(13)=A'PDOT
VARSR(14)=A'QDOT
VARSR(15)=A'RDOT
VARSR(16)=A'QHBMR
VARSR(17)=A'LHBMR
VARSR(18)=A'MHBMR
VARSR(19)=A'ZP1
VARSR(20)=A'ZP2
&RETURN &
```

Sample Command File for Mod ML Model Dynamic Run (Lateral input)

For brevity, only one Mod ML model command file is provided.

```
ED
ML
D
6
D
6
D
6
D
6
D
15
I
INPUTB
15
&RETURN &
I
INPUTA
```

```
16
&RETURN &
E
C
I
1
ST
XA(2)
N
-4.46447
&RETURN &
I
2
ST
XC(2)
N
-7.87920
&RETURN &
I
3
ST
XP(2)
N
-3.76958
&RETURN &
E
E
S
WEIGHT=22000
FSCG=360
HTRIM=3000
V=40
OAT=48.32
TIMLIM=10
DSASSW=.T.
ASASSW=.T.
MXTHR(1)=24.9
ENGIN=.F.
TRMPRT=.F.
TFILMR=0.29
TFILTM=0.0
VARPB(1)=A'XA(3)
VARPB(2)=A'XC(3)
VARPB(3)=A'XP(3)
FILENMPB='795_048.CTDIF
SLOADPB=.T.
RMBIASPB=.T.
ADAPS=.T.
VNAMEWPB(1)='LATSTKI
VNAMEWPB(2)='COLLSTKI
VNAMEWPB(3)='PEDI
TMVRSR(1)=A'WEIGHT
TMVRSR(2)=A'FSCG
```

```
TMVRSR(3)=A'HTRIM
TMVRSR(4)=A'V
TMVRSR(5)=A'OAT
TMVRSR(6)=A'TIMLIM
VARSR(1)=A'XAPC
VARSR(2)=A'XBPC
VARSR(3)=A'XCPC
VARSR(4)=A'XPPC
VARSR(5)=A'XAILS
VARSR(6)=A'XBILS
VARSR(7)=A'PHIB
VARSR(8)=A'THETAB
VARSR(9)=A'BETFRE
VARSR(10)=A'PDEG
VARSR(11)=A'QDEG
VARSR(12)=A'RDEG
VARSR(13)=A'PDOT
VARSR(14)=A'QDOT
VARSR(15)=A'RDOT
VARSR(16)=A'QHBMR
VARSR(17)=A'LHBMR
VARSR(18)=A'MHBMR
VARSR(19)=A'ZP1
VARSR(20)=A'ZP2
LODATA(1)\DAEPP1MP=0
LODATA(2)\DAEPP1MP=575.54
LODATA(3)\DAEPP1MP=989.22
LODATA(4)\DAEPP1MP=1169.08
LODATA(5)\DAEPP1MP=1043.18
LODATA(6)\DAEPP1MP=521.58
LODATA(7)\DAEPP1MP=0
LODATA(8)\DAEPP1MP=-521.58
LODATA(9)\DAEPP1MP=-1043.18
LODATA(10)\DAEPP1MP=-1169.08
LODATA(11)\DAEPP1MP=-989.22
LODATA(12)\DAEPP1MP=-575.54
LODATA(13)\DAEPP1MP=0
LODATA(14)\DAEPP1MP=0
LODATA(15)\DAEPP1MP=449.64
LODATA(16)\DAEPP1MP=755.4
LODATA(17)\DAEPP1MP=899.28
LODATA(18)\DAEPP1MP=771.38
LODATA(19)\DAEPP1MP=395.68
LODATA(20)\DAEPP1MP=0
LODATA(21)\DAEPP1MP=-395.68
LODATA(22)\DAEPP1MP=-771.38
LODATA(23)\DAEPP1MP=-899.28
LODATA(24)\DAEPP1MP=-755.4
LODATA(25)\DAEPP1MP=-449.64
LODATA(26)\DAEPP1MP=0
LODATA(27)\DAEPP1MP=0
LODATA(28)\DAEPP1MP=287.78
LODATA(29)\DAEPP1MP=503.6
```

```
LODATA(30)\DAEPP1MP=575.54
LODATA(31)\DAEPP1MP=503.6
LODATA(32)\DAEPP1MP=251.8
LODATA(33)\DAEPP1MP=0
LODATA(34)\DAEPP1MP=-251.8
LODATA(35)\DAEPP1MP=-503.6
LODATA(36)\DAEPP1MP=-575.54
LODATA(37)\DAEPP1MP=-503.6
LODATA(38)\DAEPP1MP=-287.6
LODATA(39)\DAEPP1MP=0
LODATA(40)\DAEPP1MP=0
LODATA(41)\DAEPP1MP=125.9
LODATA(42)\DAEPP1MP=251.8
LODATA(43)\DAEPP1MP=305.76
LODATA(44)\DAEPP1MP=251.8
LODATA(45)\DAEPP1MP=125.9
LODATA(46)\DAEPP1MP=0
LODATA(47)\DAEPP1MP=-125.9
LODATA(48)\DAEPP1MP=-251.8
LODATA(49)\DAEPP1MP=-305.76
LODATA(50)\DAEPP1MP=-251.8
LODATA(51)\DAEPP1MP=-125.9
LODATA(52)\DAEPP1MP=0
LODATA(53)\DAEPP1MP=0
LODATA(54)\DAEPP1MP=0
LODATA(55)\DAEPP1MP=0
LODATA(56)\DAEPP1MP=0
LODATA(57)\DAEPP1MP=0
LODATA(58)\DAEPP1MP=0
LODATA(59)\DAEPP1MP=0
LODATA(60)\DAEPP1MP=0
LODATA(61)\DAEPP1MP=0
LODATA(62)\DAEPP1MP=0
LODATA(63)\DAEPP1MP=0
LODATA(64)\DAEPP1MP=0
LODATA(65)\DAEPP1MP=0
LODATA(1)\DBEPP1MP=510.84
LODATA(2)\DBEPP1MP=417.98
LODATA(3)\DBEPP1MP=247.68
LODATA(4)\DBEPP1MP=0
LODATA(5)\DBEPP1MP=743.04
LODATA(6)\DBEPP1MP=619.2
LODATA(7)\DBEPP1MP=247.68
LODATA(8)\DBEPP1MP=0
LODATA(9)\DBEPP1MP=1099.08
LODATA(10)\DBEPP1MP=464.4
LODATA(11)\DBEPP1MP=61.92
LODATA(12)\DBEPP1MP=0
LODATA(1)\DAEPP2MP=0
LODATA(2)\DAEPP2MP=0
LODATA(3)\DAEPP2MP=0
LODATA(4)\DAEPP2MP=0
LODATA(5)\DAEPP2MP=0
```

```
LODATA(6)\DAEPP2MP=0
LODATA(7)\DAEPP2MP=0
LODATA(8)\DAEPP2MP=0
LODATA(9)\DAEPP2MP=0
LODATA(10)\DAEPP2MP=0
LODATA(11)\DAEPP2MP=0
LODATA(12)\DAEPP2MP=0
LODATA(13)\DAEPP2MP=0
LODATA(14)\DAEPP2MP=0
LODATA(15)\DAEPP2MP=0
LODATA(16)\DAEPP2MP=0
LODATA(17)\DAEPP2MP=0
LODATA(18)\DAEPP2MP=0
LODATA(19)\DAEPP2MP=0
LODATA(20)\DAEPP2MP=0
LODATA(21)\DAEPP2MP=0
LODATA(22)\DAEPP2MP=0
LODATA(23)\DAEPP2MP=0
LODATA(24)\DAEPP2MP=0
LODATA(25)\DAEPP2MP=0
LODATA(26)\DAEPP2MP=0
LODATA(27)\DAEPP2MP=0
LODATA(28)\DAEPP2MP=0
LODATA(29)\DAEPP2MP=0
LODATA(30)\DAEPP2MP=0
LODATA(31)\DAEPP2MP=0
LODATA(32)\DAEPP2MP=0
LODATA(33)\DAEPP2MP=0
LODATA(34)\DAEPP2MP=0
LODATA(35)\DAEPP2MP=0
LODATA(36)\DAEPP2MP=0
LODATA(37)\DAEPP2MP=0
LODATA(38)\DAEPP2MP=0
LODATA(39)\DAEPP2MP=0
LODATA(40)\DAEPP2MP=0
LODATA(41)\DAEPP2MP=0
LODATA(42)\DAEPP2MP=0
LODATA(43)\DAEPP2MP=0
LODATA(44)\DAEPP2MP=0
LODATA(45)\DAEPP2MP=0
LODATA(46)\DAEPP2MP=0
LODATA(47)\DAEPP2MP=0
LODATA(48)\DAEPP2MP=0
LODATA(49)\DAEPP2MP=0
LODATA(50)\DAEPP2MP=0
LODATA(51)\DAEPP2MP=0
LODATA(52)\DAEPP2MP=0
LODATA(53)\DAEPP2MP=0
LODATA(54)\DAEPP2MP=0
LODATA(55)\DAEPP2MP=0
LODATA(56)\DAEPP2MP=0
LODATA(57)\DAEPP2MP=0
LODATA(58)\DAEPP2MP=0
```

```
LODATA(59)\DAEPP2MP=0
LODATA(60)\DAEPP2MP=0
LODATA(61)\DAEPP2MP=0
LODATA(62)\DAEPP2MP=0
LODATA(63)\DAEPP2MP=0
LODATA(64)\DAEPP2MP=0
LODATA(65)\DAEPP2MP=0
LODATA(1)\DBEPP2MP=0
LODATA(2)\DBEPP2MP=0
LODATA(3)\DBEPP2MP=0
LODATA(4)\DBEPP2MP=0
LODATA(5)\DBEPP2MP=0
LODATA(6)\DBEPP2MP=0
LODATA(7)\DBEPP2MP=0
LODATA(8)\DBEPP2MP=0
LODATA(9)\DBEPP2MP=0
LODATA(10)\DBEPP2MP=0
LODATA(11)\DBEPP2MP=0
LODATA(12)\DBEPP2MP=0
LODATA(9)\MDWCMP=-232
LODATA(10)\MDWCMP=-75
DQF0=2
&RETURN &
```

APPENDIX B. PROCESSED TRIM DATA

Stick Position and Attitude Data for Configuration 1: GW 16825, FSCG 364, 3000 ft DA

TEST FLIGHT DATA 16825 364 3000

TEST	RUN NO	A/S [KT]	WEIGHT [lb]	DA [ft]	B1S LONG [%]	A1S LAT [%]	COLL [%]	PEDAL [%]	PHIB [deg]	THETAB [deg]	SIDESLIP [deg]	ATTACK [deg]
744	26	52	17246	2924	45	40	42	58	-1.3	4.3	-5.7	3.5
	25	70	17264	2961	43	43	37	63	-0.3	5.6	-4.3	6.2
	24	87	17274	3002	37	45	44	63	-0.1	6.3	-0.8	3.9
	27	103	17242	2882	37	48	47	65	0	5.1	-1.5	3.1
	28	122	17227	2916	35	47	62	65	-1.1	3.6	-0.4	-1.7
	29	144	17211	2910	33	49	78	64	0.3	1.1	0.3	-3.7
	30	152	17180	2932	29	47	90	63	0.8	1.2	-0.2	-4.8

BASELINE GENHEL DATA 16825 364 3000

HQ GenHel

WEIGHT [lb]	A/S [KT]	HTRIM [ft]	B1S LONG [%]	A1S LAT [%]	COLL [%]	PEDAL [%]	PHIB [deg]	THETAB [deg]	BETFRE [deg]	ALFREE [deg]
16825	40	3000	48	46	43.3	55	-1.43	3.12	0	
16825	60	3000	45	50	40	57	0	2.44	4.95	
16825	80	3000	39	53	41	62	0	3.57	2.19	
16825	100	3000	37	55	45	66	0	2.52	0.712	
16825	120	3000	36	57	54	68	0	0.7	0.09	
16825	140	3000	34	58	65	70	0	-1.19	-0.09	
16825	150	3000	32	58	73	71	0	-1.97	-0.03	
16825	155	3000	30	58	77	72	0	-2.13	-0.016	
16825	160	3000	29	58	82	72	0	-2.57	0.02	

ML GENHEL DATA 16825 364 3000

ML GenHel

WEIGHT [lb]	A/S [KT]	HTRIM [ft]	B1S LONG [%]	A1S LAT [%]	COLL [%]	PEDAL [%]	PHIB [deg]	THETAB [deg]	BETFRE [deg]	ALFREE [deg]
16825	40	3000	48	44	44	55	-1.23	3.13	0	3.13
16825	60	3000	48	47	40	60	0	2.47	0.3	2.47
16825	80	3000	42	50	43	66	0	2.97	-1.22	2.96
16825	100	3000	40	52	45	70	0	2.26	-1.17	2.26
16825	120	3000	38	54	53	72	0	0.7041	-0.65	0.7
16825	140	3000	36	55	65	74	0	-1.15	-0.73	-1.15
16825	150	3000	34	55	73	75	0	-2.17	-0.743	-2.16
16825	155	3000	33	54	78	76	0	-2.45	-0.71	-2.44
16825	160	3000	32	54	82	76	0	-2.8	-0.721	-2.79

MOD ML GENHEL DATA 16825 364 3000

ML GenHel No Left Stab Int and 2 X Right Inf with -75 ft^3 MDWCMP and Delta Drag = 2 square feet

WEIGHT [lb]	A/S [KT]	HTRIM [ft]	B1S LONG [%]	A1S LAT [%]	COLL [%]	PEDAL [%]	PHIB [deg]	THETAB [deg]	BETFRE [deg]	ALFREE [deg]
16825	40	3000	46	44	44	54	-1.46	2.99	0	2.98
16825	60	3000	47	47	40	61	0	2.53	0.399	2.53
16825	80	3000	41	50	43	66	0	3.1	-1.15	3.1
16825	100	3000	39	53	46	69	0	2.34	-1.06	2.34
16825	120	3000	36	54	55	72	0	1	-0.542	1
16825	140	3000	33	55	67	74	0	-0.625	-0.56	-0.623
16825	150	3000	29	55	76	75	0	-1.17	-0.51	-1.16
16825	155	3000	27	54	80	76	0	-1.16	-0.47	-1.15
16825	160	3000	26	54	84	77	0	-1.42	-0.46	-1.41

MR and Stab Bending Data for Configuration 1: GW 16825, FSCG 364, 3000 ft DA

Test Data RDF 953_744 — 16825 — 364 — 3000

First Harmonic Shaft Extender Bending

Airspeed	Run	Amplitude [in-lb]	Phase Angle [deg] From Contact Pos Dir Of Rot	Amplitude [ft-lb]	Phase Angle [deg] From Nose Pos Permutation	Resloved L [ft-lb]	Resolved M [ft-lb]	Q [ft-lb]	STBNBM1R [in-lb] local	STBNBM1L [in-lb] local	STAB INCIC [deg]	TPS196FL [psi] local	TPS196FR [psi] local	TPS196AR [psi] local	TPS196AL [psi] local
0	14	108000	117	9000.00	247.3	-3473.15	-8302.84	32485.00	5500.00	3600.00	38.5	736.00	458.00	505.00	177.00
52	26	131000	98	10916.67	266.3	-704.48	-10893.91	24187.00	4600.00	3800.00	29.4	-67.00	953.00	-351.00	-100.00
70	25	137000	99	11416.67	265.3	-935.46	-11378.28	19120.00	3600.00	3400.00	13.1	-21.00	860.00	-278.00	-125.00
87	24	187000	103	15583.33	261.3	-2357.15	-15404.03	23671.00	-4300.00	-300.00	3.9	-238.00	968.00	-397.00	-62.00
103	27	175000	105	14583.33	259.3	-2707.64	-14329.77	24250.00	-4600.00	-700.00	1.9	-96.00	937.00	-421.00	-141.00
122	28	161000	112	13416.67	252.3	-4079.11	-12781.54	34950.00	-11800.00	-3200.00	2.6	-1053.00	1326.00	-1230.00	170.00
144	29	154000	123	12833.33	241.3	-6162.87	-11256.71	45557.00	-19800.00	-4700.00	2.7	-2428.00	1854.00	-1867.00	559
152	30	166000	125	13833.33	239.3	-7062.51	-11894.62	53975.00	-25900.00	-7100.00	3.1	-3340.00	2222.00	-2024.00	827.00

HQ GenHel — 16825 — 364 — 3000

Shaft Extention Dist= 8 in

Stab lift length= 72 in
Point bend measured= 50 in

	Resultant Bending Moment @ shaft ext	Resultant Phase @shaft ext	H (+aft) @center rot Shaft Axis lb	J (+left wing) @center rot Shaft Axis lb	L @center rot Shaft Axis ft-lb	M @center rot Shaft Axis ft-lb	Q @center rot Shaft Axis ft-lb	L @shaft ext Shaft Axis ft-lb	M @shaft ext Shaft Axis ft-lb	Q @shaft ext Shaft Axis ft-lb	R STABIL PT LOAD [lb] local	L STABIL PT LOAD [lb] local	R STABIL MOM @x=62in [in-lb] local	L STABIL MOM @x=62in [in-lb] local
40	5664.61	256.33	-400	358	-1264	-5195	25297	-1502.67	-5461.67	25297	-108	-108	1875.00	1875.00
60	5911.87	260.94	-411	248	-884	-5544	22030	-1049.33	-5818.00	22030	-156	-156	2708.33	2708.33
80	12469.48	266.34	-900	170	-758	-11839	22317	-871.33	-12439.00	22317	-2	-2	34.72	34.72
100	13112.33	266.89	-906	129	-679	-12486	24874	-765.00	-13090.00	24874	67	67	-1163.19	-1163.19
120	12624.64	266.59	-815	96	-719	-12057	30181	-783.00	-12600.33	30181	145	145	-2517.36	-2517.36
140	12489.45	266.01	-754	107	-833	-11954	38517	-904.33	-12456.67	38517	277	277	-4809.03	-4809.03
150	13520.08	265.39	-819	110	-1042	-12928	44359	-1115.33	-13474.00	44359	382	382	-6631.94	-6631.94
155	14579.14	265.29	-879	108	-1148	-13942	47376	-1220.00	-14528.00	47376	440	440	-7638.89	-7638.89
160	14837.40	264.85	-881	115	-1279	-14188	51034	-1355.67	-14775.33	51034	496	496	-8611.11	-8611.11

ML GenHel — 16825 — 364 — 3000

Shaft Extention Dist= 8 in

Stab lift length= 72 in
Point bend measured= 50 in

	Resultant Bending Moment @ shaft ext	Resultant Phase @shaft ext	H (+aft) @center rot Shaft Axis lb.	J (+left wing) @center rot Shaft Axis lb	L @center rot Shaft Axis ft-lb	M @center rot Shaft Axis ft-lb	Q @center rot Shaft Axis ft-lb	L @shaft ext Shaft Axis ft-lb	M @shaft ext Shaft Axis ft-lb	Q @shaft ext Shaft Axis ft-lb	R STABIL PT LOAD [lb] local	L STABIL PT LOAD [lb] local	R STABIL MOM @x=62in [in-lb] local	L STABIL MOM @x=62in [in-lb] local
40	5708.09	249.41	-412	408	-1883	-5011	25670	-2155.00	-5285.67	25670	-95	-124	1649.31	2152.78
60	4563.08	248.30	-299	319	-1589	-3993	21935	-1801.67	-4192.33	21935	-122	-181	2118.06	3142.36
80	10273.62	259.95	-792	261	-1696	-9574	23116	-1870.00	-10102.00	23116	57	-41	-989.58	711.81
100	10764.37	260.91	-770	198	-1617	-10108	24502	-1749.00	-10621.33	24502	144	-11	-2500.00	190.97
120	11216.13	260.52	-761	178	-1762	-10550	29683	-1880.67	-11057.33	29683	273	1	-4739.58	-17.36
140	10924.65	258.59	-672	188	-2069	-10254	37935	-2194.33	-10702.00	37935	483	40	-8385.42	-694.44
150	11075.74	257.29	-682	213	-2333	-10341	43650	-2475.00	-10795.67	43650	674	90	-11701.39	-1562.50
155	12089.25	257.01	-773	223	-2597	-11258	47247	-2745.67	-11773.33	47247	788	126	-13680.56	-2187.50
160	12252.09	256.10	-758	245	-2816	-11379	50356	-2979.33	-11884.33	50356	883	127	-15329.86	-2204.86

Mod ML GenHel — 16825 — 364 — 3000

Shaft Extention Dist= 8 in

Stab lift length= 72 in
Point bend measured= 50 in

	Resultant Bending Moment @ shaft ext	Resultant Phase @shaft ext	H (+aft) @center rot Shaft Axis lb	J (+left wing) @center rot Shaft Axis lb	L @center rot Shaft Axis ft-lb	M @center rot Shaft Axis ft-lb	Q @center rot Shaft Axis ft-lb	L @shaft ext Shaft Axis ft-lb	M @shaft ext Shaft Axis ft-lb	Q @shaft ext Shaft Axis ft-lb	R STABIL PT LOAD [lb] local	L STABIL PT LOAD [lb] local	R STABIL MOM @x=62in [in-lb] local	L STABIL MOM @x=62in [in-lb] local
40	6415.90	250.47	-469	415	-2015	-5680	26175	-2291.67	-5992.67	26175	-81	-110	1406.25	1909.72
60	5154.37	250.32	-355	322	-1636	-4574	22130	-1850.67	-4810.67	22130	-96	-162	1666.67	2812.50
80	10981.33	260.55	-862	257	-1706	-10245	23384	-1877.33	-10819.67	23384	92	14	-1597.22	-243.06
100	12022.26	261.54	-899	197	-1678	-11286	25308	-1809.33	-11885.33	25308	204	72	-3541.67	-1250.00
120	13062.52	261.32	-948	173	-1875	-12278	30525	-1990.33	-12910.00	30525	375	121	-6510.42	-2100.69
140	13887.90	259.99	-982	164	-2298	-13023	39374	-2407.33	-13677.67	39374	619	214	-10746.53	-3715.28
150	15859.84	259.68	-1181	188	-2699	-14819	46040	-2824.33	-15606.33	46040	832	317	-14444.44	-5503.47
155	17085.83	259.53	-1288	177	-2947	-15950	49013	-3065.00	-16808.67	49013	918	357	-15937.50	-6197.92
160	17604.11	259.20	-1314	186	-3134	-16424	52064	-3258.00	-17300.00	52064	1017	391	-17656.25	-6788.19

Stick Position and Attitude Data for Configuration 2: GW 22000, FSCG 360, 3000 ft DA

TEST FLIGHT DATA 22000 360 3000

TEST	RUN NO	A/S [KT]	WEIGHT [lb]	DA [ft]	B1S LONG [%]	A1S LAT [%]	COLL [%]	PEDAL [%]	PHIB [deg]	THETAB [deg]	SIDESLIP [deg]
793	34	51	22231	3211	46	42	56	58	-1.1	5.3	0.3
	33	69	22243	3157	44	44	57	62	-0.6	5.3	-1.8
	32	85	22255	3093	38	46	56	63	-0.3	6.6	-1.2
	35	104	22203	3009	40	46	60	69	-1.3	5.2	-3.4
	36	124	22186	2926	36	48	70	67	-0.2	4.1	-1.6
	37	146	22152	2922	30	47	86	62	-0.9	2.6	-2.2

BASELINE GENHEL DATA 22000 360 3000

HQ GenHel

WEIGHT [lb]	A/S [KT]	HTRIM [ft]	B1S LONG [%]	A1S LAT [%]	COLL [%]	PEDAL [%]	PHIB [deg]	THETAB [deg]	BETFRE [deg]
22000	40	3000	49	44	58	53	-1.35	3.27	0
22000	60	3000	46	49	54	57	0	2.85	5.8
22000	80	3000	40	52	54	64	0	3.82	2.7
22000	100	3000	39	54	57	68	0	2.84	0.787
22000	120	3000	39	55	64	72	0	1.12	-0.104
22000	140	3000	35	56	76	73	0	-0.328	-0.12
22000	150	3000	32	55	83	74	0	-0.59	-0.062
22000	155	3000	30	55	87	74	0	-0.8	-0.0484
22000	160	3000	29	54	91	74	0	-1.24	-0.019

ML GENHEL DATA 22000 360 3000

ML GenHel

WEIGHT [lb]	A/S [KT]	HTRIM [ft]	B1S LONG [%]	A1S LAT [%]	COLL [%]	PEDAL [%]	PHIB [deg]	THETAB [deg]	BETFRE [deg]
22000	40	3000	49	43	58	53	-1.033	2.99	0
22000	60	3000	49	46	54	61	0	2.6	-0.046
22000	80	3000	44	48	56	68	0	2.91	-1.73
22000	100	3000	43	50	58	73	0	2.27	-1.89
22000	120	3000	42	52	63	76	0	0.88	-1.49
22000	140	3000	40	52	75	78	0	-0.87	-1.45
22000	150	3000	36	51	84	78	0	-1.17	-1.25
22000	155	3000	35	51	85	79	0	-1.32	-1.28
22000	160	3000	34	50	91	79	0	-1.78	-1.24

ML GENHEL DATA 22000 360 3000

ML GenHel No Left Stab Int and 2 X Right Inf with -75 ft^3 MDWCMP and Delta Drag = 2 square feet

WEIGHT [lb]	A/S [KT]	HTRIM [ft]	B1S LONG [%]	A1S LAT [%]	COLL [%]	PEDAL [%]	PHIB [deg]	THETAB [deg]	BETFRE [deg]
22000	40	3000	49	43	59	53	-1	3.14	0
22000	60	3000	48	45	55	60	0	2.81	0.145
22000	80	3000	42	48	56	68	0	3.13	-1.49
22000	100	3000	41	50	58	73	0	2.62	-1.66
22000	120	3000	38	51	66	75	0	1.47	-1.21
22000	140	3000	33	52	78	77	0	0.412	-1.03
22000	150	3000	29	51	86	78	0	0.281	-0.878
22000	155	3000	29	51	87	79	0	0.127	-0.923
22000	160	3000	27	49	94	78	0	-0.139	-0.81

MR and Stab Bending Data for Configuration 2: GW 22000, FSCG 360, 3000 ft DA

Test Data **RDF 953_793** **22000** **360** **3000**
First Harmonic Shaft Extender Bending

Airspeed	Run	Amplitude [in-lb]	Phase Angle [deg] From Contact Pos Dir Of Rot	Amplitude [ft-lb]	Phase Angle [deg] From Nose Pos Permutation	Resloved L [ft-lb]	Resolved M [ft-lb]	Q [ft-lb]	STBNBM1R [in-lb] local	STBNBM1L [in-lb] local
51	34	99000	92	8250.00	272.3	331.09	-8243.35	31934.00	4300.00	3000.00
69	33	110000	98	9166.67	266.3	-591.55	-9147.56	31524.00	100.00	1200.00
85	32	152000	100	12666.67	264.3	-1258.05	-12604.04	29267.00	-5400.00	0.00
104	35	126000	103	10500.00	261.3	-1588.24	-10379.19	30047.00	-5800	-300
124	36	102000	112	8500.00	252.3	-2584.28	-8097.62	37651.00	-10400.00	-1700.00
146	37	119000	123	9916.67	241.3	-4762.22	-8698.37	51321.00	-19800.00	-6200.00

HQ GenHel **22000** **360** **3000**

Shaft Extention Dist= 8 in

Stab lift length= 72 in
Point bend measured= 50 in

	Resultant Bending Moment @ shaft ext	Resultant Phase @shaft ext	H (+aft) @center rot Shaft Axis lb	J (+left wing) @center rot Shaft Axis lb	L @center rot Shaft Axis ft-lb	M @center rot Shaft Axis ft-lb	Q @center rot Shaft Axis ft-lb	L @shaft ext Shaft Axis ft-lb	M @shaft ext Shaft Axis ft-lb	Q @shaft ext Shaft Axis ft-lb	R STABIL PT LOAD [lb] local	L STABIL PT LOAD [lb] local	R STABIL MOM @x=62in [in-lb] local	L STABIL MOM@x=62in [in-lb] local
40	4939.38	251.24	-472	564	-1452	-4274	35657	-1828.00	-4588.67	35657	-37	-37	642.36	642.36
60	5315.35	259.35	-526	428	-908	-4829	29591	-1193.33	-5179.67	29591	-109	-109	1892.36	1892.36
80	10787.14	265.91	-1063	306	-718	-10039	28181	-922.00	-10747.67	28181	-17	-17	295.14	295.14
100	10605.18	267.29	-1007	243	-470	-9915	29277	-632.00	-10586.33	29277	51	51	-885.42	-885.42
120	8812.18	267.95	-769	230	-297	-8288	33759	-450.33	-8800.67	33759	96	96	-1666.67	-1666.67
140	9291.75	267.03	-765	250	-454	-8761	43246	-620.67	-9271.00	43246	229	229	-3975.69	-3975.69
150	11036.86	266.62	-926	270	-613	-10391	49635	-793.00	-11008.33	49635	336	336	-5833.33	-5833.33
155	11683.79	266.44	-983	278	-685	-10996	53003	-870.33	-11651.33	53003	440	440	-7638.89	-7638.89
160	11563.54	266.13	-961	317	-736	-10884	57467	-947.33	-11524.67	57467	446	446	-7743.06	-7743.06

ML GenHel **22000** **360** **3000**

Shaft Extention Dist= 8 in

Stab lift length= 72 in
Point bend measured= 50 in

	Resultant Bending Moment @ shaft ext	Resultant Phase @shaft ext	H (+aft) @center rot Shaft Axis lb	J (+left wing) @center rot Shaft Axis lb	L @center rot Shaft Axis ft-lb	M @center rot Shaft Axis ft-lb	Q @center rot Shaft Axis ft-lb	L @shaft ext Shaft Axis ft-lb	M @shaft ext Shaft Axis ft-lb	Q @shaft ext Shaft Axis ft-lb	R STABIL PT LOAD [lb] local	L STABIL PT LOAD [lb] local	R STABIL MOM @x=62in [in-lb] local	L STABIL MOM@x=62in [in-lb] local
40	4692.61	240.51	-440	636	-2079	-3676	35663	-2503.00	-3969.33	35663	-13	-57	225.69	989.58
60	3833.47	241.57	-337	545	-1646	-3040	29990	-2009.33	-3264.67	29990	-57	-141	989.58	2447.92
80	8075.60	256.92	-827	444	-1691	-7276	29389	-1987.00	-7827.33	29389	97	-44	-1684.03	763.89
100	7893.99	258.79	-769	369	-1427	-7202	29200	-1673.00	-7714.67	29200	155	-62	-2690.97	1076.39
120	6927.79	257.98	-616	350	-1349	-6334	33045	-1582.33	-6744.67	33045	264	-97	-4583.33	1684.03
140	6534.13	254.10	-502	391	-1682	-5904	42354	-1942.67	-6238.67	42354	519	-61	-9010.42	1059.03
150	8420.10	253.95	-723	433	-2177	-7569	49956	-2465.67	-8051.00	49956	710	-13	-12326.39	225.69
155	8214.50	253.76	-665	428	-2156	-7400	51038	-2441.33	-7843.33	51038	785	1	-13628.47	-17.36
160	8512.56	252.40	-694	490	-2410	-7598	56671	-2736.67	-8060.67	56671	905	1	-15711.81	-17.36

Mod ML GenHel **22000** **360** **3000**

Shaft Extention Dist= 8 in

Stab lift length= 72 in
Point bend measured= 50 in

	Resultant Bending Moment @ shaft ext	Resultant Phase @shaft ext	H (+aft) @center rot Shaft Axis lb	J (+left wing) @center rot Shaft Axis lb	L @center rot Shaft Axis ft-lb	M @center rot Shaft Axis ft-lb	Q @center rot Shaft Axis ft-lb	L @shaft ext Shaft Axis ft-lb	M @shaft ext Shaft Axis ft-lb	Q @shaft ext Shaft Axis ft-lb	R STABIL PT LOAD [lb] local	L STABIL PT LOAD [lb] local	R STABIL MOM @x=62in [in-lb] local	L STABIL MOM@x=62in [in-lb] local
40	4924.74	241.91	-473	638	-2091	-3918	35869	-2516.33	-4233.33	35869	7	-37	-121.53	642.36
60	4417.21	243.66	-413	558	-1775	-3585	30459	-2147.00	-3860.33	30459	-15	-106	260.42	1840.28
80	9255.11	258.20	-971	436	-1750	-8380	29858	-2040.67	-9027.33	29858	140	36	-2430.56	-625.00
100	9615.48	260.39	-978	355	-1491	-8807	29876	-1727.67	-9459.00	29876	216	2	-3750.00	-34.72
120	9866.79	260.30	-989	346	-1547	-9046	34692	-1777.67	-9705.33	34692	370	65	-6423.61	-1128.47
140	11836.09	258.91	-1199	374	-2116	-10798	45319	-2365.33	-11597.33	45319	660	178	-11458.33	-3090.28
150	13870.51	258.65	-1413	362	-2539	-12647	51898	-2780.33	-13589.00	51898	831	264	-14427.08	-4583.33
155	13709.20	258.79	-1349	346	-2486	-12538	53038	-2716.67	-13437.33	53038	895	301	-15538.19	-5225.69
160	14676.34	258.32	-1517	428	-2758	-13346	59623	-3043.33	-14357.33	59623	1029	346	-17864.58	-6006.94

LIST OF REFERENCES

1. Padfield, Gareth D., "Helicopter Flight Dynamics: The Theory and Application of Flying Qualities and Simulation Modeling" AIAA Education Series, 1996.

2. SER-702183, Sikorsky Engineering Report, "Growth Rotor Blade Feasibility Demonstration Flight Test Report", Sikorsky Aircraft Corporation, 1996.

3. SER-70452, Sikorsky Engineering Report, "UH-60A Black Hawk Engineering Simulation Volumes I and II" Prepared under NASA Contract NAS2-10626 by Sikorsky Aircraft, 1980.

4. "GenHel® Familiarization Course", Lecture Notes of Thomas Lawrence, 1997.

5. Enclosure(1) to AVO-U1-98-0020R1 "UH-60L Mass Data (w/ Main Rotor Growth Blades) 1998.

6. SER-520792, Sikorsky Engineering Report, "SH-60B Loads Survey/Envelope Expansion Structural Flight Test Report, 1989.

7. Prouty, R. W., "Helicopter Performance, Stability, and Control," Krieger Publishing Company, Malabar, Fl., 1995.

8. Hanselman D., and Littlefield B., "Mastering Matlab," Prentice Hall Upper Saddle River, N.J., 1995.

9. Matlab Help Desk, file://waverly/matlab$/help/helpdesk.html

10. Wood, E. R., "An Introduction to Helicopter Dynamics," AA3402 Helicopter Aerodynamics class notes 1998.

INITIAL DISTRIBUTION LIST

1. Defense Technical Information Center 2
   8725 John J. Kingman Rd., Suite 0944
   Ft. Belvoir, VA 22060-6218

2. Dudley Knox Library 2
   Naval Postgraduate School
   411 Dyer Rd.
   Monterey, CA 93943-5101

3. Chairman, Code AA/Co 1
   Department of Aeronautics and Astronautics
   Naval Postgraduate School
   Monterey, CA 93943-5000

4. Prof. E. Roberts Wood, Code AA/Wd 2
   Department of Aeronautics and Astronautics
   Naval Postgraduate School
   Monterey, CA 93943-5000

5. Thomas H. Lawrence 2
   Sikorsky Aircraft Corporation
   6900 Main Street, P.O. Box 9729, Mail Stop S336A
   Stratford, CT 06615-9129

6. CPT Robert L. Barrie, Jr. 2
   12812 Camino Del Valle
   Poway, CA 92064